Modelling impacts of climate variability and change on wheat cropping across New South Wales

Submitted by

Bin Wang

BSc., Nanjing Agri. U., China

A thesis submitted for the degree of Doctor of Philosophy

of University of Technology Sydney

School of Life Sciences, Faculty of Science,

University of Technology Sydney

January 2017

Certificate of original authorship

I certify that the work in this thesis has not previously been submitted for a degree nor has it been submitted as part of requirements for a degree except as part of the collaborative doctoral degree and/or fully acknowledged within the text.

I also certify that the thesis has been written by me. Any help that I have received in my research work and the preparation of the thesis itself has been acknowledged. In addition, I certify that all information sources and literature used are indicated in the thesis.

Signature of Student:

Date: 23/01/2017

Acknowledgements

I would like to thank my principal supervisor Prof. Qiang Yu and co-supervisor Prof. Derek Eamus for their supervision, advice and guidance during my PhD. It was Prof. Yu who encouraged me to study in UTS and gave me great support to help me to apply for scholarships from Chinese Scholarship Council. It was also him who suggested me to study at NSW Department of Primary Industries (DPI) Wagga Wagga agricultural institute and undertake this research project. I was not only given all the support but encouraged to publish research findings throughout the whole period. I am also indebted to my co-supervisor, principal research scientist Dr. De Li Liu for his invaluable assistance and suggestions in the academic studies. I must admit that without his constant encouragements, support and supervision I would not have done this. He has walked me through all the stages of the writing of this thesis and spent much time reading through each draft and provided me with inspiring advice. Without his patient instruction, insightful criticism and expert guidance, this PhD thesis could not have reached its present form. His supervision plays a crucial role in the completion of this thesis and will have profound impact on my future career.

I am grateful to staff in Climate Unit, NSW DPI, especially to team leader Timothy Sides for his assistance in various ways. The university staff in particular gave me every support when required for which I am thankful to them. I'm also thankful to my collaborators Prof. Senthold Asseng, Dr. Ian Macadam, Dr. Chao Chen and Dr. Xihua Yang for their tremendous efforts in improving the early manuscripts that have been published.

This PhD research is impossible unless the unfailing support and courage given by my beloved partner Dr. Yanyun Li. I know she is the one who suffered a lot during this process and I feel very lucky to have her around me. My special thanks to my parents and sister in China for their encouragement and understanding. They have always been helping me out of difficulties and supporting without a word of complaint. I also owe my sincere gratitude to my friends and my fellow classmates who gave me their help and time in listening to me and helping me work out my problems during the difficult course of the thesis.

I wish to gratefully acknowledge that the Chinese Scholarship Council provided the scholarship and the NSW DPI provided facilities for conducting this work.

Publications arising from this thesis

Journal Publications

1. **Wang B**, Chen C, Liu DL, Asseng S, Yu Q, Yang X (2015a) Effects of climate trends and variability on wheat yield variability in eastern Australia. Climate Research 64:173-186, https://doi.org/10.3354/cr01307.

2. **Wang B**, Liu DL, Asseng S, Macadam I, Yu Q (2015b) Impact of climate change on wheat flowering time in eastern Australia. Agricultural and Forest Meteorology 209:11-21, http://dx.doi.org/10.1016/j.agrformet.2015.04.028.

3. **Wang B**, Liu DL, Macadam I, Alexander LV, Abramowitzc G, Yu Q (2016) Multi-model ensemble projections of future extreme temperature change using a statistical downscaling method in south eastern Australia. Climatic Change, 1-14, http://dx.doi.org/10.1007/s10584-016-1726-x.

4. **Wang B**, Liu DL, Asseng S, Macadam I, Yu Q (2017) Modelling wheat yield change under CO_2 increase, heat and water stress in relation to plant available water capacity in eastern Australia. (submitted).

5. **Wang B**, Liu DL, Asseng S, Macadam I, Yu Q, Yang X (2017) Spatiotemporal changes of wheat phenology, yield and water use efficiency under the CMIP5 multimodel ensemble projections in eastern Australia. Climate Research, https://doi.org/10.3354/cr01458.

Conference Proceedings

Wang B, Liu DL, Macadam I, Alexander LV, Abramowitz G, Yu Q Multi-model ensemble projections of future extreme temperature change using a statistical downscaling method in eastern Australia. MODSIM2015, Gold Coast; 11/2015.

Contents

Summary

Wheat is the most important crop in Australia in terms of the gross value of production. However, in Australia wheat yield is extremely variable from year to year among major production regions, such as New South Wales (NSW), with its agricultural system being significantly affected by water stress and ongoing climate change. To accurately quantify crop yield, and estimate greenhouse gas emissions (GHG) at specific sites and regional scales, it is essential to link spatial information of agro-resources and crop simulation model to assess crop growth in response to agricultural management and environmental variation. The outcomes of this project will enhance the capability of farmers and policy makers to adapt and manage farm outcomes in the face of climate change/variability.

For this study, I extracted the historical daily climate data (1900-2010), known as SILO patched point dataset (PPD, http://www.longpaddock.qld.gov.au/silo/ppd/index.php), for maximum and minimum temperature, rainfall, and solar radiation at 894 weather stations evenly distributed across the NSW wheat belt. Wheat yields at shire level during 1922-2000 (data in some shires were not available in some years) across the NSW wheat belt were obtained from Fitzsimmons (2001). Statistical methods were used to quantify the relationship between reported shire wheat yields and climate factors during the wheat-growing season across the NSW wheat belt in eastern Australia from 1922 to 2000. I found that wheat yields were positively correlated to rainfall and minimum temperature while negatively correlated to maximum temperature at a significant level ($p<0.05$). Growing season rainfall is usually the main direct climatic driver affecting wheat yields variation in this semi-arid area, but the indirect effects of temperature and solar radiation are also important. A detailed understanding of how historical climate variation has impacted on wheat yield can provide useful insights for the development of sustainable agricultural systems in the face of future climate change.

I used the statistical downscaling and bias-correction method developed by Liu and Zuo (2012) to generate realistic daily site-specific climate data from monthly GCM output on a coarse-resolution grid. Briefly, monthly GCM output data (solar radiation, rainfall, daily maximum and minimum temperature) from each of the selected GCMs were downscaled to the 894 observation sites using an inverse distance-weighted interpolation method. Biases were then corrected using a transfer function derived from interpolated GCM data and observed data for the sites. Daily climate data for each of 894 sites under two RCPs for 1900-2100 were generated by a modified stochastic weather generator (WGEN) with parameters derived from the bias-corrected monthly data. The results show that wheat growing season rainfall is projected to decrease under different future scenarios across the NSW

wheat belt. Future climate projected an averaged warming of 2.1 ˚C for RCP4.5 and 3.8 ˚C for RCP8.5 across this region in 2061-2100 compared to the baseline period 1961-2000.

A crop simulation model (APSIM) driven by statistical downscaling data was used to simulate wheat productivity and water use efficiency under the CMIP5 multimodel ensemble projections across the NSW wheat belt. Despite an acceleration of crop development and shortening of growth duration together with declining growing season rainfall, GCMs projected that multi-model median yields could increase by 0.4% (4704 kg/ha) for RCP4.5 and 7.3% (5027 kg/ha) for RCP8.5 by 2061-2100. These results show that drier area would benefit more from elevated CO_2 than wetter area in the NSW wheat belt. Without the increase in CO_2 concentration simulated wheat yield decrease rapidly under RCP4.5 by 2061-2100 and much more so under RCP8.5 compared to the present. The simulated evapotranspiration (ET) decreased by 11.9% (282 mm) for RCP4.5 and 18.8% (260 mm) for RCP8.5 over the whole wheat belt. Increasing yields combined with decreasing ET resulted in simulated water use efficiency increasing by 11.4% (15.4 kg ha^{-1} mm^{-1}) for RCP4.5 and 29.3% (17.8 kg ha^{-1} mm^{-1}) for RCP8.5. Wheat production in water-limited, low yielding environments appears to be less negative impacted or in some cases even positively affected under future climate change and elevated CO_2, compared to other growing environments in the world.

Agro-ecosystems have high spatial heterogeneity and temporal variation of productivity, arising from the spatial and temporal variability of climate, soil texture/water, and management practices. Furthermore, the projected yield increase in the future could be overestimated because the crop model generally does not sufficiently account for yield reduction due to diseases, pests and weeds. I did not explicitly consider certain aspects such as efficient management practices, breeding new crop cultivars, which will obviously have a significant impact on wheat yield in the future. Therefore, these current simulated results would provide a baseline for future adaptive strategies such as incorporating new traits into new cultivars in new management systems not currently available.

Chapter 1

Introduction

Australia has the world's most variable climate (Stokes & Howden 2010) and climate variability has significantly affected Australian agricultural production. Since 2000, the planting areas for crops have decreased due to drought conditions. The production of wheat has decreased in all states except Victoria and in 2009-2010, NSW production decreased by 23% to 5.3 million ton (http://www.daff.gov.au/abares) compared to the decade prior to this period. With climate change and likely increased climate variability in the near future, together with increasing frequency of extreme events, such as droughts, floods and heat waves, crop yields are at risk of decline (Stokes & Howden 2010). However, the inevitable concomitant increased atmospheric CO_2 concentrations will increase plant photosynthesis and possibly decrease transpiration (i.e. water-use) and this may increase crop resistance to water stress (Lawlor & Mitchell 1991, Parry et al. 2004, Long et al. 2006). The diverse effects of climate change/variability and CO_2 increase in the wheat-belt of New South Wales are complex and poorly understood. Therefore, there is an urgent need for agricultural systems model to synthesise this knowledge and extend it beyond experimental sites and testing years so that agricultural resources can be optimized with the lowest risk under a changing climate across all sites and times especially for determining optimal response strategies for the future.

This study will provide a mechanistic understanding of the interactive impacts of climate warming, variable rainfall, and enriched atmospheric CO_2 concentration on wheat productivity over NSW wheat-belt from baseline period to different future periods, and reveal spatial and temporal patterns of water use and greenhouse gas emissions (GHG). As such, this project will provide answers to the following important questions:

(1) How did climate variability alter wheat yield over the past 100 years?

(2) How will wheat yield respond to more frequent extreme climate events (e.g. more/less rainfall; increased temperature extreme events like frost and heat stress) under diverse CO_2 emission scenarios in the future?

The specific aims of this study are to:

(1) Reveal wheat yield change in response to climate change/variability in the NSW wheat-belt over the past century at sites, shire and state scales using yield record and long term simulations by Agricultural Production Systems Simulator (APSIM).

(2) Evaluate the capacity of statistically downscaled data from IPCC AR5 multiple global circulation models (GCM) projections to represent recent trends in extreme temperature events, to describe the possible magnitude of the changes in the extreme climate events in the future.

(3) Quantify wheat development, crop yield and water-use under a changing climate over NSW wheat-belt using APSIM model driven by statistical downscaling IPCC AR5 GCM projections.

1.2 Research background

1.2.1 Climate change and wheat yield in NSW

In the past decade (2003-2013), total annual wheat production in NSW ranged between 2477 and 104,488 kt and the harvested area varied annually ranging from 2995 to 4322 kha, resulting in the yield produced per hectare varied greatly from 0.62 to 2.75 t/ha or in a range of more than four-fold (http://www.daff.gov.au/abares). Across the entire wheat belt of NSW, the mean annual temperature and rainfall varies from 13-20 ^{o}C and 200-700 mm, respectively, with large inter-annual variations. Spatially, the climate is hotter from south to north and drier from east to west (Liu et al. 2014). How much of the variations in wheat yield are caused by variation in climate are still unclear. Furthermore future climate scenarios, generated from the outputs of different GCMs, predict a significant decrease in winter rainfall in the south-western NSW by 2050 (CSIRO & BoM 2015), although with a slight increase in summer rainfall in the northeast. This will be accompanied by an increase of 2-3 ^{o}C in winter and spring maximum temperatures. As such it is expected that future wheat yield will be even more variable in NSW due to changing climate. A detailed understanding of how historical climate variation has impacted on wheat yield can provide useful insights for the development of sustainable agricultural systems in the face of future climate change.

1.2.2 Modelling impacts of climate change on crop production

Crop models, such as APSIM (**A**gricultural **P**roduction **S**ystems s**IM**ulator) developed by the Agricultural Production Systems Research Unit (APSRU) in Australia, are powerful tools for diagnosing crop growth, predicting crop yield and evaluating environmental impacts at multiple scales (Asseng et al. 1998, Keating et al. 2003). The management of agriculture resources is of paramount importance because the world has an ever increasing demand for food, while trying to reduce potential adverse environmental impacts. As a consequence, agricultural scientists have conducted numerous demonstration projects worldwide using modelling to analyze strategies for maximising crop production and minimizing adverse impacts. These agricultural system models include CERES (Crop Environment Resource Synthesis) from the US (Allan et al. 1986), WOFOST (WOrld FOod

STudies) from Europe (Diepen et al. 1989) and ORYZA2000 for lowland rice from IRRI (Bouman 2001). Many studies not only focused on simulating the individual effects of higher temperature (Asseng et al. 2011), elevated CO_2 (Tubiello et al. 2007a), changed rainfall (Jamieson et al. 1998) but also concentrated on how different aspects of climate change interact with each other (Van Ittersum et al. 2003, Ludwig & Asseng 2006). However, the results or recommendations are, at best, site-specific and time-dependent. Furthermore, a large uncertainty exists in predictions of future climate due to human activities. Therefore, crop model integration into spatial analyses is needed for analysing the impacts of the changing climate to crop growth at regional scales.

1.2.3 Climate change impacts and adaptations based on GCM downscaling data

Global climate change has been expected to threaten food supply, for example, through changing patterns of rainfall, increasing incidences of extreme weather, which could lead to greater variability of production, increased price volatility and changes in trade flows (Tubiello et al. 2007b, Lobell et al. 2008). GCMs are currently major tools in simulating climate change (Xu 1999, Mehrotra et al. 2013) and are used in assisting the future food and fiber productions. These numerical coupled models represent various earth systems including the atmosphere, oceans, land surface and sea-ice and offer considerable potential for the study of climate change and variability (Fowler et al. 2007). Although GCMs are recognized as the most appropriate tool to explore future climate change in response to rising concentrations of anthropogenic greenhouse gases, they remain relatively coarse in spatial resolution, even for the latest AR5 GCMs projections no less than one hundred kilometers and are unable to realistically simulate precipitation and other climate variables at regional and local scales (a few kilometers). For example, assessments of future river flows (hydrological model) (Crosbie et al. 2011) or agricultural potential (crop model) (Zhang 2005) require daily data, such as temperature, precipitation at catchments, or even station, field scales. Furthermore, archived daily sequences simulated by GCMs are currently available only for specific periods (time slices) of a few decades (Li Liu & Zuo 2012). Therefore, it is important to develop methods that make use of the available raw GCM output to produce scenarios of higher temporal and spatial resolutions to develop the best climate change adaptation strategies and policy development.

1.3 Significance

Agro-ecosystems have high spatial heterogeneity and temporal variation of productivity, arising from the spatial and temporal variability of climate, soil types, and management practices. In order to accurately quantify crop phenology, yield and water use efficiency under future climate change, and estimate GHG emissions at sites and regional scales, it is essential to link spatial information of

agro-resources and crop models to assess crop growth in response to agricultural management and environmental variation. The outcomes of this project will enhance the capability of farmers and policy makers to adapt and manage farm outcomes in the face of climate change/variability.

1.4 Proposed thesis outline

The proposed outline for this thesis is as follows:

- Introduction
- Literature review
- Effects of climate trends and variability on wheat yield variability in eastern Australia
- Multi-model ensemble projections of future extreme temperature change using a statistical downscaling method in south eastern Australia
- Impact of climate change on wheat flowering time in eastern Australia
- Modelling changes in wheat yield under future climate conditions in relation to plant available water capacity in eastern Australia
- Spatial changes of wheat phenology, yield and water use efficiency under the CMIP5 multimodel ensemble projections in eastern Australia.
- Final conclusion

Chapter 2

Literature review

The objective of this section is to provide a comprehensive review of literature related to the assessment of climate change impacts on crop productivity and adaptation options. It is intended to provide useful background information for this PhD research in understanding the impacts of climate change on agriculture and food security and to provide suitable adaptation options.

2.1 Climate change

In September 2013, the Intergovernmental Panel on Climate Change (IPCC) released its Fifth Assessment Report by Working Groups Ⅰ (AR5 WG Ⅰ) (IPCC 2013). Among the key conclusions of the report are the following findings:

- Warming of the climate system is unequivocal based on the facts that the atmosphere and ocean have warmed, the amounts of snow and ice have diminished, sea level has risen, and the concentrations of greenhouse gases have increased.

- Total radiative forcing is positive, and has led to an uptake of energy by the climate system. The largest contribution to total radiative forcing is caused by the increase in the atmospheric concentration of CO_2 since 1750.

- Continued emissions of greenhouse gases will cause further warming and changes in all components of the climate system. Limiting climate change will require substantial and sustained reductions of greenhouse gas emissions.

Australia's annual mean temperatures have increased by about 0.9 °C since 1910 with significant regional variations (Pearce et al. 2007). Daytime maximum temperatures have warmed by 0.8°C since 1910, while overnight minimum temperatures have warmed by 1.1 °C, and 2013 was Australia's warmest year on record, being 1.2 °C above the 1961-1990 average of 21.8 °C and 0.17 °C above the previous warmest year in 2005 (CSIRO & BoM 2015). The climate later in the twenty-first century is virtually certain to be warmer than at present. CMIP5 model projections indicate that average temperatures in Australia will rise by about 1.0 to 5.0 °C by 2070; a long-term drying over southern areas during winter, particularly in the southwest (IPCC 2013). The projections also indicate that extreme events such as heat waves and droughts are likely to become more frequent and intensive (Alexander & Arblaster 2009).

2.2 Downscaling methods

2.2.1 Change factors (CFs)

In the last a few decades, a number of downscaling techniques have been employed to bridge the gap between the resolution of climate models and local scales (Frei et al. 2003, Mearns et al. 2003, Diaz-Nieto & Wilby 2005, Hewitson & Crane 2006, Charles et al. 2007, Benestad 2010, Mehrotra et al. 2013). The most straightforward method for rapid impact assessment is to apply large-scale climate change projections to local observed climate baseline-change factors (CFs) (Arnell 1992, Arnell & Reynard 1996, Xu 1999, Anandhi et al. 2011).

Differences between the control and future GCM simulations are applied to baseline observations by simply adding or scaling the mean climatic values to each day (Fowler et al. 2007). There are two steps to produce climate scenarios in this simple method. First, estimate the mean changes in precipitation and temperature using GCM simulated baseline and future climates (e.g., $\triangle T$= +1, +2 and +3 ^{o}C and $\triangle P$= 0, $\pm$10%, $\pm$20%). Second, obtain local scaled future values by adding $\triangle T$ and by multiplying the values by (1+$\triangle P$) for temperature and precipitation, respectively (Xu 1999).

Although CFs can be rapidly applied to several GCMs to generate a range of climate scenarios, there are some problems with this approach. For example, the procedure only scaled the means, maxima and minima, ignoring climatic range and variability and assuming the spatial pattern of present climate remains constant in the future. Furthermore the temporal sequencing of wet and dry days is generally unchanged for precipitation, so CFs may not be helpful in circumstances where changes in event frequency and spell lengths are important to the impact assessment (Diaz-Nieto & Wilby 2005, Fowler et al. 2007, Anandhi et al. 2011).

2.2.2 Dynamical and statistical downscaling

Another two main methods, the dynamical downscaling method and statistical (empirical) downscaling method, have been widely applied to translate the large-scale GCM output into a finer resolution. The first is a dynamical downscaling approach embedding a higher-resolution climate model within a GCM. The second approach is to use statistical methods to generate empirical relationships between GCM-resolution climate variables and local climate.

2.2.2.1 Dynamical downscaling

Dynamical downscaling nests a regional climate model (RCM) into GCMs to produce a higher grid box resolution within the region of interest. An important advantage of this method is that RCMs explicitly account for many of the physical process such as orographic features and spatially more detailed depictions of gradients within the atmosphere than GCMs (Fowler et al. 2007, Yin et al. 2011). However, the dynamical method tends to inherit systematic biases from the driving GCM models and is dependent upon the veracity of GCM outputs as boundary conditions and also strongly depends on the presence and strength of regional scale forcing including such as orography, land-sea contrast, vegetation cover (Wang et al. 2004). Dynamical downscaling is also highly computational demanding and is as expensive to run as a global GCM (Wilby & Wigley 1997). Moreover, model integrations have been restricted to 'time slices'. For example, most RCMs are run only for a time-slice from 2070 to 2100, which makes climate change impacts for other periods difficult to assess (Fowler et al. 2007).

Nonetheless, this method has the ability to produce finer resolution information from GCM-scale output that can resolve atmospheric processes on a smaller scale and may ultimately provide atmospheric data for impact assessments that reflect the natural heterogeneity of climate at regional scales (Wilby & Wigley 1997, Fowler et al. 2007). Because of the complex topography and diverse climate regimes studies within the western U.S., Europe, and New Zealand, often report that more skillful dynamical downscaling for capturing regional climate than in regions such as the U.S., Great Plains and China where regional forcings are weaker (Kidson & Thompson 1998, Frei et al. 2003, Leung et al. 2003a, Wang et al. 2004).

Dynamical downscaling produced more realistic estimates of hydrologic impacts in mountainous regions such as the western U.S. derived from an ensemble of regional climate simulations (Leung et al. 2003b). This approach also can provide improved simulation of meso-scale precipitation and higher moment climate statistics (extreme climate such as intense precipitation, extreme high/low temperatures and frost conditions, and diurnal, seasonal, and inter-annual variability) for the control climate, and hence produce more plausible climate change scenarios for extreme events and climate variability at the regional scale (Wang et al. 2004). Since human society has been more vulnerable to changes in the frequency or intensity of extreme events (floods, droughts, heat waves) rather than median climate states, so dynamical downscaling will remain an important method for providing valuable needed information to assess climate change impact.

2.2.2.2 Statistical downscaling

Many statistical downscaling techniques have been developed to translate large-scale GCM output onto a finer spatiotemporal resolution. They are regression models, weather typing schemes and stochastic weather generators. Regression models capture the relationships between the local meteorological variables and the large scale atmospheric variables (predictors) (Wigley et al. 1990, von Storch et al. 1993, Crane & Hewitson 1998, Huth 1999, Zorita & Von Storch 1999). Weather typing schemes or weather classification methods group days into a finite number of discrete weather types or "states" according to their synoptic similarity (Conway et al. 1996, Goodess & Palutikof 1998, Hewitson & Crane 2002, Bardossy et al. 2005). Weather generators are statistical models that provide sequences of weather variables by simulating key properties of observed meteorological records (i.e. daily means, frequencies, extremes, variance and covariance) (Semenov & Barrow 1997, Wilks & Wilby 1999, Zhang 2005, Kilsby et al. 2007).

Statistical downscaling is based on some key assumptions that (i) predictor variables should be characterized well by GCMs. (ii) the observed, empirical relationship is assumed to be stationary under future climate conditions. If these assumptions hold, then it is possible to produce scenarios of regional and smaller-scale climate from GCMs projections, that are both more reliable and of finer resolution than the 'raw' GCM data (Wilby & Wigley 2000).

In comparison with dynamical downscaling, the main advantages of statistical downscaling are: (1) it is comparatively cheap and computationally efficient; (2) it can be applied easily to point-scale climatic variables from GCM output; (3) it is based on standard and accepted statistical procedures and the statistical relationships can be explained rather easily; and (4) it can be easily transferable to other regions and provide site-specific estimations (Fowler et al. 2007). Due to such advantages, statistical methods have been widely used in the regional climate change impact assessments, especially in the hydrologic response assessment (Hay & Clark 2003, Wood et al. 2004, Crosbie et al. 2011, Chen et al. 2012). However, this method also has disadvantages that need to be taken into account in its practical applications. First, it generally requires long and reliable observed historical time series for calibrating and validating the appropriate statistical relationship. Second, it depends upon choice of predictors and GCM boundary forcing. Third, it assumes that statistical relationships will be valid in the future, which is called stationarity in the predictor-predictand relationship.

New techniques have been introduced to improve the realism of downscaling data, such as Zhang (2007) downscaled monthly GCM temperature and precipitation to the station level using transfer functions and then used a Richardson-type weather generator to generate daily climate series based on

spatially downscaled monthly GCM output. Liu and Zuo (2012) applied an inverse distance-weighted (IDW) interpolation method to first downscale to specific sites through the monthly climate projections from global climate models (GCMs), a bias correction procedure was then used to the monthly GCM values of each site and daily climate projections for the site are generated by using a stochastic weather generator, WGEN. These approaches bridge the spatiotemporal gaps between coarse resolution projections of GCMs and fine resolution of data requirements of agricultural systems models, which can further demonstrate the site-specific impact assessment of climate change on water resources and crop production using hydrological model and crop growth model.

2.3 Climate change impacts on crop productivity

Crop development, growth and grain yields will greatly respond to increases in atmospheric CO_2 concentration, higher temperatures, altered precipitation and solar radiation, increased frequency of extreme temperature and precipitation events (Tubiello et al. 2007a, Yu et al. 2014). Solar radiation, temperature and precipitation are closely related and affect crop yield in different ways. Consequently, understanding these factors that determine yield is essential to predicting regional crop production, altering new cultivars, improving crop management techniques, and adopting feasible strategies to deal with climate change (Yu et al. 2014). When examining trends in historic grain yield data, it is difficult to separate the effect of climate change on crop production from the effects of changes in land use, cultivars and crop management. However, the use of simulation model makes it possible to study the impact of changes in the climate while keeping other technology variables (like cultivars and management) constant. Recent research has helped to better quantify the potential outcome of these key interactions.

2.3.1 Climate warming

Average global temperature and regional temperature patterns resulting from increased atmospheric concentrations of greenhouse gases are predicted to continue to rise, which have important consequences for crop yield (Tao et al. 2006, Lobell 2007, Luo 2011). Crop growing season is greatly affected by temperature (Porter & Gawith 1999, Sadras & Monzon 2006). For example, in southern Spain, a shift in phenology of trees and crops has been observed due to increased temperature from 1986 to 2008 (García-Mozo et al. 2010). Estrella et al. (2007) found that the majority of phenology events were significantly earlier with a mean advance of 1.1-1.3 days per decade in Germany.

Increasing mean temperatures during the growing season have been reported to reduce grain

yields due to a shorter growth period, reduce light interception and limit photosynthesis rates by accelerating phenological development (Asseng et al. 2011, Teixeira et al. 2011). Lobell et al. (2003) concluded that gradual temperature changes have had a measurable impact on both corn and soybean yield trends in America. Peng et al. (2004) found a close linkage between rice grain yield and mean minimum temperature based on records from continuous field experiments during 1992-2003 at the International Rice Research Institute (IRRI). Rice yields declined by 10% for each 1 °C increase in growing season minimum temperature. Tao et al. (2006) reported that the observed changes in temperature affected the phenology and crop yields differently at different stations in China. Furthermore, Lobell et al. (2007) found that diurnal temperature range (DTR=t_{max}-t_{min}) has a relatively strong negative effect in Australia and Canada, while a positive effect in France for wheat.

Based on these studies, it can be found that continuous warming trend has had large impacts on the development and production of field crops, but the size and extent of the impacts have differed spatially and temporally (Tao et al. 2006). There is a clear and present need to synthesize crop yield and climate data from different areas with more detailed information to predict impacts of climate change on future food production (Lobell & Asner 2003).

2.3.2 Solar radiation (global dimming)

The amount of incident solar radiation governs the physiological and biophysical processes of vegetation over land surface, such as canopy photosynthesis, and evapotranspiration (ET), as well as the energy balance over diurnal/seasonal time frames (Yang et al. 2013). The global solar radiation reaching the surface declined from the beginning of widespread measurements in the 1950s until the mid-1980s while there was a partial recovery from the 1980s onward (Stanhill & Cohen 2001, Wild et al. 2005). Numerous studies have substantiated the findings of significant decadal surface solar radiation changes observed both at worldwide distributed terrestrial sites as well as in specific regions, which show that dimming and brightening occurred in different areas and related to aerosol loading of the atmosphere and the influences of aerosols on atmospheric transmittance (Cohen 2009, Norris & Wild 2009, Wild 2009, Augustine & Dutton 2013).

Reductions in solar radiation and change in radiation composition are closely coupled to evapotranspiration and water use efficiency (WUE) which could have significant effects on crop development and growth (Stanhill & Cohen 2001, Zhang et al. 2011a). Black et al. (2006) showed that the decrease in solar irradiance between 1955 and 2004 resulted in a significant decrease in calculated gross primary productivity varying from 1.25 to 3.9 t C ha^{-1} over the 50-year period. Chameides et al. (1999) found a close correlation between decrease in solar radiation and rice yield at Nanjing of China

using the CERES model. Yang et al. (2013) demonstrated that declining solar radiation from high radiation levels had no effect on wheat yield but improved water use efficiency, while under low radiation levels (mean wheat season solar radiation of 7.8 MJ m^{-2}) grain yields decreased significantly.

2.3.3 Water stress

Water resources play a vital role in crop productivity and assessment of seasonal and long-term water availability is not only of importance for sustaining human life, biodiversity and the environment, but also helpful for farmers to determine agricultural water management (Kang et al. 2009). Water availability is under threat from the changing climate because of possible rainfall decrease in some regions of the world (Wang et al. 2009d, Rowhani et al. 2011, Traore et al. 2013). In the northern wheat-belt of Australia most of the water used by the wheat crop falls as rain before the growing season, and is stored in the subsoil after fallowing while in southern Australia, although fallowing adds to the water supply in some soils in some districts, most of the water used by wheat comes from rain during April-October (French & Schultz 1984a, b). However, growing season rainfall is highly variable and usually limits production especially in rainfed environments and climate change is one of the greatest pressures on the hydrological cycle including the natural replenishment of surface and groundwater resources.

Many studies have considered climate change impacts on water use efficiency as well as crop productivity under different climate conditions. For example, Luding et al. (2006) studied the impacts of predicted climate change on wheat systems in Western Australia and found that reductions in rainfall could result in a considerable decrease in wheat yield while future climate change has been predicted to increase the potential wheat yield in the wetter and cooler southern part of the wheat-belt. Wang et al. (2011) demonstrated that the response of crop yield to future climate change is complex and the extents of response depend on many other factors like climatic regions, crop types, soil types and management practices over the Murray-Darling Basin in Australia.

2.3.4 Elevated atmospheric CO_2

Increasing concentrations of CO_2 in the atmosphere are linked to a high probability of climate change, characterized by increased surface temperatures, by changed global and regional patterns of precipitation, and by climatic shifts in both mean and variability that could threat ecosystem functions and human welfare (Tubiello & Ewert 2002). Elevated CO_2 concentrations stimulate photosynthesis, leading to increased plant productivity and modified water and nutrient cycles (Kimball et al. 2001,

Nowak et al. 2004). In particular, elevated CO_2 and associated climate change may greatly affect crop production. Therefore, it is not surprising that hundreds of studies have been conducted to analyze crop response to increased CO_2 concentrations above current levels.

Experiments under optimal conditions show doubling the atmospheric CO_2 concentration from 350 ppm to 700 ppm increases leaf photosynthesis by 30%-50% in C3 plant species including rice, soybeans and wheat, and 10%-25% in C4 crop such as maize and sorghum, despite some down-regulation of leaf photosynthesis by elevated atmospheric CO_2 concentrations (Tubiello et al. 2007b). Spring wheat grain yield increased by 10.4% (Högy et al. 2009) and rice seed yield increased 7-15% (KIM et al. 2003, Long et al. 2006) in elevated CO_2 during previous FACE studies. Long et al. (2006) found a much smaller CO_2 fertilization effect on yield using new FACE data than currently assumed derived from chamber experiments and crop models forecast. Recent analyses of FACE studies indicate that, at 550 ppm atmospheric CO_2 concentration, observed yields increase under unstressed conditions by 26% for wheat in Australian dry land (O'Leary et al. 2015). However, Tubiello et al. (2007a) reported that the response of crop yields to elevated CO_2 were similar across FACE and non-FACE experimental data and results from most crop simulations were consistent with the values from FACE experiments. They think any remaining differences in CO_2 response based on FACE results would not significantly alter projections of world food supply in the 21st century.

Modelers and plant physiologists alike recognize that the impacts of elevated CO_2, as measured in experimental settings and subsequently implemented in models, may nonetheless overestimate actual field and farm-level responses, because of many limiting factors such as pests, weeds, nutrients, competition for resources, soil water and air quality, which are neither well understood at large scales, nor well implemented in leading models. Future crop model development should therefore strive to include these additional factors to allow for more realistic climate-change simulations. In the meantime, studies projecting future yield and production under climate change should do so by incorporating sensitivity ranges for crop response to elevated CO_2 to better convey the associated uncertainty range (Tubiello et al. 2007b).

2.3.5 Increased frequency of extreme events

The effects of increased climate variability on crop production under climate change are likely to increase production losses beyond those estimated from changes in mean variables alone (Tubiello et al. 2007b). Yield damaging climate thresholds spanning periods of just a few days for crops include absolute temperature levels linked to particular developmental stages like flowering and seed formation stage (Wheeler et al. 2000, Wollenweber et al. 2003, Asseng et al. 2011). For example

spring wheat grain yield declined by 350 g/m^2 with a 10˚C increase in maximum temperature at 78 days after sowing (50% anthesis) and a 40% reduction in the number of grains per year in a field experiment (FERRIS et al. 1998). Rice spikelet sterility was positively related to the maximum temperature during the 20 days before and after anthesis (Tao et al. 2006). Maize exhibits reduced pollen viability for temperatures above 36˚C (Porter & Semenov 2005).

GCM outputs indicated that the surface temperature and precipitation might become more intense in the future, and short-term natural extremes such as storms and floods, droughts, heat waves, inter-annual and decadal climate variations as well as large-scale circulation changes such as the El Nino Southern Oscillation all have adverse effects on crop production. For example, El Nino-like conditions increase the probability of farm incomes falling below their long-term median by 75% across most of Australia's cropping regions, with impacts on gross domestic product ranging from 0.75% to 1.6% (Potgieter et al. 2002, Tubiello et al. 2007b). Europe experienced a particularly extreme climate event during the summer of 2003, with temperatures up to 6°C above long-term means and precipitation deficits up to 300 mm. A record crop yield drop of 36% occurred in Italy for corn grown in the Po valley where extremely high temperatures prevailed (Ciais et al. 2005).

2.3.6 Interactions of climate variables (temperature and rainfall) and CO_2 increase

Changes in temperature, rainfall, and atmospheric CO_2 concentration together can have significant impacts on crop productivity (Challinor & Wheeler 2008, Chavas et al. 2009). Scenarios for future global and regional climate change will include elevated atmospheric CO_2, but could also mean warmer average air temperatures and increased water deficit in rainfed agriculture due to changes in rainfall amount and distribution (Asseng et al. 2004). High temperature during the critical flowering period of a crop may lower otherwise positive CO_2 effects on yield by reducing grain number size, and quality while increased temperatures during the growing period may also reduce CO_2 effects indirectly, by increasing water demand (Howden et al. 2007).

2.3.6.1 Year patterns of climate impacts

Time series of crop yields comprise of two components. One is the increase in yield as a result of crop management improvement, including improved cultivars, fertilization development and biocide application. The other is the variation in yield caused by climatic variability (Yu et al., 2001). To evaluate the impact of climate on crop yields, the technologically driven yield increase must be eliminated by removing the yield trend from times series. To do this the first-difference method has been widely used to remove the possible confounding effects of non-climatic factors (Lobell et al.,

2003, 2005, 2007; Tao et al., 2008; Zhang et al., 2010). It creates a series of yield differences differentiating the yields of 2 successive years. Thus the effects of variations in climatic variables on crop yield variations can be identified without directly removing the technologically driven trend towards yield increase.

2.3.6.2 Process-based crop models

These effects of climate change on growth processes in the context of natural climatic and soil variability, and a large range of crop management options (e.g. N management) make it extremely difficult to foresee and quantify any consequences of future climate change on crop production (Asseng et al. 2004). A widely used approach to this prediction problem is process-based models that simulate crop growth and development. Many studies not only focused on simulating the individual effects of higher temperature, elevated CO_2, changed rainfall but also concentrated on how different aspect climate change interact each other (Van Ittersum et al. 2003, Ludwig & Asseng 2006).

For example Asseng et al. (2011) showed that observed variations in average growing-season temperature of ±2 ^oC in the main growing regions of Australia can cause reductions in wheat production of up to 50% when rainfall, radiation, genotype and cropping practices were kept constant between years. Ludwig et al. (2006) studied how higher temperature (2, 4 and 6 ^oC) elevated CO_2 (525 and 700 ppm) and five different rainfall scenarios affected wheat yield using APSIM-Nwheat. Yield increased with higher CO_2 especially at drier sites while higher temperatures had a positive effect in the cooler and wetter region. Potgieter et al., (2013) assessed the impact changes in temperature and rainfall associated with low and high CO_2 on modelled wheat yields in response to emission scenarios projected for the periods 2020 and 2050, they found that taking into account CO_2 fertilizations effects attenuated the yield reductions associated with increased temperatures and reduced rainfall by 2020, 2050.

However, large uncertainty exists in climate impacts on yield using crop simulation models, especially the uncertainty related to model structure. In recent years, a number of studies, as part of the Agricultural Model Inter-comparison and Improvement Project (AgMIP), have examined the differences through systematic crop model inter-comparison (Asseng et al. 2013, Martre et al. 2015). Palosuo et al. (2011) simulated winter wheat yield and its variability in different climates of Europe with a comparison of eight crop growth models (APES, CROPSYST, DAISY, DSSAT, FASSET, HERMES, STICS and WOFOST) and concluded that application of crop simulation models with restricted calibration leaded to a high degree of uncertainty about climate impacts on yield and yield variability. Nevertheless, the wide range of projected impacts on agriculture is associated with both

the uncertainty in climate projections (i.e. GCM projections and GHG emission scenarios) and the structural (or parameterization) differences between crop models (Osborne et al. 2013, Monier et al. 2016). Some studies pointed out GCMs being the main source of the uncertainty in magnitude, spatial pattern and even sign of projected change (Hawkins & Sutton 2009, Kassie et al. 2015). They partitioned the variation of future climate change to three main factors, namely the internal variability of climate system, the choice of GCMs (model uncertainty or response uncertainty) and the greenhouse gas emissions pathway (scenario uncertainty). Different GCMs can provide different future climate projections for a particular region. The real climate system is highly complex and it is impossible to adequately describe its processes with an individual climate model. Authors of model evaluation studies have stated that no single model can be considered 'best' and recommend using results from a range of climate models. Therefore, the use of many GCMs was important to sample the uncertainties in future climate projections that arise from differences in model structure and parameterization, as well as internal climate variability (Lobell et al. 2015).

2.3.6.3 Statistical models

Another method is statistical models in which historical data on crop yields and climate variables are used to calibrate relatively simple regression equations (Lobell & Burke 2010a). They are particularly useful when data are insufficient to calibrate more complicated process-based models. Many efforts have been made to empirically investigate climatic effects on crop yield by relating climate change observations to census yields from long-term site-specific field observations to regional, national and global scale (Tao et al. 2006, Lobell et al. 2008, Zhang et al. 2010, Teixeira et al. 2011).

In spite of these efforts, there are some arguments about effects of increased temperature on crop production. For example, Lobell (2007) found negative effects of increased diurnal temperature range (DTR) for rice yields, which contradicts the positive effect of DTR inferred by Peng et al. (2004). More interesting, Sheehy et al. (2006) reinvestigated Peng's claim of the yield decline with the IRRI dataset Peng et al. (2004) used and argued against and pointed toward covariation of rising minimum temperature and reduced solar radiation, thus, a decrease in solar radiation could also explain the reduction in yield (Zhang et al. 2010). Low solar radiation could be associated with high minimum temperature, high rainfall and low harvest index (Sheehy et al. 2006). Zhang et al. (2010) reported positive and negative yield correlation with temperature can be seen as a proxy of radiation or rain effects via correlation with them, suggesting a relative weak temperature effect on change in rice yields. Consequently, separating the contributions of solar radiation, rainfall and temperature to yield cannot be achieved using simple correlation because of co-linearity problem between predictor

variables (e.g. temperature and precipitation, temperature and radiation) (Lobell & Burke 2010b).

2.3.7 Adaptation to climate change

Adaptation to climate change will require changes in genotype (G) and management (M) to match the climate-induced changes in environment (E) (Soussana et al. 2010). For rainfed crops in the dry areas, evidence shows that variation due to E far outweighs the variation of grain yield that is due to M or G, or the interactions between these factors, and between these factors and E (Anderson 2010).

Asseng et al. (2012) found that changes in climate and CO_2 concentration last century have, in combination, had little or no impact on wheat yields in Western Australia using APSIM-Nwheat model while other changes have had much larger effects, including changes in crop cultivars, crop production technologies and farming systems, including increased fertilizer use, herbicides for weed management, reduced tillage, improved machinery allowing earlier sowing, retention of crop residues, and the use of 'break' crops, largely for management of root diseases. Anderson et al. (2005) showed that about 70% of yield improvement has come from improved management and about 30% from improved cultivars of wheat through experiments comparing old and modern management, old and modern cultivars. Jiang et al. (2003) grew a set of historical cultivars of winter wheat released over 50 years in China managed in the same environment and found that the cultivars differed by only 36% while recorded grain yield increased eightfold during this period, indicating that agronomic practices were the most important factors for grain yield. Yu et al. (2012) carried out the modeling analysis on contributions of cultivar improvement during the past three decades, which showed that rice cultivar improvement was the top most important contributor to the enhance rice production in China with cultivar (38.9%), climate (4.4%), management (9.3%).

The contributions to yield improvement of the genotype×management×environment (G×M×E) are varied in different regions for different crops. Therefore, this will require the development of regional adaptation strategies (e.g. innovative water harvesting and conservations methods, sowing dates, cultivar choice, crop rotation) as well as the development of drought and heat tolerant cultivars, which can counter the likely negative impact of climate change (Potgieter et al. 2013).

Chapter 3*

Effects of climate trends and variability on wheat yield variability in eastern Australia

Abstract

Identifying climatic drivers that dominate crop yield variations at a regional scale is important for predicting regional crop production. In this study, a statistical method was used to quantify the relationship between reported shire wheat yields and climate factors during wheat-growing season across the New South Wales (NSW) wheat belt in eastern Australia from 1922 to 2000. The results show that 8.5-21.2% of the observed wheat yield increase over the last 78 years is due to changes in climate. In the eastern slopes of NSW, growing season maximum and minimum temperatures and number of heat stress days (>34 °C) were identified to be dominant climatic factors affecting wheat yield, accounting for 36% of yield variation. In the northern region, maximum temperature, pre-growing season rainfall (December to April) and the number of frost days (<2 °C) accounted for 41% of yield variation. In the southern region, rainfall, temperature, the number of frost and heat stress days accounted for 47% of yield variation, while in southwest NSW, rainfall was the main factor accounting for 31% of yield variation. Frost was less important in the eastern slopes because farmers manage frost occurrence by sowing late and using late-flowering cultivars. However, frost had more impact on yield variation in the northern parts of the wheat belt as farmers sow earlier and select short-season cultivars to avoid heat stress. Understanding the impact of climate variations on crop yield is important for developing sustainable agricultural production under future climate change.

Keywords: climate variation, wheat yield variability, NSW wheat belt, first difference

3.1 Introduction

Inter-annual variability of crop yields is largely determined by climate variables such as temperature, rainfall, and solar radiation (Chen et al. 2004, Rowhani et al. 2011, Trnka et al. 2012, Traore et al. 2013). These climate factors are closely related and affect grain yield in different ways for different crops; moreover, climate-yield relationships are also region-dependent (Lobell & Asner 2003, Lobell et al. 2005, Tao et al. 2008, Ludwig et al. 2009, Zhang et al. 2010, Potgieter et al. 2013). For example, Zhang et al. (2010) found that solar radiation was the primary climate variable to cause inter-annual variations in rice yield in southern China, based on experimental data during the period

*: This chapter has been published in Climate Research 64:173-186, 2015.

of 1981-2005. In Mexico, most of the wheat yield variability can be attributed to cool nighttime temperatures during the wheat-growing season, which explained approximately 69% of yield variation in irrigated systems (Lobell et al. 2005). Lobell et al. (2007) reported that growing season temperatures accounted for at least 29% of year-to-year variation of grain yields for six of the most widely grown crops globally. However, in rain-fed conditions, the variation in seasonal rainfall is the major climate factor to affect yield variation (Seif & Pederson 1978, Cooper et al. 2008, Traore et al. 2013). Therefore, it is important to identify the major climate factors that cause yield variation and quantify their effects on yield for specific crops in specific regions. This can provide a foundation to understand regional crop production and variability and can help to develop feasible strategies for adapting to future climate change (Lobell et al. 2007).

Wheat is the most important crop in Australia in terms of the gross value of its production. However, Australian wheat yield is extremely variable from year to year across major production regions (Potgieter et al. 2002). In the past decade (2003-2013), New South Wales (NSW) annual wheat production ranged between 2,477 and 10,488 kt. Harvested area varied from 2,995 to 4,322 kha with wheat yields varying from 0.62 to 2.75 t/ha (http://www.daff.gov.au/abares). Although advances in technology and improved cultivars have been identified to contribute to yield increase, much of the variation in Australian wheat yields is related to growing season rainfall variability. For example, in South Australia approximately 65% of wheat yield variation has been reported to be associated with the variability of rainfall during April-October, with rainfall during winter months (June to August) being more effective to produce high yields than that during other times (Cornish 1950). However, Seif and Pederson (1978) found that spring rainfall, from 3 weeks before flowering to 2 weeks after, contributed to 86% of the variation in yield in the central west of New South Wales. Extreme weather events, such as frost and heat stress, affect wheat yields and represent a significant risk that needs to be managed to maintain profitable production (Asseng et al. 2011, Zheng et al. 2012). Several studies have investigated the climate effects on wheat in Australia using the yield data at a regional level (Potgieter et al. 2002, Hansen et al. 2004), state level (Yu et al. 2014), and national scale (Nicholls 1997). However, there have been few comprehensive studies of the climate-yield relationship at a district or shire level, which can provide a higher spatial resolution of yield and climate, including diverse compositions of solar radiation, rainfall, and temperature. Moreover, the results of recent studies on the impact of climate trends in Australia have been contradicting. For example, Nicholls (1997) concluded that 30% to 50% of Australian wheat yield increase during the period 1952-1992 was caused by temperature increase. In a multiple linear regression model with three climate variables, Nicholls (1997) found that increase in minimum temperature caused wheat yield increase with small contributions from rainfall changes. However, Godden et al. (1998) and Gifford et al. (1998) argued

that Nicholls's conclusion was not justified and overestimated the effects of climate trends on wheat yields. Gifford et al. (1998) suggested that the response of wheat yield to climate variation is more specific to regional conditions and growing season climate variability and many other factors contribute to the change in yields.

Statistical models that rely on past observations of climate and crop yields have been widely used to evaluate the impacts of climate change on crop performance (Lobell & Burke 2010a). They are particularly useful when data are insufficient to calibrate dynamic process-based models. The main requirement of statistical models is long time series data for historical climate and crop yields. Among statistical approaches, the multiple linear regression method is traditionally used because it can explain the relative contributions of different climate factors to crop yield with relatively simple multiple linear regression equations (Lobell et al. 2005, Sheehy et al. 2006, Lobell et al. 2007, Lobell & Burke 2010b, Rowhani et al. 2011). However, a multiple linear regression method is limited by excluding collinearity among climate factors when consider individual predictor effects (Sheehy et al. 2006, Lobell & Burke 2010b).

In this study, I systematically investigated climate-yield relationships and the effects of climate variation on wheat yields in four geographical-climate regions at shire scale across the NSW wheat belt in eastern Australia during 1922-2000. Stepwise regression analysis was used to identify the most relevant climate variables for yield variation, and empirical regression models were then developed to quantify the effect of climate trends on yield. The objectives of this study were to: 1) provide a quantitative understanding of the relationship between wheat yield and climate in the past few decades; 2) identify the major climatic drivers for yield variation and 3) analyze the impact of climate trend on wheat yields.

3.2 Materials and methods

3.2.1. Study area

The New South Wales (NSW) wheat belt is geographically located in 66 shires of the state in eastern Australia. It has an area of 360,000 km^2, accounting for 45% of the state land area of 809,444 km^2 (Liu et al. 2014). Here wheat is mainly grown under rain-fed conditions. The crop can be sown in autumn or early winter (May to July) to ensure that flowering will take place after the last frost, and maturity will occur before any summer humidity across the wheat belt, depending on local climatic conditions (rainfall) and soil types.

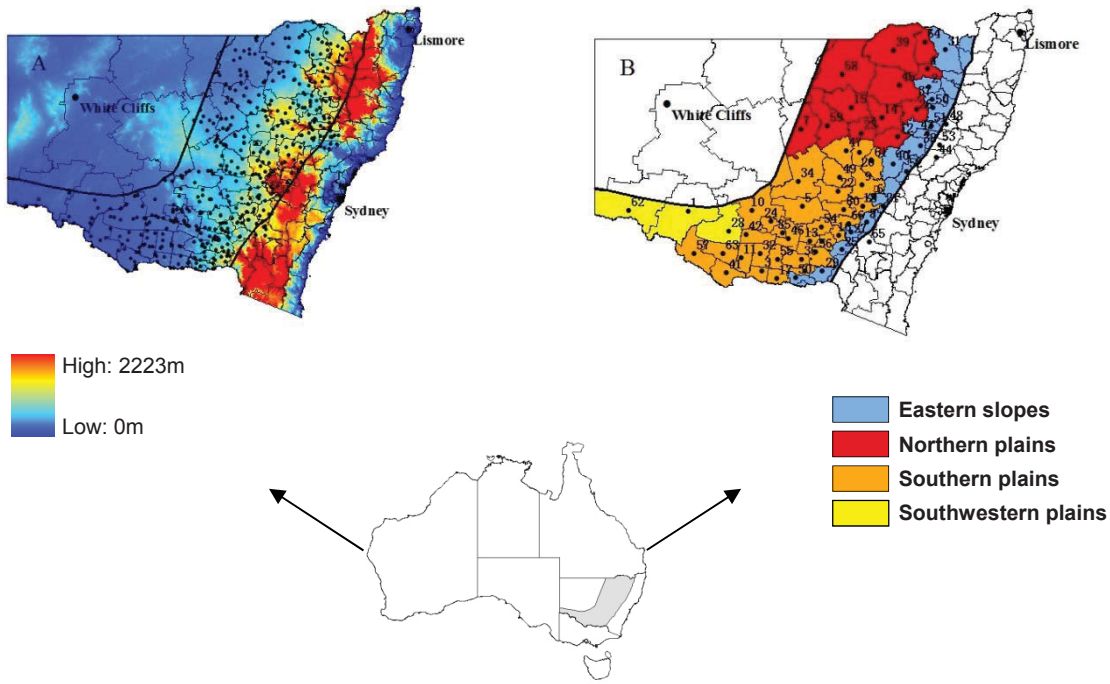

Fig. 3.1 Spatial distributions of 466 weather stations (A) and four regions including 66 shires (B) over the NSW wheat belt used in this study.

Wheat usually flowers in early to mid-spring, and matures in late spring to early summer. Although the sowing date and mature date vary, May to November is typical growing season for wheat in eastern Australia (Gomez-Macpherson & Richards 1995). The wheat belt is characterized by variable topography and climate conditions (Fig. 3.1A). Topographically, the eastern part of the wheat belt is occupied by hills, known as "slopes", with elevation above 500 m. The other areas are mainly occupied by plains. Climatically, the wheat belt has a broad range of variable environments (Fig. 3.2). It is warm and dry in the northern and southwestern plains, where growing season rainfall (GSR) is less than 250 mm and growing season mean temperature (GST) is above 14.0 °C. In the southern plains, GSR is about 300 mm and GST is about 12.5 °C. In the eastern slopes, the GSR is more than 400 mm with GST being lower than 12 °C. Accordingly, I divided the wheat belt into four regions based on the climate and topography characteristics obtained from the topographical landscape of a Digital Elevation Model (DEM): the eastern slopes (I), northern plains (II), southern plains (III) and southwestern plains (IV) (Table 3.1, Fig. 3.1B).

Table 3.1 Time period of sixty-six selected shires and number of weather stations for each shire included in this study. Region I included 20 shires in the east of NSW wheat belt; region II included 12 shires in the north; region III included 31 shires in the south and region IV included three shires in the southwest.

Region	ID[a]	Shire	Stations	Time period	Region	ID	Shire	Stations	Time period
I	29	Holbrook	7	1922-1996	III	32	Jerilderie	5	1922-2000
	25	Gundagai	4	1922-1996		17	Corowa	6	1922-2000
	27	Harden	2	1922-2000		55	Urana	4	1922-2000
	65	Yass	7	1922-1996		19	Culcairn	3	1922-2000
	8	Boorowa	4	1922-2000		36	Lockhart	6	1922-2000
	6	Blayney	5	1922-1996		56	Wagga	11	1922-2000
	21	Evans	6	1922-1996		46	Narrandera	9	1922-2000
	52	Rylstone	3	1922-1996		35	Leeton	4	1927-2000
	40	Mudgee	8	1922-1996		5	Bland	9	1922-2000
	38	Merriwa	7	1922-2000		13	Coolamon	6	1922-2000
	44	Muswellbrook	5	1922-1996		33	Junee	10	1922-2000
	53	Scone	7	1922-1996		54	Temora	3	1922-2000
	43	Murrurundi	7	1922-2000		16	Cootamundra	5	1922-2000
	51	Quirindi	8	1922-2000		11	Conargo	8	1922-2000
	48	Nundle	1	1922-1996		47	Narromine	10	1922-2000
	50	Parry	4	1922-2000		20	Dubbo	3	1922-2000
	37	Manilla	1	1922-1996		61	Wellington	7	1922-2000
	31	Inverell	10	1922-2000		66	Young	6	1922-2000
	2	Barraba	5	1922-1996		49	Parkes	9	1922-2000
	30	Hume	6	1922-2000		9	Cabonne	11	1922-2000
II	58	Walgett	25	1966-2000		18	Cowra	6	1922-2000
	39	Moree plains	13	1922-2000		60	Weddin	6	1922-2000
	64	Yallaroi	7	1922-2000		22	Forbes	2	1922-2000
	15	Coonamble	12	1922-2000		63	Windouran	6	1922-1996
	45	Narrabri	14	1922-2000		41	Murray	5	1922-2000
	26	Gunnedah	11	1922-2000		10	Carrathool	7	1922-2000
	14	Coonabarabra n	9	1922-2000		42	Murrumbidgee	7	1922-2000
	23	Gilgandra	5	1922-2000		34	Lachlan	15	1922-2000
	59	Warren	9	1958-2000		24	Griffith	7	1927-2000
	7	Bogan	8	1958-2000		57	Wakool	8	1922-2000
	12	Coolah	7	1922-2000	IV	1	Balranald	8	1960-2000
	4	Bingara	4	1922-1996		62	Wentworth	5	1968-2000
III	3	Berrigan	4	1922-2000		28	Hay	14	1961-2000

[a] The ID number corresponds to those in Fig. 1B.

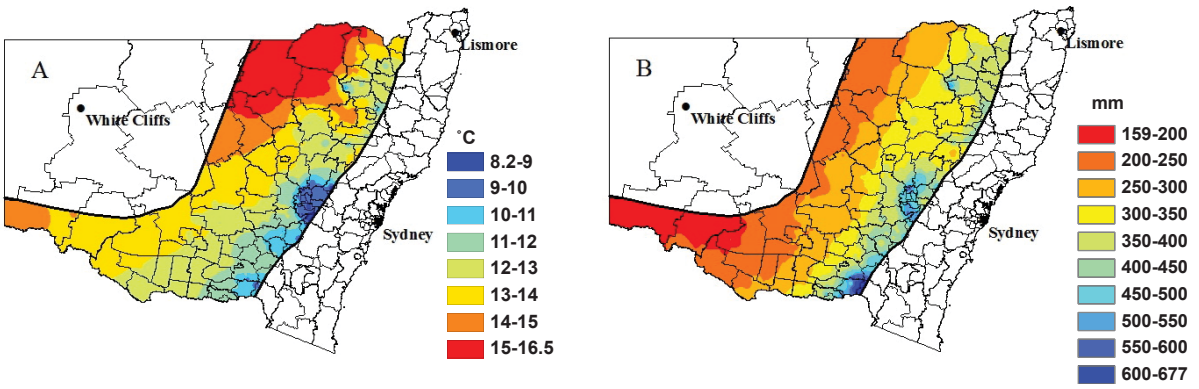

Fig. 3.2 Spatial distributions of growing season mean temperature (GST) (A) and rainfall (GSR) (B) over the NSW wheat belt during 1922-2000.

3.2.2 Climate and yield data

For this study, I extracted the historical daily climate data (1922-2000), known as SILO patched point dataset (PPD, http://www.longpaddock.qld.gov.au/silo/ppd/index.php), for maximum and minimum temperature, rainfall, and solar radiation at 466 weather stations evenly distributed across the NSW wheat belt (Fig. 3.1A). Wheat yields at shire level during 1922-2000 (data in some shires were not available in some years) across the NSW wheat belt were obtained from Fitzsimmons (2001) (Table 3.1).

To obtain climate variables that characterize the climate conditions of each shire, the daily maximum and minimum temperatures, rainfall, and solar radiation during 1922-2000 were assembled from the weather stations located within the shire (Table 3.1) to produce shire-average daily climate data. I then averaged the calculated daily climate data for the main growing season from May 1 to November 30 to obtain shire-scale climatic variables of the wheat-growing season. Number of days with T_{max} >34 °C (boundary to define heat stress) and number of days with T_{min} <2 °C (boundary to define frost) (Asseng et al. 2011, Liu et al. 2011, Barlow et al. 2015) during the wheat-growing season were calculated for each shire.

3.2.3 De-trending method

The year-to-year variations of crop yield are largely driven by climate (Yu et al. 2001, Chen et al. 2004, Porter & Semenov 2005), but studies have shown that crop management improvements including improved cultivars, fertilization development, and biocides application have contributed to crop yield increase in the past decades (Anderson et al. 2005, Asseng & Pannell 2012, Yu et al. 2012). To evaluate the impact of climate variation on crop yield, the yield increase driven by technological

improvement needs to be excluded. A first-difference method has been widely used to remove the possible confounding effects of non-climatic factors (Nicholls 1997, Lobell & Asner 2003, Tao et al. 2008, Zhang et al. 2010). This approach can minimize the influence of management factors, allowing the ability to examine the response of crop yields to climatic variables from year to year (Lobell & Field 2007, Trnka et al. 2012). First difference is defined as the difference of a parameter between two successive years:

$$\Delta X_i = X_i - X_{i-1} \qquad i=1, 2, \ldots n \qquad (3.1)$$

Where ΔX_i is the first difference of the parameter for *i*th year; X_i is the parameter value for the *i*th year; and $X_{i\text{-}1}$ is the parameter value for the *(i-1)*th year. The first differences of maximum temperature (ΔT_{max}), minimum temperature (ΔT_{min}), rainfall (ΔR), solar radiation (ΔS), number of frost days (T_{min} <2 °C， ΔF), number of heat stress days (T_{max} > 34°C， ΔH) and wheat yield (ΔY) for the growing season during the period of 1922-2000 were calculated. Then ΔY, ΔT_{max}, ΔT_{min}, ΔR, ΔS, ΔF and ΔH were used to evaluate the effects of variation in climate factors on yield.

3.2.4 Stepwise regression analysis

Stepwise regression analysis is particularly useful to identify major climatic variables to affect crop yield variations (Yu et al. 2001, Liu et al. 2010b). It evaluates all climate variables for their potential contributions to crop yield variation and excludes variables not statistically significant in the multiple regression model (P≤0.01). Procedures to use stepwise regression are relatively computationally efficient and have advantages to allow to use a small subset of least correlated variables without losing a significant portion of the explanatory power of the data, thus minimizing the effects of multicollinearity on the regression model (Huang & Townshend 2003). The stepwise regression analysis combines both forward selection and backward elimination methods to establish a regression model. Firstly, the procedure starts a forward selection by trying out one explanatory variable at a time and includes it in the regression model if it is statistically significant (P<0.01). The second step involving in the stepwise procedure will use backward elimination method to retest the coefficients of the added variables and delete these variables if the test judges them to be insignificant. Because the addition of one variable can lead to a change in the performed *p* value associated with another variable, the third step in the stepwise process will reselect the variables by allowing a variable to enter the equation at one step, deleting the variable at a later step and allowing the variable to reenter at an even later step (Dielman 2001). Finally, the stepwise regression procedure terminates when no more variables can be justifiably entered or removed from the model.

In this study we use stepwise method to select significant climate variables with statistical software SAS (version 9.2). The multiple liner regression model without intercept (intercept forced to zero, to avoid trend effect) (Nicholls 1997) was:

$$\Delta Y = a_0 \Delta T_{\max} + a_1 \Delta T_{\min} + a_2 \Delta R + a_3 \Delta S + a_4 \Delta F + a_5 \Delta H \quad (3.2)$$

a_0, a_1, a_2, a_3, a_4 and a_5 represent the regression coefficients to be fit.

3.3 Results

3.3.1 Variability of climate and wheat yield

Fig. 3.3 shows the variations of climate variables during the wheat-growing season from 1922 to 2000 in four regions. Growing season maximum temperature (GST_{max}) had the biggest variability in the eastern slopes (region I) due to a large range of latitudes in this region, ranging from 13.2 to 23.5 ^{o}C with a mean of 18.3±2.1 ^{o}C (Fig. 3.3A). For the northern and southern plains (region II and III, respectively), there were similar amplitudes of the variations in GST_{max}, but the northern plains had the highest mean GST_{max} of 21.5 ^{o}C. GST_{max} had the least variability (±0.6 ^{o}C) ranging from 18.4 to 21.3 ^{o}C with a mean of 20.0 ^{o}C in the southwestern plains (region IV). For growing season minimum temperature (GST_{min}) (Fig. 3.3B), the patterns of their variations were similar to GST_{max}. In eastern slopes GST_{min} varied between 1.6 and 8.2 ^{o}C with a mean of 5.1±1.2 ^{o}C, and the mean value of GST_{min} was highest in the southwestern plains, with the value of 7.4±0.6 ^{o}C.

The largest variability of growing season solar radiation (GSS) (Fig. 3.3C) occurred in the eastern slopes, ranging from 2,738 to 3,961 MJ m^{-2} yr^{-1} with a mean of 3,294±232 MJ m^{-2} yr^{-1}, while the southwestern plains had the smallest variability from 3,040 to 3,567 MJ m^{-2} yr^{-1} with a mean of 3,243±103 MJ m^{-2} yr^{-1}. The largest averaged GSS value was 3,600 MJ m^{-2} yr^{-1} in the northern plains.

Growing season rainfall (GSR) ranged between 97.6 and 935.1 mm with a mean of 407.1±141.4 mm among all the years and shires in the eastern slopes (Fig. 3.3D). The median GSR was 400 mm, 75% of years and shires had more than about 300 mm in this region. The northern and southern plains had a similar rainfall range with a mean of 302.5±117.8 and 307.2±115.2 mm in growing season, respectively. Notably, the southwestern plains received less than half of GSR of eastern slopes ranging between 46.2 and 376.9 mm with a mean of 199.8±65.9 mm. Rainfall was less than 290 mm in 90% of years and shires in this region.

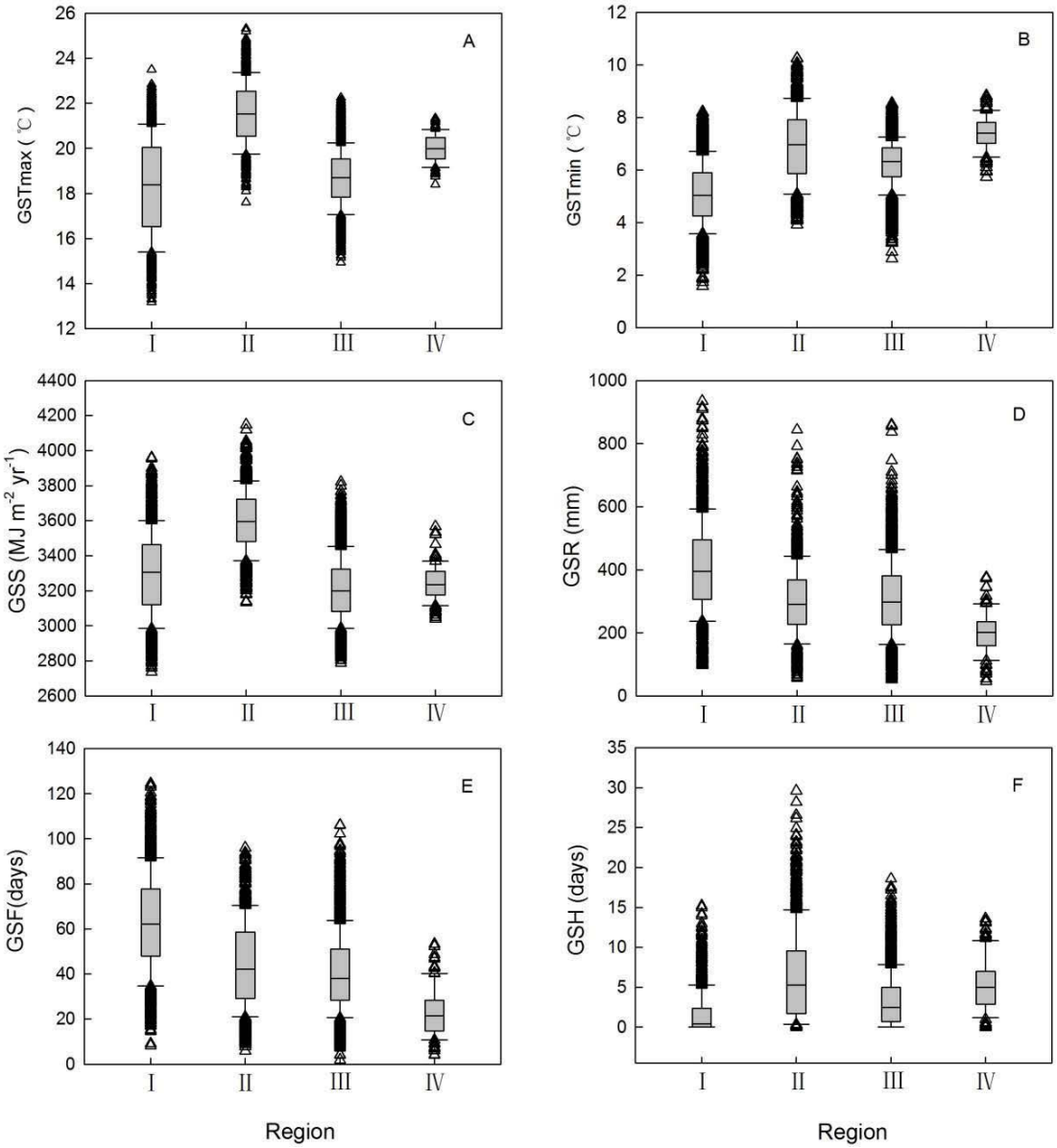

Fig. 3.3 Mean growing season maximum temperature (GST_{max}, A), minimum temperature (GST_{min}, B), solar radiation (GSS, C), rainfall (GSR, D), number of frost (GSF, E) and heat stress days (GSH, F) from 1922 to 2000 in four regions. The horizontal line inside boxes indicates the median value, box-boundaries are the 25th and 75th percentiles, whiskers are the 10th and 90th percentile and triangles indicate outliers.

The occurrence probability of frost (GSF) and heat stress (GSH) varied greatly across the NSW wheat belt during the period of 1922-2000 (Fig. 3E, F). The number of frost days was the highest (63 days) in the eastern slopes occurring during the wheat-growing season in more than 50% of years and shires due to lower temperature (Fig. 3.2A). The number of frost days in the northern plains (44 days)

was slightly more than that in the southern plains (41 days). However, frost days occurred least in the southwestern plains (23 days). By contrast, heat stress days during the wheat-growing season in the northern plains and southwestern plains occurred approximately 5 days in more than 50% of years and shires due to higher temperature (Fig. 3.3F). The eastern slopes and southern plains had fewer heat events due to the relatively lower temperature during the wheat-growing season. Spatially, the number of heat days occurred gradually more from south to north and from east to west, which was opposite to the occurrence of frost days (Fig. 3.4).

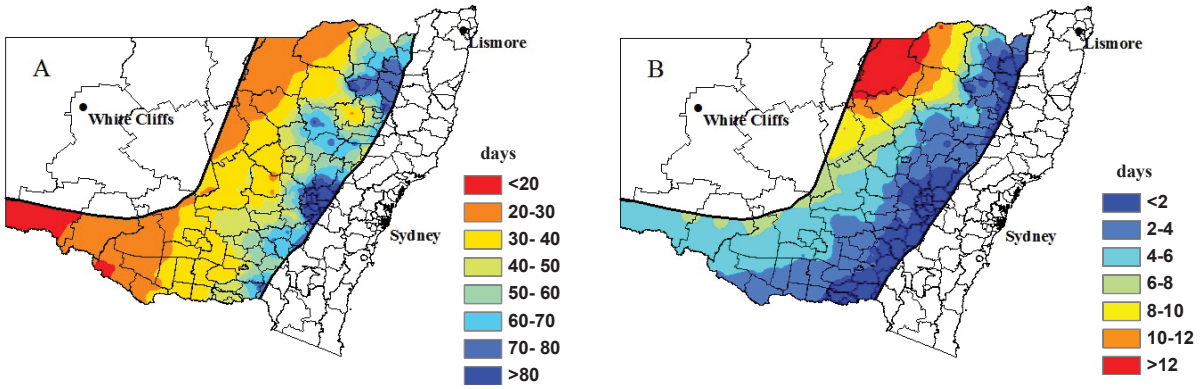

Fig. 3.4 Spatial distributions of the number of frost days (<2 °C) (A) and heat stress days (>34 °C) (B) during wheat growing season over the NSW wheat belt during 1922-2000.

Observed wheat yields at all four regions varied greatly from year to year (Fig. 3.5). Wheat yields had the largest variability in the southern plains, ranging from 0.20 to 3.12 t ha^{-1} with a mean of 1.39±0.66 t ha^{-1}. In the eastern slopes, yields varied from 0.44 to 3.32 t ha^{-1} with a mean of 1.39±0.63 t ha^{-1}. The northern and southwestern plains had lower amplitudes of variations in yield, but yields in the southwestern plains had a higher mean value of 1.37±0.48 t ha^{-1}. Compared with climate variables, the yield variation among the four regions was relatively small, indicating that crop yields were not only affected by climate but also influenced by crop management.

3.3.2 Wheat yield-climate relationships

Inter-annual wheat yield (ΔY) response to climate variation is consistent across four regions (Fig. 3.6). ΔY is positively correlated to ΔR and $\Delta T_{\min}$ while negatively correlated to ΔS, ΔT_{max}, ΔF and ΔH. The correlation coefficient of the first difference of wheat yield with the first difference of rainfall was 0.55, minimum temperature was 0.24, solar radiation was -0.51, maximum temperature was -0.54, number of frost days was -0.36, and number of heat stress days was -0.37 on average in the four regions. All of these coefficients were statistically significant at level of $p<0.05$. These results suggest that higher rainfall and minimum temperature resulted in higher yield, while

higher maximum temperature and solar radiation could lead to lower yield in rain-fed conditions, frost and heat stress had negative effects on wheat yield across the whole wheat belt.

Table 3.2 shows the correlation coefficients of six climate variables ΔR, ΔS, ΔT_{max}, $\Delta T_{\min}$, ΔF, and ΔH at each region. Rainfall was positively correlated to minimum temperature but negatively correlated to maximum temperature and solar radiation, number of frost days, and number of heat stress days. For the four regions together, the correlation coefficient of the first difference of rainfall with the first difference of solar radiation, maximum temperature, minimum temperature, number of frost days and number of heat stress days was -0.76, -0.65, 0.51, -0.58 and -0.51, respectively. All of these relationships were statistically significant at the level of $p<0.01$. Drought years in the wheat belt tended to be less cloudy with higher solar radiation and maximum temperature, but had lower minimum temperature. Higher solar radiation days were always accompanied by lower rainfall over the NSW wheat belt which explains why higher solar radiation could result in lower yield.

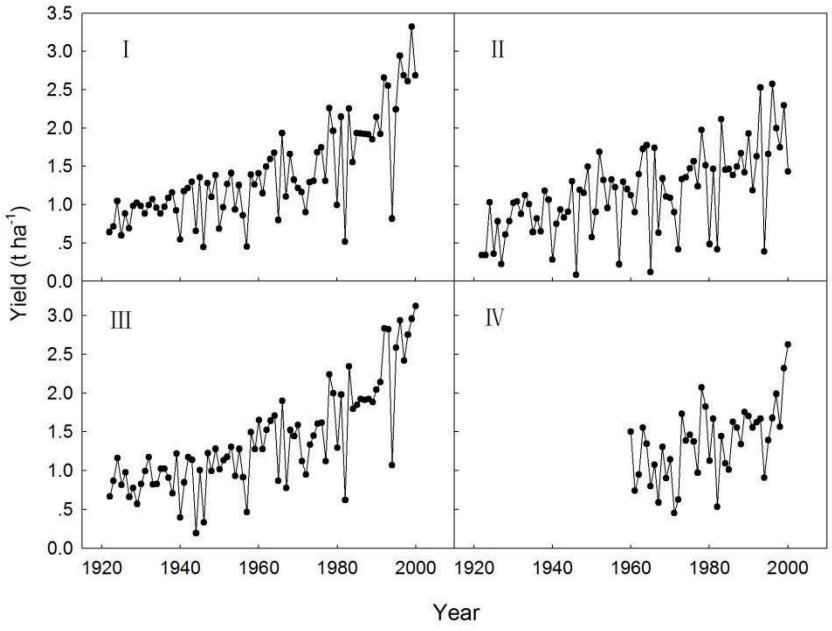

Fig. 3.5 Averaged wheat yields in four regions during the period of 1922-2000. Prior to 1960 statistical data for region IV (three shires) were not included.

Table 3.2 Pearson correlation matrix of different climate variables in four regions. All the variables used are still highly correlated with each other despite using the difference method.

	ΔR (mm)	ΔS (MJ m^{-2})	ΔT_{max} (°C)	ΔT_{min} (°C)	ΔF (days)	ΔH (days)
Region I						
ΔR (mm)	1	-0.75**	-0.63**	0.57**	-0.67**	-0.50**
ΔS (MJ m^{-2})	-	1	0.68**	-0.54**	0.59**	0.58**
ΔT_{max} (°C)	-	-	1	-0.02	0.27**	0.63**
ΔT_{min} (°C)	-	-	-	1	-0.86**	-0.17**
ΔF (days)	-	-	-	-	1	0.27**
ΔH (days)	-	-	-	-	-	1
Region II						
ΔR (mm)	1	-0.80**	-0.63**	0.52**	-0.62**	-0.55**
ΔS (MJ m^{-2})	-	1	0.71**	-0.46**	0.53**	0.60**
ΔT_{max} (°C)	-	-	1	0.11**	0.20**	0.71**
ΔT_{min} (°C)	-	-	-	1	-0.80**	-0.03
ΔF (days)	-	-	-	-	1	0.17**
ΔH (days)	-	-	-	-	-	1
Region III						
ΔR (mm)	1	-0.74**	-0.72**	0.49**	-0.62**	-0.56**
ΔS (MJ m^{-2})	-	1	0.75**	-0.41**	0.47**	0.57**
ΔT_{max} (°C)	-	-	1	0.00	0.31**	0.63**
ΔT_{min} (°C)	-	-	-	1	-0.80**	-0.14**
ΔF (days)	-	-	-	-	1	0.31**
ΔH (days)	-	-	-	-	-	1
Region IV						
ΔR (mm)	1	-0.75**	-0.62**	0.44**	-0.40**	-0.43**
ΔS (MJ m^{-2})	-	1	0.82**	-0.16	0.19*	0.49**
ΔT_{max} (°C)	-	-	1	0.19*	0.05	0.52**
ΔT_{min} (°C)	-	-	-	1	-0.76**	-0.08
ΔF (days)	-	-	-	-	1	0.17
ΔH (days)	-	-	-	-	-	1

**significant at $p<0.01$; *significant at $p<0.05$.

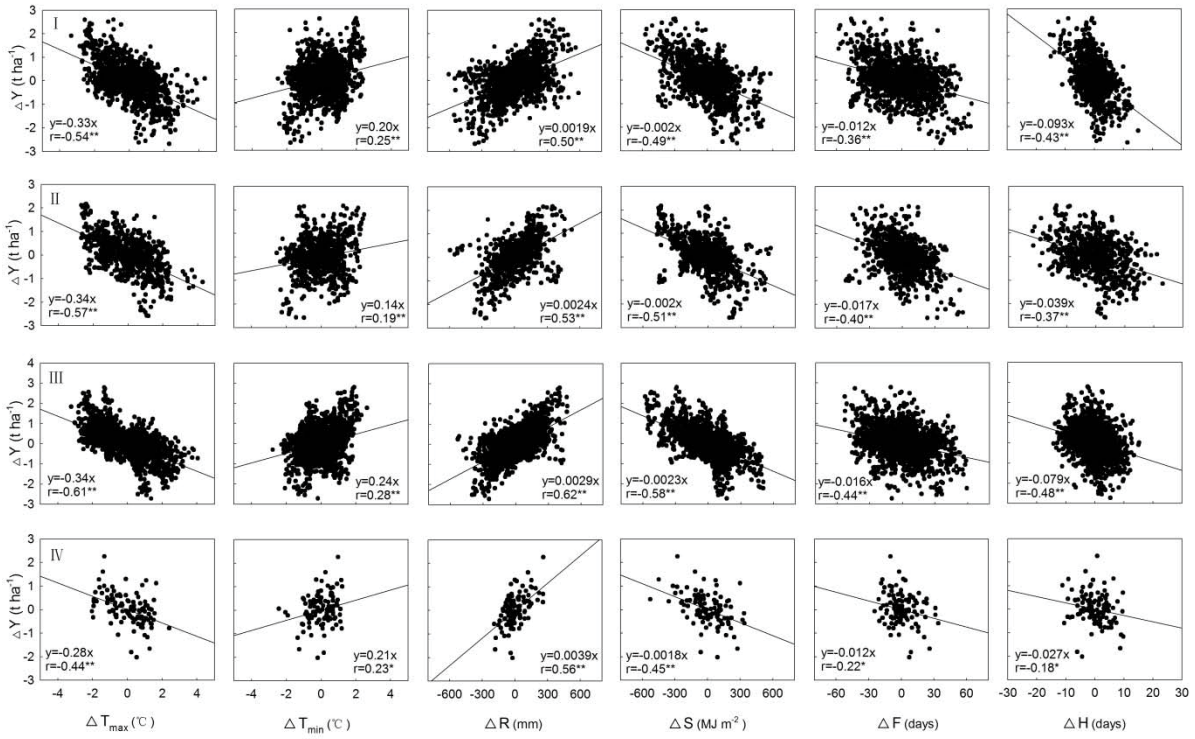

Fig. 3.6 Correlation of first difference of wheat yield (ΔY) and first difference of growing season maximum (ΔT_{max}), minimum temperature ($\Delta T_{\min}$), rainfall (ΔR), solar radiation (ΔS) and number of frost (<2 °C) (ΔF) and heat stress days (>34 °C) (ΔH) in four regions. Best-fit regression line and correlation coefficients r are shown. **significant at p<0.01; *significant at p<0.05.

Table 3.3 shows the regression analysis for wheat yields and climate factors. In the eastern slopes of the NSW wheat belt, wheat yield variation was primarily dominated by growing season minimum temperature, maximum temperature, and number of heat stress days which contributed to 36% of wheat yield variation. In the northern plains, wheat yield variation significantly correlated with growing season maximum temperature, number of frost days, and pre-growing season rainfall (December to April). These climate variables could explain 41% of yield variation. In the southern plains, the major climate factors determining yield were growing season rainfall, maximum and minimum temperature, and number of frost and heat stress days. These factors contributed to 47% variation in wheat yield. However, as the main factor, rainfall caused 31% of wheat yield variability in the southwestern plains. When the effects of variations in climate factors on wheat yield were considered in the whole NSW wheat belt, the year-to-year variability in yield was dominated by growing season rainfall, maximum temperature, minimum temperature, and number of frost days, which accounted for 41% of yield variation over the past few decades.

3.3.3 Effects of climate trend on wheat yield

Table 3.4 shows the trends in major climatic drivers and their effects on yield increase. The estimated yield change was calculated as the percentage of climate-trend yield change accounting for observed yield increase from 1922 to 2000 according to the regression model in Table 3.3. In the eastern slopes, growing season maximum temperature showed a small decreasing trend by 0.0080 °C yr^{-1} ($p<0.05$) during 1922-2000. Minimum temperature significantly increased by 0.011 °C yr^{-1} ($p<0.01$) and number of heat stress days decreased but not significantly. These three major climatic drivers resulted in 14.8% yield increase. In the northern plains, growing season maximum temperature decreased by 0.0064 °C yr^{-1} ($p>0.05$), pre-growing season rainfall increased by 0.88 mm yr^{-1} ($p>0.05$) and the number of frost days decreased significantly by 0.16 days yr^{-1} ($p<0.01$), which could explain yield increase of 21.2%. In the southern plains, decreasing maximum temperature (-0.0078 °C yr^{-1}, $p<0.05$) and other climatic drivers changed but not significantly led to 8.5% yield increase. However, growing season rainfall increased by 0.59 mm yr^{-1} ($p>0.05$) accounting for a yield increase of 9.3% (2.3 kg ha^{-1} yr^{-1}) in the southwestern plains. For the four regions together, recent climatic trends had a positive effect on wheat yield increased by 8.5-21.2% over the last few decades.

3.4 Discussion

In this study, the year-to-year first-difference method was used for de-trending wheat yield to remove technology effects. This method is easier to calculate compared with other de-trending methods such as robust regression technique (Finger 2010, Newlands et al. 2014), which is superior in handling data with outliers. A stepwise regression model was applied to identify significant or major climate variables ($p<0.01$) affecting wheat yield variation in four contrasting climatic regions across the NSW wheat belt. However, this method does not explicitly address predictor collinearity in the regression model. When multicollinearity exists it will affect the regression coefficient estimates, but it does not affect the ability to obtain a good fit of regression (higher R^2) and the quality of forecasts or predictions from the regression (Dielman 2001). Namely, multicollinearity does not reduce the predictive power or reliability of the model as a whole. Hence, if the regression model is used strictly for forecasting or for an overall estimation of climate effects as in our study, the multicollinearity may not be problematic, but if the contribution of individual variables is estimated it should be cautiously applied in interpreting results.

Table 3.3 The regression coefficients of stepwise regression analysis ($p<0.01$) between first difference of wheat yield (ΔY) and climatic variables including growing season temperature (ΔT_{max}, ΔT_{min}), rainfall (ΔR), solar radiation (ΔS), number of frost (<2 °C, ΔF) and heat stress days (>34 °C, ΔH) and pre-growing season (December to April) rainfall (ΔR_{pre}) in each region I, II, III, IV and the whole NSW wheat belt during the period 1922-2000. The 99% confidence intervals (lower limit and upper limit) are shown in brackets.

Climate drivers	I	II	III	IV	NSW
ΔR (10^{-3} mm)	-	-	0.70 (0.35/1.1)	3.9 (2.4/5.3)	0.45 (0.22/0.70)
ΔS (MJ m^{-2})	-	-	-	-	-
ΔT_{max} (°C)	-0.29 (-0.34/-0.25)	-0.29 (-0.34/-0.25)	-0.23 (-0.27/-0.19)	-	-0.28 (-0.31/-0.25)
ΔT_{min} (°C)	0.18 (0.14/0.22)	-	0.099 (0.03/0.17)	-	0.099 (0.049/0.15)
ΔR_{pre} (10^{-3} mm)	-	0.40 (0.02/0.77)	-	-	-
ΔF (10^{-2} days)	-	-1.3 (-1.6/-0.96)	-0.35 (-0.62/-0.07)	-	-0.37 (-0.58/-0.15)
ΔH (10^{-2} days)	-1.9 (-3.4/-0.35)	-	-1.5 (-2.3/-0.68)	-	-
R^2	0.36	0.41	0.47	0.31	0.41

Table 3.4 Trends in observed wheat-growing season climatic drivers and their estimated impacts on yield change (%) according to the regression model in Table 3.3 at four regions across the NSW wheat belt during 1922-2000.

Climate drivers	I	II	III	IV
ΔT_{max} (°C yr^{-1})	-0.0080*	-0.0064	-0.0078*	-
ΔT_{min} (°C yr^{-1})	0.011**	-	0.0015	-
ΔR (mm yr^{-1})	-	-	0.72	0.59
ΔR_{pre} (mm yr^{-1})	-	0.88		
ΔF (days yr^{-1})	-	-0.16**	0.086	-
ΔH (days yr^{-1})	-0.0002	-	-0.012	-
Estimated yield change	14.8%	21.2%	8.5%	9.3%

**trends are significant with p<0.01; *trends are significant with p<0.05.

Inter-annual variability of crop yields is well known to depend on climate factors (Chen et al. 2004). The results presented here show that wheat yields in the NSW wheat belt were positively correlated to growing season rainfall and minimum temperature but negatively correlated to maximum temperature, which is consistent with a previous study conducted for wheat in Australia (Yu et al. 2014). However, Lobell et al. (2005) showed that growing season minimum temperature was the major factor to contribute to yield increase and had a negative effect on wheat yield variation for irrigated systems in Mexico, which was different from our results in rain-fed environments. In southern Mali cotton production was particularly affected by rainfall distribution (Traore et al. 2013). Zhang et al. (2010) found that irrigation water availability in different regions played a key role in determining a switch of dominant climatic drivers (solar radiation or rainfall) to affect rice yields variation in China. In the eastern Australian wheat belt, which is located in a semiarid region with the climate becoming warmer from south to north and drier from east to west, seasonal rainfall was the major direct factor that affects crop sowing date, water supply and consequently yields. If only

considering a single climatic factor, about 31% of yields variability can be attributed to rainfall variation during the wheat-growing season (May to November) across the wheat belt (Fig. 3.6), which is consistent with previous studies (Cornish 1950, Seif & Pederson 1978, Stephens et al. 1994).

It should be noted that there are interactive impacts of rainfall, temperature and solar radiation on yield variation (Gifford et al. 1998). For example, growing season solar radiation had a negative effect on wheat yield variation due to strong negative correlation between rainfall and radiation in the present study (Table 3.2). Here I assumed that solar radiation effects on yield can be attributed to rainfall variation, suggesting an indirect rainfall impact on variability in wheat yields, which was different to temperature as a proxy of radiation and rainfall effects on rice yields in China (Zhang et al. 2010).

Water stress caused by low rainfall and high evaporative demands is the major limitation on wheat yield in many parts of the wheat belt (except the eastern slopes) (French & Schultz 1984b, Turner & Asseng 2005, Ludwig & Asseng 2006). It should be noted that in region I and II, the growing season rainfall (ΔR) was not selected into the multi-linear equations (Table 3.3). However, this doesn't mean that rainfall had no significant impacts on the year-to-year wheat yield variations (see the high correlation with rainfall in Fig. 3.6). Rainfall was not identified as a significant factor to affect wheat yield variation probably because the impacts of rainfall were almost accounted for by the maximum temperature due to the coherence between them, i.e. maximum temperature was negatively related to rainfall in a highly significant level ($P<0.01$, Table 3.2). Moreover, in the eastern slopes, the wheat-growing season received over 400 mm of rainfall, which roughly meets the wheat water demand from May to November for most of years. Therefore, yields were less correlated to rainfall, and growing season rainfall was not selected as major climate factor to limit wheat yield in this region. Compared with the eastern slopes, there were more drought impacts in the other three regions because of lower rainfall during most growing seasons (Fig. 3.7). It is worthwhile to note that the non-growing season rainfall can contribute to stored soil water at the end of summer in the northern plains, which can be used for water uptake of the crop (Angus et al. 1980). In such cases, pre-growing season rainfall can be an important factor on wheat yield variability, and wheat growth appears to be less relying on growing season rainfall. This is similar to southern Queensland where wheat is predominantly grown on stored water in fine-textured soils with high water-holding capacity (Angus et al. 1980). Most of the water transpired is from the store accumulated in the preceding summer, when rainfall ranges between 300 and 400 mm (December to April). Therefore, the contribution of rainfall to yield variation shifts from winter dominated in the southern plains to summer dominated in the northern plains across the NSW wheat belt.

In addition to rainfall, other climate factors such as maximum and minimum temperature also had significant impacts on wheat yields variation in eastern Australia. In particular, extreme weather events such as frost and heat stress can have a large impact on yield variation (Asseng et al. 2011). For dry land wheat in Australia, the damage from early spring frost is a major constraint to yields (Marcellos & Single 1975, McDonald et al. 1983). High temperatures can increase the rate of grain filling and above 30 ^{o}C can result in an acceleration of leaf senescence, which leads to a reduction in yield (Lobell et al. 2012). An earlier study showed that the optimum sowing and flowering dates were determined by the incidence of early spring frosts and high spring temperatures in the NSW wheat belt (McDonald et al. 1983). Although farmers select cultivars for a targeted flowering window, such selection is often based on an average with limited success (Liu et al. 2010a). The results presented here show that frost was less important in the eastern slopes but more important in the northern parts of the NSW wheat belt. This can be at least partially attributed to the fact that most farmers in the eastern slopes manage frost occurrence well by sowing late and using late flowering cultivars to minimize frost risk. However, this also can increase heat stress risk due to delaying the flowering date. Fortunately, the occurrence of heat stress in the eastern region is less frequent than other regions; hence, farmers can extend the wheat flowering dates far later than in other regions. In regions with a high frequent occurrence of heat stress, such as the northern plains, farmers have to sow earlier and plant short-season cultivars to avoid heat stress. In turn, this increases the frost risk at anthesis. In Australia, wheat yields can be severely damaged by frost and heat stress when occurring during flowering (Godden et al. 1998, Asseng et al. 2011). Farmers in Australia have traditionally been concerned about frost and heat risks but it is often hard to manage them well in extreme cases. One of these extreme cases is late frost. For example, NSW wheat was badly damaged in 2002 when frost occurred in late October (28 October). The year-to-year mean growing season temperature variation can be about 2 to 3 ^{o}C. For example, in 2013, the winter temperature was about 2 ^{o}C higher than the long-term average, but frost still occurred (http://www.bom.gov.au/climate/). Wheat yields were badly damaged in many areas as the higher temperature accelerated crop growth development with early flowering and widespread frost damage.

Several reports have shown that the recent climate trend has had significant impacts on crop yields (Tao et al. 2008, Lobell et al. 2011, Traore et al. 2013). Nicholls (1997) concluded that 30-50% of the observed yield increase was due to an increase in minimum temperature and decrease in the diurnal temperature range resulting in less frost damage in Australia. This contribution of climatic trends to Australian wheat yield increase was considered to be overestimated and attracted serious criticism (Gifford et al. 1998, Godden et al. 1998, Anderson et al. 2005). The correlation of yield variation with minimum temperature was not significant at 5%, and the equation showed, contrarily,

that rainfall had a negative effect on wheat yield variation. Mean annual minimum temperature had a larger contribution to yield increase only because it increased mostly since 1952 to 1992 (by 1.02 °C) in Nicholls's study. The results from stepwise regression described here demonstrate that 8.5-21.2% of the observed wheat yield increase over the last 78 years in the NSW wheat belt was due to climatic trends. Unlike the relative short period of data used by Nicholls (1997), I used nearly twice the length of shire data and calculated climate variables during the wheat-growing season. In addition I applied stepwise regression analysis to select significant climate variables in the regression model. Each leading variable in the multiple regression equation had a significant level ($p \leq 0.01$). The climate trends contribution estimated by this method was less than that of Nicholls (1997). It is certain that management changes over time, meaning that new cultivars, the development of new land with different soil characteristics, and changes in land use all affected yield increases across the NSW wheat belt during the past decades.

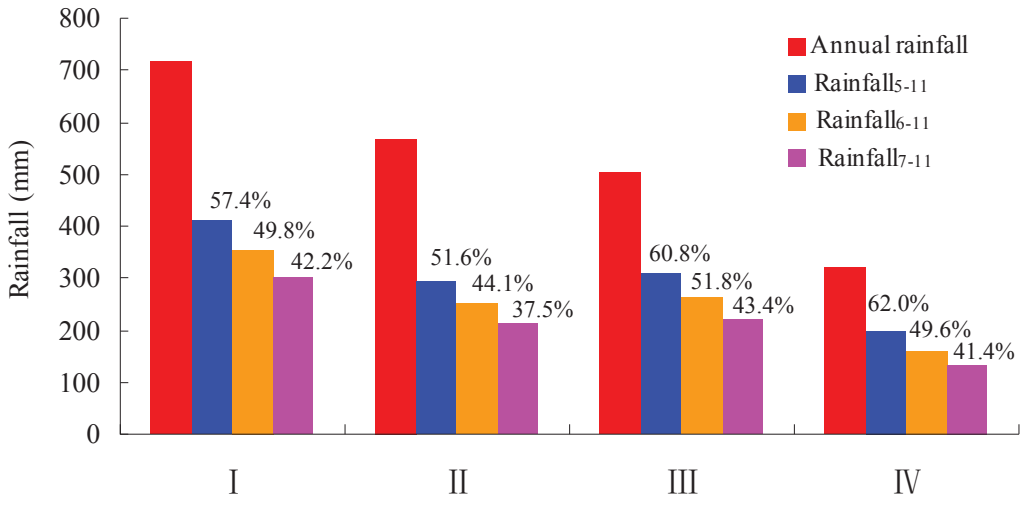

Fig. 3.7 Seasonal and annual rainfall for four regions in the NSW wheat-belt. May-November, June-November and July-November rainfall as possible growing season rainfall were calculated as wheat sowing date varies depending on time of initial rainfall at start of the season. The values above the bar are the percentages that seasonal rainfall accounts for annual rainfall.

These results show that the yield variation in the NSW wheat belt was mainly affected by variability of growing season rainfall and temperature while solar radiation was not a major climate driver (Table 3.3). Climate change scenarios suggest that eastern Australia is likely to become warmer and drier in the future (Pearce et al. 2007). Although the positive effect of higher CO_2 concentration is likely to benefit rain-fed crop production by improving water-use efficiency (KIM et al. 2003, Asseng

et al. 2004, Ludwig & Asseng 2006), this effect may not be sufficient to outweigh the negative effect of increasing temperature and decreasing rainfall (Piao et al. 2010). Farmers in NSW can adapt to rainfall variability. For example, they often will not sow a wheat crop in drought years with late starts of the growing season or only sow in some areas with sufficient stored soil water. Wheat phenology is expected to accelerate with global warming in the future resulting in a shorter growing period. Later maturing cultivars could be used to mitigate the shortening of the phenology and enable to capture enough solar radiation for biomass accumulation (Zheng et al. 2012). To some extent earlier maturing cultivars can avoid severe terminal drought, but the risk of heat stress around flowering will still increase due to higher temperature, potentially resulting in substantial yield losses for heat sensitive cultivars in the future (Semenov & Shewry 2011). Therefore, new wheat cultivars with improved water-use efficiency and heat resistance will be needed to better adapt to reduced water availability and increased heat stress. Breeding for such traits is particularly important if the projections of rainfall reductions are realized and the frequency of high-temperature days will further increase in the future (Asseng & Pannell 2012).

3.5 Conclusions

In the eastern Australia wheat belt, wheat yields were positively correlated to growing season rainfall and minimum temperature while negatively correlated to maximum temperature at a significant level ($p<0.05$). Recent climatic trends have contributed 8.5-21.2% to the observed wheat yield increase in different climatically regions. Rainfall is usually the main direct climatic driver affecting wheat yields variation in the NSW wheat belt, but it also indirectly affects temperature and solar radiation.

In the eastern slopes, growing season temperatures and number of heat stress days were major factors affecting yield variation. In the northern parts of the wheat belt, major climatic drivers for yield variation were growing season maximum temperature and pre-growing season (December to April) rainfall and number of frost days. In the southern region, growing season rainfall, temperatures, number of frost and heat stress days had major contribution to yield variation. In the southwestern plains, growing season rainfall was the main direct climate factor to determine yield variation. Understanding these effects of climate variations on crop yield is important for developing sustainable agricultural production to adapt to future climate change.

Chapter 4*

Multi-model ensemble projections of future extreme temperature change using a statistical downscaling method

Abstract

Projections of changes in temperature extremes are critical to assess the potential impacts of climate change on agricultural and ecological systems. Statistical downscaling can be used to efficiently downscale output from a large number of general circulation models (GCMs) to a fine temporal and spatial scale, providing the opportunity for future projections of extreme temperature events. This chapter presents an analysis of extreme temperature data downscaled from 7 GCMs selected from the Coupled Model Intercomparison Project phase 5 (CMIP5) using a skill score based on spatial patterns of climatological means of daily maximum and minimum temperature. Data for scenarios RCP4.5 and RCP8.5 for the New South Wales (NSW) wheat belt, south eastern Australia, have been analysed. The results show that downscaled data from most of the GCMs reproduces the correct sign of recent trends in all the extreme temperature indices (except the index for cold days) for 1961-2000. An independence weighted mean method was used to calculate uncertainty estimates, which shows that multi-model ensemble projections produce a consistent trend compared to the observations in most extreme indices. Large warming occurs in the east and northeast of the NSW wheat belt by 2061-2100 and increases the risk of exposure to hot days around wheat flowering date, which might result in farmers needing to reconsider wheat cultivars suited to maintain yield. This analysis provides a first overview of projected changes in climate extremes from an ensemble of 7 CMIP5 GCM models with statistical downscaling data in the NSW wheat belt.

Keywords: Warm indices; Cold indices; GCMs; Observations; Independence weighted mean; Australia

4.1 Introduction

Anthropogenic contributions have already significantly influenced global and regional climate (Stott et al. 2004, Sillmann & Roeckner 2008, Lewis & Karoly 2013). It is estimated that the global mean surface temperature has risen by 0.85 ˚C during the last century (IPCC, 2013) and Australia's climate has warmed by 0.9 °C since 1910 (State of the Climate 2014, http://www.bom.gov.au/state-of-the-climate/). Shifts in the mean of climatic distributions can result in very large percentage changes in the frequency of extremes such as heatwaves, which could have a critical impact on human society (Fischer & Schär 2010), natural ecosystems (Welbergen et al. 2008)

*: This chapter has been accepted for publication in Climatic Change, 2016.

and agricultural crops (Asseng et al. 2011, Zheng et al. 2012).

In recent years, a number of studies have attempted to identify observed changes in extreme temperature events across the globe (Alexander et al. 2006, Perkins et al. 2012, Donat et al. 2013) as well as in Australia (Alexander & Arblaster 2009). These have shown statistically significant increases in occurrences of hot days and warm nights and decreases in occurrences of cool days and cold nights over the past few decades. Changes in extreme temperatures have the potential to impact crop growth and development, such as accelerating phenological development and leaf senescence, as well as grain yield. Extreme heat events around flowering and grain filling periods and untimely frost in spring cause serious damage to wheat production in Mediterranean climates like that of eastern Australia (Zheng et al. 2015). For example, heat stress during the reproductive phase can lead to reductions in wheat grain production of up to 50% (Asseng et al. 2011). The greatest yield losses (about 50%) can be found when heavy frosts occur in early October (Boer et al. 1993).

Future changes in extreme temperature have been projected by different general circulation models (GCMs) (Tebaldi et al. 2006, Sillmann & Roeckner 2008). However, GCM output data are at spatial resolutions of hundreds of kilometres, and so are often too coarse to be used directly in regional scale analysis or resolve small-scale climate processes. This mismatch is a major obstacle for assessing the site-specific impacts of climate change on agricultural systems (Zhang 2005, Macadam et al. 2014). Three methods have been used to overcome this obstacle. First, *scaling* is a relatively straightforward procedure whereby the changes in future climate projected by GCMs, relative to a baseline period, are applied to observed data for the same baseline period. Often, this method does not account for any changes in climate variability (Prudhomme et al. 2002, Diaz-Nieto & Wilby 2005). Dynamical downscaling is used to achieve higher spatial resolutions by nesting regional climate models (RCMs) within GCM output fields. However, RCMs are computationally expensive and running RCM simulations for a region of interest for which suitable RCM output does not already exist can be a significant investment of resources (Fowler et al. 2007). Alternatively, statistical downscaling (Liu & Zuo 2012) applies statistical transfer functions to GCM output to estimate daily point-scale meteorological series. This method is easily transferable to different regions and provides site-specific estimations under a range of greenhouse gas emission scenarios so long as reliable observations of the climate variable of interest are available (Tolika et al. 2008, Ahmed et al. 2013, Jeong et al. 2013a, b). However, statistical downscaling method relies on empirical relationships between observational data and data from GCM simulations.

GCMs are a standard tool for deriving projections for future climate change. However, the real climate system is highly complex and it is impossible to adequately describe its processes with an

individual climate model. Authors of model evaluation studies have stated that no single model can be considered 'best' and recommend using results from a range of models (Tebaldi & Knutti 2007). There are different ways to combine results from multiple GCMs, such as Bayesian methods or weighting (Robertson et al. 2004, Tebaldi et al. 2005, Yang et al. 2012). Weighted averages (Giorgi & Mearns 2002), where weights are determined by examining the historical relationship between simulations and observations, perform better than simple averages, where each model is weighted equally (i.e. multi-model mean). However, the difficulty is in quantifying model skill and deriving model weights accordingly based on model performance. Using the multi-model mean (weighted equally) is the most common and widely used approach (Knutti et al. 2010). There is some evidence that the "mean model" result, obtained by averaging over the ensemble of models, provides an overall best comparison to observations for climatological mean fields (Lambert & Boer 2001). However, the multi-model mean approach is clearly not appropriate for all types of evaluation, such as variability estimates or extremes, as multi-model mean datasets have significantly less spatial and temporal variance than datasets from individual models or from observations (Bishop & Abramowitz 2013). The use of multi-model averages to estimate climatological means works best when each model provides an independent estimate (Jeong & Kim 2009). However, modelling groups share literature, data sets, parameterisations and even sections of model code, so there are several reasons to suspect a lack of statistical independence of every climate prediction in the suite of models used (Abramowitz 2010, Bishop & Abramowitz 2013). Bishop and Abramowitz (2013) derived weights (independence weighted mean method, IWM) that explicitly account for model dependence defined using covariance of model errors, and I used this approach in this study to synthesize extreme temperature events projected from different GCMs. The optimal weights were estimated to find the linear combination of an ensemble of model simulations that minimizes mean square difference (MSD) between GCM simulated and the observations.

This study focuses on the analyses of two 40-year simulations: the first examines the time period 1961-2000 (referred to as 'present'), the second the period 2061-2100 (referred to as 'future'). The analysis examines temperature extremes in statistically downscaled GCM data and demonstrates the application of the independence weighted mean approach to extreme temperature data from 7 skill-selected GCMs, out of 28 GCMs downscaled. Rather than developing a detailed physical explanation for the changes in extreme temperature events, the purpose of this paper is to evaluate the capacity of statistically downscaled data to represent recent trends in extreme temperature events, to describe the possible magnitude of the changes in the extreme climate events in the future and to provide detailed spatial information on changes in future extreme climate events. The study area is the

NSW wheat belt in south eastern Australia, where extreme temperature events have already become a significant challenge for grain producers (Wang et al. 2015b, Zheng et al. 2015).

4.2 Materials and methods

4.2.1 Study area and observed climate data

The detailed climate and topography of this study area are described in chapter 3. The eastern part of the wheat belt consists of slopes with elevation above 500 m and the other areas are mainly plains. It is warm and dry in the northern and southwestern plains but cooler and wetter in the east.

The Australian Climate Observations Reference Network-Surface Air Temperature (ACORN-SAT) dataset contains quality-controlled daily maximum and minimum temperature data for 112 stations, (Trewin 2013). Previous studies have calculated extreme indices from these data (e.g. Alexander et al., 2006; Alexander et al., 2007; Donat et al., 2013) and in particular have used methods such as angular distance weighting to create gridded values which can be compared to GCM output (e.g. Alexander and Arblaster, 2009). However, there are only about 10 ACORN-SAT sites with temperature records of 100 years or more in the NSW wheat belt and they are not distributed evenly across the region (Trewin 2013). In this study, to maximise the number of stations used, daily temperature data for 1889-2014 were used from the 894 meteorological sites in the NSW wheat belt extracted from the SILO (Scientific Information for Land Owners) patched point dataset (PPD, http://www.longpaddock.qld.gov.au/silo/ppd/index.php) (see Fig. 4.1) (Jeffrey et al. 2001). Inhomogeneities are present in many climatic time series, for example whenever a station location is moved, a recording instrument is changed, a new method of data collection is employed, or an observer changes (Vincent 1998, Lund & Reeves 2002, Trewin 2010). These are corrected in the ACORN-SAT dataset. Temporal homogeneities in the SILO annual mean maximum and minimum temperature data for 894 sites used in this study were tested by applying a revision of the two-phase regression model in this study (Lund & Reeves 2002). This of course does not mean that these stations can be guaranteed to be free from data artefacts but we assume that if present these are random and so will be averaged out in the analysis process.

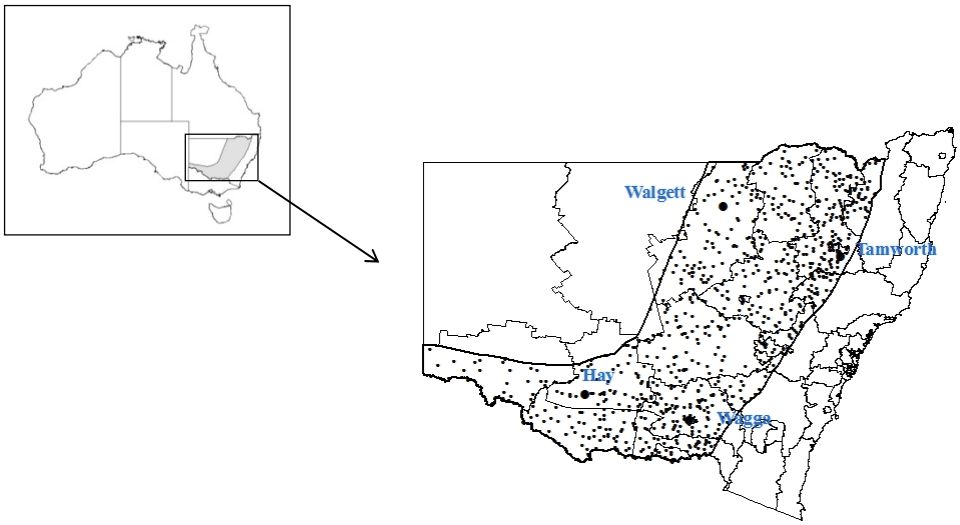

Fig. 4.1 The NSW wheat belt in south eastern Australia and location of 894 weather stations used in this study.

4.2.2 GCM selection

Data from 28 GCMs (see Table 4.1) from the Coupled Model Intercomparison Project phase 5 (CMIP5) were used. Details of these models can be found at http://cmip-pcmdi.llnl.gov/cmip5/docs/CMIP5_modeling_groups.pdf. The GCM output used consisted of monthly surface air temperature data. To identify the relatively satisfactory GCMs in simulating the climatological temperature to downscale over eastern Australia, Taylor's method was used to select GCMs after characterizing model performance from correlation and standard deviations (Taylor 2001). These two statistics were combined in a single diagram, resulting in a good visualization of model performance. This approach has been widely used and is practical for a small number of models (Sui et al. 2014, Wang et al. 2015b). Skill scores based on modified equation defined in Taylor's method were determined to consider spatial correlation and standard deviation between model simulated patterns and observations:

$$S = \frac{4(1+R)^2}{\left(\frac{\sigma_f}{\sigma_r} + \frac{\sigma_r}{\sigma_f}\right)^2 (1+R_0)^2} \tag{4.1}$$

where S is the skill score; R is the spatial correlation coefficient in climatological mean values between the simulations and observations; R_0 is the maximum correlation coefficient attainable (here we use 0.999); σ_f and σ_r are the standard deviations of the simulated and observed spatial patterns in climatological means, respectively.

Table 4.1 List of 28 GCMs under RCP4.5 and RCP8.5 future climate scenarios used in this study for statistical downscaling outputs of 894 sites over the NSW wheat belt (Liu & Zuo 2012).

Model ID	Name of GCM	Abbr. of GCM	Institute ID	Country
01	BCC-CSM1.1	BC1	BCC	China
02	BCC-CSM1.1(m)	BC2	BCC	China
03	BNU-ESM	BNU	GCESS	China
04	CanESM2	CaE	CCCMA	Canada
05*	CCSM4	CCS	NCAR	USA
06*	CESM1(BGC)	CE1	NSF-DOE-NCAR	USA
07*	CMCC-CM	CM2	CMCC	Europe
08	CMCC-CMS	CM3	CMCC	Europe
09*	CSIRO-Mk3.6.0	CSI	CSIRO-QCCCE	Australia
10*	EC-EARTH	ECE	EC-EARTH	Europe
11	FIO-ESM	FIO	FIO	China
12	GISS-E2-H-CC	GE2	NASA GISS	USA
13*	GISS-E2-R	GE3	NASA GISS	USA
14	GFDL-CM3	GF2	NOAA GFDL	USA
15	GFDL-ESM2G	GF3	NOAA GFDL	USA
16	GFDL-ESM2M	GF4	NOAA GFDL	USA
17	HadGEM2-AO	Ha5	NIMR/KMA	Korea
18	INM-CM4	INC	INM	Russia
19	IPSL-CM5A-MR	IP2	IPSL	France
20	IPSL-CM5B-LR	IP3	IPSL	France
21	MIROC5	MI2	MIROC	Japan
22	MIROC-ESM	MI3	MIROC	Japan
23	MIROC-ESM-CHEM	MI4	MIROC	Japan
24	MPI-ESM-LR	MP1	MPI-M	Germany
25	MPI-ESM-MR	MP2	MPI-M	Germany
26*	MRI-CGCM3	MR3	MRI	Japan
27	NorESM1-M	NE1	NCC	Norway
28	NorESM1-ME	NE2	NCC	Norway

*Represents the models chosen for analysis.

Equation (4.1) was applied to calculate skill scores for the 28 GCM simulations using climatological temperatures for the 50-year average of the reference period 1961-2010. Skill scores were calculated for monthly maximum and daily minimum temperatures averaged across winter (June-July-August, JJA), spring (September-October-November, SON), summer (December-January-February) and autumn (March-April-May, MAM) and the entire year (Fig. 4.2). The 7 GCMs (i.e., CCS, CE1, CM2, CSI, ECE,

GE3 and MR3) that achieved a skill score greater than 0.55 for both maximum and minimum temperatures during the different seasons and the entire year were selected for use in the subsequent analysis (Table 4.1).

4.2.3 Climate projections

Monthly mean daily maximum and daily minimum air temperature data for 1900-2100 were extracted from GCM simulations in the World Climate Research Programme's (WCRP's) Coupled Model Intercomparison Project phase 5 (CMIP5) dataset (Taylor et al. 2012). The simulations considered began in the 1800s and continued through the 21st century, with greenhouse gas emissions being consistent with a range of different Representative Concentration Pathways (RCPs) (Van Vuuren et al. 2011). In this chapter, simulations of two different RCPs, RCP4.5 and RCP8.5, are considered. They are identified by their approximate total radiative forcing in 2100 relative to 1750: 4.5 W m^{-2} for RCP4.5 and 8.5 W m^{-2} for RCP8.5. In RCP4.5, annual greenhouse gas emissions peak around 2040 and then decline. In RCP8.5, annual greenhouse gas emissions continue to increase throughout the 21st century. These two scenarios were selected because they more closely represent current conditions of radiative forcing and emissions and have more raw monthly GCMs projected temperature data for statistically downscaling. I considered radiative forcing and CO_2 emission prescribed by two Representative Concentration Pathway scenarios (RCP4.5 and RCP8.5) (Van Vuuren et al. 2011). These closely represent current conditions of radiative forcing and emissions and have more monthly GCM temperature data in the CMIP5 archive than the other RCPs. The monthly gridded data simulated by the GCMs were statistically downscaled to the meteorological observation sites using the method described by Liu and Zuo (2012). This method has been used in recent climate change impact studies (Yang et al. 2014, Anwar et al. 2015). It is capable of generating realistic time series of daily data from monthly gridded GCM. It corrects biases in the GCM data and, in contrast to dynamical downscaling, is sufficiently computationally efficient to be applied to multiple GCMs with ease. Hence the method facilitates the sampling of uncertainties in future climate changes.

The statistical downscaling method used in this study is different from many other statistical downscaling methods that need data involving atmospheric circulation or sea surface temperature as predictors. This method used GCM monthly climate data and historical observed data for the variables of interest. It can be easily applied to anywhere if a reliable daily historical climate record is available. The downscaling process consists of two parts: spatial downscaling and temporal downscaling. Spatial downscaling involves downscaling monthly GCM projections of maximum and minimum temperature from GCM grid cells to monthly values for each of the sites of interest, in this case 894 sites in the NSW wheat belt, using an inverse distance-weighted (IDW) interpolation method and then bias correction is applied by transferring the resulting monthly site data using functions obtained from

analysing observed and GCM data for a historical training period, in this case 1961-2000. Daily maximum and minimum temperature sequences for each site are then downscaled from the spatially downscaled monthly GCM projections using the WGEN stochastic weather generator.

WGEN (Richardson & Wright 1984) generates these climate variables using serial-correlation (matrix A) and cross-correlation coefficients (matrix B):

$$X_i(j) = AX_{i-1}(j) + B\epsilon_i(j) \qquad (4.2)$$

where $X_i(j)$ is a matrix including three climate variables (maximum temperature, minimum temperature and radiation) for day i. ϵ_i is a vector of independent random components. A and B are matrices that are calculated by:

$$A = M_1 M_0^{-1} \qquad (4.3)$$

$$BB^T = M_0 - M_1 M_0^{-1} M_1^T \qquad (4.4)$$

where the elements of M_0 are the correlation coefficients between these three variables on the same day and those of M_1 are the lag-1-day correlation coefficients. In the original version of WGEN, only one set of elements for matrix A and B were given and applied across the whole country of USA (Richardson and Wright 1984). The same matrix A and B were applied in other countries when WGEN was used because there were no reports on an analytic solution to matrix B in the literature. Liu and Zuo (2012) first provided a derivation of the elements of the matrix B so that the WGEN model can be applied to downscale to a site with parameters derived specifically from the site. Therefore, the parameters involved in generating daily values in Liu and Zuo (2012) are based on the site-specific relations derived from locally observed data and GCM projections so that the underlying relationships that determine the daily temperature distribution vary depending on sites and GCMs.

4.2.4 Climate extremes indices

Several measures of extreme temperatures were used, as recommended by the CCl/WCRP/JCOMM Expert Team on Climate Change Detection and Indices (ETCCDI) (http://etccdi.pacificclimate.org/indices_def.shtml). A set of 11 temperature indices was selected for this study, 8 recommended by ETCCDI and 3 that have been calculated for this study because of their impacts on wheat specifically (Table 4.2). These indices are calculated from daily maximum, minimum temperature and have been developed to assess changes in intensity, duration and frequency of extreme temperature events (Zhang et al. 2011b). Some are threshold indices defined as the number of days on which a temperature falls above or below a fixed threshold. As meteorological observed temperature data were measured by standard instruments located in a Stevenson screen at a height of

about 1.25 m above the ground (Liu et al. 2010a), the meteorological recorded temperature is generally higher than that at the ground. Thus, frost days (FD2) occur for a wheat crop when daily minimum temperatures are lower than 2 ˚C (Wang et al. 2015b). Hot days (HD) occur when daily maximum temperatures are higher than 30 ˚C. The 30 ˚C threshold was used as part of a standard climatological index that is applicable to more places across the globe than just Australia (Orlowsky & Seneviratne 2012), though we recognise that further work using thresholds demonstrated to be important for wheat growth in NSW would be valuable. Other indices are absolute indices representing maximum or minimum values within a year. These include maximum daily maximum temperature (TXx), maximum daily minimum temperature (TNx), minimum daily maximum temperature (TXn), minimum daily minimum temperature (TNn). The remainder are percentile-based indices, and include occurrence of cold nights (TN10p), occurrence of warm nights (TN90p), occurrence of cold days (TX10p) and occurrence of warm days (TX90p). They are calculated as the number of days on which temperature falls above or below the 90th or the 10th percentiles for each climate model at each site. The percentiles are calculated relative to the time of the year, centred on a 5-day window for each calendar day and using a 1961-2000 reference period (Klein Tank & Können 2003, Vincent et al. 2005, Zhang et al. 2011b). Extreme temperature range (ETR) has also been computed as the difference between TXx and TNn to provide a measure of extreme temperature variability. All of the indices were calculated as annual values.

4.2.5 Multi-model ensembles and model dependence

The idea that the performance of a forecast can be improved by averaging or combining results from multiple models is based on the fundamental assumption that errors tend to cancel if the models are independent, and thus uncertainty should decrease as the number of models increases (Tebaldi & Knutti 2007). However, the CMIP5 GCMs cannot be considered to be fully independent. Here I used a novel dependence weighted mean method to account for model dependence to calculate a multi-model mean for each extreme temperature index. Extreme temperature indices were calculated first, and then annual values of each index after secondary bias correction were used to fit the optimal weights based on 7 selected GCMs during the period 1900-2010 (7×111 data points). The independence measure technique was developed by Bishop and Abramowitz (2013) which used the covariance in model errors as the basis for a definition of model dependence. Here I briefly summarize the main points of their approach for completeness. The below is model error covariance matrix **A** derived from Bishop's method:

$$\mathbf{A} = \frac{\sum_{j=1}^{J}(\mathbf{x}^j - \mathbf{y}^j)(\mathbf{x}^j - \mathbf{y}^j)^T}{J-1} \tag{4.5}$$

where $\mathbf{x}^j = \left[x_1^j, x_{2,}^j, \ldots x_k^j, \ldots x_K^j\right]^T$; x_k^j is the extreme temperature index for the *j*th time step of *k*th GCM

model; $\mathbf{y}^j$ is the *j*th time step observed extreme temperature index; $(1, \dots, j, \dots, J)$ are time steps of annual index values and $(1, \dots, k, \dots, K)$ for GCM models. In this case, J=111 and K=7.

Next, optimal weights (**w**) are derived from the error covariance matrix (**A**) of different GCM models to minimize the mean square difference (MSD) between multi-model ensemble and the observations (see Bishop and Abramowitz (2013) for details):

$$\mathbf{w} = \frac{\mathbf{A}^{-1}\mathbf{1}}{\mathbf{1}^T\mathbf{A}^{-1}\mathbf{1}} \tag{4.6}$$

where $\mathbf{w} = [w_1, w_2, \dots, w_k, \dots, w_K]^T$, w_k is the *k*th model coefficient in the linear combination; $\mathbf{1}^T$ =[1,1,…,1].

$$\mu_e^j = \mathbf{w}^T\mathbf{x}^j = \sum_{k=1}^{K} w_k x_k^j \tag{4.7}$$

where μ_e^j is the multi-model ensemble of extreme temperature index for the *j*th time step.

4.2.6 Secondary bias correction

The Liu and Zuo (2012) downscaling procedure used in this study is somewhat effective at correcting the biases in the monthly GCM. However, the bias correction approach used in the downscaling procedure is largely limited to correcting stationary biases in the GCM output and cannot fully account for biases that are non-stationary during the training period. Therefore, the downscaled daily data for a period that might be different from the training period and may have residual biases in some cases. In order to minimise the impact of these on outputs of a biophysical model, Yang et al. (2016) applied a simple additional bias correction (delta approach) called secondary bias correction to the outputs of model simulations forced with the downscaled data. We observe the same effects in the extreme indices in our study and apply a similar solution. The extreme indices were first calculated from the statistical downscaled GCM daily data and then corrected by the secondary bias correction for each site.

$$Y_G' = Y_G - (\overline{X_G} - \overline{X_O}) \tag{4.8}$$

where Y_G' is GCM simulated value after correction, Y_G is GCM simulations for 1900-2100, $\overline{X_G}$ is GCM simulated mean value for a historical baseline period 1900-2010, $\overline{X_O}$ is the corresponding observed mean value over the same historical period.

4.2.7 Multi-model means

I investigated two different methods of calculating multi-model mean values of the indices. Indices were first calculated for individual GCMs and were then averaged together. Both the arithmetic mean (AM) and IWM were calculated and compared.

Table 4.2 Definitions of 11 extreme temperature indices used in this study. All indices are those recommended by ETCCDI (Zhang et al. 2011b), except HD, FD2 and ETR which are specifically calculated for this study as indices of relevance to agriculture.

ID	Index	Definition	Units
TXx	Warmest daily Tmax	Annual maximum value of daily maximum temperature	˚C
TNx	Warmest daily Tmin	Annual maximum value of daily minimum temperature	˚C
TXn	Coldest daily Tmax	Annual minimum value of daily maximum temperature	˚C
TNn	Coldest daily Tmin	Annual minimum value of daily minimum temperature	˚C
HD	Number of Hot days	Frequency of daily maximum temperature >30 ˚C	days
$FD2$	Number of Frost days	Frequency of daily minimum temperature <2 ˚C	days
$TX90p$	Warm days	Number of days in a year with daily maximum temperature >90th percentile	days
$TN90p$	Warm nights	Number of days in a year with daily minimum temperature >90th percentile	days
$TX10p$	Cold days	Number of days in a year with daily maximum temperature <10th percentile	days
$TN10p$	Cold nights	Number of days in a year with daily minimum temperature <10th percentile	days
ETR	Extreme temperature range	Difference between highest daily maximum and lowest daily minimum temperature during the year	˚C

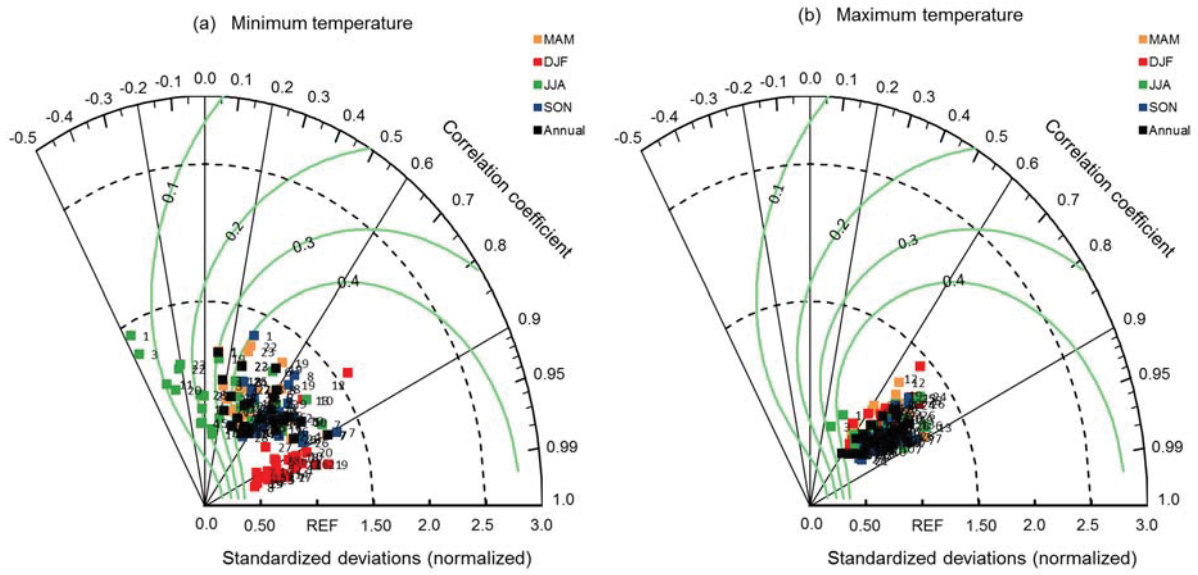

Fig. 4.2 Taylor diagram (Taylor, 2001) displaying normalized pattern statistics of climatological annual and seasonal (a) maximum temperature and (b) minimum temperature in south eastern Australia between 28 GCMs and observation for the reference period of 1961-2010. Each number represents a model ID (see Table 4.1). Orange, red, green, blue and black rectangles show simulations of MAM (March-April-May, autumn), DJF (December-January-February, summer), JJA (June-July-August, winter), SON (September-October-November, spring) and annual means, respectively. The correlation coefficient between a model and the reference is given by the azimuthal position of the model, with oblique solid lines showing different coefficient values. The radial distance from the origin is the normalized standard deviation of a model, with cambered dotted lines showing values of 1.5 and 2.5. Normalized centered root mean square difference between a model and the reference is their distance apart, with cambered solid line showing value of 1.0. The green solid lines are isolines of measure of skill as defined by equation (4.1) in (Taylor, 2001).

4.3 Results

4.3.1 Comparison between observed and downscaled extreme indices

The observed and downscaled values for each index from 1961 to 2000 averaged across the NSW wheat belt are shown in Fig. 4.3. There was an increasing trend for observed warm indices (TXx, TNx, TX90p, TN90p, HD) while there was a decreasing trend in cold extremes (TX10p, FD2) during the historical period 1961-2000. In all cases, changing trends were calculated using ordinary

least square (OLS) regression and trend significance was calculated at the 5% level using Student's T test.

Table 4.3 shows trends and significance for the observations and each GCM for the 11 indices. It is noteworthy that, of the 11 indices, only TN90p (warm nights) showed a significant increase ($p<0.05$) in the observations and 6 of the 7 models exhibited a statistically significant increase in TN90p (Table 4.3). Although, observed trends in other indices were not significant, the majority of the GCM models obtained the correct sign of trend for each extreme temperature indicator except TN10p (cold nights), when averaged across the region. At least 6 of 7 models produced trends in seven indices (TNx, TX90p, TN90p, TXn, TNn, FD2, ETR) of the same sign as the observed trends. 5 of 7 models agreed with the observations in terms of sign of trend in TX10p and 4 of 7 models displayed a consistent trend with the observations in TXx. While the sign of the extreme temperature trends in the downscaled daily data generally matched the trends for the observations, the magnitude of change varied between different GCMs and was different from the observed values. No single GCM was consistently 'best' at reproducing the observed magnitude of trends across all extreme temperature indicators and some GCMs overestimated or underestimated the observed trends in some of the temperature extremes indices during 1961-2000 (Table 4.3).

Both the observed and GCM-based extreme temperature indices show large inter-annual variability over historical period 1961-2000, especially for model GE3 (Fig. 4.3 and Table 4.3). The GE3 indicated no significant trends ($p<0.05$) in these 11 extreme temperature indices. However, the IWM and AM simulations from 7 GCMs had less variability in the baseline time series than individual models and observations due to its averaged nature, leading to a significant trend in 6 of 11 extreme temperature indices. In addition, the observed and the IWM simulations had a good consensus in the magnitude of the trend in TN90p (Table 4.3). For example, observed TN90p increased by 3.42 days per decade while IWM indicated TN90p rose by 3.24 days per decade during the period 1961-2000.

Root-mean-square error (RMSE) values were calculated for both the AM and IWM, using area-averaged values and comparing against observations. For each index, individual GCMs usually had larger RMSE values than the AM (Table 4.4). Meanwhile, the RMSE of IWM for all 11 eleven temperature indices was lower than that of AM.

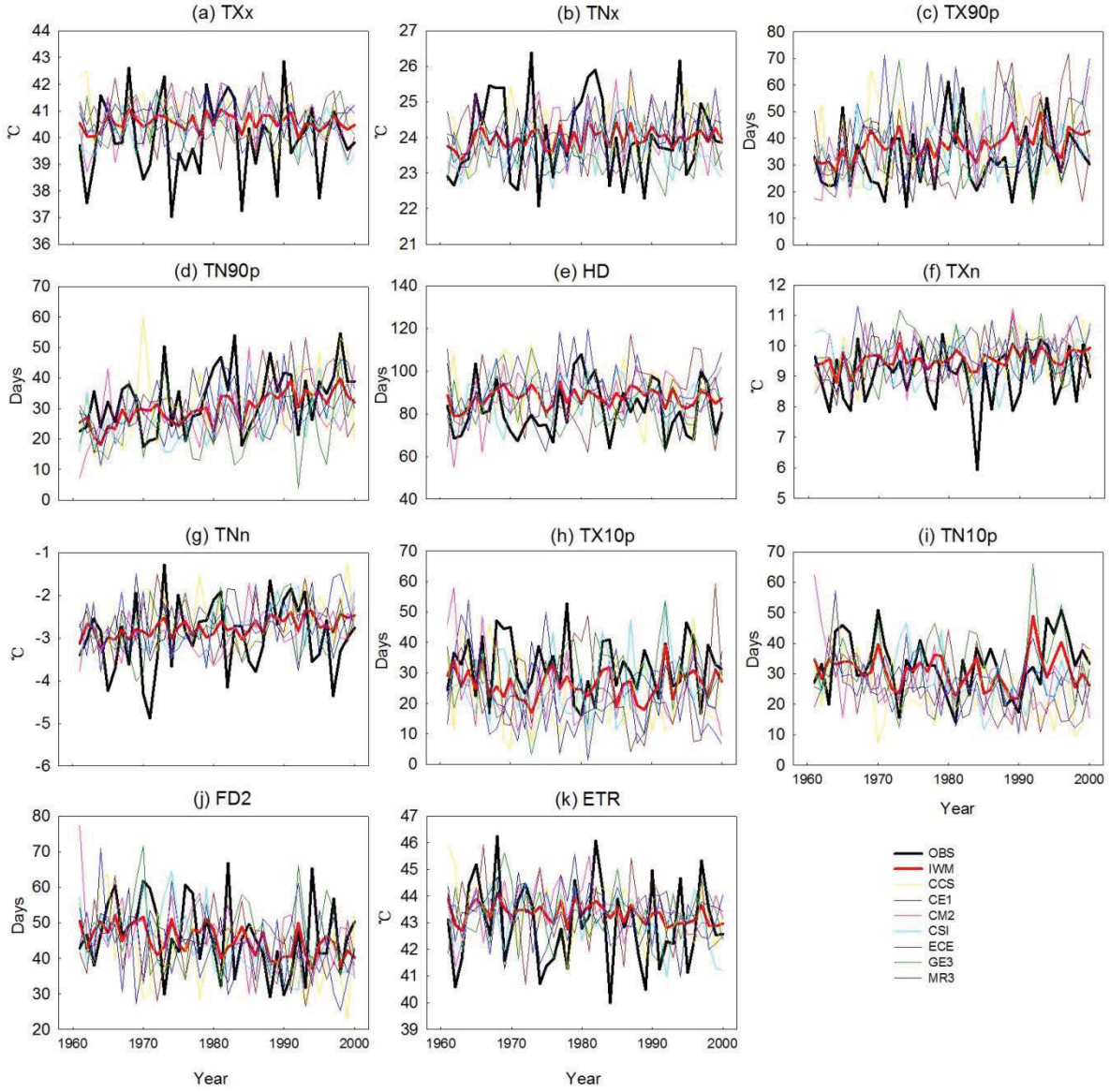

Fig. 4.3 The observed (black line) and each GCM simulated including multi-model independence weighted mean (IWM, red line) time series of extreme temperature indices from 1961 to 2000 averaged across the NSW wheat belt.

4.3.2 Multi-model ensemble projections of temperature extremes

Fig. 4.4 shows spatial changes in multi-model ensemble simulated (IWM) extreme temperature indices between 1961-2000 and 2061-2100 for RCP8.5 using inverse distance weighted (IDW) interpolation. In addition, the temporal evolution in temperature indices averaged across the NSW wheat belt from 1900 to 2100 under RCP4.5 and RCP8.5 for the IWM results is shown in Fig. 4.5.

Table 4.3 Observed and GCMs simulated trends for the 11 extreme temperature indices calculated over 1961-2000. Standard errors for trends for individual models are shown in brackets. Boldface signifies trends that are significant at 5% level. Units as Table 4.2 (per decade).

GCM	TXx	TNx	$TX90p$	$TN90p$	HD	TXn	TNn	$TX10p$	$TN10p$	$FD2$	ETR
CCS	-0.13 (±0.10)	0.07 (±0.09)	1.68 (±1.75)	**3.41** (±1.35)	-0.67 (±1.57)	0.18 (±0.09)	0.12 (±0.08)	-1.45 (±1.64)	**-2.73** (±1.24)	**-2.81** (±1.21)	-0.25 (±0.13)
CE1	0.07 (±0.09)	**0.21** (±0.08)	**3.88** (±1.83)	**3.07** (±1.02)	1.40 (±1.43)	**0.17** (±0.08)	**0.17** (±0.06)	-2.60 (±1.45)	**-2.50** (±1.09)	**-3.32** (±1.09)	-0.10 (±0.11)
CM2	0.11 (±0.11)	0.05 (±0.09)	**4.21** (±1.35)	**3.02** (±1.13)	2.56 (±1.42)	**0.21** (±0.10)	**0.17** (±0.06)	**-3.01** (±1.44)	**-3.21** (±1.16)	**-3.05** (±1.03)	-0.06 (±0.11)
CSI	-0.01 (±0.09)	0.02 (±0.09)	0.28 (±1.30)	**3.58** (±1.00)	-0.01 (±1.27)	-0.03 (±0.09)	**0.22** (±0.05)	1.64 (±1.38)	**-2.60** (±0.95)	**-4.16** (±0.97)	-0.23 (±0.12)
ECE	-0.11 (±0.12)	0.00 (±0.10)	**3.90** (±1.91)	**3.63** (±1.11)	0.83 (±1.77)	**0.19** (±0.09)	0.08 (±0.07)	-1.73 (±1.68)	-2.26 (±1.19)	**-2.27** (±1.12)	-0.20 (±0.15)
GE3	0.03 (±0.10)	-0.02 (±0.09)	1.78 (±1.68)	1.67 (±1.30)	-0.67 (±1.58)	0.04 (±0.10)	0.06 (±0.08)	1.70 (±1.46)	0.88 (±1.42)	-0.86 (±1.31)	-0.03 (±0.14)
MR3	0.01 (±0.10)	0.12 (±0.09)	0.44 (±1.48)	**1.96** (±0.86)	-0.76 (±1.58)	0.04 (±0.09)	0.04 (±0.08)	-0.15 (±1.40)	-0.28 (±0.90)	-0.77 (±1.06)	-0.03 (±0.13)
IWM	0.01 (±0.04)	0.07 (±0.04)	**2.24** (±0.58)	**3.24** (±0.46)	0.36 (±0.57)	**0.11** (±0.04)	**0.11** (±0.02)	-0.02 (±0.68)	-0.41 (±0.77)	**-2.03** (±0.49)	**-0.12** (±0.05)
AM	0.00 (±0.04)	0.06 (±0.03)	**2.91** (±0.59)	**3.01** (±0.42)	0.38 (±0.56)	**0.11** (±0.04)	**0.13** (±0.02)	-0.80 (±0.57)	**-1.81** (±0.45)	**-2.46** (±0.40)	**-0.13** (±0.04)
Obs	0.05 (±0.20)	0.01 (±0.16)	1.70 (±1.58)	**3.42** (±1.28)	0.67 (±1.68)	0.07 (±0.13)	0.10 (±0.11)	-0.42 (±1.31)	0.29 (±1.31)	-1.83 (±1.36)	-0.06 (±0.22)

4.3.2.1 Warm extremes

Fig. 4.4a-e indicates increases in the warm extremes across the NSW wheat belt between 1961-2000 and 2061-2100. The spatial changes in daily maximum Tmax (TXx) and Tmin (TNx) for RCP8.5 are presented in Fig. 4.4a and b. The increase was more pronounced in the northeast for TXx (in a range of 4.4-5.1 ˚C) and in the south for TNx (in a range of 4.3-5.2 ˚C). As demonstrated in Fig. 4.5a and b, the time series of TXx and TNx show similar features, characterized by increases and, before the year 2050, no distinguishable differences between the two scenarios. In the last 40 years of the 21st century, area-averaged TXx increases by around 2.4 ˚C for RCP4.5 and 4.1 ˚C for

RCP8.5 compared to 1961-2000. The corresponding increases for TNx are approximately 2.3 ˚C and 3.9 ˚C for RCP4.5 and RCP8.5, respectively.

Warm days (TX90p) and warm nights (TN90p) also exhibit increases across the wheat belt and the spatial patterns are presented in Fig. 4.4c and d. The most striking increase is found in the north and east for TX90p (over 120 days). In contrast to TX90p, the rise in TN90p is noteworthy in the northeast with more than 130 days. Fig. 4.5c and d show that TX90p and TN90p have consistent increases over the 21st century for both RCP4.5 and RCP8.5. At the end of the 21st century, TX90p increases dramatically by around 168.2% for RCP4.5 and 314.8% for RCP8.5 compared to the 1961-2000. TN90p increases by approximately 208.6% and 414.7% for RCP4.5 and RCP8.5, respectively.

The number of hot days (HD) increases by between about 23.0 to 72.0 days across the region (Fig. 4.4e). The increase is more significant in the northeast with a range of 62-72 days. As shown in Fig. 4.5e the temporal evolution of HD shows a consistent increase under RCP8.5, which is similar to other warm extreme indices. The increase in HD is around 34.7% for RCP4.5 and 58.9% for RCP8.5 compared to the 1961-2000 at the end of the 21st century.

Table 4.4 Root mean square error (RMSE) between the multi-model arithmetic mean (AM), independence weighted mean (IWM), each GCM and observed values for the 11 temperature indices during 1961-2000.

GCMs	TXx (˚C)	TNx (˚C)	$TX90p$ (days)	$TN90p$ (days)	HD (days)	TXn (˚C)	TNn (˚C)	$TX10p$ (days)	$TN10p$ (days)	$FD2$ (days)	ETR (˚C)
CCS	1.74	1.29	16.89	13.92	16.48	1.37	0.99	17.49	15.69	12.87	1.67
CE1	1.58	1.20	18.07	9.94	16.10	1.23	0.98	17.25	13.27	12.79	1.65
CM2	1.59	1.20	15.49	13.49	15.85	1.26	0.97	14.55	13.43	12.78	1.76
CSI	1.52	1.28	13.31	12.85	13.76	1.19	0.85	11.98	12.08	12.05	1.60
ECE	1.76	1.40	20.35	12.61	18.90	1.20	0.97	17.11	15.27	12.71	1.82
GE3	1.65	1.29	16.83	13.95	16.21	1.24	0.90	15.10	10.36	11.62	1.84
MR3	1.55	1.26	14.90	11.97	13.99	1.39	0.98	14.10	11.96	13.41	1.58
AM	1.48	1.11	12.52	10.08	12.16	1.11	0.82	11.59	10.45	9.97	1.47
IWM	1.40	1.07	12.28	9.57	11.82	1.05	0.79	10.45	8.52	9.77	1.42

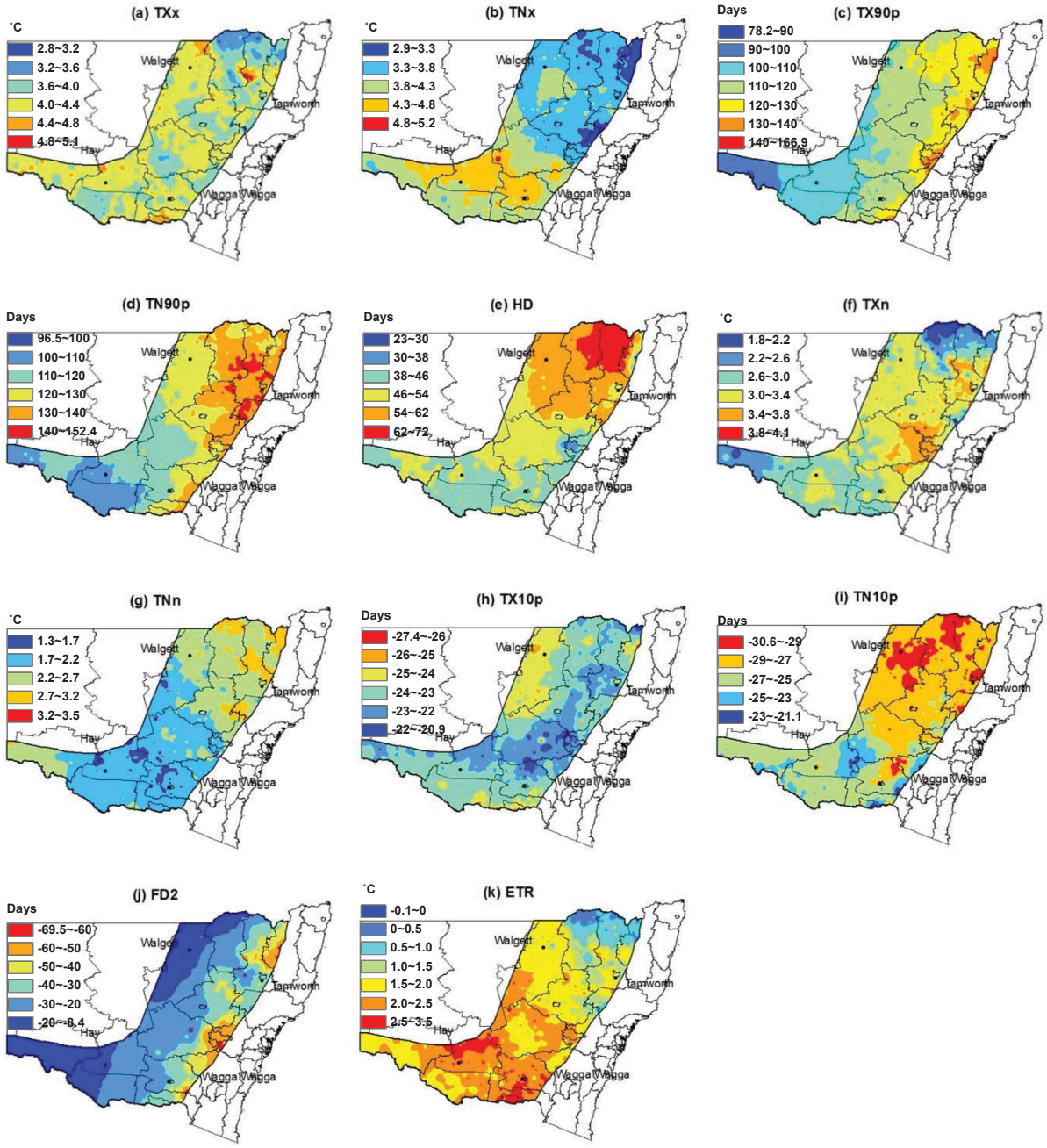

Fig. 4.4 Changes in multi-model ensemble (independence weighted mean, IWM) simulated extreme temperature indices during the period 2061-2100 compared to 1961-2000 under RCP8.5.

4.3.2.2 Cold extremes

The spatial distribution of simulated changes in the cold extremes is shown in Fig. 4.4f-j. Fig. 4.4f-g show increases across the region for daily minimum Tmax (TXn) and daily minimum Tmin

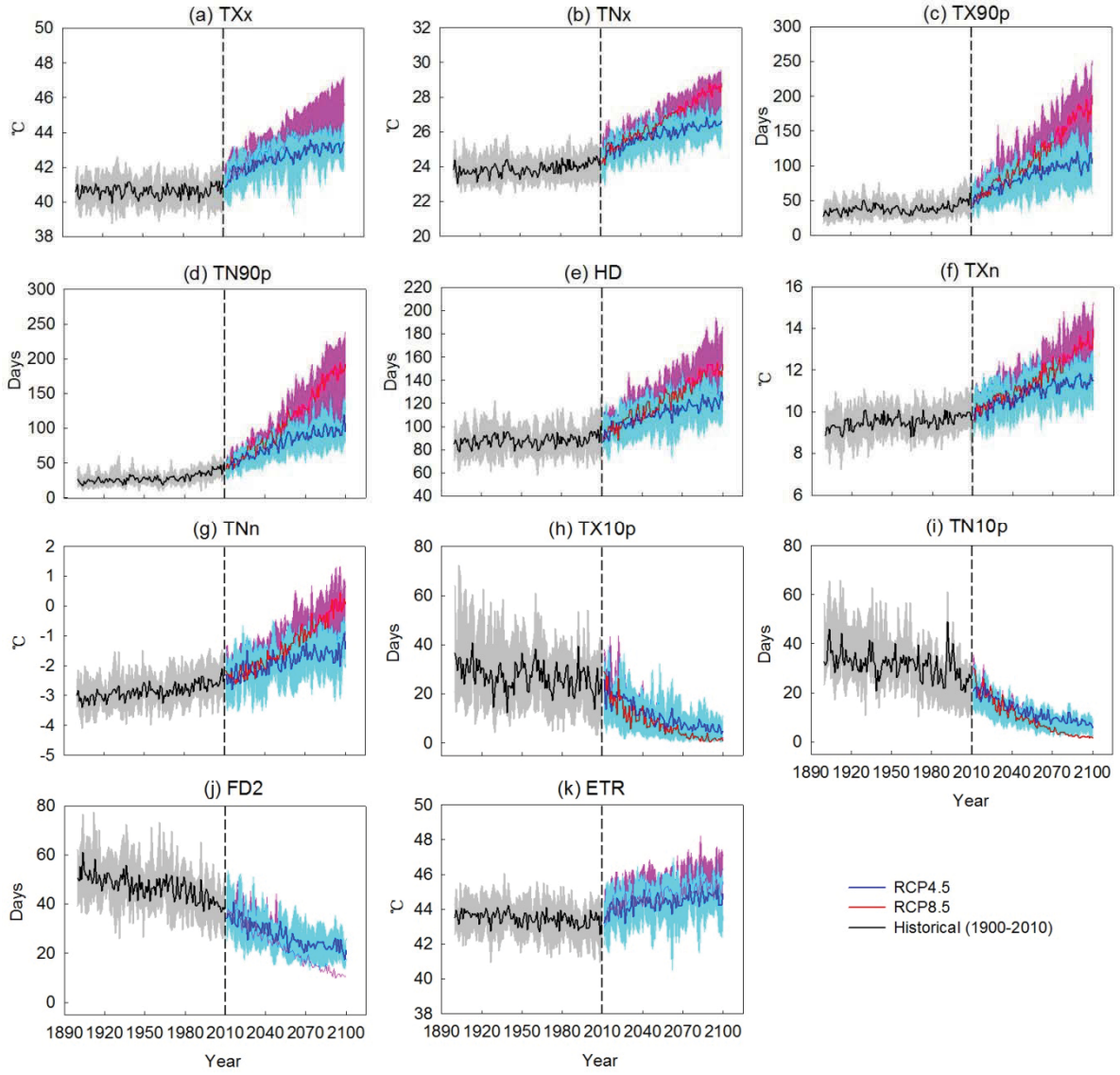

Fig. 4.5 Time series (1900-2100) of multi-model ensemble (independence weighted mean, IWM) simulated extreme temperature indices under RCP4.5 and RCP8.5 averaged across the NSW wheat belt. The top and bottom bounds of shaded area are the 90th and 10th percentile of the annual value respectively from the 7 GCMs simulations. The light blue and pink colours reflect the shading under RCP4.5 and RCP8.5, respectively.

(TNn). For TXn, these are most significant, 3.4-4.1 ˚C, in the east. For TNn, the changes are most significant, 2.7 to 3.5 ˚C, in the north. For TXn the increase in the area average is around 1.8 ˚C for RCP4.5 and 3.0 ˚C for RCP8.5 by the end of the 21st century (Fig. 4.5f). The increase in TNn is close to that in TXn, by about 1.2 ˚C for RCP4.5 and 2.2 ˚C for RCP8.5 (Fig. 4.5g). Conversely, cold

days (TX10p) and cold nights (TN10p) show a decreasing trend in the future, which is consistent with warming. Fig. 4.4h shows very large decreases in the occurrence of TX10p in the north, of 24-27.4 days. The magnitude of decreases in the area average by the end of 21st century is 73.4% for RCP4.5 and 89.7% for RCP8.5 (Fig. 4.5h). For TN10p, there is a larger decline mainly in the north, of 27-30.6 days (Fig. 4.4i). The area average of TN10p declines by 70.9% for RCP4.5 and 88.2% for RCP8.5 by the end of the 21st century (Fig. 4.5i). The results show that there are no longer any cold days and cold nights (as defined with respect to the 1961-2000 period) under high emission RCP8.5 by the end of the century.

The occurrence of frost days (FD2) generally decreases across the region (Fig. 4.4j) over the 21st century, by about 8.4 to 69.5 days. The largest decrease is in the east (50-69.5 days) and the smallest in the west (8.4-20 days). As shown in Fig. 4.5j, the area average of FD2 shows a consistent drop under the two RCPs in the 21st century, of around 48.8% for RCP4.5 and 68.0% for RCP8.5 compared to the 1961-2000 period.

4.3.2.3 Extreme temperature range

Extreme temperature range (ETR) shows an increase consistent with greater increases in daytime maxima (spatially averaged 4.1˚C in TXx Fig. 4.4a) compared to night-time minima (spatially averaged 2.2˚C in TNn, Fig. 4.4g). The largest increase is found in the south and a small increase can be seen in the north (Fig. 4.4k). The time series of area averaged ETR shows a consistent increase but with large fluctuations, and there is a small difference between results for the two scenarios in the 21st century (Fig. 4.5k). The amount of ETR increase by the end of the century is approximately 1.3 ˚C for RCP4.5 and 1.8 ˚C for RCP8.5.

4.4 Discussion

In this study, observed TN10p (cold nights) showed a non-significant increase due to large inter-annual variability. However, most GCMs projected a significant decrease in TN10p. The trends of some extreme temperature indices (e.g. TNx) in the downscaled data for some individual GCMs (e.g. model GE3) were opposite to observed values (Table 4.3). These results are possibly linked to the temporal downscaling procedure and/or unforced variability. Like many other statistical downscaling methods, this method relies on empirical relationships between observational and GCM simulated data (Liu & Zuo 2012). Although WGEN parameters derived from observations are improved in this method, extreme events may not be realistically represented in the output. Even though secondary bias correction was applied to correct multi-year averages for temperature indicators, each GCM simulated extreme climate indices still had large differences with the

observations (Fig. 4.3). Differences may be reduced by improving the WGEN parameters with fine scale outputs of dynamically downscaled results, rather than using coarse scale GCM data, in combination with historical records. Confidence in projections of future changes in climate extremes can be improved by combining extremes data from multiple models, assuming that errors tend to be cancelled if models are independent.

General findings and results in detecting changes in temperature extremes over the whole continent of Australia have been presented in recent studies (Collins et al. 2000, Alexander et al. 2007, Perkins & Alexander 2013). My results show that the significant trend in TN90p was particularly well simulated by 6 out of 7 GCMs analysed. An increase in warm nights would arise through the local impact of the enhanced greenhouse effect. The result is consistent with the results of the Alexander and Arblaster (2009) study of Australian climate extremes. However, Alexander and Arblaster (2009) focused on projections of temperature extremes across Australia to the end of the 21st century on the grid scale of the GCM, which is generally too coarse a scale to accurately estimate changes in extreme events in a specific region such as the NSW wheat belt. Moreover, that study used the arithmetic ensemble mean and consequently uncertainties due to the dependence of different GCMs remained. In contrast to previous work, this study strives to construct more spatially detailed scenarios of future climate extremes over a specific region using the IWM method.

Temperature extremes have the potential to affect wheat growth. The occurrence of extreme high temperature during sensitive stages of crop development, such as near flowering and /or during early grain filling, could reduce grain yield due to its direct effect on grain number and grain mass (Talukder et al. 2014), while a continuous period of extreme high temperature could result in large yield losses (Asseng et al. 2011, Lobell et al. 2015). Many experiments have been carried out to assess the effect of heat stress on wheat yield. For example, Nuttall et al. (2013) studied wheat growth under heat stress conditions (heat shock in the Australian dryland environment) and the results show that heat stress (37 ˚C for 3 days) imposed six days after anthesis caused a 12% reduction in grain number and a 13% reduction in grain yield. In the climate projections for the 21st century, the higher emission scenario RCP8.5 has a higher rate of increase for warm extremes and decrease for cold extremes than RCP4.5 (Fig. 4.5). Consistent with a warming trend, we find the potential for more frequent hot days, and more warm days and nights, decreases in the number of frost days, and fewer cold days and nights in the future. These results, based on standard climatological extreme indices, suggest that wheat crops may experience more severe heat stress but decreases in frost risk in the eastern part of the NSW wheat belt. Further work using indices tailored to correspond to crop physiological processes would be required to confirm and quantify the effect of this on yields and other relevant aspects of wheat production. Since the sensitivity of wheat to temperature extremes varies over the

growing season, such indices would likely include consideration of extremes in different periods within the year.

The eastern area is occupied by slopes and has broad climate variability due to larger latitudes (Wang et al. 2015a). Most farmers in this region manage frost occurrence well by sowing late and using late flowering cultivars to minimize frost risk. However, as frost days are projected to decrease in frequency and hot days are projected to increase, this will increase the risk of exposure to hot days around the flowering date. Grain growers need to choose suitable cultivars and sow in autumn or early winter, which can allow flowering to occur during the period with minimum stress of frost and heat. In addition, extreme temperature can accelerate leaf senescence (Asseng et al. 2011), which potentially leads to yield loss. Therefore, it is important to breed some cultivars capable of coping with an increased frequency and magnitude of heat stress around flowering and grain filling. Although frost days are projected to decrease in the future, it will be equally important to maintain tolerance to low temperatures when sowing earlier in the year.

Estimates of future changes in temperature extremes are essential information for stakeholders and policymakers. Although this analysis contributes to this effort, there are many uncertain factors in assessing changes in extreme indices at the regional scale. For example, the strong effects of ENSO on Australian climate, which can improve predictability on seasonal timescales can also enhance inter-annual variability, making attribution on climate time scales more difficult for GCM projections (Arblaster et al. 2014, King et al. 2014). More work on generating projections from more advanced, higher resolution GCMs with advanced multi-model ensemble methods, as well as on analysing uncertainties related to model structure and internal parameters and improving downscaling and bias correction techniques (Jeong et al. 2015a, Jeong et al. 2015b), are needed for a better understanding of future changes in extremes over the NSW wheat belt.

4.5 Conclusion

The downscaling procedure used in this study was effective at correcting the bias associated with the site-based monthly GCM values by relating observed historical climate data to that simulated by GCMs. The SILO daily time series of meteorological data at point locations were used as a basis for spatial downscaling and bias correction of 7 skill-selected CMIP5 GCMs. We evaluated the ability of the downscaled data from each of the 7 GCMs to reproduce trends in values of extreme temperature indices over eastern Australia over the period 1961-2000. In general, most GCM models captured the sign of historical observed trends in temperature extremes, but no one model was consistently good at reproducing all indices. The observed and the multi-model ensemble projections agreed well in the

magnitude of warm nights trend for the period 1961-2000 across this region. Despite less inter-annual variability in temperature extremes, the independence weighted mean method simulations had a lower RMSE with observations compared to the unweighted mean. Moreover, future projections show that more warm days (TX90p), warm nights (TN90p) and hot days (HD), less cold nights (TN10p) and frost days (FD2) will occur in the east and northeast of the NSW wheat belt in the future by 2061-2100. Exposure to extreme heat stress can severely damage crop production. Therefore, breeding for improved heat tolerance should remain a priority for the eastern Australian wheat industry.

Chapter 5*

Impact of climate change on wheat flowering time in eastern Australia

Abstract

The flowering time of wheat is strongly controlled by temperature and is potentially highly sensitive to climate change. In this study, I analysed the occurrence of last frost (days with minimum temperature under 2°C) and first heat (days with maximum temperatures exceeding 30°C) events of the year to determine the optimum flowering date in the wheat belt of New South Wales (NSW), eastern Australia. I used statistically downscaled daily maximum and minimum temperature data from 19 Global Climate Models (GCMs) with a vernalizing-photothermal model in order to simulate future flowering dates and the changes in frost and hot days occurrence at flowering date (+/- 7 days) for two future scenarios for atmospheric greenhouse gas concentrations (RCP4.5 and RCP8.5) in 2040s (2021-2060) and 2080s (2061-2100). Relative to the 1961-2000 period, the GCMs projected increased daily maximum and minimum temperatures for these future periods, accompanied by reduced frost occurrence and increased incidence of heat stress. As a consequence, by the 2080s, simulations suggest a general advance in spring wheat flowering date by, on average, 10.2 days for RCP4.5 and 17.8 days for RCP8.5 across the NSW wheat belt. Winter wheat flowering dates were delayed by an average of 2.4 days for RCP4.5 and 14.3 days for RCP8.5 in the warmest parts of the region (the northwest) due to reduced cumulative vernalization days (requiring cool conditions). In the cooler regions (the northeast, southeast and southwest), flowering date occurred earlier by 6.2 days for RCP4.5 and 6.7 days for RCP8.5 on average. Moreover, in the western parts of the wheat belt the delay of winter wheat flowering date was about 9.5 days longer than that in the eastern parts. As a result of phenological responses to increasing temperatures, current wheat cultivars may not be suitable for future climate conditions, despite reduced frost risk.

Keywords: wheat phenology, vernalizing-photothermal model, climate change, NSW wheat belt, frost days, hot days

5.1 Introduction

Global average surface temperatures have increased over the past century, and the warming trend in the last 50 years has been 0.18°C per decade. The Intergovernmental Panel on Climate Change

*: This chapter has been published in Agricultural and Forest Meteorology 209:11-21, 2015.

(IPCC) Fifth Assessment has projected that the increase in global mean temperature by 2018-2100will likely be 1.8±0.5°C for RCP4.5 and 3.7±0.7°C for RCP8.5, relative to 1986-2005. In Australia, mean temperature has been increasing by approximately 0.09°C per decade during the last century and by 0.19°C per decade for the latest 40 years (Murphy & Timbal 2008). There has been an increased intensity and frequency of hot daytime temperatures since the 1990s (Bureau of Meteorology and CSIRO, 2014; http://www.bom.gov.au/state-of-the-climate). The annual mean temperature in Australia is projected to increase up to 2.3±0.5 °C for RCP4.5 and 4.2±0.9 °C for RCP8.5 scenarios by the year 2080-2099 compared with the climate of 1980-1999, leading to more frequent hot days and less frequent cold days in the future (Irving et al. 2012).

Global climate changes are expected to have significant effects on crop growth and development (Wheeler et al. 2000, Asseng et al. 2011). Changing phenology is one of the most important crop responses to climate change (Wolkovich et al. 2012). Flowering is a critical stage of development in the life cycle of most crops; it affects the chances of pollination and other crop processes, such as leaf expansion, root growth, and nutrient uptake (Fitter & Fitter 2002), and determines seed number and ripening (Craufurd & Wheeler 2009). The timing of flowering is a complex trait affected by a range of environmental factors, such as photoperiod, ambient temperature, and vernalization (Halse & Weir 1970, Angus et al. 1981, Liu 2007, Springate & Kover 2014).

Temperature has been demonstrated as one of the most important factors for crop flowering dates. For any given cultivar, increasing temperatures accelerate phenological development, so the timing of anthesis becomes earlier (Craufurd & Wheeler 2009, Asseng et al. 2011). Earlier flowering of crops has been observed worldwide during the last few decades, although the specific response of crop phenology to recent climate change varies with location, season, and genotype (Chmielewski et al. 2004, Hu et al. 2005, Menzel et al. 2006, Tao et al. 2006, Estrella et al. 2007, Amano et al. 2010). For example, Tao et al. (2006) observed that wheat anthesis became earlier by 2.86 days per decade from 1981 to 2000 at Tianshui in China. Hu et al. (2005) observed a consistent trend of earlier winter wheat heading or flowering dates by 0.8-1.8 days per decade across six sites in the United States Great Plains during the past 70 years. However, it is uncertain what magnitude the effects of an increase in air temperature on wheat flowering will have because of the strong interaction that exists with vernalization and photoperiodic responses (Miglietta et al. 1995). Vernalization is a physiological process by which plants can acquire competence to flower by prolonged exposure to cooling temperatures. Warmer temperatures during the vernalization period can delay dormancy or the fulfilment of chilling requirements, which increases the length of the vegetative phase and delays the onset of the reproductive stage (Rosenzweig & Tubiello 1996). Increased mean temperature may increase the rate of crop development, but the effect may be reduced because of lack of vernalization

(Butterfield & Morison 1992). This is particularly true for winter cultivars (Wang & Engel 1998, Liu 2007, Cook et al. 2012).

Wheat is normally grown under climatic conditions in Australia where the growing season is limited by the period of effective rainfall (Halse & Weir 1970, French & Schultz 1984a). Wheat flowering date is determined by a combination of sowing date and cultivar. Extreme weather events, such as spring frost and heat stress, can have significant impacts on crop growth and yield (Asseng et al. 2011, Sun & Huang 2011, Lobell et al. 2012). Therefore, the sowing time and cultivar are chosen to minimize frost and heat stress risk around flowering (McDonald et al. 1983, Shackley & Anderson 1995, Zheng et al. 2012). Grain growers, particularly in the wheat belt of Australia, have traditionally managed the potential loss from frost by sowing late or selecting a cultivar that flowers later (Shackley & Anderson 1995). However, delaying planting to reduce the risk of frost can result in higher losses than direct damage from frost because crops may face above-optimum temperatures during grain filling and there is increased risk of crop exposure to heat stress and terminal drought (Fuller et al. 2007). Therefore, optimum flowering periods need to be determined by analysing the tails and distributions for both frost and heat stress (Zheng et al. 2012). These distributions, and flowering dates themselves, will be affected by climate change.

There is a wide range of options for adapting cropping systems to climate change, and these may help to maintain or even increase crop yields compared to those under current conditions (Tubiello et al. 2000). Farmers can respond to changes in environmental conditions by choosing the most favourable crops, cultivars, and cropping systems (Tubiello et al. 2000, Asseng & Pannell 2013). Assessment studies should indicate which strategies have a good chance of success and which specific conditions represent a threshold for adaptation (Tubiello et al. 2000). For example, a threshold for advanced days in flowering date should identify when some wheat cultivars might not maintain yields because of a shortened growing season. However, many factors determine how crops respond to climate change. Crop models have been widely used to examine these responses. Meanwhile, these models account for the effect of multiple environmental factors (e.g., vernalization and photoperiod) and allow testing of multiple genotype-environment-management combinations (e.g., sowing date × cultivar × environment × year) (Zheng et al. 2012).

The objectives of this study were to: 1) identify future changes in wheat flowering date in the eastern Australian wheat belt; 2) identify the change in number of hot and frost days around wheat flowering date with future climate change in this region. The study accounted for uncertainties in future climate conditions by considering two scenarios for future atmospheric greenhouse gas concentrations and future climate conditions simulated by 19 Global Climate Models (GCMs). The

GCMs were selected for their skill at simulating temperatures throughout the wheat belt. The complex effects of climate on flowering date with two contrasting wheat genotypes were determined by forcing a vernalizing-photothermal model with statistically downscaled output from the GCMs.

5.2 Materials and methods

5.2.1 Study area and climate data

The study area is the New South Wales (NSW) wheat belt in eastern Australia. Data from 894 meteorological stations were used in this study (see Fig. 5.1). Daily temperature data at these stations for 1961-2000 were extracted from the SILO patched point dataset (PPD, http://www.longpaddock.qld.gov.au/silo/ppd/index.php). Annual mean maximum and minimum temperature time series data from these 894 stations have been tested separately for inhomogeneities using a revision of the two-phase regression model (Lund & Reeves 2002).

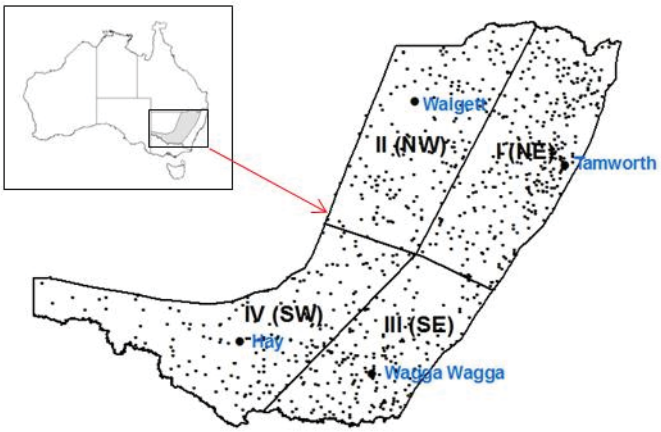

Fig. 5.1 The location of the 894 weather stations used in this study and the four regions of the NSW wheat belt considered: I: Northeast (NE); II: Northwest (NW); III: Southeast (SE) and IV: Southwest (SW).

The gridded temperatures from each GCM were first spatially interpolated to the study sites using an inverse distance weight interpolation method. Skill scores defined according to equation (4) (Taylor 2001) were used to identify the relatively satisfactory GCMs in simulating the climatological temperature over the NSW wheat belt. Equation (4.1) in chapter 4 was used to calculate skill scores for the 28 GCM simulations using climatological temperatures for 1961-2000. Skill scores were calculated for daily maximum and daily minimum temperatures averaged across the wheat-growing season (March 1 to November 30) and the entire year (Fig. 5.2). The 19 GCMs that achieved a skill

score greater than 0.4 for both maximum and minimum temperatures during the growing season and the entire year were selected for use in all subsequent analyses.

Using the method described by Liu and Zuo (2012), I downscaled gridded monthly temperature data from the 19 skill-selected GCMs to daily data for the 894 study sites. This method is based on a stochastic weather generator. Briefly, the gridded monthly GCM outputs were first interpolated to the specific sites using an inverse distance weight interpolation method. Then a bias correction procedure was applied to the monthly GCM values of each site (Liu & Zuo 2012). Daily climate data for the site were generated by a modified WGEN (Richardson & Wright 1984) with parameters determined from historical data and the monthly bias-corrected data.

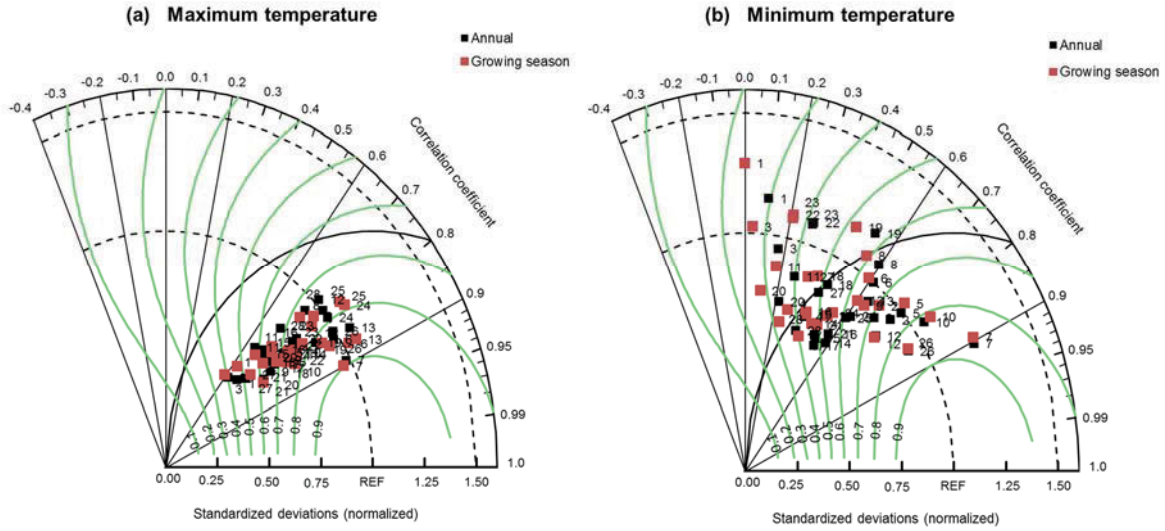

Fig 5.2 Taylor diagram (Taylor 2001) displaying normalized pattern statistics of 1961-2000 climatological mean (a) daily maximum temperature and (b) daily minimum temperature in eastern Australia for GCMs against observations. Each number represents a model ID (see Table S1). The black squares represent annual temperatures, and the red squares represent growing season temperatures (March 1 to November 30). The standard deviations for the GCMs have been normalized by the standard deviation of the reference observations (REF). The normalized standard deviation of a model is the radial distance from the origin to the points, with cambered dotted lines showing values of 1.0 and 1.5. The correlation coefficient between a model and the reference is given by the azimuthal position of the model, with oblique solid lines showing different coefficient values (-0.2, 0.2, 0.6 and 0.9). The green solid lines are isolines of measure of skill defined by equation (1).

5.2.2 Vernalizing-photothermal model

The time for wheat flowering can be simulated with a model that can represent the interaction between cold vernalization and temperature promotion, together with a photoperiod effect. The model should also identify whether the crop requires vernalization and should quantitatively measure the duration of vernalization required. Based on these general hypotheses, Liu (2007) developed a non-linear vernalization module incorporated into the thermal and photothermal additive models for modelling the time of flowering. The approach differed from that used in other wheat phenological models, which commonly simulate the development rate as a multiplicative function with a three-stage linear vernalization response (Ritchie 1991, Cao & Moss 1997, Wang & Engel 1998).

In this study, the vernalizing-photothermal model was used to simulate wheat flowering date for historical and future climate data with spring (Cunningham) and winter (Wylah) cultivars that can be sown across the NSW wheat belt with different sowing dates for different regions (Matthews et al. 2014). The phenology model and parameterisation procedures are explained in detail by Liu (2007). Briefly, the daily rate of progress toward flowering r_i is given as follows:

$$r_i = b_0 + b_1 f(V_i,\ V_f) T_i + b_2 P_i \qquad (5.1)$$

In this equation, $r_i \geq 0$; T_i is the mean temperature; P_i is the photoperiod of the day; and b_0, b_1 and b_2 are genotypic coefficients. V_i is the cumulative vernalization days, which accumulate a value of 1 if the temperature is optimal or 0 if the temperature is outside the appropriate range. V_f is a genotypic characteristic. The larger V_f is, the longer the requirement for vernalization. $2V_f$ is defined as the duration required for completion of vernalization. If $V_f = 0$, no vernalization is required, $f(V_i,\ V_f) = 1$. The flowering date is the day when the summation of daily developing rates (r_i) is greater or equal to 1.0 in the model.

Field observations of sowing and flowering dates for the two cultivars were collected from field experiments conducted from 2002 to 2006 at 15 locations in the NSW wheat belt to determine the parameters for equation (5.1) and for evaluating the prediction of flowering dates for spring and winter wheat using the vernalizing-photothermal model. In the experiment, cultivars were sown at five different sowing times from early April to early July in each year at each location. Each cultivar was sown as a separate block in each sowing time in a single one-meter long row with 25-cm row space. Air temperature data were recorded at each location with electronic data recorders sampling at 30-minute intervals to determine the daily maximum and minimum temperature. The date when 50% of ears in each row had commenced flowering was recorded.

Least-squares multiple regressions were used to determine the parameters for the two cultivars from the field observations for the different sowing dates, locations and years (Liu, 2007). I also applied a cross validation (Liu, 2007) so that the predictability of the model for the two cultivars used in this study was independently validated with the observed data. Table 1 shows the fitting parameters of the vernalizing-photothermal model for spring (Cunningham) and winter (Wylah) wheat cultivar. Fig. 5.3 displays the fitting and cross validation of the model for the number of days from sowing to flowering. The spring wheat flowering dates predicted by the model were consistent with the observational data (Fig. 5.3a), with the root mean square error (RMSE) of 6.93 days (N=40, R^2=0.87) for validation of fitting and 7.56 days (N=40, R^2=0.84) for cross-validation. RMSE for winter wheat was 6.92 days (N=122, R^2=0.93) and 7.06 days (N=122, R^2=0.92) (Fig. 5.3b).

Table 5.1 Parameters for the two wheat genotypes for the vernalizing-photothermal model used in this study.

Wheat genotypes	Parameters			
	b_0	b_1	b_2	V_f
Spring (Cunningham)	-21.0357	0.650004	2.017451	0.00
Winter (Wylah)	-6.03995	0.709042	0.633144	12.71

5.2.3 Climate analysis

5.2.3.1 Optimum sowing date for current climate

Observed daily minimum and maximum temperatures for 1961-2000 were used to analyse the occurrence of frost and heat events. For each growing season and each site, the last frost day was defined as the last day of the year with a minimum air temperature below 2°C (Liu et al. 2011); the first heat day was defined as the first day after July 1 with a maximum air temperature greater than 30°C (Porter & Gawith 1999, Asseng et al. 2011). Years with no frost and/or heat days were assigned the minimum last frost day (April 11) and maximum first heat day (December 31) across all sites (Zheng et al. 2012). The probabilities of occurrence of last frost and first heat days were calculated to determine historical flowering date for the period of 1961-2000. The optimum flowering date was defined as the date halfway between the date of 10% risk of last frost and the date of 10% risk of first heat day (i.e., the low-risk flowering window). The development of two cultivars was simulated using the vernalizing-photothermal model for different sowing dates at 1-day intervals (from March 1 to

August 1) at each site. Using the optimum flowering dates, we identified the optimum sowing dates for spring and winter wheat at each site.

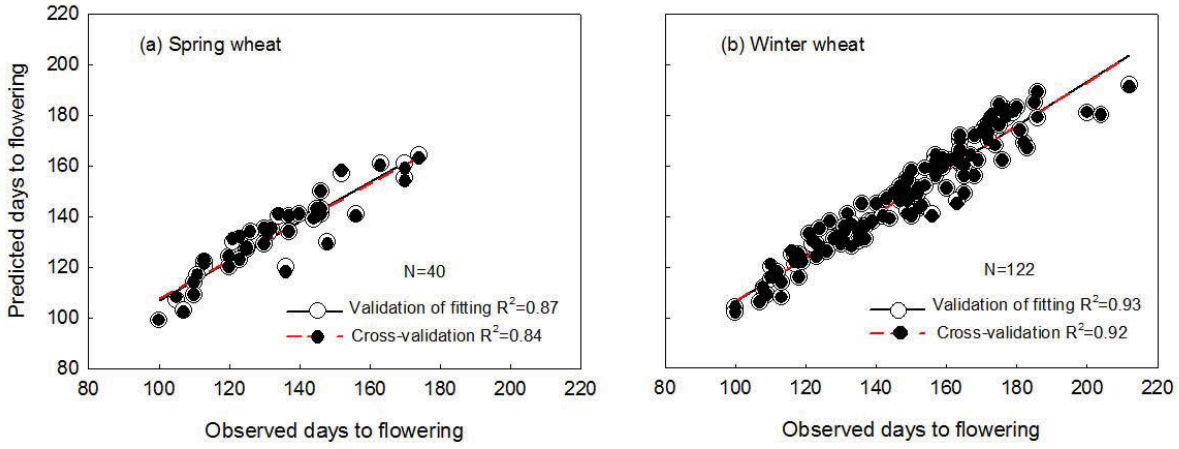

Fig. 5.3 Comparison of observed and the phenological model predicted days from sowing to flowering for spring (a) and winter (b) wheat. The root mean square error (RMSE) for spring wheat was 6.93 days (N=40, R^2=0.87) for validation of fitting and 7.56 days (N=40, R^2=0.84) for cross-validation. RMSE for winter wheat was 6.92 days (N=122, R^2=0.93) and 7.06 days (N=122, R^2=0.92). The solid black line corresponds to the linear regression for parameter fitting, and the red dashed line corresponds to cross validation.

5.2.3.2 Simulation for future climate scenarios

The daily maximum and minimum temperature downscaled from the 19 selected GCMs were used to drive the vernalizing-photothermal model to investigate changes in flowering date by 2040s (2021-2060, near future) and by 2080s (2061-2100, far future) under the RCP4.5 and RCP8.5 scenarios. The optimum sowing dates for two cultivars for each site determined by downscaled historical climate data from each GCM were used as future sowing dates to simulate flowering date change using the vernalizing-photothermal model. Moreover, I calculated the number of hot days (daily maximum temperature exceeding 30°C) and frost days (daily minimum temperature under 2°C) occurring at anthesis dates (+/- 7 days) to investigate changes in the occurrence of temperature extremes during flowering. Future changes for flowering date and the number of frost and hot days were calculated as downscaled future (2040s and 2080s) values minus downscaled historical (1961-2000) values.

5.2.3.3 Spatial analysis

Results were generated for four regions of the NSW wheat belt, including the Northeast (NE, I), Northwest (NW, II), Southeast (SE, III), and Southwest (SW, IV) (see Fig. 5.1). I used the Climate Change Adaptation Strategy Tool (CCAST) to calculate regional results from values calculated for the 894 study sites. Developed by Liu et al. (2011), CCAST is a stand-alone GIS framework that analyses climate change impacts, defines the agricultural and geographical areas most sensitive to climate change, and identifies appropriate adaptation responses (Liu et al. 2011). Once a target index was selected (for example, a change in flowering date), spatial analysis was performed to obtain a pattern of changes across a region. Here, the 50th percentile of the selected index across all the sites in the specific region was calculated as a spatial regional value using inverse distance weighted (IDW) interpolation.

5.3 Results

5.3.1 Projected changes in temperature

Table 5.2 presents trends in annual mean daily maximum and minimum temperature statistically downscaled from 19 GCMs over the NSW wheat belt from 2020 to 2100 under scenarios RCP4.5 and RCP8.5. For annual maximum and minimum temperature, all the models show a positive trend for both future climate scenarios. However, the projections show apparent differences between scenarios RCP4.5 and RCP8.5. The trend for RCP8.5 was much larger than that of RCP4.5, owing to the different evolution of radiative forcing in the future. Under RCP4.5, the trends of annual maximum temperature ranged between 0.07°C and 0.34°C per decade across the 19 GCMs with an ensemble mean trend of 0.17°C per decade. For scenario RCP8.5, the ensemble mean rate of increase in annual maximum temperature was 0.45°C per decade, more than double that of RCP4.5. For the annual minimum temperature, the mean trend for RCP8.5 was 0.47°C per decade. In contrast, RCP4.5 predicted a lower mean warming rate of 0.16°C per decade.

RCP4.5 and RCP8.5 are considered as two cases of different evolution in greenhouse gas concentrations. The RCPs represent a range of 21st century climate policies. For RCP4.5, radiative forcing stabilizes by 2100, but for RCP8.5 it does not peak by year 2100 due to high greenhouse gas emissions. In the present study, the two scenarios produced similar temperatures for the NSW wheat belt until the middle of the 21st century based on the median value from the 19 GCMs (Fig. 5.4). In the time series of annual maximum and minimum temperature during the period 1961-2100 across the

NSW wheat belt, distinguishable differences between the two scenarios do not occur until the year 2040, considering the ensembles of projections.

The annual mean temperatures for RCP4.5 and RCP8.5 projected by the 19 GCMs for the 2040s and 2080s differed between the four regions of the wheat belt (Fig. 5.5). The projected temperature in the 2040s showed large differences between the four regions. By the 2040s, the highest simulated temperature was found in northwestern parts of NSW wheat belt (region NW, II) with ensemble median temperatures of 20.5°C for RCP4.5 and 20.8°C for RCP8.5. The lowest simulated annual temperatures appeared in the southeast (region SE, III), 17.0°C for RCP4.5 and 17.2°C for RCP8.5. The simulated annual mean temperature of the 2080s was similar to the results of the 2040s, with highest temperature in region NW (21.0-22.6°C) and lowest temperature in SE (17.6-19.3°C) for RCP4.5 and RCP8.5. However, the projected changes of temperature and the dispersion between the two scenarios turned out to be larger in the 2080s. By the 2080s, region NE (I) and SE were projected to warm the most, with an ensemble median warming of 2.9°C; region SW (IV) was projected to warm the least, with an ensemble median warming of 2.7°C.

5.3.2 Optimum sowing and flowering dates for historical climate data

Optimum flowering date was determined as the date halfway through the low-risk period for extreme temperature, between 10% risk of last frost and 10% risk of first heat day (e.g., for Wagga Wagga in Fig. 5.6). To identify optimum sowing dates, simulations were performed with sowing at 1-day intervals from March 1 to August 1. The optimum sowing dates for each site for the two wheat cultivars were identified from the simulations, given the optimum flowering date. For example, based on the patterns of frost and heat stresses for Wagga Wagga (Fig. 5.6), the optimum flowering date was October 13; the optimum sowing date for spring wheat (Cunningham) was May 27; and the optimum sowing date for winter wheat (Wylah) was May 22.

Fig. 5.7a and b show the spatial distribution of optimum sowing dates for spring and winter wheat based on observed historical climate data for 1961-2000. The sowing date became later in the year from west to east across the NSW wheat belt, and the winter cultivar was sowed earlier than the spring cultivar by an average of 26 days. The optimum flowering date also became delayed in the year from west to east (Fig. 5.7c).

5.3.3 Changes in flowering date for future climate scenarios

The results from these simulations indicate that the future climate changes considered will have a large impact on wheat flowering date. Fig. 5.8a shows changes in spring wheat flowering date for the 2040s and 2080s relative to the baseline period (1961-2000) for the four regions in the NSW wheat

belt. The time of spring wheat flowering is clearly advanced in future climate scenarios due to increasing temperature.

Table 5.2 Projected trends in annual mean daily maximum and daily minimum temperature (°C per decade) statistically downscaled from 19 GCMs for RCP4.5 and RCP8.5 during the period 2020-2100 in the NSW wheat belt. Standard errors for trends for individual models are shown in brackets. For the multi-model mean trends, numbers in brackets are standard deviations across all GCMs. All trends are significant with $p<0.05$.

Model ID	Maximum temperature				Minimum temperature			
	RCP4.5		RCP8.5		RCP4.5		RCP8.5	
	Trend	R^2	Trend	R^2	Trend	R^2	Trend	R^2
02	0.07(±0.028)	0.07	0.36(±0.031)	0.63	0.07(±0.026)	0.07	0.43(±0.029)	0.74
05	0.19(±0.029)	0.35	0.55(±0.035)	0.75	0.13(±0.025)	0.27	0.45(±0.025)	0.81
06	0.14(±0.029)	0.24	0.49(±0.039)	0.67	0.12(±0.018)	0.37	0.40(±0.021)	0.83
07	0.20(±0.032)	0.34	0.62(±0.028)	0.86	0.23(±0.024)	0.53	0.67(±0.021)	0.93
08	0.27(±0.037)	0.39	0.65(±0.041)	0.76	0.26(±0.026)	0.57	0.65(±0.030)	0.86
09	0.34(±0.030)	0.62	0.56(±0.028)	0.84	0.21(±0.019)	0.61	0.60(±0.018)	0.93
10	0.15(±0.036)	0.17	0.39(±0.048)	0.46	0.22(±0.025)	0.50	0.53(±0.027)	0.83
12	0.14(±0.027)	0.26	0.36(±0.025)	0.72	0.12(±0.021)	0.30	0.42(±0.020)	0.84
13	0.15(±0.029)	0.26	0.27(±0.026)	0.58	0.17(±0.019)	0.49	0.36(±0.019)	0.83
14	0.29(±0.039)	0.42	0.49(±0.040)	0.66	0.26(±0.022)	0.63	0.55(±0.021)	0.89
15	0.10(±0.033)	0.10	0.36(±0.034)	0.59	0.07(±0.025)	0.09	0.41(±0.024)	0.79
16	0.12(±0.038)	0.11	0.36(±0.038)	0.54	0.13(±0.032)	0.18	0.41(±0.030)	0.69
18	0.16(±0.025)	0.33	0.29(±0.027)	0.59	0.06(±0.022)	0.09	0.22(±0.021)	0.58
19	0.20(±0.027)	0.42	0.55(±0.023)	0.88	0.18(±0.018)	0.58	0.52(±0.022)	0.87
21	0.18(±0.036)	0.24	0.42(±0.036)	0.62	0.17(±0.028)	0.32	0.53(±0.026)	0.84
24	0.15(±0.042)	0.14	0.48(±0.045)	0.59	0.13(±0.023)	0.30	0.45(±0.025)	0.80
25	0.13(±0.038)	0.14	0.46(±0.040)	0.63	0.14(±0.021)	0.36	0.44(±0.027)	0.76
26	0.15(±0.030)	0.25	0.38(±0.034)	0.61	0.17(±0.016)	0.57	0.48(±0.019)	0.89
27	0.17(±0.026)	0.35	0.47(±0.029)	0.77	0.11(±0.021)	0.25	0.36(±0.018)	0.84
Mean	0.17(±0.07)	0.27	0.45(±0.11)	0.67	0.16(±0.06)	0.37	0.47(±0.11)	0.82

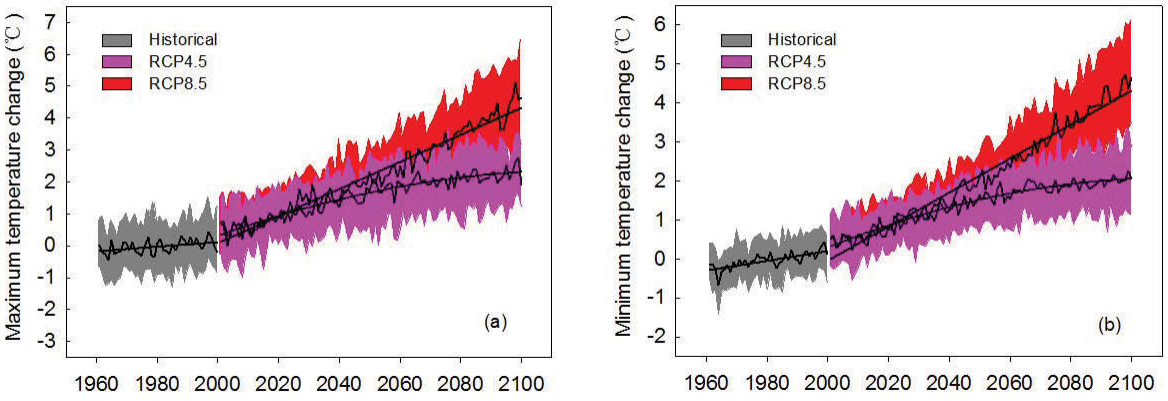

Fig. 5.4 Projected changes in annual mean daily maximum (a) and daily minimum (b) temperature during the 21st century under RCP4.5 and RCP8.5 relative to the 1961-2000 for the NSW wheat belt. The heavy black curves represent the median value from the 19 GCMs, calculated for each year. The top and bottom bounds of shaded area are the 90th and 10th percentile of the annual value from the 19 GCMs simulations.

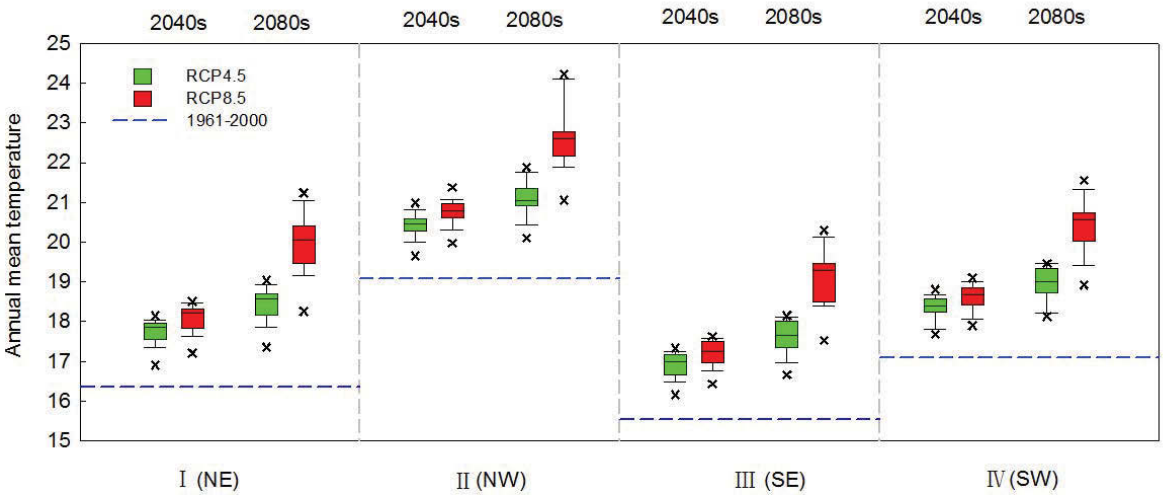

Fig. 5.5 Simulated annual mean temperature from the 19 selected GCMs under RCP4.5 and RCP8.5 in the 2040s and 2080s in the four regions over the NSW wheat belt. The dotted lines represent the mean temperature for the period 1961-2000. Box plots are constructed from results from 19 GCMs. Box boundaries indicate the 25th and 75th percentiles; the black line within the box marks the median; whiskers below and above the box indicate the 10th and 90th percentiles; and crosses indicate outliers.

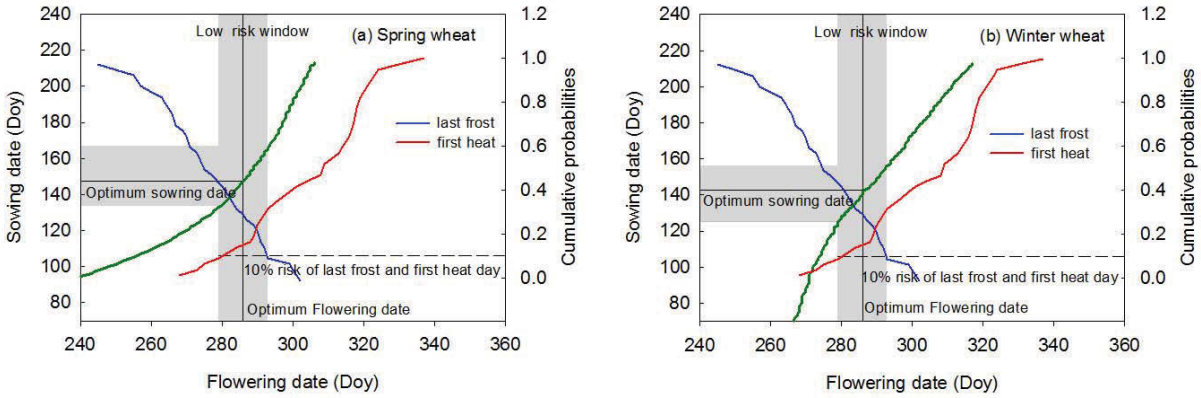

Fig. 5.6 Spring (a, Cunningham) and winter (b, Wylah) wheat optimum flowering and sowing dates determined by the occurrence of extreme temperature events for Wagga Wagga during the period 1961-2000. Probabilities of last frost days (blue line) and first heat days (red line) are calculated as the percentiles of last frost and first heat days from 1961 to 2000. The green line shows the variation in flowering date for different sowing dates. The 10% risk of last frost and first heat day is given to determine low-risk flowering window (horizontal dashed line). The grey shading shows the low-risk period for flowering and the corresponding sowing window. The optimum flowering date is the middle date of the low-risk flowering window (vertical solid line). The optimum sowing date is determined by the corresponding optimum flowering date (horizontal solid line).

The time to flowering was shortened with rising temperature for all four regions, and the effect was more pronounced where temperatures increased the most. The largest shift in flowering date was found in region NE, especially under the high-emission RCP8.5 scenario, followed by region NW; the smallest changes in flowering date were found in regions SW and SE. By the 2040s, spring wheat flowering date was expected to become earlier by an ensemble median of 6.8 days for RCP4.5 and 8.4 days for RCP8.5 across the NSW wheat belt. However, the impact of further temperature increases leads to a greater effect on the time of flowering. By the 2080s, flowering date shifted earlier by an ensemble median of 10.2 and 17.8 days for the two scenarios across the wheat belt. The difference in the size of the effect between the two scenarios is larger for the 2080s than for the 2040s. This is related to large differences in temperatures between RCP4.5 and RCP8.5 after about 2040 (Fig. 5.4).

Fig. 5.8b shows the changes in winter wheat flowering date for the two future climate scenarios. Flowering date advances under RCP4.5 and RCP8.5 by both the 2040s and 2080s for all regions except region NW; ensemble median changes under RCP4.5 are 6.8 (NE), 7.3 (SE), and 4.6 (SW) days, and 6.8 (NE), 9.1 (SE) and 4.1 (SW) days under RCP8.5. Increasing temperatures accelerated the growth rate of winter wheat and thereby advanced the flowering date. However, it is noteworthy

that the date of flowering for winter wheat was delayed by higher temperature in the warmest region (region NW). On average, winter wheat flowering date shifted 2.4 days later for RCP4.5 and 14.3 days later for RCP8.5.

Fig. 5.9 displays the sensitivity of wheat flowering date to annual mean temperature change in the four regions of the NSW wheat belt based on two scenarios from 19 GCMs with two time periods (2040s and 2080s). Spring wheat flowering date showed a negative response to an increase in mean annual temperature (Fig. 5.9a) in all four regions. For regions NE, NW, and SW, a 1°C increase in temperature resulted in an earlier shift for flowering date by approximately 4.9 days. A smaller change occurred in region SE, 4.0 days°C^{-1}. However, winter wheat had a negative correlation between flowering date and temperature only for region SE, the coolest region (Fig. 5.9b); in this region, a 1°C increase in mean temperature resulted in an earlier shift for flowering date by 2.2 days. The warmest region (region NW) showed delays in flowering date by 11.7 days°C^{-1}.

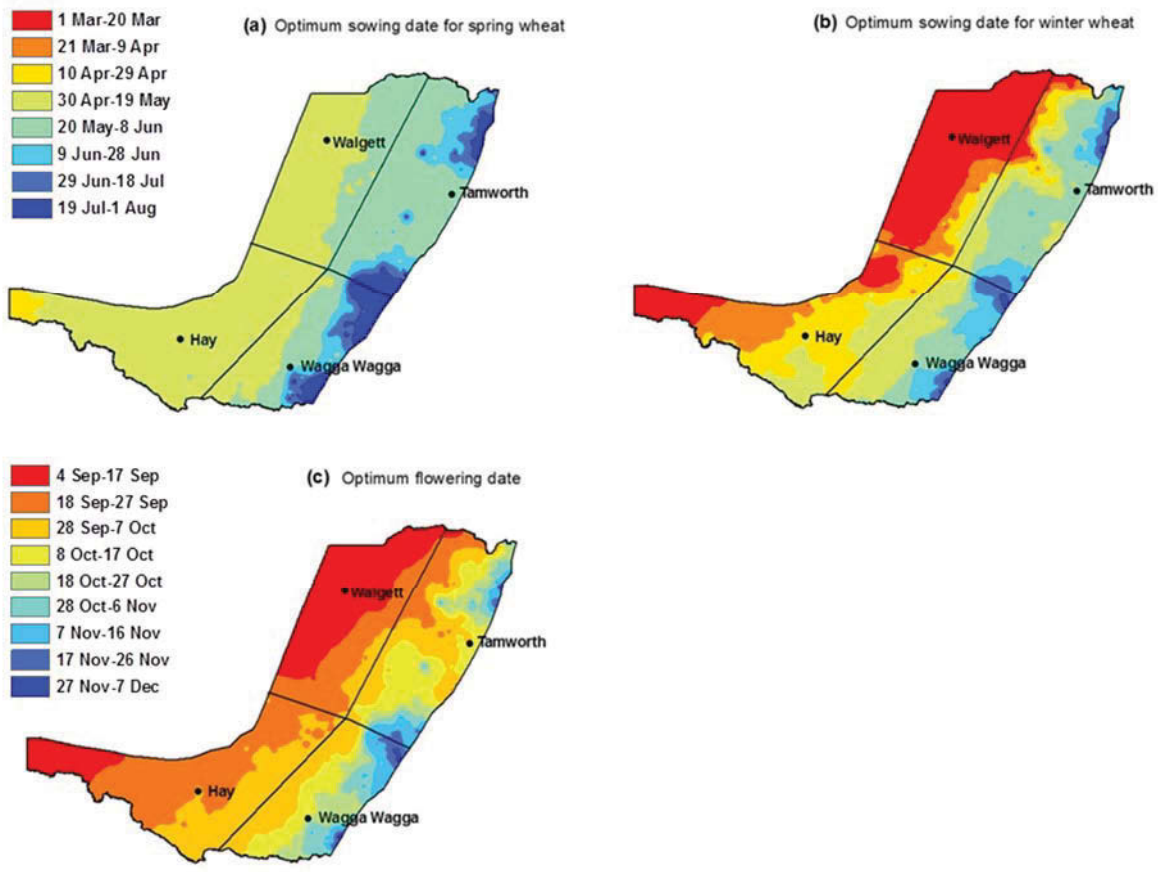

Fig. 5.7 Maps of optimum sowing date for spring wheat (a), winter wheat (b), and optimum flowering date (c), based on observed historical climate data during the period of 1961-2000.

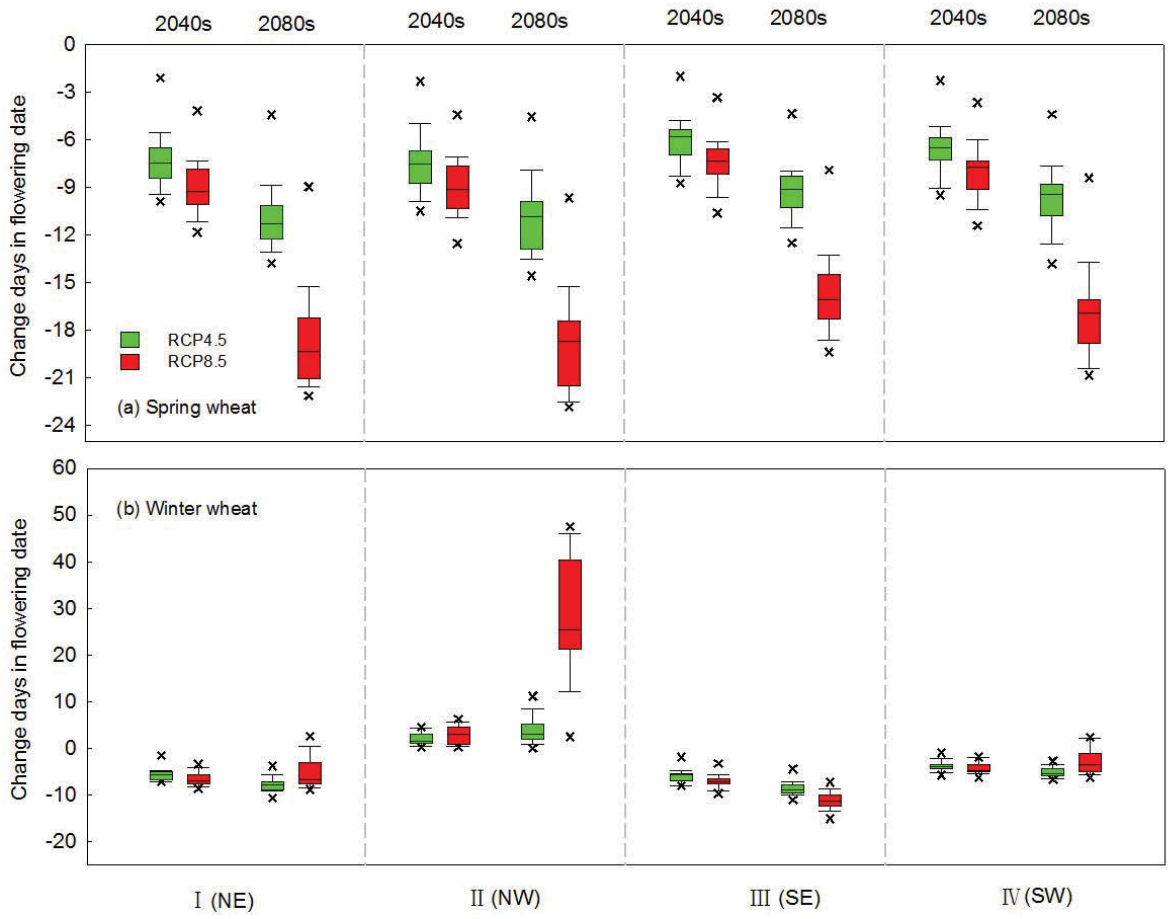

Fig. 5.8 Simulated changes in flowering date for spring (a) and winter (b) wheat in the 2040s and 2080s relative to the period 1961-2000 for four regions in the NSW wheat belt. Box plots are constructed from results from 19 GCMs. Box boundaries indicate the 25th and 75th percentiles; the black line within the box marks the median; whiskers below and above the box indicate the 10th and 90th percentiles; and crosses indicate outliers.

5.3.4 Changes in number of hot and frost days at flowering date

The risk of heat stress during flowering was found to be more severe in the future than at present. Fig. 5.10a shows increases in the number of hot days (maximum temperature exceeding 30°C) around spring wheat flowering (flowering date +/- 7 days) under RCP4.5 and RCP8.5 in 2040s and 2080s at the four regions of the NSW wheat belt. By the 2040s, changes in the number of hot days were almost all less than 1 day for both RCP4.5 and RCP8.5. By the 2080s, the increase in the occurrence of hot days at flowering date was the most in region NW (ensemble median change of 1.6 days for RCP4.5 and 3.5 days for RCP8.5) followed by region NE (ensemble median change of 1.5 days for RCP4.5 and 3.0 days for RCP8.5); the smallest increase in the number of hot days was found in region SW

(ensemble median change of 1.2 days for RCP4.5 and 2.5 days for RCP8.5). The results for winter wheat are similar (Fig. 5.10b), although for region NW increases in the number of hot days by the 2040s exceed 1 day for most of the GCMs (ensemble median changes of 1.1 days for RCP4.5 and 1.7 days for RCP8.5).

The number of frost days with daily minimum temperature below 2°C occurred around wheat flowering date (+/- 7 days) reduced by less than one day for both future scenarios relative to the 1961-2000 period due to climate warming (Fig. 5.11). By 2040s decreased number of frost days was less than 0.1 for spring wheat for both RCP8.5 and RCP4.5 at the four regions (Fig. 5.11a). By 2080s the highest decrease in the occurrence of frost days was in region NW (ensemble median change of 0.3 days for RCP4.5 and 0.4 days for RCP8.5); the lowest decrease in the number of frost days was found in region SW (ensemble median change of 0.2 days for RCP4.5 and 0.3 days for RCP8.5). The results for winter wheat are analogous to spring wheat (Fig. 5.11b).

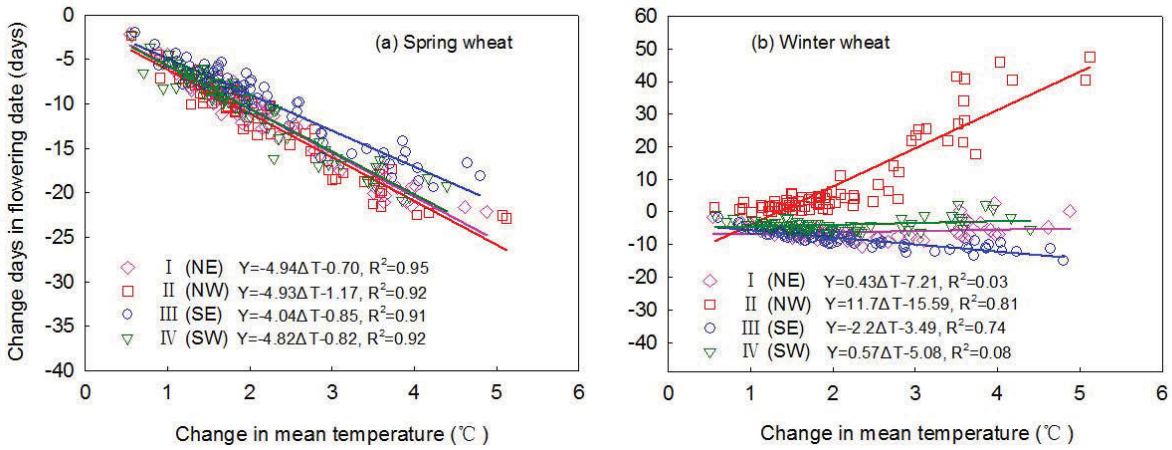

Fig. 5.9 Relationship between simulated changes in wheat flowering date and annual mean temperature change in four regions of the NSW wheat belt for spring (a) and winter (b) wheat. The effect of a change in temperature (ΔT) was fitted using linear regression.

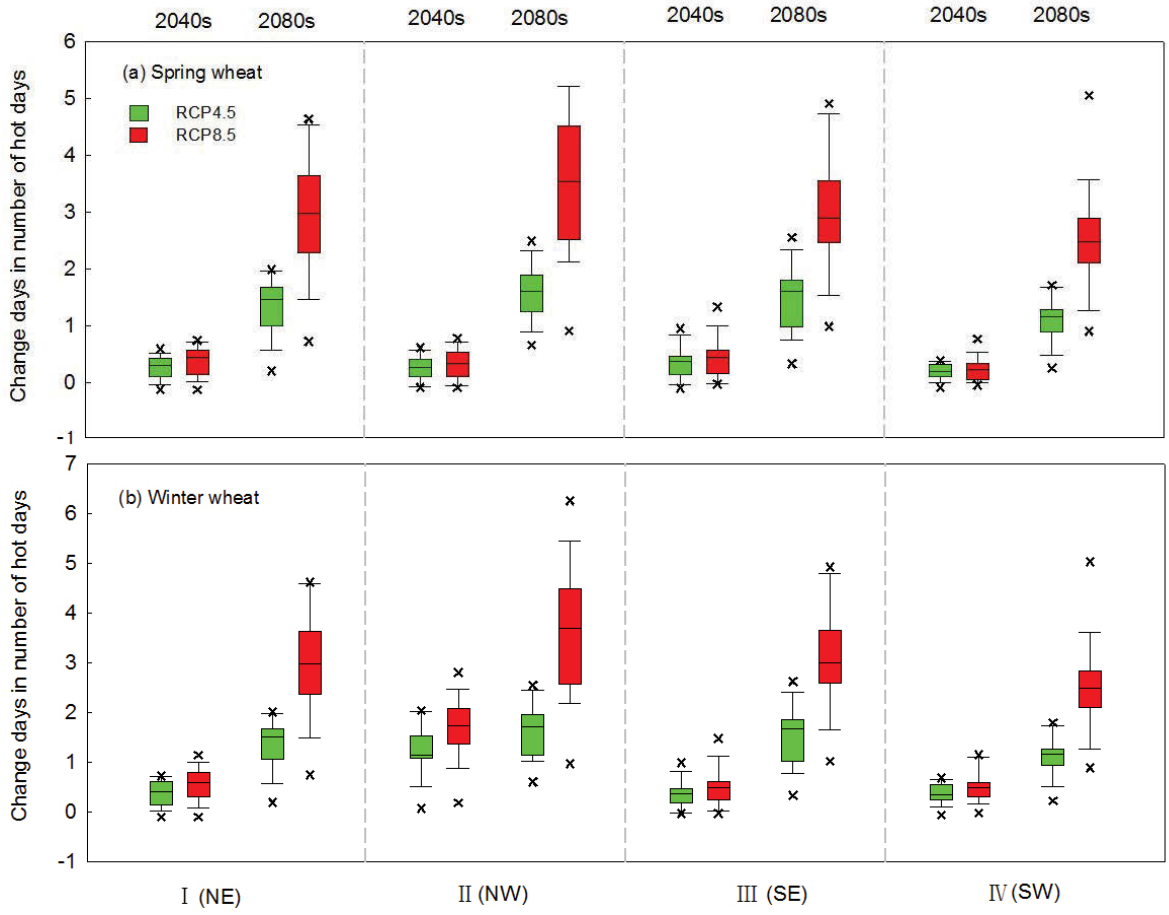

Fig. 5.10 Changes in average number of hot days with daily maximum temperature exceeding 30°C during flowering (flowering date +/- 7 days) for spring (a) and winter (b) wheat under RCP4.5 and RCP8.5 by the 2040s and 2080s, relative to the 1961-2000 period for four regions in the NSW wheat belt based on downscaled data from 19 GCMs. Box boundaries indicate the 25th and 75th percentiles; the black line within the box marks the median; whiskers below and above the box indicate the 10th and 90th percentiles; and crosses indicate outliers.

5.4 Discussion

In this study, the combination of downscaled GCM output and the phenological model were used to assess the effects of climate change on wheat flowering dates across the NSW wheat belt. The overall response of wheat phenology to changes in temperature in the four regions considered is an obvious result of the temperature-driven development model. Compared with the baseline, if farmers do not change the cultivars grown and do not improve management practices, the simulations of

future climate scenarios indicated that climate change would shorten the growing period for spring wheat due to an advance in flowering date. The warmer climate would speed development and lead to a reduction in the number of days in the vegetative period for spring wheat.

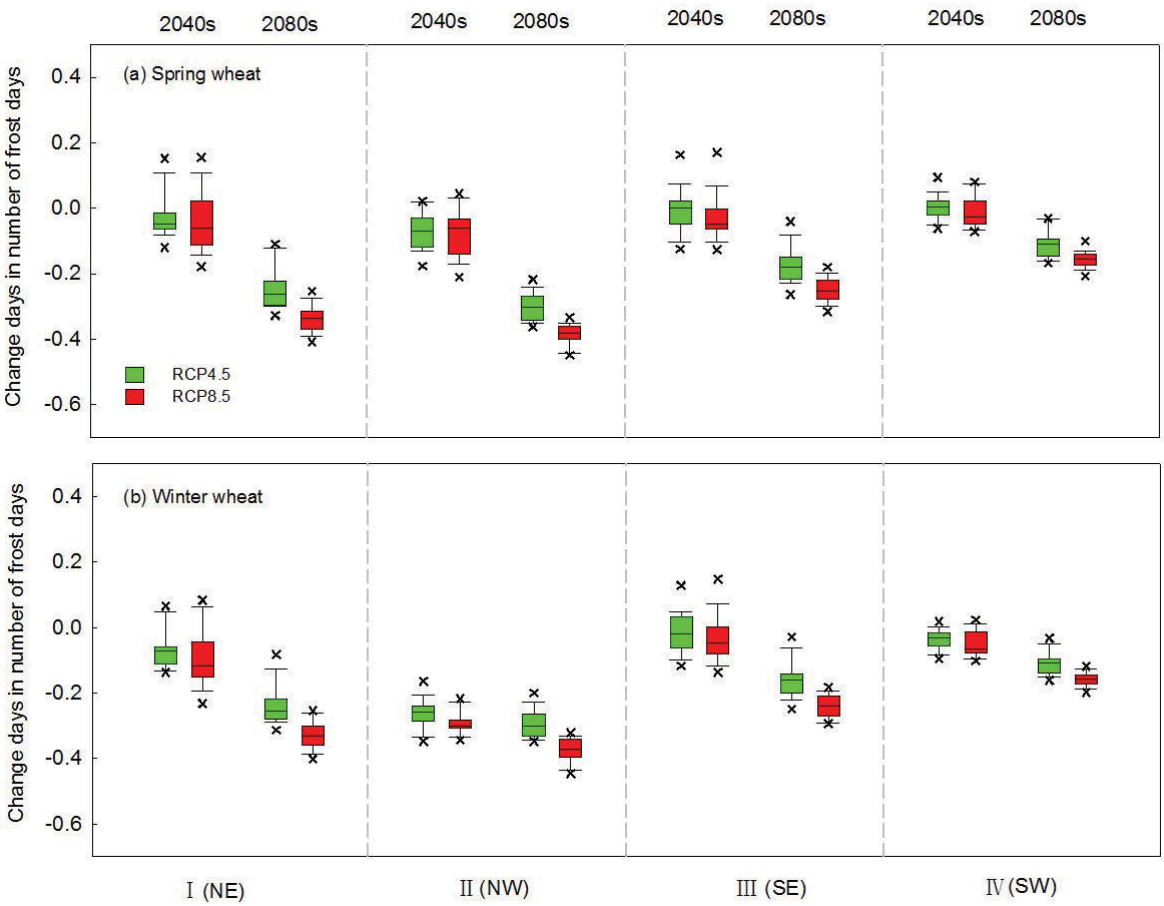

Fig. 5.11 Changes in average number of frost days with daily minimum temperature under 2°C during flowering (flowering date +/- 7 days) for spring (a) and winter (b) wheat under RCP4.5 and RCP8.5 by the 2040s and 2080s, relative to the 1961-2000 period for four regions in the NSW wheat belt based on downscaled data from 19 GCMs. Box boundaries indicate the 25th and 75th percentiles; the black line within the box marks the median; whiskers below and above the box indicate the 10th and 90th percentiles; and crosses indicate outliers.

Winter wheat flowering dates also changed but these change varied by region. In the warmest region, the NW, flowering dates were delayed due to higher temperature resulting in unsuccessful vernalization, especially by the 2080s under the high-emission RCP8.5 scenario (Fig. 5.8b). In the coolest region, the SE, flowering date occurred earlier (Fig. 5.8b). I found that simulated flowering

date would advance by an ensemble median of 10.2 days for RCP4.5 and 17.8 days for RCP8.5 for spring wheat averaged across the entire wheat belt in the 2080s. In contrast, flowering date for winter wheat would advance by 4.8 days under RCP4.5 and delay by 1.0 days under RCP8.5 in the 2080s.

Although simulated wheat flowering date became earlier or delayed (Fig. 5.8), the number of hot days with maximum temperature exceeding 30°C during flowering date (+/- 7 days) in 2040s and 2080s increased due to climate warming, especially for the RCP8.5 (Fig. 5.10). Simulated number of frost days with minimum temperature below 2°C during flowering (+/- 7 days) decreased slightly in 2080s for RCP8.5 (Fig. 5.11). It should be noted that hot days occurred most and frost days occurred least in the warmest region, the NW, under high emission (RCP8.5) in the future, which is consistent with the results of Zheng et al. (2012). They found that a greater number of regions would become "frost-free" and the first heat day of wheat season was earlier by 4-41 days in Australian wheat belt in the future climate. Consequently, the timing and frequency of frost and heat events were predicted to differ depending on the location and future scenario considered.

Simulated spring wheat flowering date changes displayed a strong correlation with annual mean temperature change. The results show that increased temperature had a negative effect on spring wheat flowering date with -4.7 days°C^{-1} (Fig. 5.9a), which roughly compares to previous estimates (Sadras & Monzon 2006, Tao et al. 2006, Estrella et al. 2007, Zheng et al. 2012, Yang et al. 2014). It is noteworthy that there was a significantly delayed response of winter wheat flowering time to mean temperature increase in the NW region (Fig. 5.9b). Many recent studies have suggested that plants were not advancing in their spring phenological behaviours (leaf unfolding and flowering) because they responded more to lack of winter chill than increased spring heat (Cook et al. 2012, Pope et al. 2013, Wang et al. 2014). The requirement of thermal time for wheat development was not being met because the number of cumulative vernalization days was shortened due to climate warming and became insufficient to fulfil the vegetation chilling requirement. The cumulative vernalization days for winter wheat reduced by an ensemble median of 20 and 30 days averaged across the NSW wheat belt for RCP4.5 and RCP8.5, respectively (Fig. 5.12a and b). As a result, flowering date was delayed under the two RCP scenarios in region NW (Fig. 5.8b), where annual temperature was the highest (Fig. 5.5). Interestingly, the NW region exhibited a stronger positive response to temperature than regions NE and SW; while in the coolest region, the SE, there was a negative relationship between flowering date change and mean temperature (Fig. 5.9b). This indicates that higher temperatures in the warmest region restricts winter wheat vernalization, which delays the growing season in the future and increases the risk of exposure to hot days around flowering date (Fig. 5.10b).

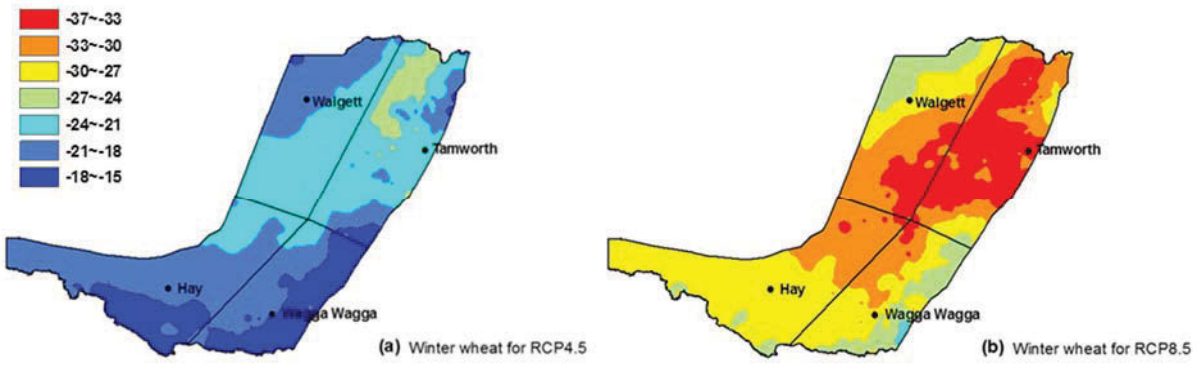

Fig. 5.12 Maps of simulated changes in cumulative vernalization days for winter wheat with an ensemble median of 19 GCMs during the period 2020-2100 under RCP4.5 (a) and RCP8.5 (b), relative to 1961-2000.

The analysis presented here demonstrated changes in anthesis processes that agree with the findings of other studies (Sadras & Monzon 2006, Wang et al. 2009c, Zheng et al. 2012). However, when driving the phenology model with statistically downscaled daily data from different GCMs, there are many uncertainties, including the choice of GCMs with the best performance to downscale. Most previous model validation studies used conventional statistics to measure the similarity between observed and modelled data (Taylor 2001, Min & Hense 2006, Reichler & Kim 2008). For example, in this study, I used Taylor's method to select GCMs after characterizing model performance from correlation and standard deviations. These two statistics were combined in a single diagram, resulting in a good visualization of the model. The projected wheat-growing season and annual maximum temperature from 28 GCMs during the period 1961-2000 all passed the skill score (0.4), except BNU-ESM, which shows better simulated results than the minimum temperature (19 of 28 GCMs passed 0.4) across the entire NSW wheat belt. This approach, however, is only practical for a small number of models and/or climate quantities (Reichler & Kim 2008). More uncertainty can come from the GCMs themselves (different spatial resolution), statistical downscaled method (bias correction), and the independence of simulated different GCMs (Bishop & Abramowitz 2013, Evans et al. 2013); these uncertainties were not considered when using multi-model ensemble median value.

Ambient temperature, photoperiod and vernalization are major environmental factors affecting crop flowering time (Wang & Engel 1998, Brooking & Jamieson 2002, Liu 2007). Other factors such as water and nitrogen stress together with temperature will have large effects on crop photosynthesis or respiration and thereby resulting in yield loss and/or gain. Therefore, as the wheat phenology

module in APSIM and CERES-Wheat both assume that crop development is determined by photoperiod and temperature (Keating et al. 2003, Lobell & Ortiz-Monasterio 2007), the phenological model used in this study is based on a non-linear vernalization module incorporating thermal and photothermal additive models for the time of flowering. It is an effective approach for determining phenological parameters from field experiment data and separating the confounding effects of temperature and vernalization in phenological development (Liu 2007). However, like all other commonly-used phenological models, uncertainty exists in the model results as the values of the model parameters are determined by fitting limited field observations.

Increasing temperatures during the 21st century will have large consequences on crops. Some cultivars will benefit from a warmer climate, while others will disappear (Piao et al. 2010). Our simulated results indicate that continued warming of the NSW climate will have serious consequences for some wheat cultivars grown there. For spring wheat, accelerated phenology could reduce yield and fitness because earlier flowering could constrain vegetative development, leading to a lower amount of radiation being intercepted and affecting soil water extraction. For winter wheat, flowering date will be delayed due to lack of necessary vernalization in the model. Fortunately, switching to different cultivars may be able to compensate for the negative impacts of climate change (Liu et al. 2010b). Adopting wheat cultivars that require weaker or zero vernalization in the future may be a good strategy in some areas. Our results demonstrate that in the western parts of the wheat belt (regions NW and SW) flowering date for winter wheat delayed more than in the eastern parts (regions SE and NE) (Fig. 5.8b). Therefore, limiting sowing of winter cultivars in the western plains may be one strategy to mitigate the impacts of future climate change in the wheat belt.

The present study clearly demonstrates the need to consider changes in both genotype and sowing date in climate change impact studies. In some of my simulations, which did not consider adaptation, the magnitude of impact was strongly related to the change in temperature because of the associated reduction in growing season duration. In this study, the optimum sowing dates based on downscaled historical climate data (1961-2000) for each GCM were used as future sowing dates to simulate future flowering changes. Optimum sowing date was only determined by the vernalization-photothermal model according to the optimum flowering date calculated by the low-risk window of frost and heat stress. The effect of rainfall on sowing date was ignored and so was crop response. This may be significant, as the timing of the first autumn rains in eastern Australia can be highly variable. In fact, optimum flowering date will change due to global warming resulting in increased number of hot days with maximum temperature exceeding 30°C (Fig. 5.10) and decreasing number of frost days with minimum temperature below 2°C (Fig. 5.11) around flowering date (+/- 7 days) in future climate conditions. Sowing dates may advance as a consequence of earlier flowering

date to minimize frost and heat stress at anthesis dates in the future (Zheng et al. 2012). In reality, farmers have already sowed earlier, and wheat yield has improved in recent decades, particularly because of the adoption of new planting practices and cultivars (Gomez-Macpherson & Richards 1995, Stephens & Lyons 1998). Moreover, sowing early at the break of season is now possible because of the use of herbicides to maintain soil water conditions and minimum tillage techniques that preserve soil water (Anderson & Smith 1990, Zheng et al. 2012).

As a result of phenological responses to increasing temperatures, current wheat cultivars may not be suitable for future climate conditions due to a shorter growth cycle and exposure to extreme high temperatures during flowering date, despite reduced frost risk. The growing season and extreme events risk might determine the plant-able year for current wheat cultivars. Different cultivars will be limited by different climatic thresholds. For example, in the vernalizing-photothermal model, if the cumulative vernalization days are $\leq 2v_f$ (approximately 25.4 days), winter wheat cannot complete vernalization, affecting the time of the transition from vegetative to reproductive development and leading to a potentially high-yield penalty. In contrast, spring wheat does not require vernalization. In the future, our current long-season wheat cultivars will have a growth period similar to the current medium-season cultivars (Zheng et al. 2012); our current medium, short-season, and winter cultivars may disappear due to warming in the next few decades. Late-maturing cultivars will be needed to maintain the current crop cycle duration, to provide for the use of resources (radiation, CO_2, water, and nutrients) of long-season cultivars, and to allow earlier sowing (Zhang et al. 2006, Zheng et al. 2012). For some regions, it is important to breed long-season cultivars capable of coping with an increased frequency and magnitude of heat stress around flowering and grain filling. In some regions, it will be equally important to maintain tolerance of low temperatures (spring frost) when sowing earlier. Breeding is often slow (e.g., 10-12 years to develop a new crop cultivar, 20 years or more to develop a new cultivar to the point of commercial production) (Asseng & Pannell 2013), so it is urgent to examine adaptation of wheat genotypes to future climate. This also points to the need to consider the effects of climate change on crops and incorporate those findings into future breeding programmes. That is why it is useful to study the results of crop simulation models with different phenotypic characteristics combined with climate data representing different climate change scenarios.

5.5 Conclusions

The flowering date of wheat is strongly controlled by temperature and is potentially highly sensitive to climate change. The results of simulations presented in this chapter suggest a general advance in spring wheat flowering date between 1961-2000 and the 2080s, on average, by 10.2 days

for RCP4.5 and 17.8 days for RCP8.5 across the NSW wheat belt. Changes in flowering dates for winter wheat were also simulated, but these varied in sign by region. In the warmer sub-region, flowering dates delayed by an average of 2.4 days for RCP4.5 and 14.3 days for RCP8.5 due to higher temperature resulting in unsuccessful vernalization. In the cooler regions (NE, SE, SW) flowering dates occurred earlier by 6.2 days for RCP4.5 and 6.7 days for RCP8.5 on average. Moreover, in the western parts of the wheat belt the delay of winter wheat flowering date was about 9.5 days longer than that in the eastern parts. Thus limiting sowing of winter cultivars in the western plains may be one strategy to mitigate the impacts of future climate change in the wheat belt. It should be noted that the number of hot days with maximum temperature exceeding 30°C during flowering date (+/- 7 days) increased while simulated number of frost days with minimum temperature below 2°C decreased due to climate warming. Therefore, sowing dates may advance as a consequence of flowering date change to minimize frost and heat stress at anthesis dates in the future. Late-maturing cultivars with increased heat-stress resistance will be needed to maintain the current crop cycle duration, to provide for the use of resources (radiation, CO_2, water, and nutrients) of long-season cultivars in eastern Australia.

Chapter 6*

Modelling changes in wheat yield under future climate conditions in relation to plant available water capacity in eastern Australia

Abstract

Increasing heat and water stress are important threats to wheat growth in rain-fed conditions. Using climate scenario-based projections from the Coupled Model Intercomparison Project phase 5 (CMIP5), I analysed changes in the probability of heat stress around wheat flowering and relative yield loss due to water stress at six locations in eastern Australia. As a consequence of warmer average temperatures, wheat flowering occurred earlier, but the probability of heat stress around flowering still increased by about 3.8% to 6.2%. Simulated potential yield across six sites increased on average by about 2.5% regardless of the emission scenario. However, simulated water-limited yield tended to decline at wet and cool locations under future climate while increased at warm and dry locations. Soils with higher plant available water capacity (PAWC) showed a lower response of water-limited yield to rainfall changes except at very dry sites, which means soils with high PAWC were less affected by rainfall changes compared with soils with low PAWC. These results also indicated that a drought stress index decreased with increasing PAWC and then stagnated at high PAWC. Under the high emission scenario RCP8.5, drought stress was expected to decline or stay about the same due to elevated CO_2 compensation effect. Therefore, to maintain or increase yield potential in response to the projected climate change, increasing cultivar tolerance to heat stress and improving crop management to reduce impacts of water stress on lower plant available water holding soils should be a priority for the genetic improvement of wheat in eastern Australia.

Keywords: GCMs; heat stress; water stress; wheat yield; APSIM model; PAWC

6.1 Introduction

Global Climate Models from the Coupled Model Intercomparison Project phase 5 (CMIP5) multi-model dataset point to a significant increase in mean temperature and marked shifts in the distribution of rainfall patters (IPCC 2013). In a warmer future climate, most GCMs also predict a substantial increase in the frequency and severity of extreme weather events. Changes in climate and extreme weather events are likely to affect agricultural crops (Porter & Semenov 2005, Gornall et al. 2010, Moriondo et al. 2011, Barlow et al. 2015).

*: This chapter has been submitted for publication.

The occurrence of extreme high temperature during sensitive stages of crop development, such as the period around anthesis, could reduce grain yield due to its direct effect on grain number and grain weight (Stone & Nicolas 1994, Wollenweber et al. 2003, Talukder et al. 2014). The individual grain mass and the grain set can be substantially reduced if a cultivar, sensitive to heatstress, is exposed to even a short period of high temperature around flowering (Talukder et al. 2010). For example, in a field experiment on the combine effects of CO_2 and temperature on the grain yield Nuttall et al. (2013) showed that a temperature of 36 to 38 ˚C around flowering (6 days after anthesis) could result in a high number of sterile grains (grain number reduced by 12%) and therefore 13% grain yield loss. A modelling study for the main wheat growing regions in Australia showed that variations in average growing-season temperature of 2 ˚C caused reductions in grain production of up to 50% (Asseng et al. 2011). Therefore, mitigating the impacts of heat stress on crop yield is one of crucial tasks for securing food under a future changing and variable climate.

Numerous simulation studies, linking projected climate data from climate models to crop models, have assessed the effects of heat and drought stress in combination or isolation on crop yield under future climate change in rainfed cropping systems (Semenov & Shewry 2011, Gourdji et al. 2013, Deryng et al. 2014, Lobell et al. 2015). Using climate projections from the CMIP3 multi-model ensemble with LARS-WG weather generator, Semenov and Shewry (2011) demonstrated that droughts would not increase vulnerability of wheat in Europe. It is noteworthy that relative yield losses from water stress were likely to decrease due to earlier maturity avoiding terminal drought stress. Lobell et al. (2015) found that the significant direct damage to wheat crop from heat stress was increasing and estimated that aggregate yield impacts of heat stress might equal drought impacts for wheat by the mid-21st century. The combination of increasing CO_2 and associated climate changes was likely to gradually reduce the drought exposure in northeast Australia. However, previous analyses modelling the effect of water stress on wheat have been limited to using single soil type at specific sites. Furthermore, there are many uncertainties in these projections due to uncertainty in future greenhouse gas emissions. Finally, linking crop simulation models to projected climate data for the future from climate models at specific locations is not straightforward. Indeed, the spatio-temporal scale mismatches between GCMs and crop simulation models must be bridged through downscaling methods.

It is well-know that under the same climatic conditions, soil characteristics are the key to sustaining agricultural production. Soil can provide a buffer to store water and supply it to the crop and therefore minimize the effects of severe drought. However, the soil's ability to support crop growth is largely dependent upon its water-holding and supply capacity. Soils with larger plant available water holding capacity (PAWC) are generally higher yielding as high PAWC can lead to

more water use and reduce water leakage below the crop root zone, resulting in increased rainfall use efficiency and decreased offsite impacts (Morgan et al. 2003, Wong & Asseng 2006, 2007, Wang et al. 2009a). Wong and Asseng (2006) showed a linear increased of measured wheat yield with soil PAWC of the top 100 cm of the soil profile in West Australia, which was consistent with crop model simulated results from Wang et al. (2009a). However, soil PAWC does not change the crop water use efficiency, but change the availability of water to crops (Wang et al. 2009a). Although efforts have been made to evaluate the impact of PAWC on crop yields, little evidence is available to prove how water stress responds to soil PAWC as a result of climate change.

The New South Wales (NSW) wheat belt contains 29.3% of the Australian wheat planted area and accounts for 28.7% of Australia's wheat production (averaged by 2003-2014) (http://www.abs.gov.au). It is among the most vulnerable regions in Australia due to its great reliance on climate. Extreme events in the NSW wheat belt have been predicted to increase in frequency, length and intensity by the end of the century (Alexander & Arblaster 2009, Lewis & Karoly 2013, Wang et al. 2016). However, it is not yet clear what the extent of yield losses resulting from water stress or heat stress will be under future climate change in this particular region. In addition, the lack of daily temperature and rainfall data for future climate has been a major obstacle to demonstrate the site-specific impact assessment of climate change on crop production. This study accounted for uncertainties in future climate conditions by considering two scenarios for future atmospheric greenhouse gas concentrations. I used a statistical downscaling method to downscale GCM projections from the CMIP5 ensemble to a local scale. The use of statistical downscaling in climate change studies allows exploration of the effect of changes in mean climate as well as changes in climatic variability and extreme events (Ahmed et al. 2013, Wang et al. 2016). A wheat simulation model was used to simulate impacts of climate change on wheat yield based on different soil types across a range of wheat cropping regions in eastern Australia.

The objectives of this study were to (1) quantify change in the probability of heat stress around flowering; (2) quantify the relative yield loss due to water stress across different soils. I focus on the analyses of two 30-year simulations: the first examines the time period 1961-1990 (referred to as 'present'), the second the period 2061-2090 (referred to as 'future'), based on the latest greenhouse gas emissions and GCM projections. Here I present the results of a study of the impacts of heat stress and water stress on wheat yield involving 12 soil types for a great degree of soil variability and six represented sites across the NSW wheat growing area.

6.2 Materials and methods

6.2.1 Study sites, climate and soil data

The NSW wheat belt is located between the arid interior of Australia and the Great Dividing Range to the east. The topography is characterized by plains in the west and slopes in the east. The climate is Mediterranean (with winter-dominant rainfall) characterized by large inter-annual variations in rainfall. Six sites, representing different agro-climatic zones within the wheat belt, were selected for this study (Fig. 6.1). The principal characteristics of these sites are summarized in Table 6.1. The two northern sites (WA, MP) are relatively warm and the three western sites (WA, LA and BA) are relatively dry. Sites to the south and east are cooler and wetter, respectively.

Daily climate data (maximum and minimum temperature, rainfall and solar radiation) for 1961-1990 for the six study sites were extracted from the SILO patched point observational dataset (PPD, http://www.longpaddock.qld.gov.au/silo/ppd/index.php) (Jeffrey et al. 2001). Daily climate data for 2061-2090 were also derived for each site from simulations of 28 different CMIP5 GCMs (Wang et al. 2015b) of two different Representative Concentration Pathways (RCPs) (Van Vuuren et al. 2011) (RCP4.5 and RCP8.5) using a statistical downscaling method. Briefly, monthly GCM output data (solar radiation, rainfall, daily maximum and minimum temperature) from 28 GCMs were firstly downscaled to the observed sites using an inverse distance-weighted interpolation method. Biases were then corrected using a transfer function derived from interpolated GCM data and observed data for the sites. Daily climate data for each site for 1900-2100 were generated by a modified stochastic weather generator (WGEN) with parameters derived from the bias-corrected monthly data. The detailed description of this method can be found in Liu and Zuo (2012). This method has been widely applied in recent climate change impact studies in Australia (Wang et al. 2015b, Guo et al. 2016, Liu et al. 2016).

Table 6.1 Average wheat growing season (April to November) temperature and rainfall (1961-1990) at the six study sites.

Site	Acronym	Latitude	Longitude	Maximum T (˚C)	Minimum T (˚C)	Mean T (˚C)	Rainfall (mm)
Walgett	WA	-29.66	148.12	23.9	9.6	16.7	268.2
Moree Plains	MP	-29.50	149.90	23.0	9.0	16.0	331.8
Lachlan	LA	-33.10	146.85	20.6	7.8	14.2	287.3
Mudgee	MU	-32.60	149.60	19.4	5.6	12.5	450.5
Balranald	BA	-34.20	143.50	20.7	7.6	14.1	212.9
Wagga Wagga	WW	-35.05	147.35	18.1	6.6	12.4	396.8

Soils vary widely in their soil water retention characteristics, ranging from shallow sandy soil, with minimal capacity to retain soil water, to deep clay soils, with great capacity to retain soil water (Table 6.2). Each study site has at least one soil type that is representative of the area. These 12 soils were selected from the APSOIL database according to PAWC ranging from 72 to 293 mm, step by approximately 20 mm (Liu et al. 2014). These soils provide a potential maximum rooting depth of the wheat crop, which ranges from 120 to 180 cm. Although some of the soils may not be found at all the six study sites, it was assumed that the spatial variation of the soils at any one site can give a range of PAWC and therefore that the range represented by the soils in Table 6.2 is reasonable (Wang et al. 2009a). Soil hydraulic parameters are shown in Fig. 6.2.

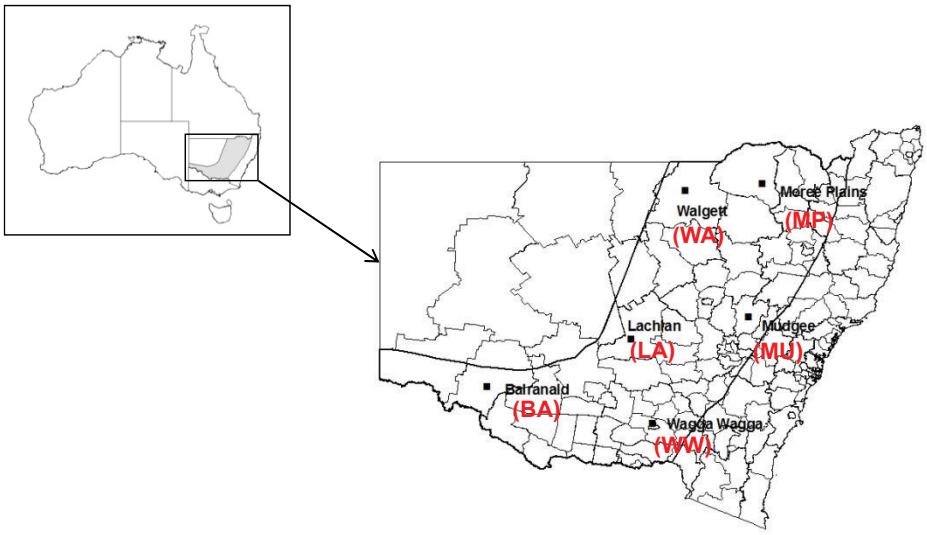

Fig. 6.1 The six selected sites used in this study.

6.2.2 Wheat simulations

APSIM (Agricultural Production System sIMulator) version 7.7 (www.apsim.info) (Holzworth et al. 2014) was used to evaluate the effect of future climate change on wheat yields at the six sites. The APSIM model has been well-tested for many modern wheat cultivars and is able to sufficiently simulate the behaviour of crops exposed to a wide range of conditions including those in the Australian wheat belt (Asseng et al. 1998, Keating et al. 2003, Ludwig & Asseng 2006). It has been widely used in studies of the effects of climate change on wheat productivity and water use in Australia (Chenu et al. 2013, Lobell et al. 2015, Yang et al. 2016). The model is an appropriate tool for determining potential yield which is defined as the yield of an adapted crop cultivar grown under favourable conditions without growth limitations from water, nutrients, pests or diseases. A potential

yield (Y_p) calculated using the APSIM model in this study is defined as the yield of an adapted crop cultivar when grown under favourable conditions without growth limitations of water, nutrients, pests, disease or other non-climatic factors (Evans 1996). It is a benchmark for systems in semi-arid climates with insufficient water supplies to avoid water stress. In this case, automatic irrigation (full irrigation) in APSIM was set to eliminate water stress. The definition of water-limited crop yield (Y_w) is similar to Y_p, but crop growth is limited by water supply. Water-limited yield is equivalent to water-limited potential yield for rain-fed crops.

The Liu and Zuo (2012) downscaling procedure used in this study is somewhat effective at correcting the biases in the monthly GCM. However, the bias correction approach used in the downscaling procedure is largely limited to correcting stationary biases in the GCM output and cannot fully account for biases that are non-stationary during the training period. Therefore, the downscaled daily data for a period that might be different from the training period and may have residual biases in some cases. In order to minimise the impact of these on crop model outputs, Yang et al. (2016) applied a simple additional bias correction called secondary bias correction to the outputs of model simulations forced with the downscaled data. In this study, crop simulation outputs Y_w and Y_p were also corrected by a secondary bias-correction procedure according to Yang et al. (2016) in order to minimise the impact of biophysical biases in the downscaling procedure on outputs of crop model simulations.

Table 6.2 The 12 soils used in this study including soil type, soil depth, plant available water capacity (PAWC).

No.	Mainly distributed region	Soil type	Soil depth (cm)	PAWC (mm)
S1	Riverina	Loam (Caldwell-Womboota 2 No616-YP)	150	72
S2	Upper Western	Sandy Clay over Clay (Wirracanna site 8 No561-YP)	120	86
S3	Upper Western	Clay (Wirracanna site 6 No563-YP)	120	111
S4	North West Slopes and Plains	Grey Vertosol (Walgett No1016)	180	131
S5	North West Slopes and Plains	Grey Vertosol (Pilliga No1014)	180	155
S6	Riverina	Sandy Loam over Clay (Rand No211)	150	170
S7	Central West Slopes and Plains	Grey Vertosol (Forbes No546-YP)	150	188
S8	Central West Slopes and Plains	Clay over Sandy Clay (Eugowra No196)	180	209
S9	North West Slopes and Plains	Grey Vertosol-Light Brigalow (Tulloona No102)	150	239
S10	Riverina	Grey Vertosol (Urana No541-YP)	150	251
S11	North West Slopes and Plains	Grey Vertosol-Heavy Brigalow (Tulloona No101)	150	266
S12	Riverina	Wunnamurra Clay (Jerilderie No542)	180	293

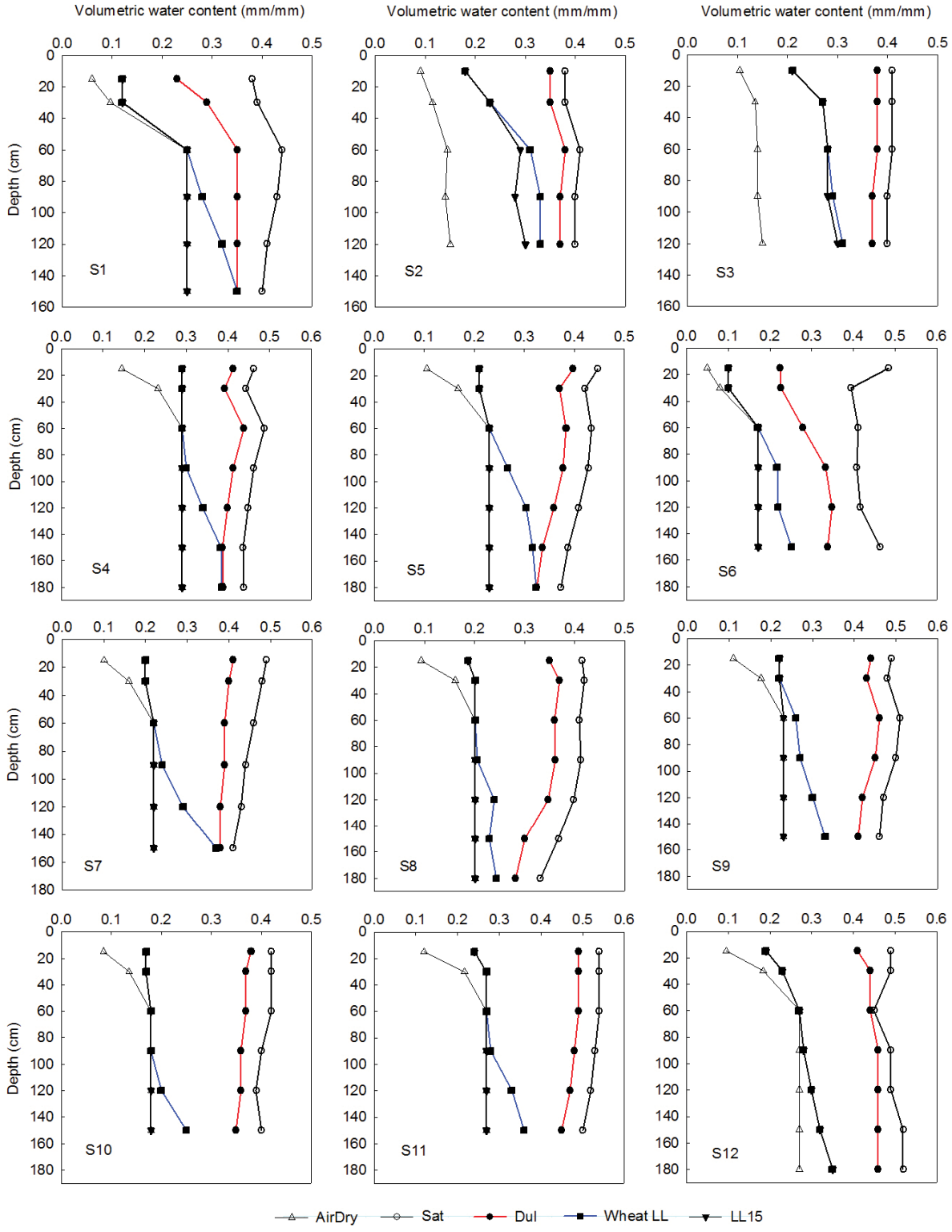

Fig. 6.2 APSIM soil parameters used to define plant available water capacity (PAWC) and values of soil water reset for 12 soil types (S1-S12) used in this study. Sat is the saturated water content. DUL represents the drained upper limit of soil water. Wheat LL stands for crop lower limit. LL15 is the

15Bar lower limit of soil water. Soil water reset to wheat LL each year on 1 January.

Elevated levels of atmospheric CO_2 in the plant module of APSIM affects crop growth by influencing RUE, transpiration efficiency and critical leaf nitrogen concentration. However, APSIM has no facility to ingest time-varying values of CO_2 concentration. Therefore, a function was added to APSIM whereby yearly atmospheric CO_2 concentrations were calculated using empirical functions of calendar year during 1900-2100 (Liu et al. 2014). For RCP4.5 scenario, the atmospheric CO_2 concentration was calculated by:

$$[CO_2]_{year} = 650.18 + \frac{0.000075326*y-0.16276}{0.00022299-\frac{727.97}{y^2}} - 0.00018747 * (y - 2045)^3 \qquad (1)$$

For RCP8.5, it was fitted by:

$$[CO_2]_{year} = 1034.3 + \frac{267.78-1.6188*y}{4.0143+\frac{53.342}{y^{5.2822}}} + 21.746 * \left(\frac{y-2010}{100}\right)^3 + 100.65 * \left(\frac{y-1911}{100}\right)^3 \qquad (2)$$

These equations set atmospheric CO_2 concentrations approximately equal to the multi-model mean mid-range carbon cycle projections for RCP4.5 (520 ppm) and RCP8.5 (720 ppm) during study period 2061-2090 (Van Vuuren et al. 2011).

The difference in volumetric water content between drained upper limit (DUL) and wheat lower limit (wheat LL) is calculated as plant available water capacity (PAWC), which represents the 'bucket' size for water stored by the soil that is available for use by a crop (Asseng et al. 2001, Yang et al. 2014). DUL is defined as the amount of water that a soil can hold after drainage has been significantly slowed and wheat LL refers to the lowest water content at which a wheat crop can extract water. In practice, high wheat yield has been associated with high PAWC in rain-fed conditions (Oliver et al. 2006, Wang et al. 2009a). With rainfall and surface evaporation being equal which depends on the amount and frequency of rainfall, a soil with a low PAWC provides less water to a crop than a soil with a high PAWC. This study focuses on the effect of PAWC on the impact of climate change on wheat yields simulated by APSIM. Other soil parameters, such as soil pH, were set to the same value between the 12 soil types considered.

In simulations presented in this chapter, the wheat sowing window was set from 1 April to 31 July (Zhao et al. 2013). Wheat was sown every year when cumulative rainfall in ten consecutive days exceeded 25 mm, or when the end of sowing window was reached (Wang et al. 2009c). Two wheat cultivars, Waagan and Bolac, were widely sown in NSW wheat belt (Matthews et al. 2014). To

optimally use the available resources (light, temperature, water and nutrients), Bolac was selected for sowing date between April 1 and May 20 (early start to season) and Waagan between May 21 to July 31 (late start to season). Sowing density was 120 plants m^{-2}, at a depth of 3 cm. Summer rainfall is important in the northern NSW wheat belt. However, to exclude the "carry-over" effects from previous seasons, simulations were reset on 1 January of every year, with soil organic carbon (OC) reset to 1.2% and soil profile mineral N reset to 35 kg ha^{-1} nitrate-N and 15 kg ha^{-1} ammonium-N in the top of soil, rapidly declining with depth, with wheat stubble reset to 1000 kg ha^{-1} and a soil C:N ration of 12, soil water reset to wheat crop lower limit (Fig. 6.2) (Asseng et al. 2000, Oliver et al. 2010b). Each year, 100 kg ha^{-1} N fertiliser was applied at sowing date and another 50 and 100 kg ha^{-1} N fertiliser were added at the juvenile and initial flowering stage, respectively (Luo et al. 2009, Wang et al. 2009c). The high level of N application used was to avoid any nitrogen stress of the crop so that simulated wheat yield was a reflection of climate change rather than fertiliser management in the APSIM model.

6.2.3 Heat and drought stress indices

In this study, heat stress around flowering date (P_{HSF}) was defined as probability of the daily maximum temperature exceeding 30 ˚C from 100 ˚Cd before flowering to 100 ˚Cd after flowering. I mainly focused on extreme temperature during the short period surrounding anthesis in which grain set is particularly sensitive to heat stress. A drought stress index (DSI) (Semenov 2009, Vanuytrecht et al. 2014) was defined as:

$$DSI = \frac{Y_p - Y_w}{Y_p} * 100\% \qquad (3)$$

where Y_w and Y_p are water-limited and potential grain yields. The greater the DSI, the higher the water stress because DSI measures the percentage of the yield reduction from the potential yield due to water stress.

6.3 Results

6.3.1 Projected changes in growing season temperature and rainfall

Fig. 6.3 shows changes in growing season (April to November) temperature and rainfall by 2061-2090, relative to 1961-1990, based on the downscaled data for the 28 GCMs for RCP4.5 and RCP8.5. The data for all GCM simulations show warming for all six sites. The increases in

temperature were greatest for the high-concentration scenario (RCP8.5) than for the low-concentration scenario (RCP4.5). Although the eastern sites (MP, MU and WW) have lower mean temperatures (Table 6.1), the simulated temperature increases were more for these sites than for the western sites (WA, LA and BA) (Fig. 6.3a). The largest warming occurred in MU, with ensemble-mean warmings of 2.3 ˚C for RCP4.5 and 3.8 ˚C for RCP8.5. In contrast, the lowest increase was found in BA, with ensemble-mean warmings of 1.9 ˚C for RCP4.5 and 3.2 ˚C for RCP8.5.

The changes in growing season rainfall showed large variations between GCMs, which indicates large uncertainty. Some GCMs projected increasing rainfall but most GCMs indicated decrease. Changes in rainfall were more pronounced for RCP8.5 than for RCP4.5. Overall, projected rainfall at northern sites (WA and MP) declined more than that at the remaining four sites. The greatest ensemble-mean decreases in rainfall occurred in MP, 7.1% for RCP4.5 and 9.4% for RCP8.5, while the smallest decreases were for MU, 3.2% and 4.5% for RCP4.5 and RCP8.5, respectively.

6.3.2 Change in days to flowering and probability of heat stress around flowering

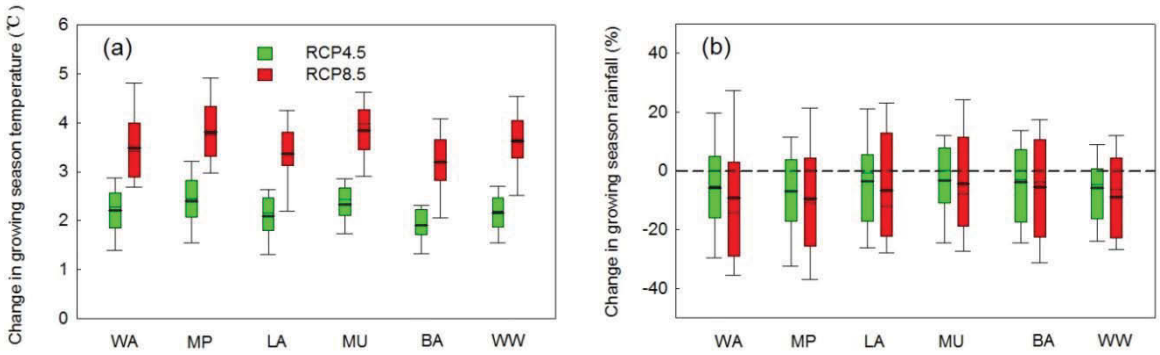

Fig. 6.3 Projected changes in wheat growing season (April-November) (a) mean temperature and (b) rainfall in 2061-2090 relative to the baseline (1961-1990) under RCP4.5 and RCP8.5 using 28 GCMs for six sites in the NSW wheat belt. Box boundaries indicate the 25th and 75th percentiles; the black thin and thick lines within the box mark the median and mean, respectively; whiskers below and above the box indicate the 10th and 90th percentiles.

APSIM simulated results indicate that the future climate changes could have a large impact on wheat flowering. Fig. 6.4a shows change in days to flowering for 2061-2090 relative to 1961-1990 under RCP4.5 and RCP8.5. The length of period from sowing to flowering was clearly shortened

under future climate scenarios for all six sites due to increasing temperature. For RCP4.5, the ensemble-mean days to flowering averaged across the six sites was shortened by 15.8 days. For RCP8.5, the equivalent value is 23.8 days. The largest shift in days to flowering was found in MU with an ensemble mean of 19.8 and 32.0 days for RCP4.5 and RCP8.5, respectively. The smallest change in vegetative period occurred in WA, where the number of days was shortened by 12.0 and 17.7 days for RCP4.5 and RCP8.5, respectively. Fig. 6.5a shows days to flowering were negatively correlated to growing season mean temperature. It was shortened by approximately 5.2-8.4 days for each 1 ˚C rise in growing season mean temperature, depending on locations. Changes in days to flowering in cool sites (MU and WW) were more sensitive to temperature change than in warm sites (WA and MP).

Fig. 6.4b shows changes in the probability of heat stress (daily maximum temperature exceeding 30 ˚C within 100 ˚Cd of flowering). Although increases in temperature accelerate wheat development, bringing forward flowering date, the risk of heat stress around anthesis is still severe in the future. Overall, heat stress probability increased more under RCP8.5 than under RCP4.5 for all six locations. Heat stress increased most at the two northern sites (WA and MP) for RCP8.5 due to higher temperature and less shift in days to flowering than the other sites. In contrast, the smallest increase was found at the cool MU and WW sites, which can be partly attributed to larger advances in flowering date. Fig. 6.5b shows the relationships between simulated ΔP_{HSF} and growing season maximum temperature (ΔT_{max}). ΔP_{HSF} was positively correlated to ΔT_{max} across the six sites. The response of ΔP_{HSF} to ΔT_{max} varied among locations. In the three western sites, on average, ΔP_{HSF} increased by 3.5% for each 1 ˚C increase in maximum temperature, which is higher than that in the three eastern sites (on average, 2.2% $^{\circ}C^{-1}$). It is noteworthy that the largest response was found in the warm site MP (3.0 % $^{\circ}C^{-1}$) while the smallest response was observed in the cool site MU (0.5% $^{\circ}C^{-1}$).

6.3.3 Changes in potential yield

Potential yields were simulated by APSIM under full irrigation conditions and thereby only affected by changing temperature, solar radiation and atmospheric CO_2 concentration. Y_p showed small variations between the 28 GCMs for each soil type (Fig. 6.6). Soil conditions play an important role in determining yield. However, the yield response plateaus at high PAWC values (greater than about 210 mm). Ensemble-mean Y_p based on the 28 GCMs increased by 2.7-6.0% for RCP4.5 and 2.5-5.8% for RCP8.5 for four sites (WA, LA, BA and WW). There was no large overall difference in potential yield change between the two RCPs. However, Y_p decreased by 2.0% in MP and by 0.8% in MU under the high-concentration RCP8.5 scenario, which can be attributed to greater warming

accelerating phenological development, resulting in less received solar radiation and nutrients to grow over the course of the growing season.

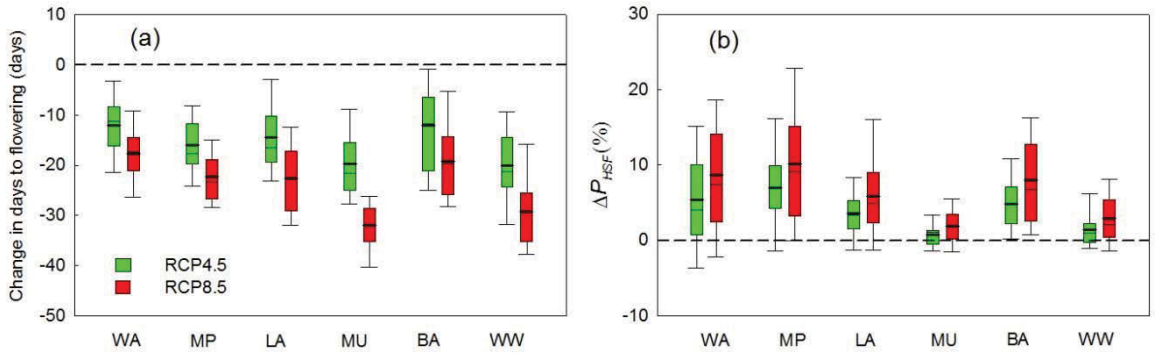

Fig. 6.4 Simulated change in days to flowering and probability of the occurrence of heat stress with daily maximum temperature exceeding 30 ˚C around flowering (± 100 ˚C days) (ΔP_{HSF}) in 2061-2090 relative to baseline (1961-1990) under RCP4.5 and RCP8.5 using 28 GCMs for six sites in the NSW wheat belt. Box boundaries indicate the 25th and 75th percentiles; the black thin and thick lines within the box mark the median and mean, respectively; whiskers below and above the box indicate the 10th and 90th percentiles.

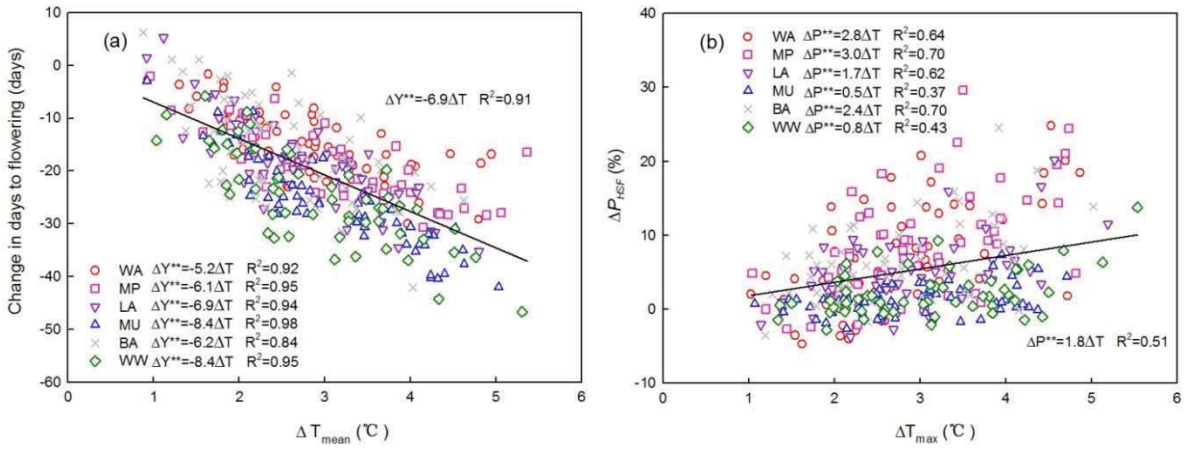

Fig. 6.5 Relationships between simulated change in days to flowering and change in growing season (April to November) mean temperature (ΔT_{mean}) (a), change in heat stress around flowering date (ΔP_{HSF}) and change in growing season maximum temperature (ΔT_{max}) (b) across six sites in the NSW wheat belt. The effect of a change in temperature was fitted using linear regression. ** indicates the significant level of P<0.01.

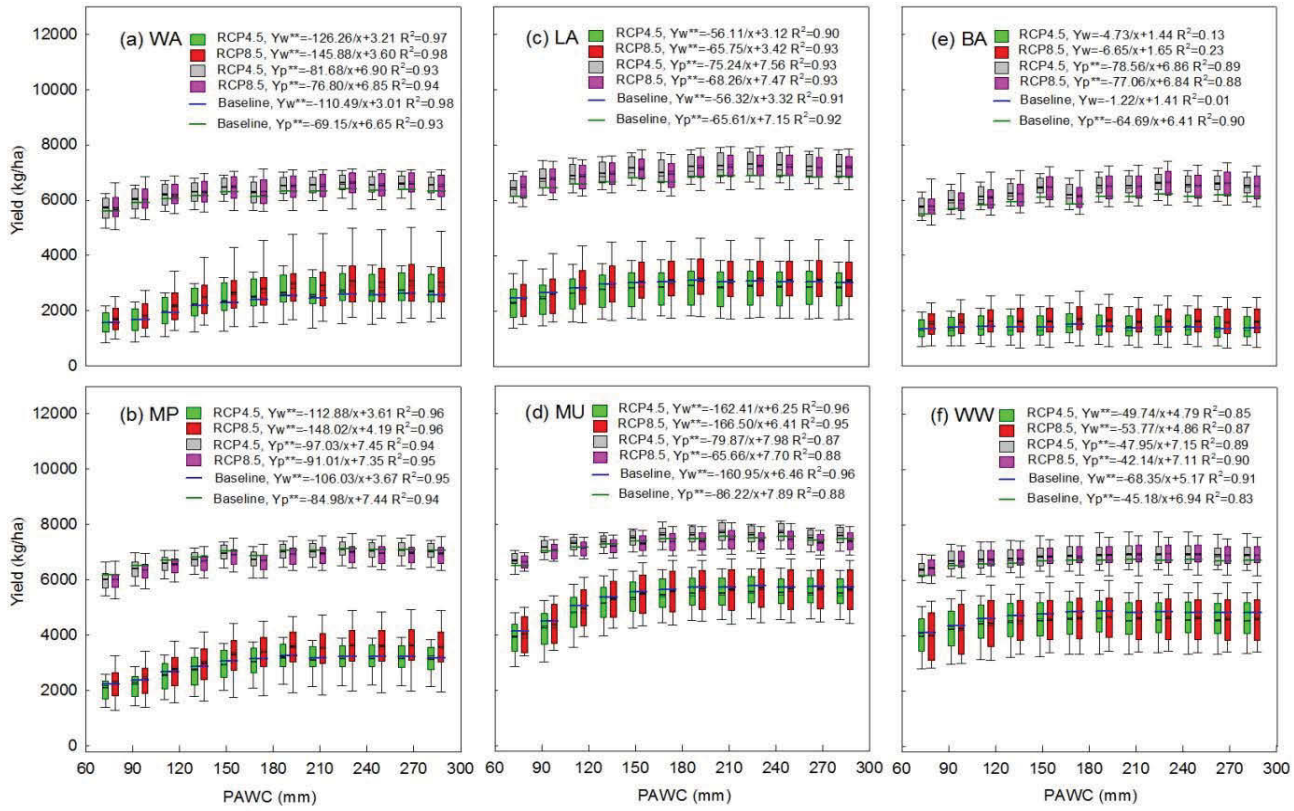

Fig. 6.6 APSIM simulated potential (Y_p) and water-limited (Y_w) wheat yield for the baseline (1961-1990) and for 2061-2090 using 28 GCMs under RCP4.5 and RCP8.5 across plant available water capacities (PAWC) for six sites (a-f) in the NSW wheat belt. Box boundaries indicate the 25th and 75th percentiles; the black thin and thick lines within the box mark the median and mean, respectively; whiskers below and above the box indicate the 10th and 90th percentiles. Regression coefficients of the relationship between wheat yield (Y_p and Y_w) and plant available water capacity (PAWC, x) for baseline and two RCPs for six sites in the NSW wheat belt, as descripted by $Y = a/x + b$. The fitted coefficients a and b are the order of magnitude of 10^3. ** indicates the significant level of P<0.01 for the regression model.

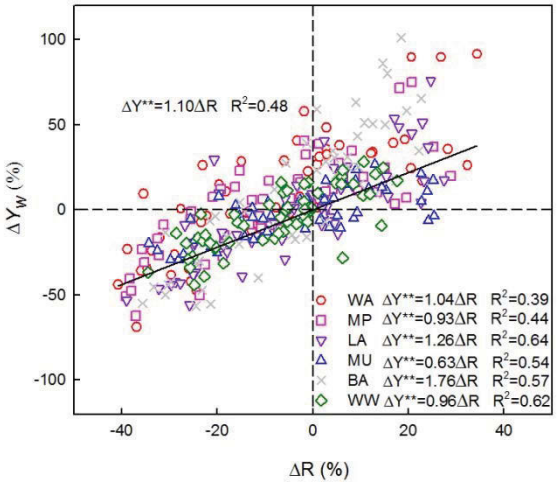

Fig. 6.7 Relationships between APSIM simulated change in water limited yield (ΔY_w) and growing season rainfall (ΔR) for six sites in the NSW wheat belt. The effect of a change in rainfall was fitted using linear regression. ** indicates the significant level of P<0.01.

6.3.4 Changes in water limited yield

In addition to temperature, radiation and CO_2 concentration, Y_w is also limited by water supply, and hence by rainfall and soil properties in APSIM model. Increasing yield with increasing PAWC occurs when the crops need to use water stored deep in the profile. A high PAWC can provide a buffer to crops, reducing the sensitivity to the temporal distribution of rainfall. The response of Y_w to PAWC differs due to the amount of growing season rainfall. Similar to Y_p, a curvilinear response to yield can be seen in Y_w. At wet sites (e.g. MU), soils with higher PAWC have a greater water reserve to meet crop water demand. By contrast, at dry sites (e.g. BA) there was no significant relationship between yield and PAWC as wheat mostly survives from current low rainfall. Water storage in soils with higher PAWC is not fully utilized due to incomplete profile wetting by limited growing season rainfall. In addition, most rain-fed crops suffer at least short-term water deficit at some point during the growing season, and thus the climate impacts are more variable for Y_w compared to Y_p. There were large variations in Y_w between the 28 GCMs for each soil type (Fig. 6.6). Simulation results showed that water limited yield is substantially affected by growing season rainfall (Fig. 6.7) and this large variation is likely due to the large variation in rainfall changes between the GCMs. The highest Y_w occurred for the wet sites MU and WW (Fig. 6.6d and f) while lowest Y_w was found in dry site BA (Fig. 6.6e). There was an overall strong positive relationship between yield change and growing season rainfall (R^2=0.48) (Fig. 6.7). This suggests that growing season rainfall is the most important yield determining factor at these six study sites. Moreover, the western dry sites have larger response

to growing season rainfall than that of eastern wet sites. However, increasing PAWC resulted in low response of Y_w to rainfall except dry site BA (Fig. 6.8). In other words, soils with higher PAWC are less affected by growing season rainfall compared with soils with lower PAWC.

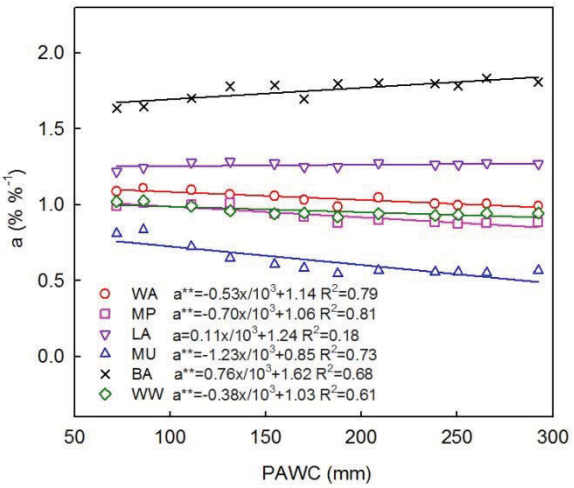

Fig. 6.8 Impact of plant available water capacities (PAWC) on the regression slope a ($\Delta Y_w = a\Delta R$) between change in APSIM simulated water-limited yield (ΔY_w) and change in growing season rainfall (ΔR) for six sites in the NSW wheat belt. The slope a is % yield change per % rainfall change. ** indicates the significant level of P<0.01.

The ensemble-mean Y_w value was higher for RCP8.5 than for RCP4.5 in the warm and dry sites (Fig. 6.6a and e), which indicates that higher atmospheric CO_2 concentrations can offset the increasing negative effects of decreased rainfall during the growing season and shortened growth period in rain-fed conditions. There was an interaction between higher temperature, rainfall and elevated CO_2. Rising CO_2 concentration is expected to decrease plant water stress due to improved transpiration efficiency. Overall, changes in Y_w depended on location and scenario. For example, simulated Y_w increased for the warm site WA, ensemble-mean changes of 3.6% and 15.2% for RCP4.5 and RCP8.5, respectively (Fig. 6.6a). Similarly, for the dry site BA, Y_w increased by 0.5% for RCP4.5 and 14.7% for RCP8.5 (Fig. 6.6e). Earlier flowering due to higher temperatures moves the grain filling period to a cooler wetter part of the season which can increase grain yield by avoiding severe summer drought. However, Y_w decreased in MU and WW because warmer growing season temperatures reduce the length of the growth period so less nutrition and radiation are received, which results in lower biomass production.

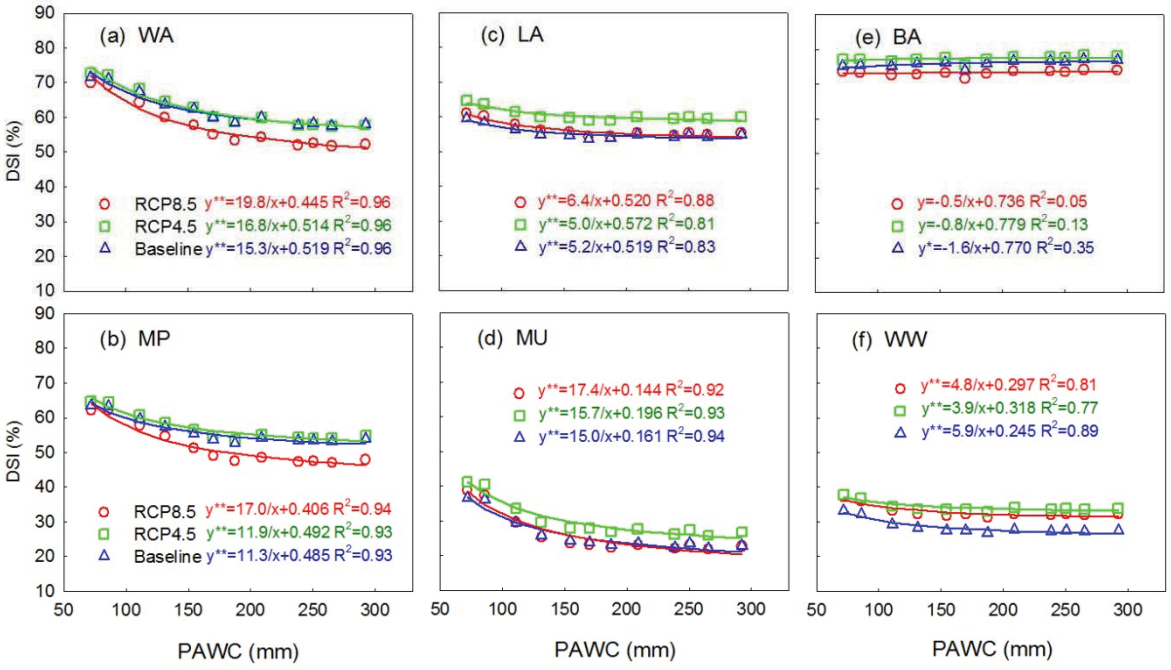

Fig. 6.9 Impact of plant available water capacities (PAWC) on drought stress index (DSI) for six sites in the NSW wheat belt. The effect of a change in PAWC was fitted by equation $DSI = a/x + b$. * and ** indicate the significant level of $P<0.05$ and $P<0.01$, respectively.

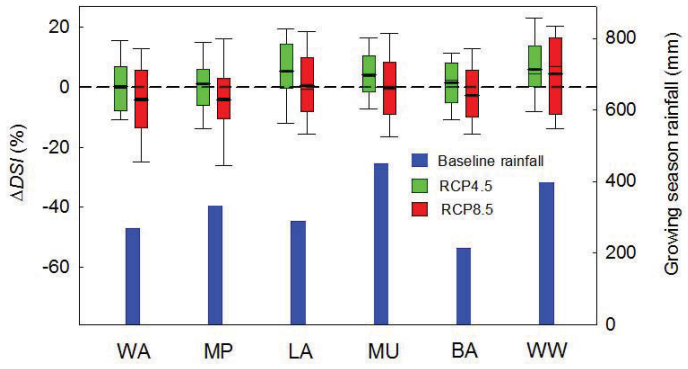

Fig. 6.10 Change in drought stress index (DSI) in 2061-2090 relative to baseline (1961-1990) under RCP4.5 and RCP8.5 using 28 GCMs averaged across 12 soils for six sites in the NSW wheat belt. Box boundaries indicate the 25th and 75th percentiles; the black thin and thick lines within the box mark the median and mean, respectively; whiskers below and above the box indicate the 10th and 90th percentiles.

6.3.5 Changes in relative yield loss

Simulated results also indicate that PAWC had a significant impact on the relative yield loss. However, the response of DSI to PAWC depended on location and soil type. For the dry site BA, where water stress is relatively severe, DSI was high for all 12 soils (about 75%, Fig. 6.9e) and there was no relationship between DSI and PAWC. In contrast, a lower DSI was found at the wetter sites MU and WW (Fig. 6.9d and f), which significantly decreases with increasing PAWC and plateaus at a higher PAWC. As a result, increase in soil PAWC tended to reduce water stress at high rainfall sites. Fig. 6.10 shows ΔDSI under RCP4.5 and RCP8.5 averaged across the 12 soils. For RCP4.5, simulated ΔDSI increased with a mean value of 5.4%, 4.1% and 6.0% in LA, MU and WW, respectively. However, for RCP8.5 ΔDSI is expected to decline or stay about the same across all six sites, except WW. Despite a decrease in rainfall during the growing season, relative yield losses from water stress are predicted to be smaller in the future than at present. Wheat can benefit from higher CO_2 concentration in the atmosphere arising from high emission RCP8.5 in 2061-2090.

6.4 Discussion

Previous studies have constructed climate scenarios by linearly manipulating historical weather records with regional average GCM-simulated climate changes (Wang et al. 2009c, Asseng et al. 2013, Potgieter et al. 2013). In this approach, the future variability of the climate is kept consistent with the variability of the historical weather records (Ludwig & Asseng 2010). Namely, the variability for the historical climate (still very large in a Mediterranean climate) and future climate scenarios is kept the same. In this study, I used statistical downscaled data derived from the state-of-the-art CMIP5 GCMs to generate future climate scenarios in which climate variability was allowed to change. This was important as the focus of the study was on stresses to wheat crops resulting from climate extremes.

The analysis considered data derived from 28 different GCMs for six sites in eastern Australia. The use of many GCMs was important to capture the uncertainty in future projections that arises from uncertainties in model structure and parameterization (Lobell et al. 2015). Multi-model mean climate changes from this method are consistent with recently developed climate change projections for Australia. Under RCP4.5, the multi-model mean growing season mean temperature increased by 2.2 ˚C averaged across locations for the period 2061-2090 relative to 1961-1990. The equivalent value for RCP8.5 was 3.6 ˚C. CSIRO and BoM (2015) projected annual mean temperature increases of 1.9 ˚C for RCP4.5 and 3.9 ˚C for RCP8.5 in eastern Australia for the time period 2080-2099. Wheat growing season rainfall decreased by 4.9% for RCP4.5 and 7.4% for RCP8.5 averaged across locations. These

changes are also consistent with the findings of CSIRO and BoM (2015), which stated that climate models projected a decrease in spring and winter rainfall in the late 21st century.

The results indicated that simulated potential yield increased for both RCPs in most study sites. However, the difference in potential yields between the RCPs were small due to interactions such as higher temperatures offsetting greater CO_2-induced yield gains for RCP8.5 (Balkovič et al. 2014, Araya et al. 2015). The effects of climate change on water limited yield depended on location. Rain-fed yield increased at warm and dry sites, which can be attributed to earlier flowering moving the grain filling period to a cooler wetter part of the season and thus increasing grain yield in case of terminal drought (Sadras & Monzon 2006, Moriondo et al. 2011). In contrast, yields decreased at wet and cool sites because warmer temperatures accelerated phenological development, resulting in less intercepted nutrition and radiation and consequently lower biomass production over the course of the growing season. However, there were interacting effects of temperature, rainfall and CO_2 concentration on wheat yields (Ludwig & Asseng 2006), which were not exhaustively explored in this study.

APSIM phenological model differed from that used in previous study with the Vernalizing-Photothermal model, which simulates the development rate as a non-linear vernalization function incorporated into the thermal and photothermal additive models (Liu 2007). In APSIM, the time to flowering and maturity is calculated as a multiplicative function with a three-stage linear vernalization response, and wheat development is mainly controlled by the daily thermal time and increased growing season temperature will increase the rate at which thermal time accumulates. Therefore wheat will flower at the same day under water-limited or full irrigated conditions. APSIM simulated results showed that, despite flowering date occurring earlier, the probability of heat stress around flowering still increased by 2061-2090 for both RCPs, which were consistent with results with the Vernalizing-Photothermal model. Therefore, future climate conditions would be likely to cause more frequent wheat failure across this region. Additionally, higher temperatures reduce the length of the growing season, which results in lower biomass production (Asseng et al. 2011, Stratonovitch & Semenov 2015). It might be beneficial to develop cultivars with higher thermal requirements and later maturity that are capable of coping with an increased heat stress around flowering.

The two cultivars were used in the same APSIM simulations to represent the fact that farmers choose different cultivars in different years to minimize the chance of frost or heat stress during flowering. The two cultivars were not simulated in separate simulations. Results reflect the single set of cultivar-choice simulations and are not intended to compare different cultivars. In addition, the

only difference between the simulated cultivars was in phenological response, and there were no physiological differences.

PAWC is a key determinant of crop productivity (Asseng et al. 2001, Wang et al. 2009a, Yang et al. 2014) and crops grown in a soil with high PAWC have a better chance of surviving drought conditions than with a low PAWC (Yang et al. 2014). Good soils (i.e. high PAWC) can provide a large buffer that moderates the impact of within-season variability in rainfall on yield (Wang et al. 2009a). High PAWC soils were less responsive to reductions in rainfall due to climate change. Our results showed that at wetter sites, soils with high PAWC had larger simulated water limited yields. Wheat yields increased with increasing PAWC and then the yield response stagnated at a high PAWC. However, PAWC had little impact on the yield range at a dry site like BA due to water limitation. The results presented here are partly consistent with findings of Wang et al. (2009a).

My simulation results showed DSI was higher at a dry site and PAWC also had little effect on DSI due to lack of rainfall reaching deeper soil layers. In contrast, wetter sites had low DSI, which decreased with increasing PAWC when water stored in the soil profile was available. The main limitation imposed by climate change for wheat cropping system in the NSW wheat belt is rainfall. Despite growing season rainfall decreasing under climate change for the six sites, relative yield losses for the period of 2061-2090 compared to baseline were predicted to be small, especially for high atmospheric greenhouse gas concentrations (RCP8.5). This is consistent with results from Semenov and Shewry (2011) in Europe, who demonstrated that drought would not increase vulnerability of wheat. They suggested that climate warming could result in earlier wheat flowering and maturity dates, which shift the grain filling period to a cooler and wetter part of the season, where soil water deficit still stayed at the same level, and allows the crop to avoid severe summer drought. In many Mediterranean and winter-dominant rainfall environments, grain yields are often limited by terminal drought in which case early flowering can be an advantage. Although flowering earlier with increasing temperature allowed the crop to escape increasing terminal drought (Semenov & Shewry 2011), higher atmospheric CO_2 concentrations under RCP8.5 compared to RCP4.5 can also offset the increased negative effects of decreased rainfall and shortened growth period. Therefore, a successful adaptation strategy in a drying region could be to develop an early flowering cultivar, but only up to a point where shortened growing season does not limit yields, to mitigate the impacts of water stress.

Nevertheless, drought is the most significant environmental stress in agriculture worldwide and improving yields in water-limited environments is a major goal of agronomy and plant breeding (Oliver et al. 2010a, Soussana et al. 2010). The future impacts of drought on yield will depend on soil types and the spatial and temporal patterns of climate change. An emerging threat for wheat

production in eastern Australia may result from an increase in frequency and magnitude of heat stress around flowering with potentially significant yield losses for heat sensitive wheat cultivars commonly grown in the northern parts of the NSW wheat belt. However, it is important to realize that the present study assumed no adaptive management strategies were put into practice in response to climate change and this is clearly an unrealistic assumption. However, the study did provide a clear picture of the adverse effects of climate change on wheat yield given no adaptive management strategies. In reality, farmers would likely gradually adapt to climate change. Indeed, even under current climate conditions, farmers often avoid sowing wheat crops in drought years with late starts to the growing season or only sow in some areas with sufficient stored soil water (Gomez-Macpherson & Richards 1995, Wang et al. 2015a).

Changing the sowing window could be an 'escape' strategy for avoiding adverse impacts of heat and water stress on yield. As the risk of frost strongly decreases when mean temperature increases (Zheng et al. 2012, Wang et al. 2015b), it might be viable to expand the sowing window to take advantage of some earlier planting opportunities. Moreover, the reduction in rainfall under future climate scenarios in eastern Australia has mainly occurred during the winter and spring months but not during autumn (CSIRO & BoM 2015), so farmers could benefit from the relatively wet autumns by sowing earlier. Another strategy is developing different cultivars that are better adapted to future climates. Having limited time and resources, crop scientists and breeders must select the most appropriate traits for crop improvement and should, therefore, focus on the development of wheat cultivars with higher thermal requirements (longer growing season), which are resistant to high temperature around flowering. Additionally improved water use efficiency through, for example, more efficient root systems and morphology in soils may provide some protection against excessive drought in the future.

6.5 Conclusion

I conclude that despite accelerated phenological development and earlier in flowering date in a warming climate across six sites in NSW, the probability of heat stress around flowering still increased by about 3.8% for RCP4.5 and 6.2% for RCP8.5. The risk of heat stress around flowering was especially high for warm sites under RCP8.5. Simulated potential yield across six sites increased in average by about 2.5% regardless of the emission scenario. However, simulated water limited yield tended to decline at wetter and cooler locations (MU and WW) under future climate while increased at warmer and drier locations (WA and BA). Soils with high PAWC provided a larger buffer to store water from variable rainfall and to supply it to crops during dry periods and therefore were less affected by rainfall decreases compared to soils with low PAWC. Although projected growing season

rainfall decreased, relative yield loss due to water stress was expected to decline or stay the same as a result of increased CO_2 concentration and, to some extent, earlier flowering allowing wheat to avoid severe summer drought. Therefore, to maintain or increase yield potential and respond to climate change, increasing tolerance to heat stress and improving crop management to reduce impacts of water stress on lower plant available water holding soils should be priorities for the genetic improvement of wheat in eastern Australia.

Chapter 7*

Spatial changes of wheat phenology, yield and water use efficiency under the CMIP5 multi-model ensemble projections for eastern Australia

Abstract

The New South Wales (NSW) wheat belt is one of the most important regions for winter crops in Australia, with its agricultural system being significantly affected by water stress and ongoing climate change. Statistical downscaled scenarios from selected 13 GCMs with RCP4.5 and RCP8.5 were combined with a crop simulation model to simulate wheat productivity and water use. It was found that projected multi-model median yields could increase by 0.4% for RCP4.5 and 7.3% for RCP8.5 by 2061-2100. Although the RCP4.5 showed a small decrease in median yield in the dry southwestern parts of the wheat belt, the higher CO_2 concentration in RCP8.5 compensated some of the negative effects resulting in 11.5% yield increase. These results show that drier area would benefit more from elevated CO_2 than wetter area. Without the increase in CO_2 concentration wheat yield decrease rapidly under RCP4.5 by 2061-2100 and much more so under RCP8.5 compared to the present. A decline in growing season length and a decrease in rainfall resulted in a reduction of crop water consumption. As a consequence, simulated evapotranspiration decreased by 11.9% for RCP4.5 and 18.8% for RCP8.5 across the NSW wheat belt. Increasing yields combined with decreasing ET resulted in simulated water use efficiency increasing by 11.4% for RCP4.5 and 29.3% for RCP8.5. Wheat production in water-limited, low yielding environments appears to be less negative impacted or in some cases even positively affected under future climate and carbon dioxide changes, compared to other growing environments in the world.

Keywords: GCMs; wheat yield; water use efficiency; evapotranspiration; APSIM

7.1 Introduction

Wheat is Australia's most important grain crop. About 80% of wheat is exported and Australia contributes around 15% of the world wheat trade annually (http://www.abs.gov.au/ausstats). Wheat is the main winter crop sown between April and July in the New South Wales (NSW) wheat belt. This region accounts for 27.5% of the Australian wheat planted area and 27% of total wheat production in the country was harvested in this region (Australian Bureau of Statistics, 2013-14; http://www.abs.gov.au/ausstats/abs@.nsf/mf/7121.0).

*: This chapter has been accepted for publication in Climate Research, 2017.

Increasing greenhouse gas concentrations are expecting to increase Australia's average surface air temperature and alter the temporal and spatial patterns of rainfall. Wheat growing season (winter and spring) rainfall is projected to decrease in most of the Australian continent under different future scenarios (CSIRO & BoM 2015). The NSW and Australian Capital Territory Regional Climate Modelling (NARCliM) project (Evans et al. 2014) predicted that NSW mean rainfall could decrease by 5%-20% for spring in 2060-2079 compared to 1990-2009. This is considered to be one of the most serious problems related to climate change, as water availability is a primary factor determining crop production in semi-arid dry land agricultural systems (Sinclair 2011).

There is increasing concern about a possible large impact of climate change on future Australian wheat productivity. Previous studies have tried to assess the impact of projected future climate changes on wheat phenology and yield using crop models driven by data derived from Global Climate Models (GCMs) or Regional Climate Models (RCMs) (Luo et al. 2009, Wang et al. 2009c, Yang et al. 2014, Anwar et al. 2015). For example, Luo et al. (2005) suggested that wheat yield in southern Australia could decrease by about 13.5% to 32% under the most likely climate change scenario. Wang et al. (2009c) found that wheat yields at Wagga Wagga in eastern Australia could be approximately 1% higher than recent yields around 2050 but 6% lower around 2070 under the SRES A1F1 scenario (Nakicenovic & Swart 2000) for future greenhouse gas and aerosol emissions. Yang et al. (2014) investigated the impact of future climate change on wheat productivity at six sites in the NSW wheat belt. Simulations showed that flowering dates at all sites shifted earlier by an average of 11 days between 1961-1990 and 2021-2040 under the SRES A2 emission scenario. The yield difference between the future and recent period varied from +3.4% to -14.7%. However, the magnitude of the climate change effect differed significantly between soil types and locations. Recent simulations have also indicated that the negative effect of climate warming may be offset by increasing CO_2 fertilization effect (Long et al. 2006, O'Leary et al. 2015, Fitzgerald et al. 2016). Therefore, a comprehensive approach that accounts for CO_2 fertilization is needed to assess the impacts of future climate on eastern Australia wheat productivity.

In addition to crop yield, future climate change may also impact the water balance of cropping systems. Several studies have investigated the impact of future climate change on evapotranspiration (ET) and water use efficiency (WUE) of wheat cropping systems (Asseng et al. 2004, Wang et al. 2009c, Wang et al. 2011a, Yang et al. 2016). Yang et al. (2016) described the impact of future climate change on WUE in relation to plant-available water capacity based on 18 GCMs for 12 soil types at six sites in eastern Australia. For all six sites, ET decreased by 7 to 28 mm while WUE increased by 0.7 to 1.3 kg ha^{-1} mm^{-1} by 2021-2040 relative to 1961-1990. Wang et al. (2009) found that under a high warming scenario, WUE of wheat may increase from 7 to 20% by 2050 and from 8 to 33% by

2070 at wetter sites in semi-arid southeast Australia, but decreased by 6-14% at drier sites, which implies that changes in crop yield may not be proportional to changes in water use.

Although increasing evidence suggests that ongoing climate change has had measurable impacts on crop development and productivity in Australia (Luo et al. 2003, Potgieter et al. 2013), future impacts have large uncertainties and remain imperfectly understood in terms of mechanisms and magnitude due to unpredictable aspects of climate change, such as the future amount of rainfall and how it will be distributed during the growing season. Moreover most recent studies on the impact of climate change on wheat cropping system in Australia use field-scale crop simulations (Anwar et al. 2015, Lobell et al. 2015, O'Leary et al. 2015, Zeleke & Nendel 2016). The method of using a representative site for a large area or area that has complex spatial heterogeneity can lead to significant errors (Wang et al. 2011b). Results for only a few locations may not represent the characteristics of a region (van Bussel et al. 2016) and may not properly represent the spatial pattern of climate change impacts. A reliable assessment of the spatio-temporal patterns of the impact of climate change across the major wheat-growing areas of Australia is required, and this will be most useful at a fine spatial scale.

In recent years, a number of studies, as part of the agricultural model intercomparison and improvement project (AgMIP), have examined the differences through systematic crop model intercomparison (Asseng et al. 2013, Martre et al. 2015). However, the wide range of projected impacts on agriculture is associated with both the uncertainty in climate projections (i.e. GCM projections and GHG emission scenarios) and the structural (or parameterization) differences between crop models (Osborne et al. 2013, Monier et al. 2016). Some studies pointed out GCMs being the main source of the uncertainty in magnitude, spatial pattern and even sign of projected change (Hawkins & Sutton 2009, Kassie et al. 2015). They partitioned the variation of future climate change to three main factors, namely the internal variability of climate system, the choice of GCMs (model uncertainty or response uncertainty) and the greenhouse gas emissions pathway (scenario uncertainty). Different GCMs can provide different future climate projections for a particular region. The real climate system is highly complex and it is impossible to adequately describe its processes with an individual climate model. Authors of model evaluation studies have stated that no single model can be considered ‘best’ and recommend using results from a range of climate models. Therefore, the use of many GCMs was important to sample the uncertainties in future climate projections that arise from differences in model structure and parameterization, as well as internal climate variability (Lobell et al. 2015).

The main objective of this study was to explore the spatial impact of future climate change on

wheat phenology, rain-fed yields, evapotranspiration and water use efficiency within the NSW wheat belt. I conducted a comprehensive analysis on how wheat yields response to climate change based on multimodel ensemble projections at sub-regional scale under future climate scenarios with and without accompanying CO_2 concentration enrichment. The aim is to provide a scientific basis for strategies to mitigate possible negative effects of climate change on the sustainable development of agro-ecosystems in the NSW wheat belt.

7.2 Materials and methods

7.2.1 Study area and climate data

The NSW wheat belt (Fig. 7.1) is located in the NSW slopes-plains region some 100-200 km inland, where annual rainfall ranges between 200 and 700 mm (Liu et al. 2014). It was classified into four subregions with different climate characteristics in this study, including two northern subregions, the Northeast (NE, I) and the Northwest (NW, II), and two southern subregions, the Southeast (SE, III) and the Southwest (SW, IV). During the 1961-2000 period, the spatially averaged growing season (April to November) mean temperature was 13.4 ˚C ranging from 8.3 ˚C in some parts of the east of the wheat belt to 17.1 ˚C in the northwest of the study area (Fig. 7.3a); growing season rainfall averaged across the study area was 381 mm ranging between 172 mm in the extreme west, to 763 mm in the extreme southeast (Fig. 7.3b). In general, the climate is hotter from south to north and drier from east to west.

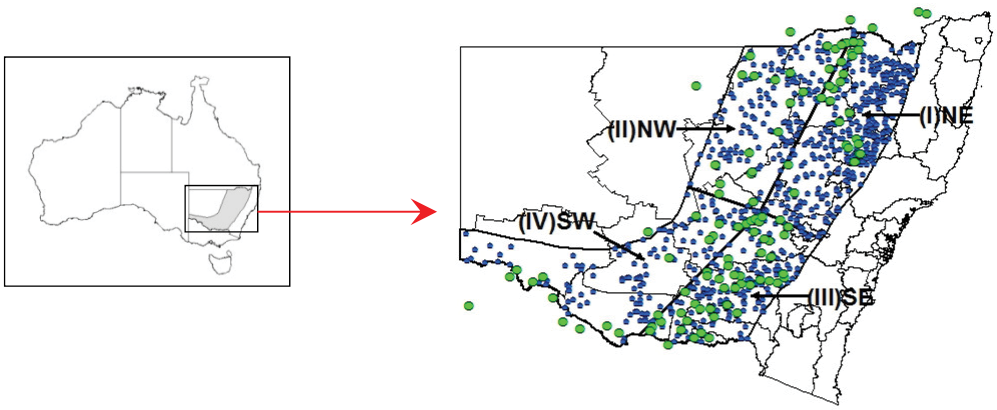

Fig. 7.1 The distribution of the 894 weather stations (black solid circle) used in this study and the four subregions of the NSW wheat belt considered: I: Northeast (NE); II: Northwest (NW); III: Southeast (SE) and IV: Southwest (SW). The green solid circles denote soil sites (121) used for this study including some soil sites from Victoria and Queensland near NSW border.

Daily solar radiation, maximum and minimum temperatures and rainfall data are available for 894 sites in the NSW wheat belt (Fig. 7.1). Data from 1900 to 2014 were extracted from the SILO patched point dataset (PPD, http://www.longpaddock.qld.gov.au/silo/ppd/index.php) (Jeffrey et al. 2001). Relevant data were available from 28 GCMs contributing to the Coupled Model Intercomparison Project Phase 5 (CMIP5) of the World Climate Research Programme. Different GCMs can provide different future climate projections for a particular region. The use of many GCMs was important to sample the uncertainties in future climate projections that arise from differences in model structure and parameterization, as well as internal climate variability (Lobell et al. 2015). All 28 GCMs have performed a 20th century experiment with all anthropogenic and natural forcing and future simulations of the RCP4.5 and RCP8.5 scenarios for atmospheric greenhouse gas concentrations (Taylor et al. 2012), resulting in 4.5 W m^{-2} and 8.5 W m^{-2} of forcing by the end of the 21st century respectively (Van Vuuren et al. 2011). I used monthly maximum temperature, minimum temperature, solar radiation and rainfall data from the GCM simulations.

To identify GCMs with satisfactory performance at simulating the climatological temperature and rainfall across the NSW wheat belt, Taylor's method was used to select GCMs after characterizing model performance using a skill score derived from correlations and standard deviations between models simulated and observed spatial patterns in climatological means. As a result, 13 out of 28 GCMs that achieved a skill score greater than 0.5 for both annual mean daily minimum, daily maximum temperature and rainfall were selected for use in the subsequent analysis (Fig. 7.2). A detailed description of the skill score can be seen in Taylor (2001).

Following several recent studies of the impact of climate change on crop growth and development (Yang et al. 2014, Anwar et al. 2015, Wang et al. 2015b), I used the statistical downscaling and bias-correction method of Liu and Zuo (2012) to generate realistic daily site-specific climate data from monthly GCM output on a coarse-resolution grid. Briefly, monthly GCM output data (solar radiation, rainfall, daily maximum and minimum temperatures) from each of the 13 selected GCMs were downscaled to the 894 observation sites using an inverse distance-weighted interpolation method. Biases were then corrected using a transfer function derived from interpolated GCM data and observed data for the sites. Daily climate data for each of 894 sites for 1900-2100 were generated by a modified stochastic weather generator (WGEN) (Richardson & Wright 1984) with parameters derived from the bias-corrected monthly data. In this study, climate data for 1961-2000 were used as a baseline climate to compare against projected future climate for 2061-2100.

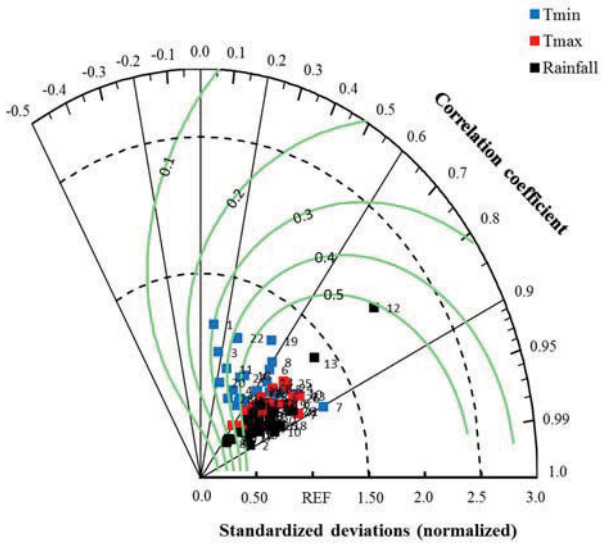

Fig. 7.2 Taylor diagram (Taylor 2001) displaying normalized pattern statistics of 1961-2000 climatological variables in eastern Australia for 28 GCMs against observations. Each number represents a model ID (see Table 4.1). The blue squares represent annual minimum temperature, red squares represent maximum temperature and black squares represent rainfall. The standard deviations for the GCMs have been normalized by the standard deviation of the reference observations (REF). The normalized standard deviation of a model is the radial distance from the origin to the points, with cambered dotted lines showing values of 1.5 and 2.5. The correlation coefficient between a model and the reference is given by the azimuthal position of the model, with oblique solid lines showing different coefficient values (-0.2, 0.0, 0.2, 0.6 and 0.9). The green solid lines are isolines of measure of skill defined by equation (1) in (Wang et al. (2015b)).

7.2.2 Crop modelling

The growth and yield of wheat were simulated using an Australian biophysical process model known as APSIM (Agricultural Production System sIMulator) version 7.7 (www.apsim.info). The APSIM model, including its Wheat, SoilN, SoilWater and Surface Organic Matter modules, has been well-tested for many modern wheat cultivars and is able to accurately simulate the behaviour of crops exposed to a wide range of Australian climatic, soil and management conditions (Asseng et al. 1998, Keating et al. 2003, Luo et al. 2005, Ludwig & Asseng 2006). It simulates phenological process, biomass accumulation and partitioning, leaf area index (LAI), as well as root, stem, leaf and grain growths in daily time steps from sowing to maturity. The APSIM-Wheat model uses both radiation use efficiency (RUE) and transpiration efficiency (TE) to calculate daily growth depending on various

conditions. Crop development is primarily based on thermal time, whereas leaf and stem growth rates are determined depending on phenological stages. Crop grain yield is a function of grain number, grain-filling and carbohydrate remobilisation. A detailed description of the APSIM model structure and processes are well documented in Keating et al. (2003) and Holzworth et al. (2014). The minimum weather input requirement for APSIM includes daily solar radiation, rainfall, maximum and minimum temperature.

7.2.3 Simulation settings

Elevated levels of atmospheric carbon dioxide (CO_2) concentration in the plant module of APSIM affects crop growth by influencing radiation use efficiency, transpiration efficiency and critical leaf nitrogen concentration. Therefore, CO_2 concentration is an important variable required in process-based crop growth models. Since APSIM cannot ingest time-varying values of CO_2 concentration, a function was added to calculate concentration using an empirical equation as function of calendar year in this study (Liu et al. 2014). The atmospheric CO_2 concentration for RCP4.5 and RCP8.5 in this study was calculated according to chapter 6.

Sowing time was controlled by a sowing rule, which involved a "sowing window" defined as the period between 1 April and 31 July, taken from the NSW Department of Primary Industries sowing guidelines (Matthews et al. 2014). Sowing occurred either on the first day within the sowing window when cumulative rainfall over the previous ten consecutive days was greater than 25 mm, or on the last day of the sowing window if this condition was not met prior to this (Wang et al. 2009c). This approach was intended to ensure that the crop was sown into moist soil. It allowed the exact date of sowing to vary from year to year and location to location according to variations in the timing of rainfall. However, since the sowing window did not change with time, this method does not represent larger changes in the seasonality of sowing, such as might be implemented by farmers as an adaptation to shorter growing seasons in a warmer climate. A time-invariant sowing window may not be realistic if farmers choose to adapt in this way, but it removed a potentially complicating factor from the study and aided interpretation of the results.

To optimally use the available resources (light, temperature, water and nutrients) and to minimise the chance of frost or heat stress during flowering, one of two different cultivars was sown in any given year. If the sowing date was before 20 May, the slow-maturing, long-season, Bolac cultivar was planted. If the sowing date was between 20 May and 31 July, the fast-maturing, short-season, Waagan cultivar was planted. The only difference between the simulated cultivars was in phenological response, and there were no physiological differences. Existing APSIM-Wheat parameters for

degree-day responses, sensitivity to vernalisation and photoperiod for calculating crop growth stages were used for the different cultivars. For both cultivars, plants were sown every year at density of 120 plants m^{-2}, and at a depth of 3 cm.

For all simulations, soil organic carbon, C:N ratio, soil mineral N and soil water content were re-set on 1 January of every year (Asseng et al. 2000, Manschadi et al. 2006). This was necessary to exclude "carry-over" effects from previous seasons and ensure that information on the direct effects of climate change on the crop could be assessed. Potential changes in the C:N ratio related to changes in biomass production and changes in mineralization rates are not accounted for. Each year, 100 kg ha^{-1} N fertiliser was applied at sowing date and another 50 and 100 kg ha^{-1} N fertiliser were added at the juvenile and initial flowering stage, respectively. The high level of N application used was to avoid any nitrogen stress of the crop so that simulated wheat yield was a reflection of climate change rather than fertiliser management.

At each site, wheat phenology, yield, soil water evaporation and crop transpiration during the growth period for different scenarios were simulated. Water use efficiency (WUE, $kg\ ha^{-1}\ mm^{-1}$) was defined as grain yield (Y, $kg\ ha^{-1}$) produced per unit of water-consumed by evapotranspiration (ET, mm) (Zhang & Oweis 1999, Mo et al. 2009, Jalota et al. 2013).

$$ET = Es + Ep \qquad (7.1)$$

$$WUE = \frac{Y}{ET} \qquad (7.2)$$

where Es and Ep were cumulative soil evaporation, crop transpiration (total water uptake from profile) from sowing date to maturity, respectively.

7.2.4 Soil data

The APSIM framework incorporates the APSoil database from which users can select soils for their simulations. APSoil contains soil water characteristics enabling estimation of plant available water capacity (PAWC) for individual soils and crops. It covers many cropping regions of Australia. There are 149 soil data sets from the APSoil database available for the NSW wheat belt (Dalgliesh et al. 2006). Each soil file contains information including soil description, soil classification, site, region, latitude, longitude and data source, which recorded the owner, project and experiment from which the data were derived. Each soil also has soil attributes including pH value (pH), layer depth (Thick), bulk density (BD), saturated water content (SAT), drained upper limit (DUL) and crop specified lower limit (LL), from which PAWC can be calculated. Generally, crop yield are closely related to soil

PAWC in semi-arid environments (Wang et al. 2009a, Yang et al. 2014). In order to minimise the bias in spatial analysis due to using an unrepresentative soil for a geographic location, the nearest soil was selected for each of 894 climate sites to simulate rain-fed potential yields (Liu et al. 2014). The spatial distribution of the selected 121 soil types relevant to the NSW wheat belt is shown in Fig. 7.1.

7.2.5 Spatial analysis

A GIS database was developed and used to process and present simulation results. The database contained climate information and crop model output. In detail, it included growing season mean temperature, rainfall, simulated wheat phenology, wheat yield, the cumulative ET during the growing period and WUE for each site. Using this database, point data for each site were interpolated to generate maps for the entire NSW wheat belt using a climate change adaptation strategy tool (CCAST) developed by Liu et al. (2011). There are many different kinds of methods for spatial interpolation. For example Kriging method, although it also gives an estimate of error for each grid point, the downside of this approach is the need to define a global or local variogram and selection of the appropriate variogram can be problematic. The integration process used in this study was the inverse distance weighting (IDW) method (Mueller et al. 2004, Wu et al. 2006). IDW is a simple and easy interpolation method for predicting unmeasured values. This method uses the weights directly calculated from the inverse of powered distances. Generated maps were stratified at equal intervals according to the interpolated values.

7.3 Results

7.3.1 Projected changes in temperature and rainfall

To present the range in projected future climate, median changes across the 13 GCM simulations in growing season mean temperature and rainfall for both RCPs are computed for each of the 894 sites. RCP8.5 projects higher temperature increases than for RCP4.5. By 2061-2100, the median increase for temperature is on average 2.1˚C for RCP4.5 and 3.8 ˚C for RCP8.5 across the wheat belt (Fig. 7.3c and e) while rainfall is predicted to decrease on average by 2.5% and 4.0% for RCP4.5 and RCP8.5, respectively (Fig. 7.3d and f). All GCMs agree on a future temperature rise (Fig. 7.4a). The highest increase for temperature is located in region NE, with regionally averaged ensemble median increase of 2.2 ˚C for RCP4.5 and 4.0 ˚C for RCP8.5. The lowest simulated increase is found in region SW, 1.9 ˚C for RCP4.5 and 3.5 ˚C for RCP8.5. By the end of 21st century, changes in simulated growing season rainfall vary with GCM used, with some GCMs simulating increases in rainfall and some simulating decreases. In all regions, most GCMs simulate decreases, meaning that regionally averaged

ensemble median changes in rainfall are all decreases. The largest ensemble median decrease in rainfall, 3.7% for RCP4.5 and 7.5% for RCP8.5, is found in region NW (Fig. 7.4b). The smallest decrease, 0.7% and 3.6% for RCP4.5 and RCP8.5 respectively, is located in region NE.

7.3.2 Impacts of climate change on phenology

Simulated days from sowing to flowering (DTF) shows a spatial gradient (decrease from east to west), with the average being 143 days ranging between 64 and 200 in the NSW wheat belt (Fig. 7.5a), which was derived from APSIM simulations forced with observations for baseline period 1961-2000. The smallest DTF was found in southwestern parts of the region, whereas the largest DTF was found in the southeastern part of the wheat belt. In the future, flowering date is advanced due to gradually increasing temperature across the region. Compared with the baseline period, by 2061-2100, median DTF is expected to shorten on average by 17.0 days for RCP4.5 and 27.8 days for RCP8.5 across the NSW wheat belt (Fig. 7.5c and e). The largest decrease of the time to flowering is found in region NE, with an ensemble median change of 18.4 days for RCP4.5 and 31.5 days for RCP8.5 (Fig. 7.6a). The smallest reduction in DTF is located in region NW with 14.4 days and 21.2 days for RCP4.5 and RCP8.5, respectively.

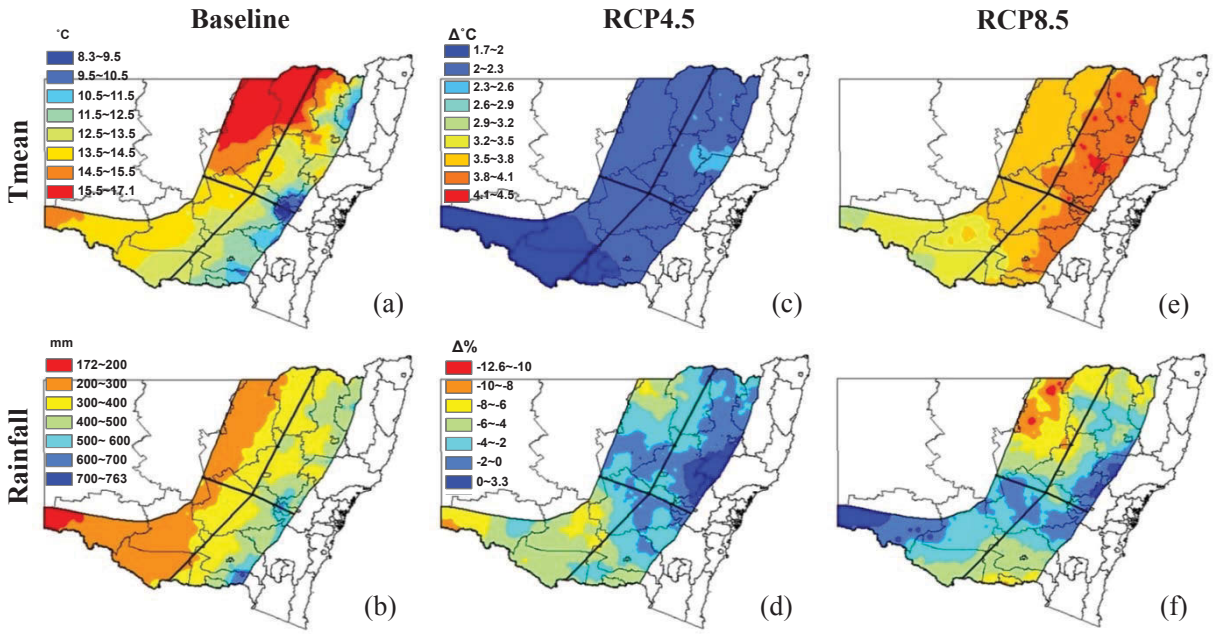

Fig. 7.3 Spatial patterns of wheat growing season (April to November) mean temperature (a) and rainfall (b) for baseline (1961-2000) and the median changes of the spatial patterns for 2061-2100 under RCP4.5 and RCP8.5 (c-f).

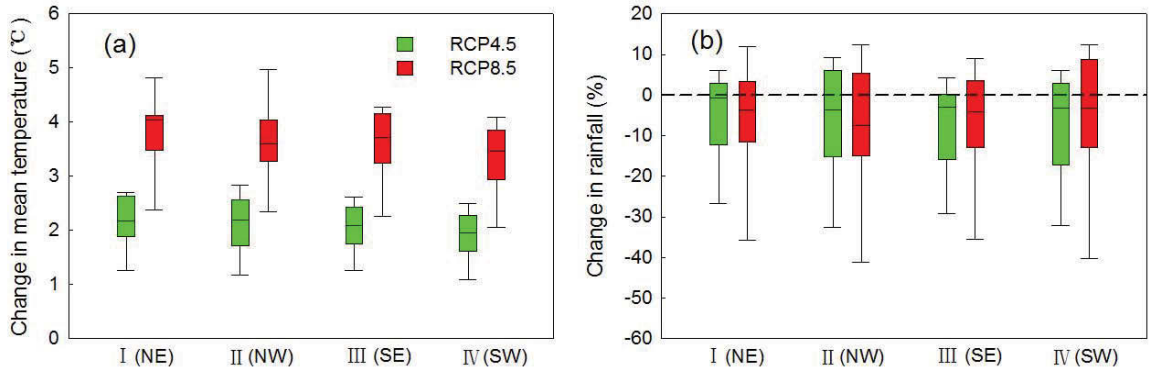

Fig. 7.4 Projected changes of wheat growing season (April to November) mean temperature (a) and rainfall (b) from the 13 selected GCMs under RCP4.5 and RCP8.5 in the 2061-2100 compared to 1961-2000 in the four regions over the NSW wheat belt. Box boundaries indicate the 25th and 75th percentiles; the black line within the box marks the median; whiskers below and above the box indicate the 10th and 90th percentiles. I: Northeast (NE); II: Northwest (NW); III: Southeast (SE) and IV: Southwest (SW).

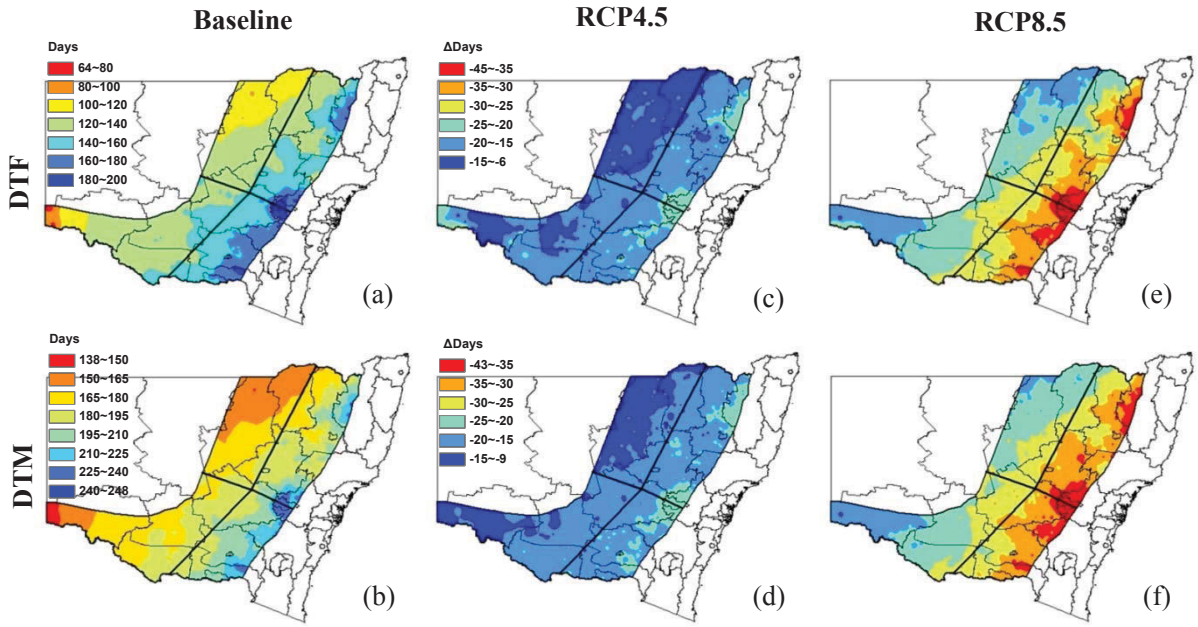

Fig. 7.5 Spatial patterns of simulated days to flowering (DTF) and days to maturity (DTM) for baseline (1961-2000) (a-b) and the median changes of the spatial patterns for 2061-2100 under RCP4.5 and RCP8.5 (c-f).

Simulated days from sowing to maturity (DTM) for 1961-2000 presented similar spatial patterns with DTF and was also reduced from east to west, with the average being 188 days ranging between 138 and 248 days in the study region (Fig. 7.5b). In the future climate, crop cycle is shortened on average by 17.6 days for RCP4.5 and 29.0 days for RCP8.5 across the wheat belt (Fig. 7.5d and f)

mostly due to advance in flowering date. The largest reduction of DTM is found in region NE, with an ensemble median of 18.8 days for RCP4.5 and 33.4 days for RCP8.5 (Fig. 7.6b). The smallest decrease in DTM is located in region NW with 14.9 days and 23.6 days for RCP4.5 and RCP8.5, respectively. The changes of DTF and DTM are significantly correlated with the change of growing season mean temperature. According to a linear regression between changes in simulated DTF and DTM and growing season temperature using regionally averaged data for 13 GCMs and two RCPs, shown in Table 7.1. The time to flowering and maturity is mainly controlled by the daily thermal time in APSIM model and the crop will die if extreme drought (water stress) occurs during any crop phases. The shortening of the time to flowering and maturity is likely to be related to projected temperature increases and, to some extent, rainfall changes. DTF could decrease by 7.6, 5.8, 8.6 and 7.2 days, respectively, in region NE, NW, SE and SW, with a decrease of 7.3 days for the entire region, as a result of an elevation of mean temperature of 1.0 ˚C. The response of crop growth duration to temperature is larger in the eastern regions than in the western regions. The similar results can be found in DTM and temperature.

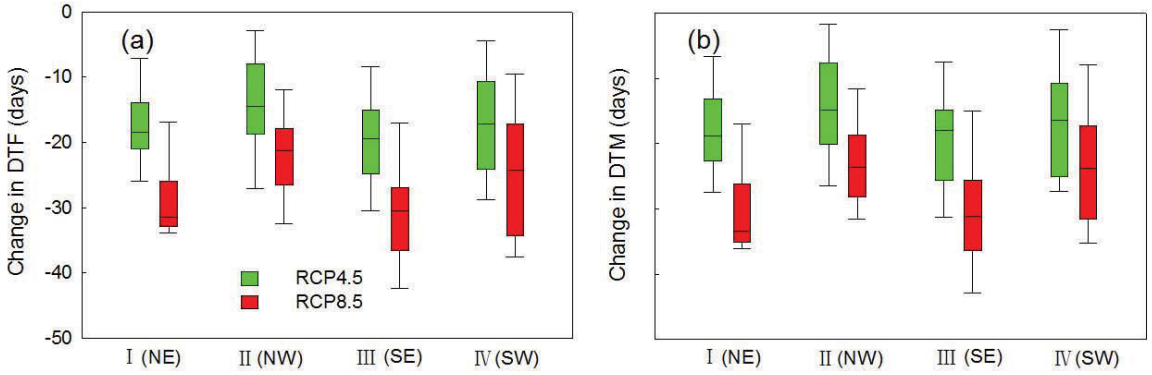

Fig. 7.6 Simulated changes in days to flowering (DTF) (a) and days to maturity (DTM) (b) from the 13 selected GCMs under RCP4.5 and RCP8.5 in the 2061-2100 compared to 1961-2000 in the four regions over the NSW wheat belt. Box boundaries indicate the 25th and 75th percentiles; the black line within the box marks the median; whiskers below and above the box indicate the 10th and 90th percentiles. I: Northeast (NE); II: Northwest (NW); III: Southeast (SE) and IV: Southwest (SW).

Table 7.1 Regression coefficients of changes for days to flowering (ΔDTF) and days to maturity (ΔDTM) with changes of wheat growing season mean temperature (ΔT) and rainfall (ΔR) in a multiple linear regression model ($\Delta Y = a\Delta T + b\Delta R$).

Region	ΔDTF			ΔDTM		
	a	*b*	R^2	*a*	*b*	R^2
I (NE)	-7.6**	0.08	0.99	-7.9**	0.12*	0.98
II (NW)	-5.8**	0.19**	0.95	-6.1**	0.16*	0.95
III (SE)	-8.6**	0.13*	0.98	-8.5**	0.17*	0.97
IV (SW)	-7.2**	0.26**	0.96	-7.1**	0.21**	0.95
Entire region	-7.3**	0.17**	0.96	-7.4**	0.16**	0.95

* indicates the significant level of P<0.05. ** indicates the significant level of P<0.01. I: Northeast (NE); II: Northwest (NW); III: Southeast (SE) and IV: Southwest (SW).

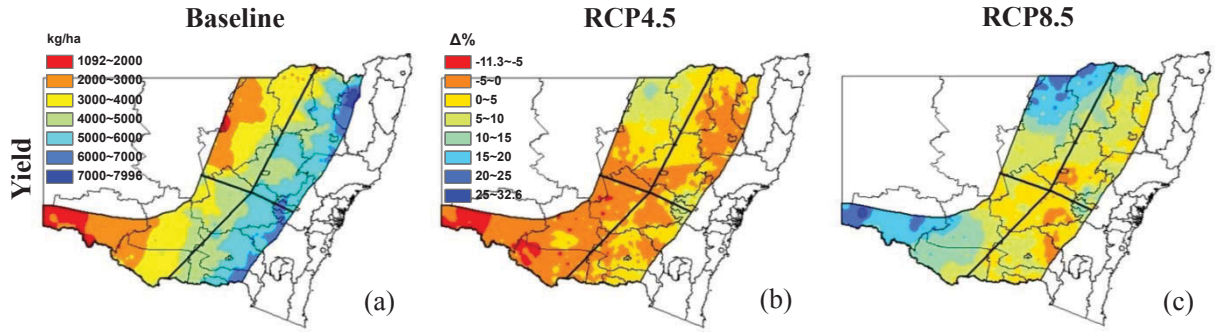

Fig. 7.7 Spatial patterns of simulated wheat yield for baseline (1961-2000) (a) and the median changes of the spatial patterns for 2061-2100 under RCP4.5 and RCP8.5 (b-c).

7.3.3 Impacts of climate change on wheat yield

In the baseline period, simulated wheat yield decreased from east to west due to lower rainfall and the shorter length of the growing period caused by higher temperature in the west. The spatially averaged wheat yield was 4685 kg ha^{-1} ranging between 1090 and 7996 kg ha^{-1} across the wheat belt (Fig. 7.7a), which is the same range as reported by Wang et al. (2009b). The average yield is higher than the averaged shire yield of 2700-3300 kg ha^{-1} in the year 2000 (Wang et al. 2015a). Considering that our simulations were based on no limitations to N, pest and weed effect, the baseline yields represent an achievable yield in this region. Compared with 1961-2000, median yields are expected to increase by on average 0.4% for RCP4.5 and 7.3% for RCP8.5 in 2061-2100 across the NSW wheat belt (Fig. 7.7b and c). It is interesting to note that the RCP4.5 shows median yield decline in the dry southwestern parts of the wheat belt (Fig. 7.7b). However, RCP8.5 leads to a multi-model median yield increase as a result of the higher CO_2 concentration compensating some negative effects. The

largest increase in wheat yield is found in region NW, with an ensemble median increase of 7.0% for RCP4.5 and 12.4% for RCP8.5 (Fig. 7.8). The smallest ensemble median increase is located in region SE with 0.1% and 5.1% for RCP4.5 and RCP8.5, respectively.

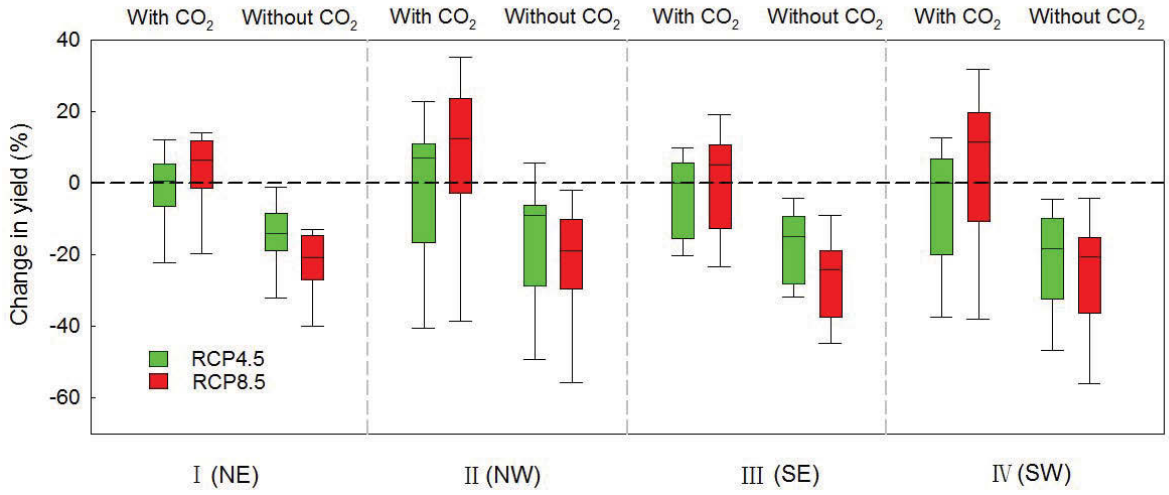

Fig. 7.8 Simulated changes of wheat yield without/with CO_2 fertilization from the 13 selected GCMs under RCP4.5 and RCP8.5 in the 2061-2100 compared to 1961-2000 in the four regions over the NSW wheat belt. Box boundaries indicate the 25th and 75th percentiles; the black line within the box marks the median; whiskers below and above the box indicate the 10th and 90th percentiles. I: Northeast (NE); II: Northwest (NW); III: Southeast (SE) and IV: Southwest (SW).

The importance of CO_2 fertilization in wheat production is demonstrated by simulating future yield with only the change in climate. Without the increase in CO_2 concentration simulated wheat yield decrease rapidly under RCP4.5 by 2061-2100 and much more so under RCP8.5 compared to the present (Fig. 7.8). It is interesting to note that some GCMs show a decrease in simulated yield even with CO_2 fertilization. These GCMs may show a greater yield reduction without CO_2 positive effects. In contrast, with the exception of region NW for RCP4.5, all GCMs show a decrease in yield without CO_2 fertilization. A descriptive statistical analysis was conducted using regional averages for 13 GCMs and two RCPs and a linear regression model. The relationships between changes of wheat yield and changes of wheat growing season rainfall, temperature and CO_2 concentration are shown in Table 7.2.

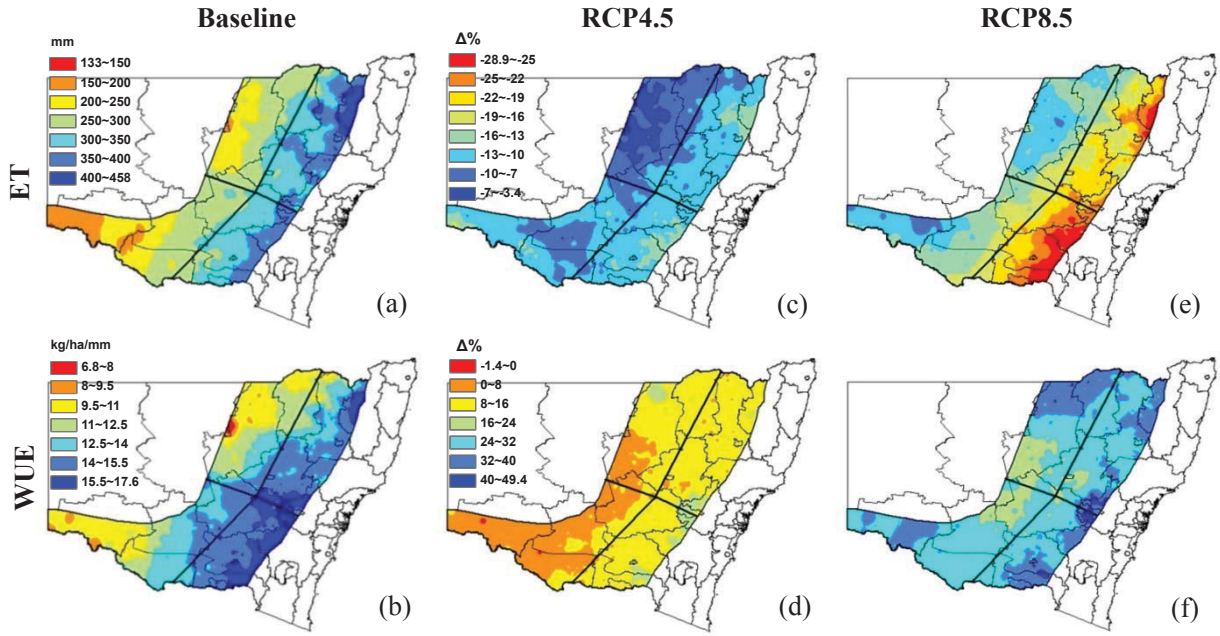

Fig. 7.9 Spatial patterns of simulated wheat ET and WUE for baseline (1961-2000) (a-b) and the median changes of the spatial patterns for 2061-2100 under RCP4.5 and RCP8.5 (c-f).

With this regression analysis the contribution of specific climate factors to yield change can be quantified. At all subregions, the change in wheat yield is significantly correlated with each lower rainfall regions. For example, there is a significant 0.65% grain yield change in SE (higher rainfall region) for each percentage change in rainfall compared to significant 1.10% grain yield changes in SW (lower rainfall region). Simultaneously, dry southwestern parts of the wheat belt have large benefit from CO_2 fertilization as APSIM simulates the CO_2 fertilization effects through an increase in transpiration efficiency (Sultan et al. 2014).

7.3.4 Changes in simulated ET and WUE

The spatial patterns of simulated cumulative ET for the growth period derived from APSIM simulations with observed baseline climate are shown in Fig. 7.9a. The ET value for wheat was lower in the west than in the east, associated with the spatial gradients of rainfall (decrease from east to west). The spatially averaged wheat ET was 320 mm ranging from 133 to 458 mm across the wheat belt. The simulated ET could decrease by 2061-2100 in response to warming conditions and reduced rainfall. The spatial pattern of median ET changes is quite similar to that of the growth period changes, suggesting that ET decreases mainly due to shortened wheat growth duration. ET decreases by 7.2% for 10 days decline in the growth period (Fig. 7.10). Compared with 1961-2000, the multi-model median ET is expected to decrease by an average of 10.7% for RCP4.5 and 18.6% for RCP8.5 by the end of this century across the NSW wheat belt (Fig. 7.9c and e). Fig. 7.11a shows the relative change

of ET compared to that for the baseline period under the RCP4.5 and RCP8.5 scenarios with and without CO_2 fertilization. The difference in the changes in ET between with/without CO_2 fertilization simulations was relatively small. The largest ensemble median decrease in simulated ET is found in region SE, especially under the high-emission RCP8.5 scenario, followed by region NE; the smallest changes in ET are located in regions SW and NW (Fig. 7.11a).

Table 7.2 Regression coefficients of changes for wheat yield (ΔY, %) with changes of wheat growing season mean temperature (ΔT, ˚C), rainfall (ΔR, %) and CO_2 concentration (ΔCO_2, ppm) in a multiple linear regression model ($\Delta Y = a\Delta T + b\Delta R + c\Delta CO_2$).

Region	*a*	*b*	*c*	R^2
I (NE)	-2.1	0.66**	0.035	0.68
II (NW)	-0.6	1.25**	0.046	0.81
III (SE)	-6.4*	0.65**	0.067**	0.68
IV (SW)	-8.3**	1.10**	0.091**	0.89
Entire region	-3.6**	0.97**	0.056**	0.73

* indicates the significant level of P<0.05. ** indicates the significant level of P<0.01. I: Northeast (NE); II: Northwest (NW); III: Southeast (SE) and IV: Southwest (SW).

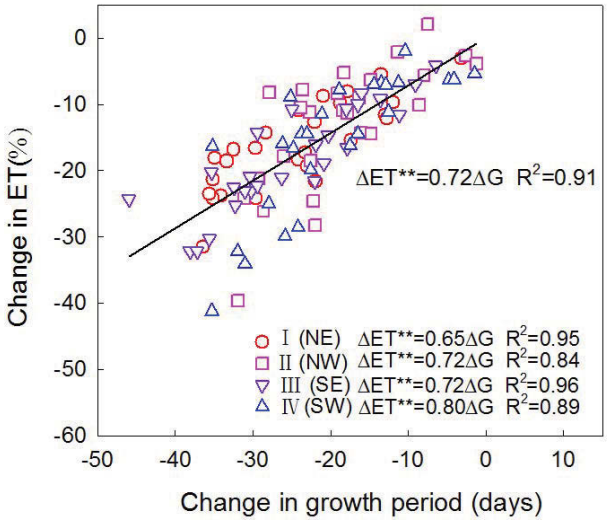

Fig. 7.10 Relationship between simulated change in ET and wheat growth period across four regions in the NSW wheat belt. I: Northeast (NE); II: Northwest (NW); III: Southeast (SE) and IV: Southwest (SW). ** indicates the significant level of P<0.01.

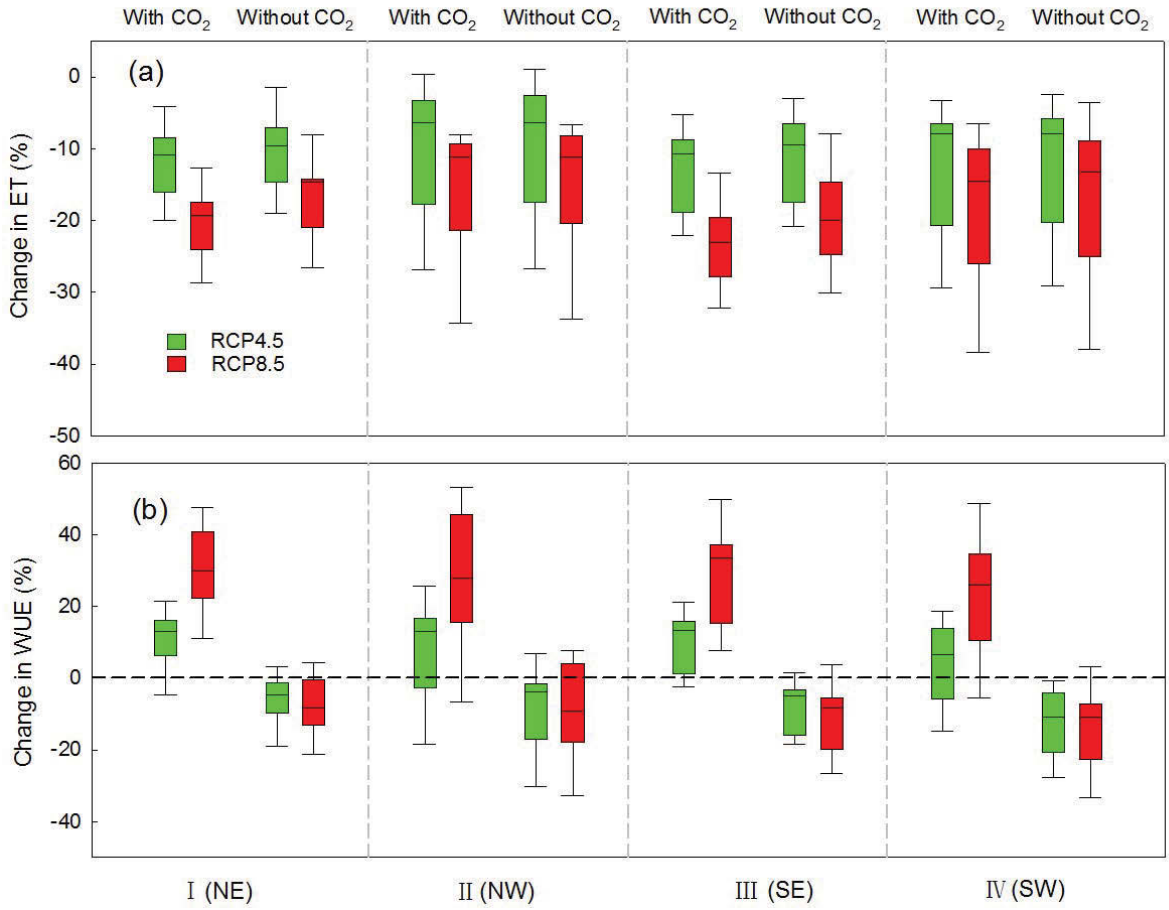

Fig. 7.11 Simulated changes of wheat ET (a) and WUE (b) without/with CO_2 fertilization from the 13 selected GCMs under RCP4.5 and RCP8.5 in the 2061-2100 compared to 1961-2000 in the four regions over the NSW wheat belt. Box boundaries indicate the 25th and 75th percentiles; the black line within the box marks the median; whiskers below and above the box indicate the 10th and 90th percentiles. I: Northeast (NE); II: Northwest (NW); III: Southeast (SE) and IV: Southwest (SW).

The spatial distribution of wheat water use efficiency (WUE) under the baseline climate is shown in Fig 7.9b. It shows that WUE decreased from east to west. The spatially averaged wheat WUE was 13.8 kg ha^{-1} mm^{-1} ranging from 6.8 to 17.6 kg ha^{-1} mm^{-1} over the wheat belt. The spatial patterns of median WUE changes in relation to the baseline under RCP4.5 and RCP8.5 in the 2061-2100 are presented in Fig. 7.9d and f. In contrast with ET changes, median WUE clearly depicts an increase trend across the wheat belt. By 2061-2100, median WUE is expected to increase by an average of 11.0% for RCP4.5 and 30.3% for RCP8.5 across the NSW wheat belt.

Fig. 7.11b shows the relative change of WUE under RCP4.5 and RCP8.5 with and without CO_2 fertilization for the four subregions. In general, with CO_2 fertilization the majority, and sometimes all,

GCMs show an increase in WUE. In all cases, most of the GCMs present decreases in WUE without CO_2 fertilization. The largest ensemble mean increase in WUE is found in region SE, especially under the high-emission RCP8.5 scenario, followed by region NE; the smallest changes in WUE are located in regions NW and SW (Fig. 7.11b). The greatest decrease for WUE appears in region SW under RCP8.5 with the value of 11.0%.

7.4 Discussion

GCMs typically provide gridded data at a spatial resolution of several hundreds of kilometres. In impact studies it is too coarse for the output to be used directly in detailed regional scale analysis and resolve small scale processes. Therefore, before these GCMs can be used, it is necessary to select satisfactory GCMs in simulating the climate over the NSW wheat belt. Consequently, I used a skill score defined in Taylor's method that combined correlation and standard deviation between simulated and observed spatial patterns in climatological temperature and rainfall means to select satisfactory climate models across the studied region. As a result, 13 out of 28 GCMs were selected for downscaling. Monthly gridded outputs of these GCMs were downscaled to station-scale daily weather series. Future climate projections from the multi-model median values based on the 13 selected GCMs showed an averaged warming of 2.1 ˚C for RCP4.5 and 3.8 ˚C for RCP8.5 across the NSW wheat belt in 2061-2100 compared to the baseline period 1961-2000. However, not all GCMs agreed on the sign of rainfall change. Large differences in magnitude and sign existed between different climate models. Multi-model median values showed a decrease in growing season rainfall. The results generally agreed with the study from CSIRO and BoM (2015) and the NARCliM project (http://www.ccrc.unsw.edu.au/sites/default/files/NARCliM/index.html).

The growth periods from sowing to flowering and maturity are critical phenological stages for wheat crops. Although there is still a considerable degree of uncertainty of projected future climate change, my analysis demonstrated DTF would be predicted to shorten by 14-31 days across the whole study area, depending on the scenarios and locations, which are analogous to the findings of other modelling studies (Sadras & Monzon 2006, Zheng et al. 2012, Potgieter et al. 2013, Yang et al. 2014, Wang et al. 2015b). My results also showed that a decrease in DTM under future climate was consistent with reduction in DTF. Moreover, modelled DTF and DTM had a similar response to rising temperature, approximately -7 days $^{\circ}C^{-1}$. This rate compared well with rates derived from Sadras and Monzon (2006) and Anwar et al. (2015). These results implied an early flowering date may result in the advance of maturity, which means the time to flowering contributed to most of the variation in time to maturity. The duration of the post-anthesis phase was relatively stable (Sadras & Monzon 2006). However, shorter vegetative periods in the future climate reduce less time to intercept radiation

and water than current climate. Therefore, the change of phenological development has become one of the most important attributes involved in crop adaptation to climate change, such as changing the planting window (sowing earlier) to escape heat stress around flowering as frost-free seasons become more frequent due to global warming (Zheng et al. 2012) and selecting long-season wheat cultivars that are resistant to water stress and high temperature during grain filling (Ludwig & Asseng 2010).

My simulated spatial patterns of yield for the baseline period 1961-2000 were associated with spatial distribution of rainfall, which is consistent with the fact that rainfall is the main climatic factor in determining yield (Oliver et al. 2009, Yu et al. 2014, Wang et al. 2015a). Wheat yield showed obvious differences between eastern and western parts of the wheat belt as the result of spatial patterns of growing season rainfall. Spatially, multi-model median yields increased by 0.4% for RCP4.5 and by 7.3% for RCP8.5. The median yield increase for RCP4.5 was small probably due to half of GCMs predicting yield decrease while half of them increase. However, these findings were in contrast with the conclusions of Yang et al. (2014) and Anwar et al. (2015). Using the APSIM model with 18 GCMs, they found that median wheat yield decreased at some of their climatologically distinct study sites in the NSW wheat belt under SRES A2 emission scenarios. The reason for the differences in results across these studies could be due to the choice of climate models, greenhouse gas emissions scenario, time horizon and different configuration of the crop model (such as soil types and crop management practices at each site), which can strongly influence the sign and magnitude of yield response (Araya et al. 2015, Kassie et al. 2015). For example, Yang et al. (2014) focused on CMIP3 GCM data and used A2 emission with individual site, particularly in a near future period of 2021-2040. My study was based on the latest greenhouse gas emission scenarios and GCM projections and focused on a far future period (2061-2100).

Rising concentrations of CO_2 in the atmosphere are driving global warming that will impact on crop yields through changes in rainfall and increases in temperature. However, elevated CO_2 also has beneficial physiological effects on crops through the stimulation of photosynthesis and reduction of drought stress as a result of lower stomatal conductance and greater intercellular CO_2 (Lin et al. 2005). By conducting a systematic comparison between yield response to climate change with or without CO_2 effect, many studies conclude that the impacts of higher atmospheric CO_2 concentration is another major source of uncertainty in quantification of crop yield (Soussana et al. 2010, Sultan et al. 2014). Acceleration of crop development and shortening of growth duration could reduce the yield potential. However, this unfavourable effect is counterbalanced by the positive CO_2 effects on biomass production. The impact of CO_2 level is two-fold as it governs climatic changes and simultaneously triggers crop responses (Vanuytrecht et al. 2011). Although the effectiveness of CO_2 fertilization has been assessed in various modelling and experimental studies, there is still an ongoing

debate and uncertainty on the extent of effects of CO_2 fertilization on future crop yields (Ainsworth & Long 2005, Long et al. 2006). For example, Sun et al. (2009) reviewed and quantified the yield increase of C3 crops to be 18% on average, ranging from 3% to 35% under elevated CO_2 in various FACE experiments. In my simulations, I compared RCP4.5 and RCP8.5 results with the analogous simulations where the CO_2 concentration was fixed at 330 ppm to roughly estimate a magnitude of CO_2 effect on wheat yield. Without the increase in CO_2 concentration simulated wheat yield decreased remarkably for two RCPs in 2061-2100. My results showed that CO_2 fertilization significantly reduced the negative climate impacts, increasing wheat yield by about 10.6% for RCP4.5 and 23.9% for RCP8.5 in the future. Wheat in drier parts of the wheat belt would have larger benefit from the positive impact of elevated CO_2 concentration than in wetter areas. These results are consistent with previous studies in rainfed cropping system (Luo et al. 2003, Wang et al. 2011a, Sultan et al. 2014). Recent analyses of Free-Air Carbon Dioxide Enrichment studies indicate that, at 550 ppm atmospheric CO_2 concentration, observed yields increase under unstressed conditions by 26% for wheat in Australian dry land (O'Leary et al. 2015). The APSIM model simulates the CO_2 fertilization effects through an increase in transpiration efficiency as well as transpiration efficiency. However, a contribution of elevated CO_2 effects cannot be directly quantified without further examination. Correct quantification of CO_2 fertilization is complex and is believed to be associated to crop characteristics and governing environmental conditions (Vanuytrecht et al. 2011). For example, interactions of CO_2 with limiting factors, especially heat and drought stress, are increasingly well understood and capable of strongly modulating observed growth responses in crops (Lin et al. 2005). Therefore, further research based on experimental systems is urgently needed to clarify how to best model the impacts of CO_2 stimulation.

Water consumption is strongly impacted by climatic shifts in temperature and rainfall, concomitant with elevated atmospheric CO_2 in a future climate (Wang et al. 2009c). As an important water loss process in field water balance, ET during wheat growth period always decreased by 10.7-18.6% across the wheat belt under future climates. Under the warming conditions, the vegetative periods of wheat will be advanced and their reproductive periods be shortened; the enriched CO_2 concentration will reduce leaf stomatal conductance and then decrease ET rates. These somewhat trade-off effects make the response of crop transpiration to climate change complicated and non-linear (Mo et al. 2013). There was relatively small response of growing season ET to CO_2 fertilization because the shortened wheat growth period and decreased rainfall were main determining factors. Trends of decreasing wheat ET under future climate projections were similar among the four subregions and agreement with previous impact assessment studies in south eastern Australia (Wang et al. 2009c, Yang et al. 2016). However, the change in wheat yields was not proportional to the

change in water use. Overall, increases in WUE were generally associated with improved wheat yields rather than reductions in water used. The median wheat yields showed an increase while cumulative ET decreased, which resulted in WUE increase in the future climate. It should be noted that simulated WUE showed a decreasing trend without considering CO_2 fertilization, indicating that elevated CO_2 could improve the water use efficiency of wheat in a certain degree.

In our study, there is still uncertainty arising from the process within the crop model (e.g. strength of CO_2 fertilization), the choice of GCMs and the method of future climate scenario generation (Osborne et al. 2013). The projected yield increase in the future could be overestimated because the crop model generally does not sufficiently account for yield reduction due to diseases, pests, weed, effects of extreme heat and drought stress (Gornall et al. 2010). We did not explicitly consider certain aspects such as technological innovations, which will obviously have a significant impact on wheat yield in the future. In addition, we assume current two wheat cultivars can sow in the future climate. However, as a result of phenological responses to increasing temperatures, current wheat cultivars may not be suitable for future climate conditions due to a shorter growth cycle and exposure to extreme high temperatures during flowering date (Wang et al. 2015b). New wheat cultivars might provide more drought and heat resistance against warming conditions. Finally, management strategies that are optimized for present-day climate may not necessarily be optimal for future climate. It should be noted that some potential adaptation opportunities arising from managing soil water more efficiently through the wheat growing season, such as choosing cultivars, sowing time, sowing density and fertilizer timing and amount, were not included in this impact analysis. This may be a main limitation of this study. Therefore, our current simulated results should be used with caution in the development of climate change adaptation strategies. Despite these limitations, this study provides a framework for assessing the future trends in wheat yield under the latest greenhouse gas emissions and CMIP5 GCM projections to facilitate policymaking and strategic research and management.

7.5 Conclusion

The responses of wheat productivity and water use to two projected future climate change scenarios in the NSW wheat belt were simulated by using the APSIM model with the output of 13 GCMs statistically downscaled to individual locations. My results show that there was a decrease in days to flowering and maturity for 2061-2100 compared with a baseline period across the whole production region. The advance in time to flowering contributed to most of the changes in wheat phenology. Spatially, median wheat yields could increase on average by 0.4% for RCP4.5 and 7.3% for RCP8.5 across the NSW wheat belt. The largest increase was found in the northwestern parts of

the wheat belt with 12.4% for RCP8.5. Evapotranspiration could decrease by 10.7% for RCP4.5 and 18.6% for RCP8.5 by the end of this century due to the reduction in length of the wheat growing period and a decrease in rainfall. However, increasing yields combined with decreasing ET resulted in water use efficiency increasing by 11.4% for RCP4.5 and 29.3% for RCP8.5. Comparisons of simulation results with and without CO_2 fertilization indicate that an increase of CO_2 concentration with future climate change scenarios will increase wheat yields and improve water use efficiency. This study is in contrast to many other studies and showed that low-rainfall-low-yielding growing environments might benefit more from climate change due to the stimulating effects of elevated CO_2 on water-limited crop productivity.

Chapter 8

Final conclusions

In the NSW wheat belt, wheat yields were positively correlated to growing season rainfall and minimum temperature while negatively correlated to growing season maximum temperature at a significant level ($p<0.05$). Recent climatic trends from 1922 to 2000 contributed to wheat yield increase by 8.5-21.2% in different climatically regions. Rainfall is usually the main direct climatic driver affecting wheat yield variation in this semi-arid area, but the variation is also affected by temperature and solar radiation. My results show that in the eastern slopes, growing season temperatures and number of heat stress days were major factors affecting wheat yield, accounting for 36% of yield variation. In the northern parts of the wheat belt, major climatic drivers for yield variation were growing season maximum temperature and pre-growing season (December to April) rainfall and number of frost days accounted for 41% of yield variation. In the southern region, growing season rainfall, temperatures, number of frost and heat stress days accounted for 47% of yield variation. In the southwestern plains, growing season rainfall was the main direct climate factor to determine 31% of yield variation. However, frost had more impact on yield variation in the northern parts of the wheat belt as farmers sow earlier and select short-season cultivars to avoid heat stress. Understanding the impact of climate variations on crop yield is important for developing sustainable agricultural production under future climate change.

Statistical downscaling method used in this study was effective at correcting the bias associated with the site-based monthly GCM values by relating observed historical climate data to that simulated by GCMs. The SILO daily time series of meteorological data at point locations were used as a basis for spatial downscaling and bias correction of different skill-selected CMIP5 GCMs. I evaluated the ability of the downscaled data from each of the selected GCMs to reproduce trends in values of 11 extreme temperature indices across eastern Australia over the period 1961-2000. In general, most GCM models captured the sign of historical observed trends in temperature extremes, but no one model was consistently good at reproducing all indices. Future projections show that great warming occurs in the east and northeast of the NSW wheat belt by 2061-2100 and increases the risk of exposure to hot days around wheat flowering date, which might result in farmers needing to reconsider wheat cultivars suited to maintain yield.

The flowering time of wheat is strongly controlled by temperature and is potentially highly sensitive to climate change. My simulations suggest a general advance in spring wheat flowering date in 2080s, on average, by 10.2 days for RCP4.5 and 17.8 days for RCP8.5 across the NSW wheat belt.

Winter wheat flowering dates were delayed by an average of 2.4 days for RCP4.5 and 14.3 days for RCP8.5 in the warmest parts of the region (the northwest) due to reduced cumulative vernalization days (requiring cool conditions). In the cooler regions (the northeast, southeast and southwest), flowering date occurred earlier by 6.2 days for RCP4.5 and 6.7 days for RCP8.5 on average. Moreover, in the western parts of the wheat belt the delay of winter wheat flowering date was about 9.5 days longer than that in the eastern parts. As a result of phenological responses to increasing temperatures, limiting sowing of winter cultivars in the western plains may be one strategy to mitigate the impacts of future climate change in the wheat belt. Furthermore, the number of hot days with maximum temperature exceeding 30°C during flowering date (+/- 7 days) increased while simulated number of frost days with minimum temperature below 2°C decreased due to climate warming. Therefore, sowing dates may advance as a consequence of flowering date change to minimize frost and heat stress at anthesis dates in the future. Late-maturing cultivars with increased heat-stress resistance will be needed to maintain the current crop cycle duration, to provide for the use of resources (radiation, CO_2, water, and nutrients) of long-season cultivars in eastern Australia.

I selected six sites in the NSW wheat belt to analyse changes in relative yield loss due to water stress. Our results show that simulated water limited yield tended to decline at wetter and cooler locations under a future climate while increased at warmer and drier locations. Soils with high PAWC provided a larger buffer to store water from variable rainfall and to supply it to crops during dry periods and therefore were less affected by rainfall decreases compared to soils with low PAWC. Our results also indicated that a drought stress index decreased with increasing PAWC and then leveled out at high PAWC. Under the high emission scenario RCP8.5, drought stress was expected to decline or stay about the same due to the elevated CO_2 compensation effect. Therefore, to maintain or increase yield potential and respond to climate change, increasing cultivar tolerance to heat stress and improving crop management to reduce impacts of water stress on lower plant available water holding soils should be a priority for the genetic improvement of wheat in eastern Australia.

The responses of wheat phenology, yield and water use efficiency to two projected future climate change scenarios in the NSW wheat belt were simulated by using the APSIM model with the output of selected 13 GCMs statistically downscaled to individual locations. Compared with 1961-2000, multi-model median projected a +2.1 to +3.8 ˚C rise in growing season temperature, and -2.5 to -4.0% reductions in rainfall across the NSW wheat belt by 2061-2100 under the two emission scenarios. Simulated results indicated that the length of wheat growth period could decline by 17.6 days for RCP4.5 and 29.0 days for RCP8.5. Despite an acceleration of crop development and shortening of growth duration together with declining growing season rainfall, I projected that multi-model median yields could increase by 0.4% for RCP4.5 and 7.3% for RCP8.5 by 2061-2100. Although the RCP4.5

showed a small decrease in median yield in the dry southwestern parts of the wheat belt, the higher CO_2 concentration in RCP8.5 compensated some of the negative effects resulting in 11.5% yield increase. These results show that a drier area would benefit more from elevated CO_2 than a wetter area. Without the increase in CO_2 concentration simulated wheat yield decrease rapidly under RCP4.5 by 2061-2100 and much more so under RCP8.5 compared to the present. A decline in growing season length and a decrease in rainfall resulted in a reduction of crop water consumption. As a consequence, simulated evapotranspiration (ET) decreased by 11.9% for RCP4.5 and 18.8% for RCP8.5 across the NSW wheat belt. Increasing yields combined with decreasing ET resulted in simulated water use efficiency increasing by 11.4% for RCP4.5 and 29.3% for RCP8.5. Wheat production in water-limited, low yielding environments appears to be less negatively impacted or in some cases even positively affected under a future climate and carbon dioxide changes, compared to other growing environments in the world.

Nonetheless, a number of limitations in our methodology and results still remain, and further research is needed in the future. Firstly, we only provide simulation result with one crop model, APSIM. Although the model has been validated at the national scales in several previous studies, simulation results may be constrained by the fundamental assumptions and approaches used in this model. This shortcoming can be overcome by comparing results from several crop growth models, which use the same combination of climate, soil, management and other input data (Martre et al. 2015). Because a broader range of crop models may differ in the description of the basic physiology thus also add information on uncertainties in projected adaptation measures. For example, recent work as part of the agricultural model intercomparison and improvement project (AgMIP) has examined (and narrowed) these differences through systematic model intercomparison (Asseng et al. 2013, Rosenzweig et al. 2013). Secondly, the magnitude of climate change scenarios for past and future periods differ among different circulation models and therefore it is a source of uncertainty that might affect the results of the applied models (statistical downscaling, crop model and SDMs). For example, these climate-change driven alterations of growing conditions can thus lead to diverse, depending on their direction (e.g. dryer or wetter), amplitude, and the starting conditions (e.g. cold- or heat-limited growing season). It is therefore normally of utmost importance to apply a range of climate models and scenarios in order to estimate the inherent variability introduced by the choice of climate.

Reference

Abramowitz G (2010) Model independence in multi-model ensemble prediction. Australian Meteorological and Oceanographic Journal 59:3-6

Ahmed KF, Wang G, Silander J, Wilson AM, Allen JM, Horton R, Anyah R (2013) Statistical downscaling and bias correction of climate model outputs for climate change impact assessment in the US northeast. Global and Planetary Change 100:320-332

Ainsworth EA, Long SP (2005) What have we learned from 15 years of free-air CO_2 enrichment (FACE)? A meta-analytic review of the responses of photosynthesis, canopy properties and plant production to rising CO_2. New Phytologist 165:351-372

Alexander L, Zhang X, Peterson T, Caesar J, Gleason B, Klein Tank A, Haylock M, Collins D, Trewin B, Rahimzadeh F (2006) Global observed changes in daily climate extremes of temperature and precipitation. Journal of Geophysical Research: Atmospheres (1984–2012) 111

Alexander LV, Arblaster JM (2009) Assessing trends in observed and modelled climate extremes over Australia in relation to future projections. International Journal of Climatology 29:417-435

Alexander LV, Hope P, Collins D, Trewin B, Lynch A, Nicholls N (2007) Trends in Australia's climate means and extremes: a global context. Australian Meteorological Magazine 56:1-18

Allan JC, Kiniry JR, Dyke P (1986) CERES-Maize: A simulation model of maize growth and development.

Amano T, Smithers RJ, Sparks TH, Sutherland WJ (2010) A 250-year index of first flowering dates and its response to temperature changes. Proceedings of the Royal Society B: Biological Sciences:rspb20100291

Anandhi A, Frei A, Pierson DC, Schneiderman EM, Zion MS, Lounsbury D, Matonse AH (2011) Examination of change factor methodologies for climate change impact assessment. Water Resources Research 47

Anderson W (2010) Closing the gap between actual and potential yield of rainfed wheat. The impacts of environment, management and cultivar. Field Crops Research 116:14-22

Anderson W, Hamza M, Sharma D, D'Antuono M, Hoyle F, Hill N, Shackley B, Amjad M, Zaicou-Kunesch C (2005) The role of management in yield improvement of the wheat crop-a review with special emphasis on Western Australia. Crop and Pasture Science 56:1137-1149

Anderson W, Smith W (1990) Yield advantage of two semi-dwarf compared with two tall wheats depends on sowing time. Crop and Pasture Science 41:811-826

Angus J, Mackenzie D, Morton R, Schafer C (1981) Phasic development in field crops II. Thermal and photoperiodic responses of spring wheat. Field Crops Research 4:269-283

Angus J, Nix H, Russell J, Kruizinga J (1980) Water use, growth and yield of wheat in a subtropical environment. Crop and Pasture Science 31:873-886

Anwar MR, Liu DL, Farquharson R, Macadam I, Abadi A, Finlayson J, Wang B, Ramilan T (2015) Climate change impacts on phenology and yields of five broadacre crops at four climatologically distinct locations in Australia. Agricultural Systems 132:133-144

Araya A, Hoogenboom G, Luedeling E, Hadgu KM, Kisekka I, Martorano LG (2015) Assessment of maize growth and yield using crop models under present and future climate in southwestern Ethiopia. Agricultural and Forest Meteorology 214:252-265

Arblaster JM, LIM E, Hendon HH, Trewin BC, Wheeler MC, Liu G, Braganza K (2014) Understanding Australia's September on record, [in "Explaining extreme events of 2013 from a climate perspective"]. Bull Amer Met Soc 95(9):S37-S41

Arnell N, Reynard N (1996) The effects of climate change due to global warming on river flows in Great Britain. Journal of hydrology 183:397-424

Arnell NW (1992) Factors controlling the effects of climate change on river flow regimes in a humid temperate environment. Journal of hydrology 132:321-342

Asseng S, Ewert F, Rosenzweig C, Jones J, Hatfield J, Ruane A, Boote K, Thorburn P, Rötter R, Cammarano D, Brisson N, Basso B, Martre P, Aggarwal P, Angulo C, Bertuzzi P, Biernath C, Challinor A, Doltra J, Gayler S, Goldberg R, Grant R, Heng L, Hooker J, Hunt L, Ingwersen J, Ozaurralde R, Kersebaum K, Müller C, Naresh Kumar S, Nendel C, O'Leary G, Olesen J, Osborne T, Palosuo T, Priesack E, Ripoche D, Semenov M, Shcherbak I, Steduto P, Stöckle C, Stratonovitch P, Streck T, Supit I, Tao F, Travasso M, Waha K, Wallach D, White J, Williams J, Wolf J (2013) Uncertainty in simulating wheat yields under climate change. Nature Climate Change 3:827-832

Asseng S, Fillery I, Dunin F, Keating BA, Meinke H (2000) Potential deep drainage under wheat crops in a Mediterranean climate. I. Temporal and spatial variability. Crop and Pasture Science 52:45-56

Asseng S, Foster I, Turner NC (2011) The impact of temperature variability on wheat yields. Global Change Biology 17:997-1012
Asseng S, Jamieson P, Kimball B, Pinter P, Sayre K, Bowden J, Howden S (2004) Simulated wheat growth affected by rising temperature, increased water deficit and elevated atmospheric CO_2. Field Crops Research 85:85-102
Asseng S, Keating B, Fillery I, Gregory P, Bowden J, Turner N, Palta J, Abrecht D (1998) Performance of the APSIM-wheat model in Western Australia. Field Crops Research 57:163-179
Asseng S, Pannell DJ (2012) Adapting dryland agriculture to climate change: Farming implications and research and development needs in Western Australia. Climatic Change:1-15
Asseng S, Pannell DJ (2013) Adapting dryland agriculture to climate change: Farming implications and research and development needs in Western Australia. Climatic Change 118:167-181
Asseng S, Turner N, Keating BA (2001) Analysis of water-and nitrogen-use efficiency of wheat in a Mediterranean climate. Plant and Soil 233:127-143
Augustine JA, Dutton EG (2013) Variability of the surface radiation budget over the United States from 1996 through 2011 from high-quality measurements. Journal of Geophysical Research: Atmospheres 118:43-53
Balkovič J, van der Velde M, Skalský R, Xiong W, Folberth C, Khabarov N, Smirnov A, Mueller ND, Obersteiner M (2014) Global wheat production potentials and management flexibility under the representative concentration pathways. Global and Planetary Change 122:107-121
Bardossy A, Bogardi I, Matyasovszky I (2005) Fuzzy rule-based downscaling of precipitation. Theoretical and applied climatology 82:119-129
Barlow K, Christy B, O'Leary G, Riffkin P, Nuttall J (2015) Simulating the impact of extreme heat and frost events on wheat crop production: A review. Field Crops Research 171:109-119
Benestad RE (2010) Downscaling precipitation extremes. Theoretical and applied climatology 100:1-21
Bishop CH, Abramowitz G (2013) Climate model dependence and the replicate Earth paradigm. Climate Dynamics 41:885-900
Black K, Davis P, Lynch P, Jones M, McGettigan M, Osborne B (2006) Long-term trends in solar irradiance in Ireland and their potential effects on gross primary productivity. Agricultural and Forest Meteorology 141:118-132
Boer R, Campbell L, Fletcher D (1993) Characteristics of frost in a major wheat-growing region of Australia. Crop and Pasture Science 44:1731-1743
Bouman B (2001) ORYZA2000: modeling lowland rice, Vol 1. IRRI
Brooking I, Jamieson P (2002) Temperature and photoperiod response of vernalization in near-isogenic lines of wheat. Field Crops Research 79:21-38
Butterfield RE, Morison JI (1992) Modelling the impact of climatic warming on winter cereal development. Agricultural and Forest Meteorology 62:241-261
Cao W, Moss D (1997) Modelling phasic development in wheat: a conceptual integration of physiological components. The Journal of Agricultural Science 129:163-172
Challinor A, Wheeler T (2008) Crop yield reduction in the tropics under climate change: processes and uncertainties. Agricultural and Forest Meteorology 148:343-356
Chameides WL, Yu H, Liu S, Bergin M, Zhou X, Mearns L, Wang G, Kiang C, Saylor R, Luo C (1999) Case study of the effects of atmospheric aerosols and regional haze on agriculture: An opportunity to enhance crop yields in China through emission controls? Proceedings of the National Academy of Sciences 96:13626-13633
Charles SP, Bari M, Kitsios A, Bates B (2007) Effect of GCM bias on downscaled precipitation and runoff projections for the Serpentine catchment, Western Australia. International Journal of Climatology 27:1673-1690
Chavas DR, Izaurralde RC, Thomson AM, Gao X (2009) Long-term climate change impacts on agricultural productivity in eastern China. Agricultural and Forest Meteorology 149:1118-1128
Chen C-C, McCarl BA, Schimmelpfennig DE (2004) Yield variability as influenced by climate: a statistical investigation. Climatic Change 66:239-261
Chen H, Xu C-Y, Guo S (2012) Comparison and evaluation of multiple GCMs, statistical downscaling and hydrological models in the study of climate change impacts on runoff. Journal of Hydrology 434:36-45
Chenu K, Deihimfard R, Chapman SC (2013) Large-scale characterization of drought pattern: a continent-wide modelling approach applied to the Australian wheatbelt–spatial and temporal trends. New Phytologist 198:801-820
Chmielewski F-M, Müller A, Bruns E (2004) Climate changes and trends in phenology of fruit trees and field

crops in Germany, 1961–2000. Agricultural and Forest Meteorology 121:69-78
Ciais P, Reichstein M, Viovy N, Granier A, Ogée J, Allard V, Aubinet M, Buchmann N, Bernhofer C, Carrara A (2005) Europe-wide reduction in primary productivity caused by the heat and drought in 2003. Nature 437:529-533
Cohen S (2009) The role of widespread surface solar radiation trends in climate change: dimming and brightening. Climate Change: Observed Impacts on Planet Earth, Letcher TM (ed) Elsevier: Amsterdam:21-41
Collins D, Della-Marta P, Plummer N, Trewin B (2000) Trends in annual frequencies of extreme temperature events in Australia. Australian Meteorological Magazine 49:277-292
Conway D, Wilby R, Jones P (1996) Precipitation and air flow indices over the British Isles. Climate Research 7:169-183
Cook BI, Wolkovich EM, Parmesan C (2012) Divergent responses to spring and winter warming drive community level flowering trends. Proceedings of the National Academy of Sciences 109:9000-9005
Cooper P, Dimes J, Rao K, Shapiro B, Shiferaw B, Twomlow S (2008) Coping better with current climatic variability in the rain-fed farming systems of sub-Saharan Africa: an essential first step in adapting to future climate change? Agriculture, Ecosystems & Environment 126:24-35
Cornish EA (1950) The influence of rainfall on the yield of wheat in South Australia. Australian Journal of Biological Sciences 3:178-218
Crane RG, Hewitson BC (1998) Doubled co2 precipitation changes for the susquehanna basin: down-scaling from the genesis general circulation model. International Journal of Climatology 18:65-76
Craufurd P, Wheeler T (2009) Climate change and the flowering time of annual crops. Journal of Experimental Botany 60:2529-2539
Crosbie RS, Dawes WR, Charles SP, Mpelasoka FS, Aryal S, Barron O, Summerell GK (2011) Differences in future recharge estimates due to GCMs, downscaling methods and hydrological models. Geophysical Research Letters 38
CSIRO, BoM (2015) Climate Change in Australia Information for Australia's Natural Resource Management Regions: Technical Report, CSIRO and Bureau of Meteorology, Australia.
Dalgliesh N, Wockner G, Peake A Delivering soil water information to growers and consultants. In. Proc Proceedings of the 13th Australian Agronomy Conference, 10-14 September 2006, Perth, Western Australia
Deryng D, Conway D, Ramankutty N, Price J, Warren R (2014) Global crop yield response to extreme heat stress under multiple climate change futures. Environmental Research Letters 9:034011
Diaz-Nieto J, Wilby RL (2005) A comparison of statistical downscaling and climate change factor methods: impacts on low flows in the River Thames, United Kingdom. Climatic Change 69:245-268
Dielman TE (2001) Applied regression analysis for business and economics, Vol. Duxbury/Thomson Learning
Diepen Cv, Wolf J, Keulen Hv, Rappoldt C (1989) WOFOST: a simulation model of crop production. Soil use and management 5:16-24
Donat M, Alexander L, Yang H, Durre I, Vose R, Dunn R, Willett K, Aguilar E, Brunet M, Caesar J (2013) Updated analyses of temperature and precipitation extreme indices since the beginning of the twentieth century: The HadEX2 dataset. Journal of Geophysical Research: Atmospheres 118:2098-2118
Estrella N, Sparks TH, Menzel A (2007) Trends and temperature response in the phenology of crops in Germany. Global Change Biology 13:1737-1747
Evans J, Ji F, Lee C, Smith P, Argüeso D, Fita L (2014) Design of a regional climate modelling projection ensemble experiment–NARCliM. Geoscientific Model Development 7:621-629
Evans JP, Ji F, Abramowitz G, Ekström M (2013) Optimally choosing small ensemble members to produce robust climate simulations. Environmental Research Letters 8:044050
Evans LT (1996) Crop evolution, adaptation and yield, Vol. Cambridge University Press
FERRIS R, Ellis R, Wheeler T, Hadley P (1998) Effect of high temperature stress at anthesis on grain yield and biomass of field-grown crops of wheat. Annals of Botany 82:631-639
Finger R (2010) Revisiting the evaluation of robust regression techniques for crop yield data detrending. American Journal of Agricultural Economics:aap021
Fischer E, Schär C (2010) Consistent geographical patterns of changes in high-impact European heatwaves. Nature Geoscience 3:398-403
Fitter A, Fitter R (2002) Rapid changes in flowering time in British plants. Science 296:1689-1691
Fitzgerald G, Tausz M, O'Leary G, Mollah M, Tausz-Posch S, Seneweera S, Mock I, Löw M, Partington D, McNeil D (2016) Elevated atmospheric [CO_2] can dramatically increase wheat yields in semi-arid environments and buffer against heat waves. Global Change Biology 22:2269-2284

Fowler H, Blenkinsop S, Tebaldi C (2007) Linking climate change modelling to impacts studies: recent advances in downscaling techniques for hydrological modelling. International Journal of Climatology 27:1547-1578
Frei C, Christensen JH, Déqué M, Jacob D, Jones RG, Vidale PL (2003) Daily precipitation statistics in regional climate models: Evaluation and intercomparison for the European Alps. Journal of Geophysical Research: Atmospheres (1984–2012) 108
French R, Schultz J (1984a) Water use efficiency of wheat in a Mediterranean-type environment. I. The relation between yield, water use and climate. Crop and Pasture Science 35:743-764
French R, Schultz J (1984b) Water use efficiency of wheat in a Mediterranean-type environment. II. Some limitations to efficiency. Crop and Pasture Science 35:765-775
Fuller MP, Fuller AM, Kaniouras S, Christophers J, Fredericks T (2007) The freezing characteristics of wheat at ear emergence. European Journal of Agronomy 26:435-441
García-Mozo H, Mestre A, Galán C (2010) Phenological trends in southern Spain: A response to climate change. Agricultural and Forest Meteorology 150:575-580
Gifford R, Angus J, Barrett D, Passioura J, Rawson H, Richards R, Stapper M, Wood J (1998) Climate change and Australian wheat yield. Nature 391:448-449
Giorgi F, Mearns LO (2002) Calculation of average, uncertainty range, and reliability of regional climate changes from AOGCM simulations via the "reliability ensemble averaging"(REA) method. Journal of Climate 15:1141-1158
Godden D, Batterham R, Drynan R (1998) Climate change and Australian wheat yield. Nature 391:447-448
Gomez-Macpherson H, Richards R (1995) Effect of sowing time on yield and agronomic characteristics of wheat in south-eastern Australia. Crop and Pasture Science 46:1381-1399
Goodess CM, Palutikof JP (1998) Development of daily rainfall scenarios for southeast Spain using a circulation-type approach to downscaling. International Journal of Climatology 18:1051-1083
Gornall J, Betts R, Burke E, Clark R, Camp J, Willett K, Wiltshire A (2010) Implications of climate change for agricultural productivity in the early twenty-first century. Philosophical Transactions of the Royal Society B: Biological Sciences 365:2973-2989
Gourdji SM, Sibley AM, Lobell DB (2013) Global crop exposure to critical high temperatures in the reproductive period: historical trends and future projections. Environmental Research Letters 8:024041
Guo Y, Li S, Liu DL, Chen D, Williams G, Tong S (2016) Projecting future temperature-related mortality in three largest Australian cities. Environmental pollution 208:66-73
Halse N, Weir R (1970) Effects of vernalization, photoperiod, and temperature on phenological development and spikelet number of Australian wheat. Crop and Pasture Science 21:383-393
Hansen JW, Potgieter A, Tippett MK (2004) Using a general circulation model to forecast regional wheat yields in northeast Australia. Agricultural and forest meteorology 127:77-92
Hawkins E, Sutton R (2009) The potential to narrow uncertainty in regional climate predictions. Bulletin of the American Meteorological Society 90:1095-1107
Hay L, Clark M (2003) Use of statistically and dynamically downscaled atmospheric model output for hydrologic simulations in three mountainous basins in the western United States. Journal of Hydrology 282:56-75
Hewitson B, Crane R (2002) Self-organizing maps: applications to synoptic climatology. Climate Research 22:13-26
Hewitson B, Crane R (2006) Consensus between GCM climate change projections with empirical downscaling: precipitation downscaling over South Africa. International Journal of Climatology 26:1315-1337
Högy P, Wieser H, Köhler P, Schwadorf K, Breuer J, Franzaring J, Muntifering R, Fangmeier A (2009) Effects of elevated CO2 on grain yield and quality of wheat: results from a 3-year free-air CO2 enrichment experiment. Plant Biology 11:60-69
Holzworth DP, Huth NI, Zurcher EJ, Herrmann NI, McLean G, Chenu K, van Oosterom EJ, Snow V, Murphy C, Moore AD (2014) APSIM–evolution towards a new generation of agricultural systems simulation. Environmental Modelling & Software 62:327-350
Howden SM, Soussana J-F, Tubiello FN, Chhetri N, Dunlop M, Meinke H (2007) Adapting agriculture to climate change. Proceedings of the National Academy of Sciences 104:19691-19696
Hu Q, Weiss A, Feng S, Baenziger PS (2005) Earlier winter wheat heading dates and warmer spring in the US Great Plains. Agricultural and Forest Meteorology 135:284-290
Huang C, Townshend J (2003) A stepwise regression tree for nonlinear approximation: applications to estimating subpixel land cover. International Journal of Remote Sensing 24:75-90
Huth R (1999) Statistical downscaling in central Europe: Evaluation of methods and potential predictors.

Climate Research 13:91-101
IPCC (2013) Climate Change 2013: The Physical Science Basis. Contribution of Working Group I to the Fifth Assessment Report of the Intergovernmental Panel on Climate Change [Stocker, T. F., D. Qin, G.-K. Plattner, M. Tignor, S. K. Allen, J. Boschung, A. Nauels, Y. Xia,V. Bex and P. M. Midgley (eds.)]. Cambridge University Press, Cambridge, United Kingdom and New York, NY, USA.
Irving DB, Whetton P, Moise AF (2012) Climate projections for Australia: a first glance at CMIP5. Australian Meteorological and Oceanographic Journal 62:211-225
Jalota S, Kaur H, Kaur S, Vashisht B (2013) Impact of climate change scenarios on yield, water and nitrogen-balance and-use efficiency of rice–wheat cropping system. Agricultural water management 116:29-38
Jamieson P, Porter J, Goudriaan J, Ritchie J, Van Keulen H, Stol W (1998) A comparison of the models AFRCWHEAT2, CERES-Wheat, Sirius, SUCROS2 and SWHEAT with measurements from wheat grown under drought. Field Crops Research 55:23-44
Jeffrey SJ, Carter JO, Moodie KB, Beswick AR (2001) Using spatial interpolation to construct a comprehensive archive of Australian climate data. Environmental Modelling & Software 16:309-330
Jeong D, St-Hilaire A, Ouarda T, Gachon P (2013a) A multivariate multi-site statistical downscaling model for daily maximum and minimum temperatures. Climate Research 54:129-148
Jeong D, St-Hilaire A, Ouarda T, Gachon P (2013b) Projection of multi-site daily temperatures over the Montréal area, Canada. Climate Research 56:261-280
Jeong DI, Kim Y-O (2009) Combining single-value streamflow forecasts–A review and guidelines for selecting techniques. Journal of Hydrology 377:284-299
Jeong DI, Sushama L, Diro GT, Khaliq MN (2015a) Projected changes to winter temperature characteristics over Canada based on an RCM ensemble. Climate Dynamics:1-16
Jeong DI, Sushama L, Diro GT, Khaliq MN, Beltrami H, Caya D (2015b) Projected changes to high temperature events for Canada based on a regional climate model ensemble. Climate Dynamics:1-18
Kang Y, Khan S, Ma X (2009) Climate change impacts on crop yield, crop water productivity and food security–A review. Progress in Natural Science 19:1665-1674
Kassie BT, Asseng S, Rotter RP, Hengsdijk H, Ruane AC, Van Ittersum MK (2015) Exploring climate change impacts and adaptation options for maize production in the Central Rift Valley of Ethiopia using different climate change scenarios and crop models. Climatic Change 129:145-158
Keating BA, Carberry PS, Hammer GL, Probert ME, Robertson MJ, Holzworth D, Huth NI, Hargreaves JN, Meinke H, Hochman Z (2003) An overview of APSIM, a model designed for farming systems simulation. European Journal of Agronomy 18:267-288
Kidson JW, Thompson CS (1998) A comparison of statistical and model-based downscaling techniques for estimating local climate variations. Journal of Climate 11:735-753
Kilsby C, Jones P, Burton A, Ford A, Fowler H, Harpham C, James P, Smith A, Wilby R (2007) A daily weather generator for use in climate change studies. Environmental Modelling & Software 22:1705-1719
KIM HY, Lieffering M, Kobayashi K, Okada M, Miura S (2003) Seasonal changes in the effects of elevated CO2 on rice at three levels of nitrogen supply: a free air CO2 enrichment (FACE) experiment. Global Change Biology 9:826-837
Kimball B, Morris C, Pinter P, Wall G, Hunsaker D, Adamsen F, LaMorte R, Leavitt S, Thompson T, Matthias A (2001) Elevated CO2, drought and soil nitrogen effects on wheat grain quality. New Phytologist 150:295-303
King AD, Donat MG, Alexander LV, Karoly DJ (2014) The ENSO-Australian rainfall teleconnection in reanalysis and CMIP5. Climate Dynamics:1-13
Klein Tank A, Können G (2003) Trends in indices of daily temperature and precipitation extremes in Europe, 1946-99. Journal of Climate 16:3665-3680
Knutti R, Furrer R, Tebaldi C, Cermak J, Meehl GA (2010) Challenges in combining projections from multiple climate models. Journal of Climate 23:2739-2758
Lambert SJ, Boer GJ (2001) CMIP1 evaluation and intercomparison of coupled climate models. Climate Dynamics 17:83-106
Lawlor D, Mitchell R (1991) The effects of increasing CO2 on crop photosynthesis and productivity: a review of field studies. Plant, Cell & Environment 14:807-818
Leung LR, Qian Y, Bian X (2003a) Hydroclimate of the western United States based on observations and regional climate simulation of 1981-2000. Part I: Seasonal statistics. Journal of Climate 16:1892-1911
Leung LR, Qian Y, Bian X, Hunt A (2003b) Hydroclimate of the western United States based on observations and regional climate simulation of 1981-2000. Part II: Mesoscale ENSO anomalies. Journal of Climate

16:1912-1928
Lewis SC, Karoly DJ (2013) Anthropogenic contributions to Australia's record summer temperatures of 2013. Geophysical Research Letters 40:3705-3709
Li Liu D, Zuo H (2012) Statistical downscaling of daily climate variables for climate change impact assessment over New South Wales, Australia. Climatic change 115:629-666
Lin E, Xiong W, Ju H, Xu Y, Li Y, Bai L, Xie L (2005) Climate change impacts on crop yield and quality with CO_2 fertilization in China. Philosophical Transactions of the Royal Society B: Biological Sciences 360:2149-2154
Liu DL (2007) Incorporating vernalization response functions into an additive phenological model for reanalysis of the flowering data of annual pasture legumes. Field Crops Research 101:331-342
Liu DL, Anwar MR, O'Leary G, Conyers MK (2014) Managing wheat stubble as an effective approach to sequester soil carbon in a semi-arid environment: Spatial modelling. Geoderma 214:50-61
Liu DL, Martin P, Cole C, Wu H, Wang E, Bowman A (2010a) Modelling agronomically-suitable sowing date in relation to the risk of frost damage and heat stress of wheat in southern New South Wales, Australia. Journal of Agricultural Science and Technology 4:26-36
Liu DL, O'Leary GJ, Ma Y, Cowie A, Li FY, McCaskill M, Conyers M, Dalal R, Robertson F, Dougherty W (2016) Modelling soil organic carbon 2. Changes under a range of cropping and grazing farming systems in eastern Australia. Geoderma 265:164-175
Liu DL, Timbal B, Mo J, Fairweather H (2011) A GIS-based climate change adaptation strategy tool. International Journal of Climate Change Strategies and Management 3:140-155
Liu DL, Zuo H (2012) Statistical downscaling of daily climate variables for climate change impact assessment over New South Wales, Australia. Climatic Change 115:629-666
Liu Y, Wang E, Yang X, Wang J (2010b) Contributions of climatic and crop varietal changes to crop production in the North China Plain, since 1980s. Global Change Biology 16:2287-2299
Lobell DB (2007) Changes in diurnal temperature range and national cereal yields. Agricultural and forest meteorology 145:229-238
Lobell DB, Asner GP (2003) Climate and management contributions to recent trends in US agricultural yields. Science 299:1032-1032
Lobell DB, Burke M (2010a) Climate change and food security: adapting agriculture to a warmer world, Vol 37. Springer
Lobell DB, Burke MB (2010b) On the use of statistical models to predict crop yield responses to climate change. Agricultural and Forest Meteorology 150:1443-1452
Lobell DB, Burke MB, Tebaldi C, Mastrandrea MD, Falcon WP, Naylor RL (2008) Prioritizing climate change adaptation needs for food security in 2030. Science 319:607-610
Lobell DB, Cahill KN, Field CB (2007) Historical effects of temperature and precipitation on California crop yields. Climatic Change 81:187-203
Lobell DB, Field CB (2007) Global scale climate–crop yield relationships and the impacts of recent warming. Environmental Research letters 2:014002
Lobell DB, Hammer GL, Chenu K, Zheng B, McLean G, Chapman SC (2015) The shifting influence of drought and heat stress for crops in Northeast Australia. Global Change Biology 21:4115-4127
Lobell DB, Ortiz-Monasterio JI (2007) Impacts of day versus night temperatures on spring wheat yields. Agronomy Journal 99:469-477
Lobell DB, Ortiz-Monasterio JI, Asner GP, Matson PA, Naylor RL, Falcon WP (2005) Analysis of wheat yield and climatic trends in Mexico. Field crops research 94:250-256
Lobell DB, Schlenker W, Costa-Roberts J (2011) Climate trends and global crop production since 1980. Science 333:616-620
Lobell DB, Sibley A, Ortiz-Monasterio JI (2012) Extreme heat effects on wheat senescence in India. Nature Climate Change 2:186-189
Long SP, Ainsworth EA, Leakey AD, Nösberger J, Ort DR (2006) Food for thought: lower-than-expected crop yield stimulation with rising CO_2 concentrations. Science 312:1918-1921
Ludwig F, Asseng S (2006) Climate change impacts on wheat production in a Mediterranean environment in Western Australia. Agricultural Systems 90:159-179
Ludwig F, Asseng S (2010) Potential benefits of early vigor and changes in phenology in wheat to adapt to warmer and drier climates. Agricultural Systems 103:127-136
Ludwig F, Milroy SP, Asseng S (2009) Impacts of recent climate change on wheat production systems in Western Australia. Climatic Change 92:495-517
Lund R, Reeves J (2002) Detection of undocumented changepoints: A revision of the two-phase regression

model. Journal of Climate 15:2547-2554
Luo Q (2011) Temperature thresholds and crop production: a review. Climatic Change 109:583-598
Luo Q, Bellotti W, Williams M, Bryan B (2005) Potential impact of climate change on wheat yield in South Australia. Agricultural and Forest Meteorology 132:273-285
Luo Q, Bellotti W, Williams M, Wang E (2009) Adaptation to climate change of wheat growing in South Australia: Analysis of management and breeding strategies. Agriculture, Ecosystems & Environment 129:261-267
Luo Q, Williams MA, Bellotti W, Bryan B (2003) Quantitative and visual assessments of climate change impacts on South Australian wheat production. Agricultural Systems 77:173-186
Macadam I, Pitman AJ, Whetton PH, Liu DL, Evans JP (2014) The use of uncorrected regional climate model output to force impact models: a case study for wheat simulations. Climate Research 61:215-229
Manschadi AM, Christopher J, Hammer GL (2006) The role of root architectural traits in adaptation of wheat to water-limited environments. Functional Plant Biology 33:823-837
Marcellos H, Single W (1975) Temperatures in wheat during radiation frost. Animal Production Science 15:818-822
Martre P, Wallach D, Asseng S, Ewert F, Jones JW, Rötter RP, Boote KJ, Ruane AC, Thorburn PJ, Cammarano D (2015) Multimodel ensembles of wheat growth: many models are better than one. Global Change Biology 21:911-925
Matthews P, McCaffery D, Jenkins L (2014) Winter crop variety sowing guide 2014. NSW DPI Orange
McDonald G, Sutton B, Ellison F (1983) The effect of time of sowing on the grain yield of irrigated wheat in the Namoi Valley, New South Wales. Crop and Pasture Science 34:229-240
Mearns L, Giorgi F, Whetton P, Pabon D, Hulme M, Lal M (2003) Guidelines for use of climate scenarios developed from regional climate model experiments. In. Data Distribution Center of IPCC. TGCIA
Mehrotra R, Sharma A, Nagesh Kumar D, Reshmidevi T (2013) Assessing future rainfall projections using multiple GCMs and a multi-site stochastic downscaling model. Journal of Hydrology
Menzel A, Sparks TH, Estrella N, Koch E, Aasa A, Ahas R, ALM-KÜBLER K, Bissolli P, Braslavská Og, Briede A (2006) European phenological response to climate change matches the warming pattern. Global Change Biology 12:1969-1976
Miglietta F, Tanasescu M, Marica A (1995) The expected effects of climate change on wheat development. Global Change Biology 1:407-415
Min SK, Hense A (2006) A Bayesian approach to climate model evaluation and multi-model averaging with an application to global mean surface temperatures from IPCC AR4 coupled climate models. Geophysical Research Letters 33
Mo X, Guo R, Liu S, Lin Z, Hu S (2013) Impacts of climate change on crop evapotranspiration with ensemble GCM projections in the North China Plain. Climatic Change 120:299-312
Mo X, Liu S, Lin Z, Guo R (2009) Regional crop yield, water consumption and water use efficiency and their responses to climate change in the North China Plain. Agriculture, Ecosystems & Environment 134:67-78
Monier E, Xu L, Snyder R (2016) Uncertainty in future agro-climate projections in the United States and benefits of greenhouse gas mitigation. Environmental Research Letters 11:055001
Morgan CL, Norman JM, Lowery B (2003) Estimating plant-available water across a field with an inverse yield model. Soil Science Society of America Journal 67:620-629
Moriondo M, Giannakopoulos C, Bindi M (2011) Climate change impact assessment: the role of climate extremes in crop yield simulation. Climatic Change 104:679-701
Mueller T, Pusuluri N, Mathias K, Cornelius P, Barnhisel R, Shearer S (2004) Map quality for ordinary kriging and inverse distance weighted interpolation. Soil Science Society of America Journal 68:2042-2047
Murphy BF, Timbal B (2008) A review of recent climate variability and climate change in southeastern Australia. International journal of Climatology 28:859-879
Nakicenovic N, Swart R (2000) Special report on emissions scenarios. Special Report on Emissions Scenarios, Edited by Nebojsa Nakicenovic and Robert Swart, pp 612 ISBN 0521804930 Cambridge, UK: Cambridge University Press, July 2000 1
Newlands NK, Zamar DS, Kouadio LA, Zhang Y, Chipanshi A, Potgieter A, Toure S, Hill HS (2014) An integrated, probabilistic model for improved seasonal forecasting of agricultural crop yield under environmental uncertainty. Frontiers in Environmental Science 2:17
Nicholls N (1997) Increased Australian wheat yield due to recent climate trends. Nature 387:484-485
Norris JR, Wild M (2009) Trends in aerosol radiative effects over China and Japan inferred from observed cloud cover, solar “dimming,” and solar “brightening”. Journal of Geophysical Research: Atmospheres

(1984–2012) 114
Nowak RS, Ellsworth DS, Smith SD (2004) Functional responses of plants to elevated atmospheric CO2–do photosynthetic and productivity data from FACE experiments support early predictions? New Phytologist 162:253-280
Nuttall J, Brady S, Brand J, O'Leary G, Fitzgerald G (2013) Heat waves and wheat growth under a future climate. In. Proc Aust Soc Agron The 16th Australian Agronomy Conference: Climate Change Available at:http://wwwregionalorgau/au/asa/2012/climate-change/8085_nuttalljghtm
O'Leary GJ, Christy B, Nuttall J, Huth N, Cammarano D, Stöckle C, Basso B, Shcherbak I, Fitzgerald G, Luo Q (2015) Response of wheat growth, grain yield and water use to elevated CO_2 under a Free-Air CO_2 Enrichment (FACE) experiment and modelling in a semi-arid environment. Global Change Biology 21:2670-2686
Oliver Y, Robertson M, Stone P, Whitbread A (2009) Improving estimates of water-limited yield of wheat by accounting for soil type and within-season rainfall. Crop and Pasture Science 60:1137-1146
Oliver Y, Robertson M, Wong M (2010a) Integrating farmer knowledge, precision agriculture tools, and crop simulation modelling to evaluate management options for poor-performing patches in cropping fields. European Journal of Agronomy 32:40-50
Oliver Y, Wong M, Robertson M, Wittwer K (2006) PAWC determines spatial variability in grain yield and nitrogen requirement by interacting with rainfall on northern WA sandplain. In. Proc Proceedings of the 13th Australian agronomy conference
Oliver YM, Robertson MJ, Weeks C (2010b) A new look at an old practice: Benefits from soil water accumulation in long fallows under Mediterranean conditions. Agricultural Water Management 98:291-300
Orlowsky B, Seneviratne SI (2012) Global changes in extreme events: regional and seasonal dimension. Climatic Change 110:669-696
Osborne T, Rose G, Wheeler T (2013) Variation in the global-scale impacts of climate change on crop productivity due to climate model uncertainty and adaptation. Agricultural and Forest Meteorology 170:183-194
Parry ML, Rosenzweig C, Iglesias A, Livermore M, Fischer G (2004) Effects of climate change on global food production under SRES emissions and socio-economic scenarios. Global Environmental Change 14:53-67
Pearce K, Holper PN, Hopkins M, Bouma WJ, Whetton P, Hennessy KJ, Power SB (2007) Climate Change in Australia: technical report 2007, Vol. CSIRO Marine and Atmospheric Research
Perkins S, Alexander L (2013) On the measurement of heat waves. Journal of Climate 26:4500-4517
Perkins S, Alexander L, Nairn J (2012) Increasing frequency, intensity and duration of observed global heatwaves and warm spells. Geophysical Research Letters 39
Piao S, Ciais P, Huang Y, Shen Z, Peng S, Li J, Zhou L, Liu H, Ma Y, Ding Y (2010) The impacts of climate change on water resources and agriculture in China. Nature 467:43-51
Pope KS, Dose V, Da Silva D, Brown PH, Leslie CA, DeJong TM (2013) Detecting nonlinear response of spring phenology to climate change by Bayesian analysis. Global Change Biology 19:1518-1525
Porter JR, Gawith M (1999) Temperatures and the growth and development of wheat: a review. European Journal of Agronomy 10:23-36
Porter JR, Semenov MA (2005) Crop responses to climatic variation. Philosophical Transactions of the Royal Society of London B: Biological Sciences 360:2021-2035
Potgieter A, Hammer G, Butler D (2002) Spatial and temporal patterns in Australian wheat yield and their relationship with ENSO. Crop and Pasture Science 53:77-89
Potgieter A, Meinke H, Doherty A, Sadras V, Hammer G, Crimp S, Rodriguez D (2013) Spatial impact of projected changes in rainfall and temperature on wheat yields in Australia. Climatic Change 117:163-179
Prudhomme C, Reynard N, Crooks S (2002) Downscaling of global climate models for flood frequency analysis: where are we now? Hydrological processes 16:1137-1150
Reichler T, Kim J (2008) How well do coupled models simulate today's climate? Bulletin of the American Meteorological Society 89:303-311
Richardson CW, Wright DA (1984) WGEN: A model for generating daily weather variables. ARS (USA)
Ritchie JT (1991) Wheat Phasic Development. In: Hanks J, Ritchie JT (eds) Modeling Plant and Soil Systems. American Society of Agronomy, Crop Science Society of America, Soil Science Society of America
Robertson AW, Lall U, Zebiak SE, Goddard L (2004) Improved combination of multiple atmospheric GCM ensembles for seasonal prediction. Monthly Weather Review 132:2732-2744

Rosenzweig C, Jones J, Hatfield J, Ruane A, Boote K, Thorburn P, Antle J, Nelson G, Porter C, Janssen S (2013) The agricultural model intercomparison and improvement project (AgMIP): protocols and pilot studies. Agricultural and Forest Meteorology 170:166-182
Rosenzweig C, Tubiello FN (1996) Effects of changes in minimum and maximum temperature on wheat yields in the central US A simulation study. Agricultural and Forest Meteorology 80:215-230
Rowhani P, Lobell DB, Linderman M, Ramankutty N (2011) Climate variability and crop production in Tanzania. Agricultural and Forest Meteorology 151:449-460
Sadras VO, Monzon JP (2006) Modelled wheat phenology captures rising temperature trends: Shortened time to flowering and maturity in Australia and Argentina. Field Crops Research 99:136-146
Seif E, Pederson D (1978) Effect of rainfall on the grain yield of spring wheat, with an application to the analysis of adaptation. Crop and Pasture Science 29:1107-1115
Semenov MA (2009) Impacts of climate change on wheat in England and Wales. Journal of the Royal Society Interface 6:343-350
Semenov MA, Barrow EM (1997) Use of a stochastic weather generator in the development of climate change scenarios. Climatic change 35:397-414
Semenov MA, Shewry PR (2011) Modelling predicts that heat stress, not drought, will increase vulnerability of wheat in Europe. Scientific Reports 1, 66; DOI:10.1038/srep00066
Shackley B, Anderson W (1995) Responses of wheat cultivars to time of sowing in the southern wheatbelt of Western Australia. Animal Production Science 35:579-587
Sheehy JE, Mitchell P, Ferrer AB (2006) Decline in rice grain yields with temperature: models and correlations can give different estimates. Field Crops Research 98:151-156
Sillmann J, Roeckner E (2008) Indices for extreme events in projections of anthropogenic climate change. Climatic Change 86:83-104
Sinclair TR (2011) Precipitation: The thousand-pound gorilla in crop response to climate change. Handbook of Climate Change and Agroecosystems: Impacts, Adapatation, and Mitigation 1:179-190
Soussana J-F, Graux A-I, Tubiello FN (2010) Improving the use of modelling for projections of climate change impacts on crops and pastures. Journal of experimental botany 61:2217-2228
Springate DA, Kover PX (2014) Plant responses to elevated temperatures: a field study on phenological sensitivity and fitness responses to simulated climate warming. Global Change Biology 20:456-465
Stanhill G, Cohen S (2001) Global dimming: a review of the evidence for a widespread and significant reduction in global radiation with discussion of its probable causes and possible agricultural consequences. Agricultural and Forest Meteorology 107:255-278
Stephens D, Lyons T (1998) Variability and trends in sowing dates across the Australian wheatbelt. Australian journal of agricultural research 49:1111-1118
Stephens D, Walker G, Lyons T (1994) Forecasting Australian wheat yields with a weighted rainfall index. Agricultural and Forest Meteorology 71:247-263
Stokes C, Howden M (2010) Adapting agriculture to climate change. In. CSIRO Publishing, Victoria
Stone P, Nicolas M (1994) Wheat cultivars vary widely in their responses of grain yield and quality to short periods of post-anthesis heat stress. Functional Plant Biology 21:887-900
Stott PA, Stone DA, Allen MR (2004) Human contribution to the European heatwave of 2003. Nature 432:610-614
Stratonovitch P, Semenov MA (2015) Heat tolerance around flowering in wheat identified as a key trait for increased yield potential in Europe under climate change. Journal of experimental botany 66:3599-3609
Sui Y, Lang X, Jiang D (2014) Time of emergence of climate signals over China under the RCP4. 5 scenario. Climatic Change:1-12
Sultan B, Guan K, Kouressy M, Biasutti M, Piani C, Hammer G, McLean G, Lobell D (2014) Robust features of future climate change impacts on sorghum yields in West Africa. Environmental Research Letters 9:104006
Sun J, Yang L, Wang Y, Ort DR (2009) FACE-ing the global change: opportunities for improvement in photosynthetic radiation use efficiency and crop yield. Plant Science 177:511-522
Sun W, Huang Y (2011) Global warming over the period 1961–2008 did not increase high-temperature stress but did reduce low-temperature stress in irrigated rice across China. Agricultural and Forest Meteorology 151:1193-1201
Talukder A, Gill G, McDonald G, Hayman P, Alexander B (2010) Field evaluation of sensitivity of wheat to high temperature stress near flowering and early grain set. In. Proc 15th Australian Agronomy Conference, Christchurch, New Zealand

Talukder A, McDonald GK, Gill GS (2014) Effect of short-term heat stress prior to flowering and early grain set on the grain yield of wheat. Field Crops Research 160:54-63
Tao F, Yokozawa M, Liu J, Zhang Z (2008) Climate-crop yield relationships at provincial scales in China and the impacts of recent climate trends. Clim Res 38:83-94
Tao F, Yokozawa M, Xu Y, Hayashi Y, Zhang Z (2006) Climate changes and trends in phenology and yields of field crops in China, 1981–2000. Agricultural and Forest Meteorology 138:82-92
Taylor KE (2001) Summarizing multiple aspects of model performance in a single diagram. Journal of Geophysical Research: Atmospheres (1984–2012) 106:7183-7192
Taylor KE, Stouffer RJ, Meehl GA (2012) An overview of CMIP5 and the experiment design. Bulletin of the American Meteorological Society 93:485-498
Tebaldi C, Hayhoe K, Arblaster JM, Meehl GA (2006) Going to the extremes. Climatic Change 79:185-211
Tebaldi C, Knutti R (2007) The use of the multi-model ensemble in probabilistic climate projections. Philosophical Transactions of the Royal Society A: Mathematical, Physical and Engineering Sciences 365:2053-2075
Tebaldi C, Smith RL, Nychka D, Mearns LO (2005) Quantifying uncertainty in projections of regional climate change: A Bayesian approach to the analysis of multimodel ensembles. Journal of Climate 18:1524-1540
Teixeira EI, Fischer G, van Velthuizen H, Walter C, Ewert F (2011) Global hot-spots of heat stress on agricultural crops due to climate change. Agricultural and Forest Meteorology
Tolika K, Anagnostopoulou C, Maheras P, Vafiadis M (2008) Simulation of future changes in extreme rainfall and temperature conditions over the Greek area: a comparison of two statistical downscaling approaches. Global and Planetary Change 63:132-151
Traore B, Corbeels M, van Wijk MT, Rufino MC, Giller KE (2013) Effects of climate variability and climate change on crop production in southern Mali. European Journal of Agronomy 49:115-125
Trewin B (2010) Exposure, instrumentation, and observing practice effects on land temperature measurements. Wiley Interdisciplinary Reviews: Climate Change 1:490-506
Trewin B (2013) A daily homogenized temperature data set for Australia. International Journal of Climatology 33:1510-1529
Trnka M, Brázdil R, Olesen JE, Eitzinger J, Zahradníček P, Kocmánková E, Dobrovolný P, Štěpánek P, Možný M, Bartošová L (2012) Could the changes in regional crop yields be a pointer of climatic change? Agricultural and Forest Meteorology 166:62-71
Tubiello FN, Amthor JS, Boote KJ, Donatelli M, Easterling W, Fischer G, Gifford RM, Howden M, Reilly J, Rosenzweig C (2007a) Crop response to elevated CO_2 and world food supply: a comment on "Food for Thought…" by Long et al., Science 312: 1918–1921, 2006. European Journal of Agronomy 26:215-223
Tubiello FN, Donatelli M, Rosenzweig C, Stockle CO (2000) Effects of climate change and elevated CO_2 on cropping systems: model predictions at two Italian locations. European Journal of Agronomy 13:179-189
Tubiello FN, Ewert F (2002) Simulating the effects of elevated CO_2 on crops: approaches and applications for climate change. European Journal of Agronomy 18:57-74
Tubiello FN, Soussana J-F, Howden SM (2007b) Crop and pasture response to climate change. Proceedings of the National Academy of Sciences 104:19686-19690
Turner NC, Asseng S (2005) Productivity, sustainability, and rainfall-use efficiency in Australian rainfed Mediterranean agricultural systems. Crop and Pasture Science 56:1123-1136
van Bussel LG, Ewert F, Zhao G, Hoffmann H, Enders A, Wallach D, Asseng S, Baigorria GA, Basso B, Biernath C (2016) Spatial sampling of weather data for regional crop yield simulations. Agricultural and Forest Meteorology 220:101-115
Van Ittersum M, Howden S, Asseng S (2003) Sensitivity of productivity and deep drainage of wheat cropping systems in a Mediterranean environment to changes in CO< sub> 2</sub>, temperature and precipitation. Agriculture, ecosystems & environment 97:255-273
Van Vuuren DP, Edmonds J, Kainuma M, Riahi K, Thomson A, Hibbard K, Hurtt GC, Kram T, Krey V, Lamarque J-F (2011) The representative concentration pathways: an overview. Climatic Change 109:5-31
Vanuytrecht E, Raes D, Willems P (2011) Considering sink strength to model crop production under elevated atmospheric CO_2. Agricultural and Forest Meteorology 151:1753-1762
Vanuytrecht E, Raes D, Willems P, Semenov MA (2014) Comparing climate change impacts on cereals based on CMIP3 and EU-ENSEMBLES climate scenarios. Agricultural and Forest Meteorology 195:12-23
Vincent LA (1998) A technique for the identification of inhomogeneities in Canadian temperature series. Journal

of Climate 11:1094-1104
Vincent LA, Peterson T, Barros V, Marino M, Rusticucci M, Carrasco G, Ramirez E, Alves L, Ambrizzi T, Berlato M (2005) Observed trends in indices of daily temperature extremes in South America 1960-2000. Journal of climate 18:5011-5023
von Storch H, Zorita E, Cubasch U (1993) Downscaling of global climate change estimates to regional scales: an application to Iberian rainfall in wintertime. Journal of Climate 6:1161-1171
Wang B, Chen C, Liu DL, Asseng S, Yu Q, Yang X (2015a) Effects of climate trends and variability on wheat yield variability in eastern Australia. Climate Research 64:173-186
Wang B, Liu DL, Asseng S, Macadam I, Yu Q (2015b) Impact of climate change on wheat flowering time in eastern Australia. Agricultural and Forest Meteorology 209:11-21
Wang B, Liu DL, Macadam I, Alexander LV, Abramowitzc G, Yu Q (2016) Multi-model ensemble projections of future extreme temperature change using a statistical downscaling method in south eastern Australia. Climatic Change (minor revision)
Wang E, Cresswell H, Xu J, Jiang Q (2009a) Capacity of soils to buffer impact of climate variability and value of seasonal forecasts. Agricultural and Forest Meteorology 149:38-50
Wang E, Engel T (1998) Simulation of phenological development of wheat crops. Agricultural Systems 58:1-24
Wang E, Xu J, Jiang Q, Austin J (2009b) Assessing the spatial impact of climate on wheat productivity and the potential value of climate forecasts at a regional level. Theoretical and applied climatology 95:311-330
Wang J, Wang E, Li Liu D (2011a) Modelling the impacts of climate change on wheat yield and field water balance over the Murray–Darling Basin in Australia. Theoretical and Applied Climatology 104:285-300
Wang J, Wang E, Luo Q, Kirby M (2009c) Modelling the sensitivity of wheat growth and water balance to climate change in Southeast Australia. Climatic Change 96:79-96
Wang M, Li Y, Ye W, Bornman JF, Yan X (2011b) Effects of climate change on maize production, and potential adaptation measures: a case study in Jilin Province, China. Climate Research 46:223
Wang T, Ottlé C, Peng S, Janssens IA, Lin X, Poulter B, Yue C, Ciais P (2014) The influence of local spring temperature variance on temperature sensitivity of spring phenology. Global Change Biology 20:1473-1480
Wang Y, Leung LR, McGREGOR JL, Lee D-K, Wang W-C, Ding Y, Kimura F (2004) Regional climate modeling: progress, challenges, and prospects. Journal of the Meteorological Society of Japan 82:1599-1628
Wang Y, Xie Z, Malhi SS, Vera CL, Zhang Y, Wang J (2009d) Effects of rainfall harvesting and mulching technologies on water use efficiency and crop yield in the semi-arid Loess Plateau, China. Agricultural water management 96:374-382
Welbergen JA, Klose SM, Markus N, Eby P (2008) Climate change and the effects of temperature extremes on Australian flying-foxes. Proceedings of the Royal Society B: Biological Sciences 275:419-425
Wheeler TR, Craufurd PQ, Ellis RH, Porter JR, Vara Prasad P (2000) Temperature variability and the yield of annual crops. Agriculture, Ecosystems & Environment 82:159-167
Wigley T, Jones P, Briffa K, Smith G (1990) Obtaining sub-grid-scale information from coarse-resolution general circulation model output. Journal of Geophysical Research: Atmospheres (1984–2012) 95:1943-1953
Wilby R, Wigley T (2000) Precipitation predictors for downscaling: observed and general circulation model relationships. International Journal of Climatology 20:641-661
Wilby RL, Wigley T (1997) Downscaling general circulation model output: a review of methods and limitations. Progress in Physical Geography 21:530-548
Wild M (2009) Global dimming and brightening: A review. Journal of Geophysical Research: Atmospheres (1984–2012) 114
Wild M, Gilgen H, Roesch A, Ohmura A, Long CN, Dutton EG, Forgan B, Kallis A, Russak V, Tsvetkov A (2005) From dimming to brightening: Decadal changes in solar radiation at Earth's surface. Science 308:847-850
Wilks DS, Wilby RL (1999) The weather generation game: a review of stochastic weather models. Progress in Physical Geography 23:329-357
Wolkovich EM, Cook B, Allen J, Crimmins T, Betancourt J, Travers S, Pau S, Regetz J, Davies T, Kraft N (2012) Warming experiments underpredict plant phenological responses to climate change. Nature 485:494-497
Wollenweber B, Porter J, Schellberg J (2003) Lack of Interaction between Extreme High-Temperature Events at Vegetative and Reproductive Growth Stages in Wheat. Journal of Agronomy and Crop Science 189:142-150

Wong M, Asseng S (2006) Determining the causes of spatial and temporal variability of wheat yields at sub-field scale using a new method of upscaling a crop model. Plant and Soil 283:203-215
Wong M, Asseng S (2007) Yield and environmental benefits of ameliorating subsoil constraints under variable rainfall in a Mediterranean environment. Plant and Soil 297:29-42
Wood AW, Leung LR, Sridhar V, Lettenmaier D (2004) Hydrologic implications of dynamical and statistical approaches to downscaling climate model outputs. Climatic change 62:189-216
Wu D, Yu Q, Lu C, Hengsdijk H (2006) Quantifying production potentials of winter wheat in the North China Plain. European Journal of Agronomy 24:226-235
Xu C-y (1999) From GCMs to river flow: a review of downscaling methods and hydrologic modelling approaches. Progress in Physical Geography 23:229-249
Yang T, Hao X, Shao Q, Xu C-Y, Zhao C, Chen X, Wang W (2012) Multi-model ensemble projections in temperature and precipitation extremes of the Tibetan Plateau in the 21st century. Global and Planetary Change 80:1-13
Yang X, Asseng S, Wong MTF, Yu Q, Li J, Liu E (2013) Quantifying the interactive impacts of global dimming and warming on wheat yield and water use in China. Agricultural and forest meteorology 182:342-351
Yang Y, Liu DL, Anwar MR, O'Leary G, Macadam I, Yang Y (2016) Water use efficiency and crop water balance of rainfed wheat in a semi-arid environment: sensitivity of future changes to projected climate changes and soil type. Theoretical and Applied Climatology 123:565-579
Yang Y, Liu DL, Anwar MR, Zuo H, Yang Y (2014) Impact of future climate change on wheat production in relation to plant-available water capacity in a semiaridenvironment. Theoretical and Applied Climatology 115:391-410
Yin C, Li Y, Ye W, Bornman JF, Yan X (2011) Statistical downscaling of regional daily precipitation over southeast Australia based on self-organizing maps. Theoretical and applied climatology 105:11-26
Yu Q, Hengsdijk H, Liu J (2001) Application of a progressive-difference method to identify climatic factors causing variation in the rice yield in the Yangtze Delta, China. International Journal of Biometeorology 45:53-58
Yu Q, Li L, Luo Q, Eamus D, Xu S, Chen C, Wang E, Liu J, Nielsen DC (2014) Year patterns of climate impact on wheat yields. International Journal of Climatology 34:518-528
Yu Y, Huang Y, Zhang W (2012) Changes in rice yields in China since 1980 associated with cultivar improvement, climate and crop management. Field Crops Research 136:65-75
Zeleke K, Nendel C (2016) Analysis of options for increasing wheat (Triticum aestivum L.) yield in south-eastern Australia: The role of irrigation, cultivar choice and time of sowing. Agricultural Water Management 166:139-148
Zhang H, Oweis T (1999) Water–yield relations and optimal irrigation scheduling of wheat in the Mediterranean region. Agricultural Water Management 38:195-211
Zhang H, Turner N, Poole M, Simpson N (2006) Crop production in the high rainfall zones of southern Australia—potential, constraints and opportunities. Animal Production Science 46:1035-1049
Zhang M, Yu G-R, Zhuang J, Gentry R, Fu Y-L, Sun X-M, Zhang L-M, Wen X-F, Wang Q-F, Han S-J (2011a) Effects of cloudiness change on net ecosystem exchange, light use efficiency, and water use efficiency in typical ecosystems of China. Agricultural and Forest Meteorology 151:803-816
Zhang T, Zhu J, Wassmann R (2010) Responses of rice yields to recent climate change in China: an empirical assessment based on long-term observations at different spatial scales (1981–2005). Agricultural and Forest Meteorology 150:1128-1137
Zhang X-C (2005) Spatial downscaling of global climate model output for site-specific assessment of crop production and soil erosion. Agricultural and Forest Meteorology 135:215-229
Zhang X, Alexander L, Hegerl GC, Jones P, Tank AK, Peterson TC, Trewin B, Zwiers FW (2011b) Indices for monitoring changes in extremes based on daily temperature and precipitation data. Wiley Interdisciplinary Reviews: Climate Change 2:851-870
Zhao G, Bryan BA, King D, Luo Z, Wang E, Song X, Yu Q (2013) Impact of agricultural management practices on soil organic carbon: simulation of Australian wheat systems. Global Change Biology 19:1585-1597
Zheng B, Chapman SC, Christopher JT, Frederiks TM, Chenu K (2015) Frost trends and their estimated impact on yield in the Australian wheatbelt. Journal of Experimental Botany:erv163
Zheng B, Chenu K, Fernanda Dreccer M, Chapman SC (2012) Breeding for the future: what are the potential impacts of future frost and heat events on sowing and flowering time requirements for Australian bread wheat (Triticum aestivum) varieties? Global Change Biology 18:2899-2914
Zorita E, Von Storch H (1999) The analog method as a simple statistical downscaling technique: comparison with more complicated methods. Journal of climate 12:2474-2489

List of publications arising from this thesis

1. Effects of climate trends and variability on wheat yield variability in eastern Australia

Vol. 64: 173–186, 2015
doi: 10.3354/cr01307

CLIMATE RESEARCH
Clim Res

Published online July 29

Effects of climate trends and variability on wheat yield variability in eastern Australia

Bin Wang[1,2,3,*], Chao Chen[4], De Li Liu[2,3], Senthold Asseng[5], Qiang Yu[1], Xihua Yang[6]

[1]School of Life Sciences, Faculty of Science, University of Technology Sydney, PO Box 123, Broadway, New South Wales 2007, Australia

[2]NSW Department of Primary Industry, Skills and Regional Development, Wagga Wagga Agricultural Institute, New South Wales 2650, Australia

[3]Graham Centre for Agricultural Innovation (an alliance between NSW Department of Industry and Charles Sturt University), Wagga Wagga, New South Wales 2650, Australia

[4]CSIRO Agriculture Flagship, Private Bag 5, PO Wembley, Western Australia 6913, Australia

[5]Agricultural & Biological Engineering Department, University of Florida, 221 Frazier Rogers Hall, PO Box 110570, Gainesville, Florida 32611-0570, USA

[6]New South Wales Office of Environment and Heritage, PO Box 3720, Parramatta, New South Wales 2150, Australia

ABSTRACT: Identifying climatic drivers that dominate in determining crop yield variations at a regional scale is important for predicting regional crop production. In this study, a statistical method was used to quantify the relationship between reported shire wheat yields and climate factors during the wheat-growing season across the New South Wales (NSW) wheat belt in eastern Australia from 1922 to 2000. The results show that recent climatic trends have increased wheat yield by 8.5 to 21.2% in 4 different climatic regions of NSW over the last few decades: In the eastern slopes, growing season maximum and minimum temperatures and number of heat stress days (>34°C) were identified as the dominant climatic factors affecting wheat yield, accounting for 36% of its variation. The wheat yield variation in the remaining 3 regions were as follows: 41% in the northern region from maximum temperature, pre-growing season rainfall (December to April), and number of frost days (<2°C); 47% in the south from rainfall, temperature, and number of frost and heat stress days; while in southwest NSW, rainfall was the main factor responsible for 31% of the variation. Frost was less important in the eastern slopes because farmers manage frost occurrence by sowing late and using late-flowering cultivars. However, the opposite occurs in the northern parts of the wheat belt where farmers sow earlier and select short-season varieties to avoid heat stress, but thereby expose their crops to possible frost conditions. Understanding the impact of climate variations on crop yield is important for developing sustainable agricultural production under future climate change.

KEY WORDS: Climate variation · Wheat yield variability · NSW wheat belt · First difference

2. Impact of climate change on wheat flowering time in eastern Australia

Agricultural and Forest Meteorology 209 (2015) 11–21

Contents lists available at ScienceDirect

Agricultural and Forest Meteorology

journal homepage: www.elsevier.com/locate/agrformet

Impact of climate change on wheat flowering time in eastern Australia

Bin Wang[a,b,c,*], De Li Liu[b,c], Senthold Asseng[d], Ian Macadam[e], Qiang Yu[a]

[a] Plant Biology and Climate Change Cluster, University of Technology Sydney, P.O. Box 123, Broadway, NSW 2007, Australia
[b] NSW Department of Primary Industries, Wagga Wagga Agricultural Institute, NSW 2650, Australia
[c] Graham Centre for Agricultural Innovation an Alliance between NSW Department of Primary Industries and Charles Sturt University, Wagga Wagga, NSW 2650, Australia
[d] Agricultural & Biological Engineering Department, University of Florida, 221 Frazier Rogers Hall, P.O. Box 110570, Gainesville, FL 32611-0570, USA
[e] Climate Change Research Centre and ARC Centre of Excellence for Climate System Science, University of New South Wales, Sydney, NSW 2052, Australia

ARTICLE INFO

Article history:
Received 29 January 2015
Received in revised form 27 April 2015
Accepted 30 April 2015

Keywords:
Wheat phenology
Vernalizing–photothermal model
Climate change
NSW wheat belt
Frost days
Hot days

ABSTRACT

The flowering time of wheat is strongly controlled by temperature and is potentially highly sensitive to climate change. In this study, we analysed the occurrence of last frost (days with minimum temperature under 2 °C) and first heat (days with maximum temperatures exceeding 30 °C) events of the year to determine the optimum flowering date in the wheat belt of New South Wales (NSW), eastern Australia. We used statistically downscaled daily maximum and minimum temperature data from 19 Global Climate Models (GCMs) with a vernalizing–photothermal model in order to simulate future flowering dates and the changes in frost and hot days occurrence at flowering date (± 7 days) for two future scenarios for atmospheric greenhouse gas concentrations (RCP4.5 and RCP8.5) in 2040s (2021–2060) and 2080s (2061–2100). Relative to the 1961–2000 period, the GCMs projected increased daily maximum and minimum temperatures for these future periods, accompanied by reduced frost occurrence and increased heat stress incidence. As a consequence, by the 2080s, simulations suggest a general advance in spring wheat flowering date by, on average, 10.2 days for RCP4.5 and 17.8 days for RCP8.5 across the NSW wheat belt. Winter wheat flowering dates were delayed by an average of 2.4 days for RCP4.5 and 14.3 days for RCP8.5 in the warmest parts of the region (the northwest) due to reduced cumulative vernalization days (requiring cool conditions). In the cooler regions (the northeast, southeast and southwest), flowering date occurred earlier by 6.2 days for RCP4.5 and 6.7 days for RCP8.5 on average. Moreover, in the western parts of the wheat belt the delay of winter wheat flowering date was about 9.5 days longer than that in the eastern parts. As a result of phenological responses to increasing temperatures, current wheat varieties may not be suitable for future climate conditions, despite reduced frost risk. In the future, it may be necessary to use longer-season wheat varieties and varieties with increased heat-stress resistance.

3. Multi-model ensemble projections of future extreme temperature change using a statistical downscaling method in south eastern Australia

Climatic Change
DOI 10.1007/s10584-016-1726-x

Multi-model ensemble projections of future extreme temperature change using a statistical downscaling method in south eastern Australia

Bin Wang[1,2] · De Li Liu[2] · Ian Macadam[3,4] · Lisa V. Alexander[3] · Gab Abramowitz[3] · Qiang Yu[1]

Received: 27 August 2015 / Accepted: 14 June 2016

Abstract Projections of changes in temperature extremes are critical to assess the potential impacts of climate change on agricultural and ecological systems. Statistical downscaling can be used to efficiently downscale output from a large number of general circulation models (GCMs) to a fine temporal and spatial scale, providing the opportunity for future projections of extreme temperature events. This paper presents an analysis of extreme temperature data downscaled from 7 GCMs selected from the Coupled Model Intercomparison Project phase 5 (CMIP5) using a skill score based on spatial patterns of climatological means of daily maximum and minimum temperature. Data for scenarios RCP4.5 and RCP8.5 for the New South Wales (NSW) wheat belt, south eastern Australia, have been analysed. The results show that downscaled data from most of the GCMs reproduces the correct sign of recent trends in all the extreme temperature indices (except the index for cold days) for 1961–2000. An independence weighted mean method is used to calculate uncertainty estimates, which shows that multi-model ensemble projections produce a consistent trend compared to the observations in most extreme indices. Great warming occurs in the east and northeast of the NSW wheat belt by 2061–2100 and increases the risk of exposure to hot days around wheat flowering date, which might result in farmers needing to reconsider wheat varieties suited to maintain yield. This

Electronic supplementary material The online version of this article (doi:10.1007/s10584-016-1726-x) contains supplementary material, which is available to authorized users.

4. Multi-model ensemble projections of future extreme temperature change using a statistical downscaling method in south eastern Australia

21st International Congress on Modelling and Simulation, Gold Coast, Australia, 29 Nov to 4 Dec 2015
www.mssanz.org.au/modsim2015

Multi-model ensemble projections of future extreme temperature change using a statistical downscaling method in eastern Australia

Bin Wang[a,b], De Li Liu[b], Ian Macadam[c,d], Lisa V. Alexander[c], Gab Abramowitz[c] and Qiang Yu[a]

[a] *School of Life Sciences, Faculty of Science, University of Technology Sydney, PO Box 123, Broadway, NSW 2007, Australia*
[b] *NSW Department of Industry, Skills and Regional Development, Wagga Wagga Agricultural Institute, NSW 2650, Australia*
[c] *Climate Change Research Centre and ARC Centre of Excellence for Climate System Science, University of New South Wales, Sydney, NSW 2052, Australia*
[d] *Met Office, FitzRoy Road, Exeter, EX1 3PB, UK*
E: bin.a.wang@dpi.nsw.gov.au

Abstract: Projections of changes in temperature extremes are critical to assess the potential impacts of climate change on agricultural and ecological systems. Statistical downscaling can be used to efficiently downscale output from a large number of general circulation models (GCMs) to a fine temporal and spatial scale, which now provides the opportunity for future projections of extreme temperature events. This paper presents an analysis of extreme temperature in data downscaled from ensembles of 13 selected GCMs, out of 28 GCMs, contributing to the Fifth Assessment Report of the Intergovernmental Panel on Climate Change (IPCC-AR5) under two Representative Concentration Pathways (RCP4.5 and RCP8.5) in eastern Australia. The statistical downscaling procedure begins with spatial interpolation of the monthly gridded data to specific locations of interest using an inverse distance-weighted method, followed by a bias correction towards historical observed climate. Daily climate data for each location are then generated by a modified version of the WGEN stochastic weather generator. The extremes of temperature are described by eleven indices, namely, the annual maximum daily Tmax (TXx), the annual maximum daily Tmin (TNx), the annual minimum daily Tmax (TXn), the annual minimum daily Tmin (TNn), the number of hot days (HD) and frost days (FD), warm days (TX90p) and nights (TN90p), cold days (TX10p) and nights (TN10p) and extreme temperature range (ETR). The results show that downscaled data from most of the GCMs reproduced the correct sign of recent trends in all the extreme temperature indices (except TN10p) although there was much more variation between the individual model runs. An independence weighted mean method was used to calculate uncertainty estimates, which verified that multi-model ensemble projections produced a good consensus compared to the observations in magnitude of the trend in TXx, TN90p, HD, TNn, ETR for the period 1961-2000 when averaged across eastern Australia. In the 21st century the frost days, cold days and nights decrease while more frequent warm days and nights and hot days are projected in the New South Wales (NSW) wheat belt. The changes in temperature extremes under RCP8.5 are more pronounced than that under RCP4.5. Greater warming occurs in the east and northeast of the NSW wheat belt by the end of the 21st century and increases the risk of exposure to hot days around wheat flowering date, which results in farmers needing to reconsider wheat varieties suited to maintain yield. This analysis provides a first overview of projected changes in climate extremes from the ensemble of 13 CMIP5 models with statistical downscaling data in eastern Australia, and supplies important information to mitigate the adverse effects of climate extremes on NSW wheat belt and improve the regional strategy for agricultural systems.

Keywords: *Warm indices, cold indices, GCMs, observations, independence weighted mean*